THERMODYNAMIC STUDIES ON ALTERNATE BINARY WORKING FLUID COMBINATIONS AND CONFIGURATIONS FOR A COMBINED POWER AND COOLING CYCLE

By

SANJAY VIJAYARAGHAVAN

A DISSERTATION PRESENTED TO THE GRADUATE SCHOOL
OF THE UNIVERSITY OF FLORIDA IN PARTIAL FULFILLMENT
OF THE REQUIREMENTS FOR THE DEGREE OF
DOCTOR OF PHILOSOPHY

UNIVERSITY OF FLORIDA

2003

ACKNOWLEDGMENTS

The work presented in this dissertation was completed with the encouragement and support of many wonderful people. Working with Dr. Yogi Goswami has been a tremendous experience. He expects his students to be self-starters, who work independently on their projects. I appreciate his patience and mentorship in areas within and beyond the realm of research and graduate school. Dr. Sherif Sherif was a terrific source of discussion, advice, encouragement and hard to find AES proceedings. Dr. James Klausner, Dr. David Hahn, and Dr. Ulrich Kurzweg agreed to be on my committee and took the time to read and critique my work, for which I am grateful. Dr. Hahn was also on my master's committee and supervised me during my assignment as a TA for two terms.

Dr. Bill Lear has to be thanked for advice on jet pumps and Dr. Skip Ingley for his interest in the cycle. Dr. Leon Lasdon from the University of Texas sent me the FORTRAN version of the GRG code and answered my questions very promptly. Although my particular project did not require much of his marvelous skills, the senior engineering technician at the Solar Park, Chuck Garretson, was very supportive. Watching him and working with him have taught me many things. He is a wonderful resource for any student at the lab. Barbara Graham over the years and now recently Vitrell McNair at the solar office have cheerfully helped me in many ways in the course of my stay here. Mrs. Becky Hoover will have to be thanked for her help and constant reminders to finish up.

My fellow students at the solar lab have been stimulating company. Some of them particularly have to be acknowledged. Gunnar Tamm, Chris Martin and Nitin Goel took interest in my work and provided constructive feedback. Gunnar has also been at the lab almost as long as I have, and he has been fun to work with. Former students such as Viktoria and Andrew Martin, and Adrienne Cooper have stayed in touch and encouraged me.

I would like to particularly thank my family for putting up with my being so far away from home, and for their love, support and eternal optimism. This section is not complete without mentioning friends, old and new, too many to name individually, who have been great pals and confidants over the years.

TABLE OF CONTENTS

Page

LIST OF TABLES

LIST OF FIGURES

NOMENCLATURE

COP	Coefficient of Performance
c_p	Specific heat
E	Exergy
f	refrigeration weight factor
h	specific enthalpy
i	Exergy Index
lmf	Liquid mass fraction
m	mass
NTU	Number of Transfer Units
Obj	Objective function
p	Pressure
Q	Heat Interaction
T	Temperature
S	Entropy
s	specific entropy
R	Universal gas constant
r	Ratio of cooling to work output
v	Specific volume
vmf	Vapor mass fraction

W	Work Interaction
x	Mass fraction of ammonia (volatile component) in a binary mixture
y	Mole fraction of volatile component in a binary mixture

Greek Symbols

α_{21}	Volatility of component 2 w.r.t component 1
η	Efficiency

Subscripts

0	Reference state
b	Boiling
basic	Referring to basic solution stream, from absorber
Carnot	Carnot Cycle
c	Cooling
cf	Chilled Fluid
crit	Critical
eff	Effective
exergy	Exergy
exit	At Exit of a Device
fg	Liquid to gas (representing phase change from liquid to gas)
HE	Heat engine
h	Heat Source
high	High

hr	Heat rejection Fluid
hs	Heat Source Fluid
in	Input
Lorenz	Lorenz Cycle
low	Low
m	Melting
max	maximum
net	Net
out	Output
p	Pump
R	Resource Utilization Efficiency
r	Reduced
rev	Reversible
ref	Refrigeration
sys	System
useful	Useful
I	First Law
II	Second Law

Abstract of Dissertation Presented to the Graduate School
of the University of Florida in Partial Fulfillment of the
Requirements for the Degree of Doctor of Philosophy

THERMODYNAMIC STUDIES ON ALTERNATE BINARY WORKING FLUID COMBINATIONS AND CONFIGURATIONS FOR A COMBINED POWER AND COOLING CYCLE

By

Sanjay Vijayaraghavan

August 2003

Chair: D. Y. Goswami
Major Department: Mechanical and Aerospace Engineering

A combined power and cooling cycle was investigated. The cycle is a combination of the Rankine cycle and an absorption refrigeration cycle. A binary mixture of ammonia and water is partially boiled to produce a vapor rich in ammonia. This vapor is further enriched in a rectifier/condenser and after superheating, expanded through a turbine. The vapor exiting the turbine in this cycle is cold enough to extract refrigeration output. By suitable selection of operational parameters for the cycle, the useful output can have a large range of refrigeration to work ratios. This combined cycle is being proposed for applications with lower temperature heat sources, with the primary objective of producing power. Some examples of energy sources include solar, geothermal, or industrial waste heat.

Evaluating the efficiency of this cycle is made difficult by the fact that there are two different outputs, namely power and refrigeration. An efficiency expression has to suitably weight the cooling component in order to be able to compare this cycle with

other cycles. Several expressions are proposed for the first law and second law efficiencies for the combined cycle based on existing definitions in the literature. Some of the developed equations have been recommended for use over others, depending on the comparison being made.

This study extended the application of the cycle to working fluids other than ammonia-water mixtures, specifically to organic fluid mixtures. It was found that very low temperatures (well below ambient) are not achievable using organic fluid mixtures, while with an ammonia-water mixture; temperatures that were substantially below ambient were obtained under similar conditions. Thermodynamic efficiencies obtained with hydrocarbon mixtures are lower than those seen with an ammonia-water mixture as the working fluid.

Based on the exergy analysis, the cycle configuration has been modified to improve its second law efficiency. A significant improvement in the resource utilization efficiency of more than 25% was achieved with the best among the improved schemes. Increased efficiencies can also be obtained for the cases where only work output is desired.

CHAPTER 1
BACKGROUND

Introduction

The goal of this study is to investigate the use of organic fluid binary mixtures as possible alternate working fluids for a new thermodynamic power cycle (henceforth referred to as the cycle) proposed by Goswami [1]. The power cycle under study is unique in that the working fluid exiting the turbine could be cold enough to extract refrigeration. This cycle is a combination of the Rankine and absorption refrigeration cycles. The performance of the cycle has been studied extensively and optimized in earlier studies [2-8]. A mixture of ammonia and water has been considered so far for the working fluid. An experimental setup was built and a preliminary verification of ammonia boiling and condensation behavior performed [8].

The cycle has been found to be more suited to low temperature heat sources, based on earlier simulation results. The use of a volatile component such as ammonia allows vapor to be formed at high enough pressures that are useful for power generation. It is, therefore, anticipated that this cycle will be used in low temperature applications such as those involving solar, geothermal, and waste heat sources.

Traditionally, the trend in thermal energy conversion in general, is to use higher temperatures in thermal energy conversion plants. Heat associated with high temperatures has a larger availability, and therefore systems operating at higher temperatures normally achieve greater first law efficiencies of conversion. Some of the

best efficiencies (around 58% first law efficiency) achieved today are with combined cycle power plants. Attempts are being made to break the 60% efficiency barrier in some combined cycle plants being designed currently [9]. In combined cycle plants being built today, a gas turbine power cycle is the first stage, and the exhaust from the turbine is used to run a steam power plant. In the case of solar power generation, to operate at high temperatures, considerable concentration of the solar radiation is required. Solar energy being a dilute resource, the collection system is a large part of the cost of a solar power plant. The optics required for achieving high concentration increases the cost of the collection system.

Some of the biggest disadvantages of solar energy as an energy source for electricity generation are a) the dilute nature of the resource, b) the intermittent nature of the energy and c) the high cost of producing power. It is hoped that by using cheaper, low concentration collection systems and a cycle that utilizes a large percentage of the exergy in that temperature range, the cost of solar power production can be brought down. The combined power and cooling cycle is being developed to efficiently utilize the exergy of low temperature heat sources. Since the cycle can operate at low temperatures, it could be applied to other low temperature heat sources such as geothermal and waste heat.

Background

Thermal power cycles can be classified on the basis of the working fluid used, as vapor power cycles and gas power cycles. In a vapor power cycle, the gas that spins the turbine is obtained from vaporizing a liquid. An example of such a cycle is the classic Rankine cycle. In a gas power cycle, such as the Brayton cycle, the working fluid is in a gaseous state throughout the cycle.

Rankine Cycle

The most commonly used vapor power cycle is the Rankine cycle. Even though a description of the Rankine cycle can be found in any engineering thermodynamics textbook [10], it is briefly covered here. The simple Rankine cycle, shown in Fig. 1.1 consists of four steps. The working fluid is pumped to a high pressure and circulated through the boiler. The fluid is boiled at a constant pressure in the boiler after which the high-pressure vapor produced is expanded through a turbine, thus extracting work from it. The vapor exiting the turbine is condensed in a condenser by rejecting heat to a cooling fluid. There are several modifications to the Rankine cycle that are used to achieve better efficiencies. These include superheating, reheating and regeneration.

Water (Steam) is the working fluid of choice for most vapor power cycles. Water works over a broad range of temperatures and pressures, has a large heat capacity, and is stable, safe and very environmentally friendly. The energy sources used to generate steam include gas, coal, oil, and nuclear sources. A small percentage of steam power plants use geothermal and solar energy sources. The first commercially successful steam engine was the one patented by Thomas Savery in 1698. The better-known Newcomen's engine eventually displaced this engine in the early 18th century [11]. The steam power plant has come a long way in the 100 odd years since central steam generating plants started being built. The first central station steam turbine in the United States operated (in 1900) with steam conditions of 1MPa and 483 K. In contrast, a typical central steam power station today operates at high pressure turbine inlet pressures and temperatures of 16.4 MPa and 800 K respectively [11].

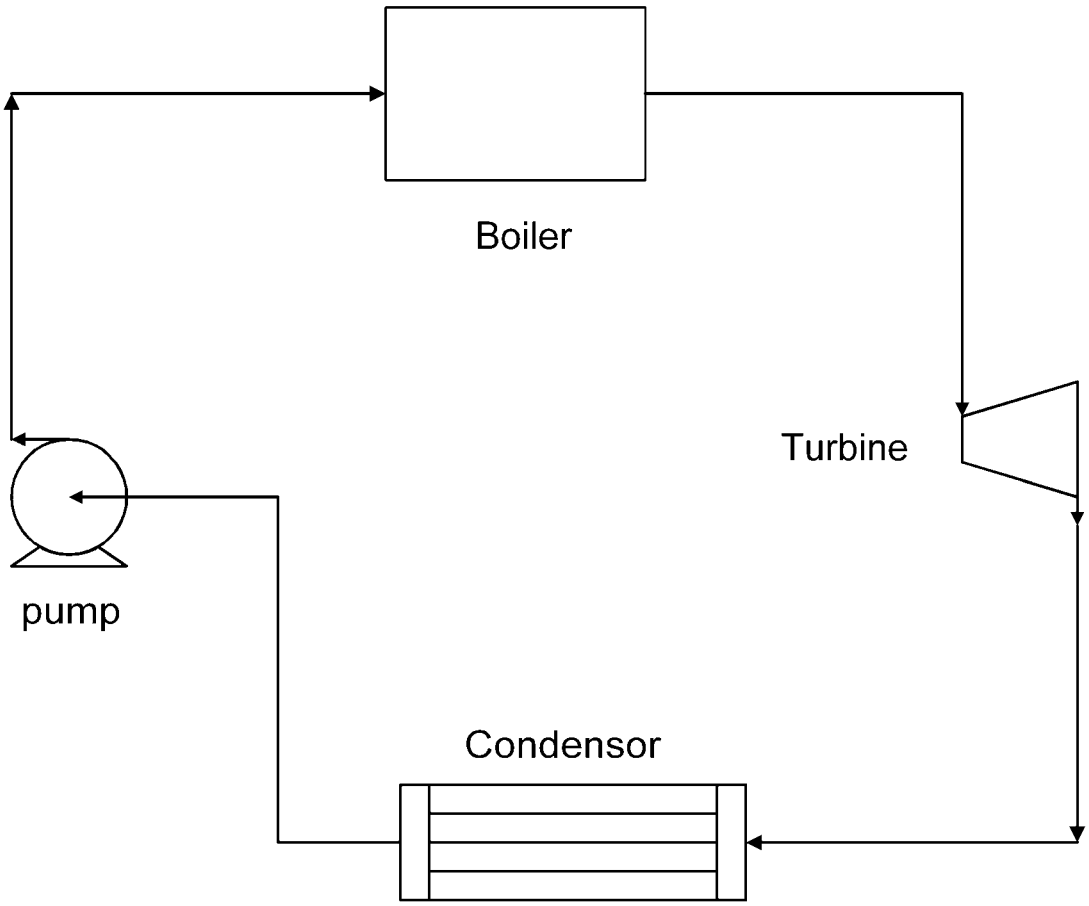

Fig. 1.1 A schematic diagram of a simple Rankine cycle

While steam is the working fluid of choice today, there are certain situations in which it does not work efficiently, particularly with low temperature resources. For example, consider the case of a binary[1] geothermal power plant. In such a plant, a fluid such as isobutane is boiled using a relatively low temperature geothermal fluid, and used to spin a turbine working on a Rankine cycle. If steam were to be used in such applications (or if the plant is designed as a flash type plant), very low pressures and large vacuums at turbine exit would result.

[1] It needs to be pointed out that in a binary geothermal power plant, a high pressure fluid is heated by a hot geofluid, boiled and expanded through a turbine. This is not the same as a plant using a binary fluid mixture for a working fluid.

Power Cycles for Low Temperature Heat Sources

The cycle being studied here appears to work well with low temperature heat sources, based on past studies. Low temperature heat sources are usually those deriving their energy from geothermal, solar or some waste heat sources. Solar energy can be used at various temperatures, depending on the collection method used. Low temperature heat sources have low availability and are not usually the energy sources of choice. Such sources would be considered useful only if some economic advantage is found in their utilization. For instance, a geothermal power plant could prove to be economically feasible to supply an area in the vicinity of a geothermal steam field.

Several power cycles that are suitable for use with low temperature heat sources have been proposed in the literature and have been used in practice. The Rankine cycle has been adapted for use with low temperature heat sources by using low boiling working fluids such as organic fluids. Organic Rankine cycles (ORC) have been extensively used in binary geothermal power plants and low temperature solar power conversion. Several ammonia-water mixture based cycles have also been proposed for low temperature applications.

Organic Rankine cycles (ORC)

Since the first Rankine cycle-based thermal power plant was built, there have been several improvements in the configuration, components, and materials used, but the working fluid of choice has almost always been water. While water has several properties that make it a very good choice as a working fluid, in low temperature applications, better choices are available. Organic working fluids are a popular choice for such applications. Despite the fact that these fluids have lower heats of vaporization than water, which requires larger flow rates, smaller turbine sizes are obtained due to the

higher density at the turbine exit conditions. A variety of fluids, both pure components and binary and ternary mixtures, have been considered for use in ORCs. These include saturated hydrocarbons such as propane, isobutane, pentane, hexane and heptane; aromatics such as benzene and toluene; refrigerants such as R11, R113, R114; and some other synthetic compounds such as Dowtherm A.

Organic Rankine cycles have been proposed and used in a variety of applications

- Binary geothermal power plants: A flash type geothermal power plant is unsuitable for low temperature, liquid dominated, geothermal resources (nominally below 180 ºC). Instead, the geofluid is used to boil an organic working fluid that is subsequently expanded in a turbine. Isobutane is an example of a common working fluid in such applications.
- Solar thermal power: ORC plants can also be applied to the conversion of low and medium temperature (say up to 300 ºC) solar heat. The Coolidge plant [12] that was a 200 kW plant built near the town of Coolidge, AZ, is a good example. For higher temperature heat sources, toluene seems to be a common choice of working fluid.
- Bottoming cycle applications: ORCs have been proposed for the bottoming cycle in some applications

Mixtures of organic fluids have also been studied for use in ORCs. The advantages of the use of mixtures will be discussed later in this chapter. Binary mixtures have been found to have a better performance compared to pure fluid ORCs [13-16]. Organic fluid turbines have been found to be very reliable and to have a relatively high efficiency even at small sizes. Due to their reliability, some people have even suggested their use in space applications, with the ORC as the bottoming stage of a Brayton or Rankine cycle power plant.

Supercritical cycles

The use of mixtures is one way to obtain good thermal matching with sensible heat sources. Other methods that have been proposed include multi-pressure boiling and supercritical operation. Multi pressure boiling has not been very popular in the industry

because of the costs involved. The other option is to use supercritical cycles. The cycle high pressure and temperature exceed that at the working fluid critical point in a supercritical cycle. The boiling process does not pass through a distinct two-phase region, and a better thermal match is obtained in the boiler. Figure 1.2 shows the boiling process in a supercritical cycle on a T-s diagram. Notice the better thermal match in a boiling heat exchanger. Supercritical cycles have to operate at a higher pressure, since the boiler pressure has to exceed the critical pressure of the working fluid. This is a disadvantage. Equipment costs go up at higher pressures, although there is an improvement in performance.

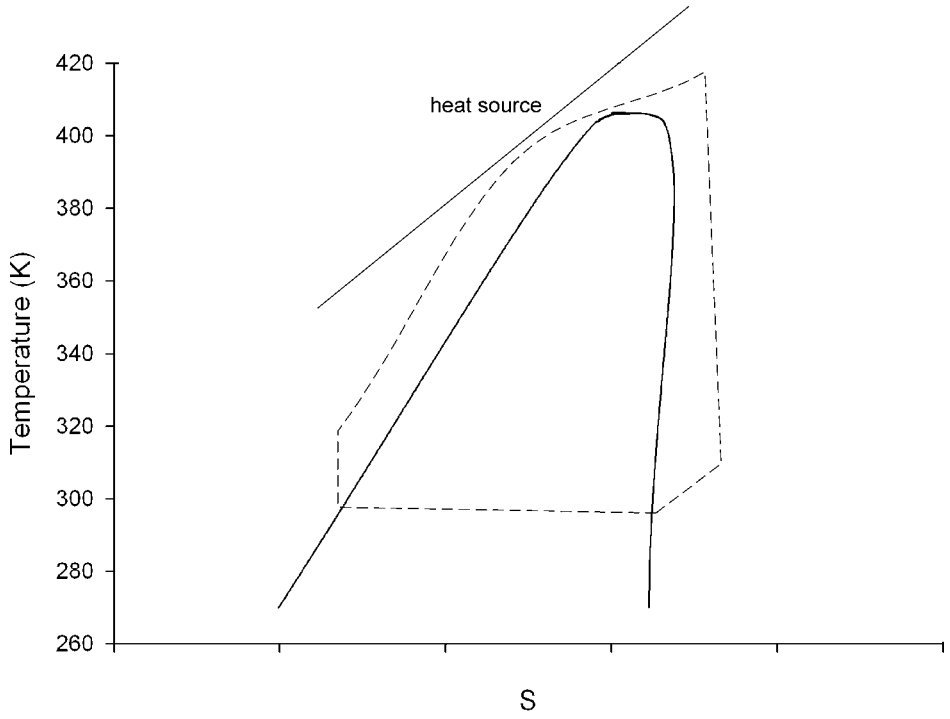

Fig. 1.2 Diagram showing a supercritical Rankine cycle on the T-s diagram for isobutane

Supercritical cycles have been studied in the United States for geothermal applications as a part of the DOE Heat Cycle Research Program [17] and have been found to improve geofluid effectiveness (power output per unit mass of geothermal fluid consumed, usually expressed as kWh/lb). Boretz [18] studied the use of supercritical operation in space applications. He suggested the use of a supercritical cycle in order to avoid the two-phase boiling encountered at subcritical conditions.

Several power cycles utilizing ammonia-water mixtures as the working fluid have been proposed in the literature. A common characteristic of most of these cycles is that all or part of the heat rejection occurs in an absorber condenser. These range from the simple Maloney and Robertson cycle to the relatively sophisticated Kalina cycle. Some of these cycles are discussed below.

Maloney and Robertson cycle

Although ammonia based cycles have been proposed earlier in the literature, in this chapter the oldest cycle considered is one by Maloney and Robertson [19]. Maloney and Robertson studied the ammonia-water binary mixture as a candidate for a simple absorption based power cycle. They studied the cycle within the range of properties available to them at that time and concluded that in all cases a steam Rankine cycle was more efficient. The range of temperatures, pressures, and compositions for which property data were available at the time of the study was limited. This is a serious shortcoming of Maloney and Robertson's results. Further, the cycle did not have a super heater included in the loop, which could have changed somewhat the efficiencies obtained.

Kalina cycle

Another ammonia-water mixture based cycle of more recent origin that shows considerable promise is the Kalina cycle [20,21]. The first Kalina cycle was first developed in the late 1970's and early 1980's. This cycle, developed by Alexander Kalina, is essentially a Rankine cycle that utilizes a binary mixture of ammonia and water as the working fluid. This results in better thermal matching in the boiler, as will be discussed later. Another feature of the Kalina cycle is the extensive internal heat recovery and exchange arrangement that minimizes irreversibilities in the heat transfer processes in the cycle. Many of the Kalina cycle configurations proposed also have an arrangement that uses the heat in the vapor leaving the turbine in a distiller to concentrate the liquid stream that is boiled and expanded in the turbine.

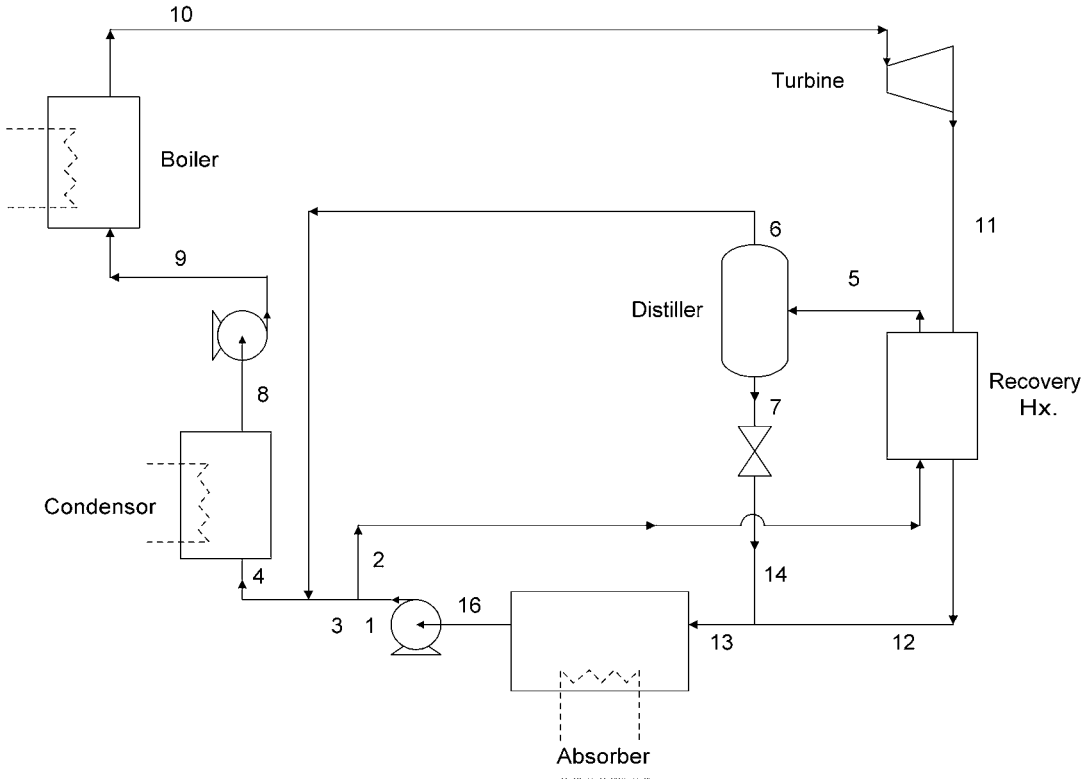

Fig. 1.3 Arrangement of a simple Kalina cycle [20]

The basic version of the Kalina cycle is shown in Fig. 1.3. The composition of the working fluid passing through the boiler (or the working solution) is different from the basic solution in the absorber. This is accomplished through the distillation method that has also been called a "thermal compression" arrangement in some papers.

The hot vapor leaving the turbine is used to distil a fraction of the pressurized basic solution (state 2) to produce vapor (state 6) rich in ammonia. The remaining liquid is combined with the cooled turbine exhaust vapor in an absorber (state 13). The turbine exhaust is normally at too high a concentration to be fully condensed at the corresponding pressure. Combining with the weak liquid enables condensation. The vapor from the distiller is combined with the rest of the basic solution and condensed (state 8) to form the working fluid. The working fluid is vaporized, and superheated (state 10) in the boiler and expanded in the turbine.

The advantages of a Kalina cycle plant are the following

- The use of a mixture results in a better thermal match in the boiler due to variable temperature boiling
- Better internal heat recovery is also possible due to use of mixtures
- The distillation arrangement along with absorption condensation allows a lower turbine exit pressure despite using a high concentration vapor. Higher work output is therefore obtained

Several studies have shown that the Kalina cycle performs substantially better than a steam Rankine cycle system [20-22]. El-Sayed and Tribus [23] showed that the Kalina cycle has 10-20% higher second law efficiency than a simple Rankine cycle operating between the same thermal boundary conditions. A second law analysis of various Kalina systems shows that using a binary fluid and the resulting reduced irreversibility generation in the boiler is one source of the improved efficiency of the cycle [24-25].

Marston [26] verified some of the results of El-Sayed, Tribus, and Kalina and through a parametric analysis concluded that composition at turbine inlet and temperature at the separator of a simple Kalina cycle are the key parameters in optimizing cycle performance.

Several Kalina cycle variations have been proposed, each optimized for different applications. A common feature of each of these "systems" as the developers of this cycle prefer to call the versions, is the improved and sometimes counterintuitive application of internal heat recovery in the cycle to minimize exergy losses. For instance, in a bottoming cycle for utility applications, (Kalina System 6) [22], the vapor is actually cooled between the IP and LP turbines and used to evaporate part of the working fluid stream.

The Kalina Cycle System 12 [27] is a variation of the Kalina cycle that was proposed for geothermal applications. This version does not have the trademark distillation arrangement. Instead, a more complicated network of recovery heat exchangers is used to improve efficiency. Figure 1. 4 shows the Kalina 12 system.

Bliem [28] studied the application of the Kalina cycle to hydrothermal (liquid dominated geothermal) energy conversion. The supercritical, recuperated Rankine cycle technology studied as part of the heat cycle research program proved to have a slightly higher second law efficiency compared to the Kalina System 12. The Heber binary geothermal plant summer design conditions were used as a reference. Both these technologies were superior to the supercritical isobutane based Rankine cycle being used at Heber.

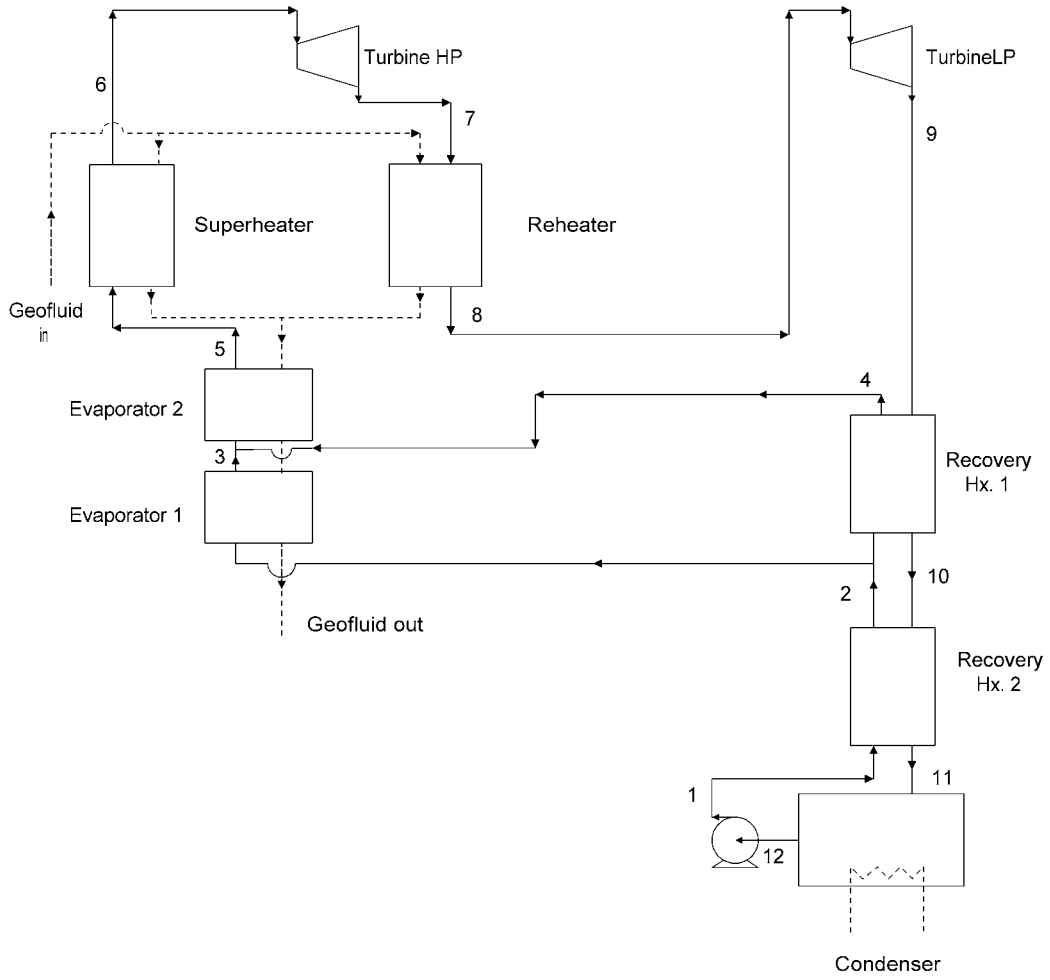

Fig. 1.4 Schematic diagram of Kalina System 12

The Kalina type distillation-condensation subsystem was also evaluated in supercritical organic cycles, but the improvement was found to be minimal. Bliem and Mines [29] also showed that the Kalina System 12 and the supercritical cycle approach a realistic upper limit of conversion, for the relatively high temperature resources (460 K and 500 K) studied.

Ibrahim and Klein [30] compared the thermodynamic performance of the Maloney and Robertson cycle and the Kalina cycle based on a second law analysis. The second law efficiency was defined as the ratio of the first law efficiency of the cycle to that of a "maximum power" cycle operating between the same thermodynamic conditions. The

maximum power cycle used is essentially the Lorenz cycle. These concepts are explained in greater detail in chapter 2. Based on the results from that study, the Kalina cycle outperforms the Maloney and Robertson cycle at large heat exchanger sizes (large NTU).

The Kalina cycle has been criticized for the fact that obtaining the output predicted by calculations for the cycle requires 100% vaporization of the working fluid in a single pass countercurrent boiler. The heat exchanger surfaces would dry out at high vapor fractions, resulting in lower overall heat transfer coefficients and a larger heat exchange area. The first Kalina geothermal plant (of 2 MWe capacity) [31] built in Husavik, Iceland, does not use the system 12 configuration. Instead, about 70 % of the flow is vaporized and the remaining liquid throttled back through a series of recovery heat exchangers. Over the last twenty years, the Kalina cycle has caught a lot of attention from the engineering community, but that has translated to very few plants actually being built. The first bottoming cycle demonstration of the plant was at the Energy Technology and Engineering Center, a DOE facility near Canoga Park, California [32]. A 3 MW demonstration plant was constructed that started operation in 1992. Tests were conducted till the end of 1996.

Other ammonia based cycles

Rogdakis and Antonopoulos [33] proposed an ammonia-water absorption power cycle. This cycle is somewhat similar to the Kalina cycle, with the major difference being that the distillation-absorption condensation process is replaced with a simple absorption condensation process. The authors calculated a substantially higher (greater than 20%) first law efficiency as compared to a steam Rankine cycle, while keeping similar superheating and condensation temperatures. The improvement is particularly

good at low heat source temperatures. An application of this cycle for recovering waste heat from gas turbine exhaust is discussed by Kouremenos et al. [34].

Use of Mixtures as Working Fluids in Thermodynamic Cycles

In a conventional Rankine cycle in which a pure fluid is used, boiling occurs at the saturation temperature corresponding to its pressure. This results in a mismatch between the temperature profile of the heat source fluid (fuel combustion products, geothermal fluids etc.) and the working fluid in the boiler. Consequently, there is significant exergy destruction during heat transfer in the boiler. One of the methods around this limitation, practiced in industry, is to boil at different pressures, resulting in a moderate increase in efficiency. The other option is to use a mixture in the working fluid. The use of mixtures as working fluids in Rankine cycles is not a new idea. As a mixture vaporizes, the changing composition of the liquid results in boiling occurring over a range of temperatures. This gives what is called a "temperature glide" between the temperatures at which the mixture starts boiling to those at which the fluid is completely vaporized.

Figure 1.5 qualitatively shows an example of the difference in boiling behavior just described. With a multi-component mixture, the fluid boils throughout in the boiler, achieving a good temperature match with the heat source fluid. While the pure fluid boils at one temperature and is then subsequently superheated, the mixture boils at varying temperatures and achieves a better thermal match in the boiler [35].

The condensation of mixtures is also a variable temperature process. This results in a better thermal match with the heat rejection fluid. The advantages of better thermal matching in the condenser are debatable. In a power plant, there is normally very little cost associated with the heat rejection fluid itself. The size of the condenser is the

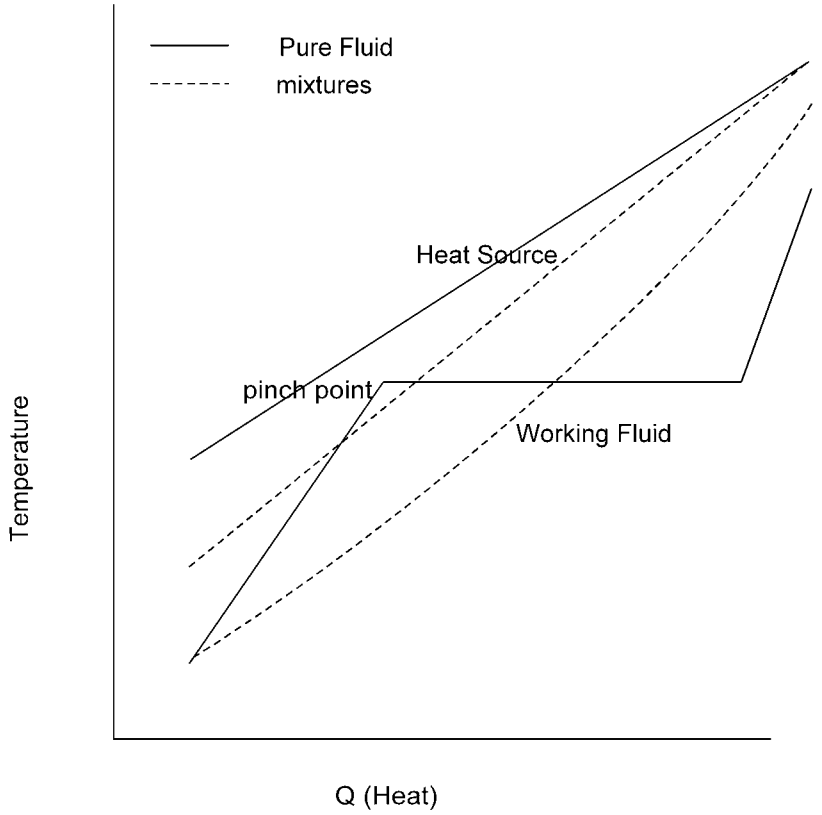

Fig. 1.5 Illustration of the difference in temperature profiles for a pure fluid being boiled and a multi-component mixture being boiled.

limitation. Also, for complete condensation of a fluid, the bubble point at the cycle low pressure has to be a little above the heat rejection fluid temperature. The use of mixtures has another advantage, particularly in geothermal power plants. Any degradation in the quality of the heat resource with time can be countered to a certain extent by changing the composition of the working fluid.

Several cycles have been developed in the literature to take advantage of mixtures. Binary mixtures have been recommended as working fluids in binary geothermal power plants. It is found that a geothermal resource is utilized more efficiently by the use of these mixtures.

The Combined Power and Cooling Cycle

Introduction

A unique feature of the combined power and cooling cycle proposed by Prof. Goswami is the simultaneous production of power and refrigeration (cooling) in the same loop. Other combined power and cooling cycles utilize the waste heat rejected from the power cycle to run a coupled heat fired cooling cycle, such as an absorption refrigeration cycle.

The cycle can be viewed as a combination of the Rankine cycle and an absorption refrigeration cycle. A binary mixture of ammonia and water has been used as the working fluid in all studies performed so far. Using that as an example, consider the schematic (basic configuration) of the cycle shown in Fig. 1.6. A mixture of ammonia and water (borrowing from absorption refrigeration literature, this mixture is called the strong solution, or basic solution) is pumped to a high pressure. This stream is preheated and pumped to the boiler, where it is partially boiled. Being the component with a lower boiling point, the vapor generated is rich in ammonia. A "rectifier" is used to increase the concentration of ammonia in the vapor by condensing some of the water out. The rectified vapor is superheated and expanded to low temperatures in an expander such as a turbine. This is possible since ammonia is a volatile component that does not condense at the temperatures and pressures at the turbine exit. The cold ammonia is used to produce refrigeration.

The remaining hot liquid in the boiler, called the weak solution, is used to preheat the working fluid in the recovery or solution heat exchanger. This high pressure liquid is then throttled back to the absorber. The vapor is absorbed into the weak solution and

condensed in the absorber. The absorber takes the place of a regular condenser in the cycle.

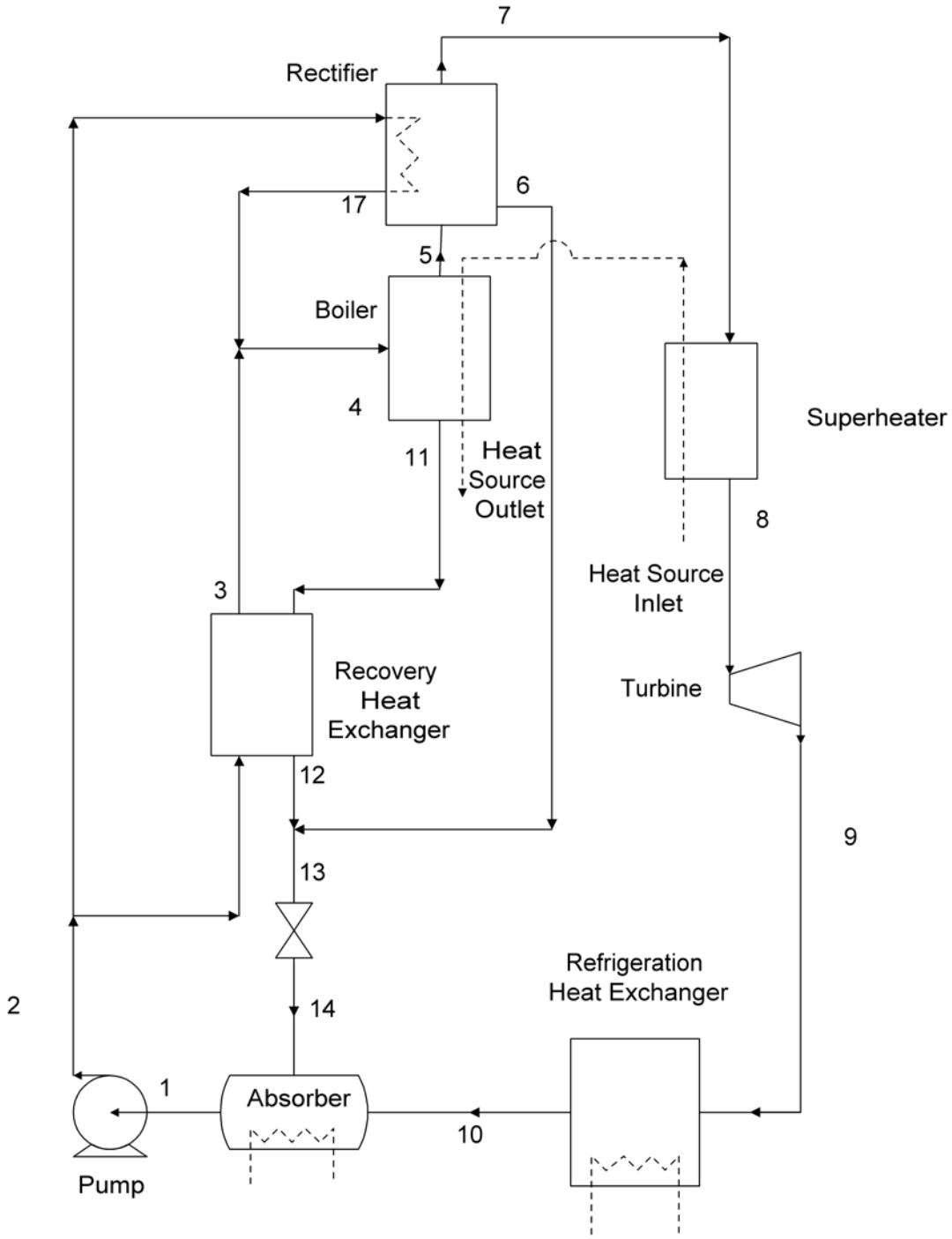

Fig. 1.6 The basic configuration of the combined power and cooling cycle

A portion of the strong solution stream is used to recover heat from the condensing vapor in the rectifier. The word rectification is used in the absorption cooling literature, by some authors, to refer to a particular configuration that employs a rectification column to purify the ammonia vapor. We use the word rectification to refer to a process used to purify vapor leaving the boiler in all the papers and reports associated with the study of this cycle.

Some of the key features of the cycle are listed below.

- Output consists of both power and cooling
- Uses a mixture as the working fluid, which makes it suitable for sensible heat sources
- Absorption condensation is used to condense the vapor
- Works best using low temperature heat sources

A summary of past research on the cycle

The combined power and cooling cycle has been the subject of a sustained research effort at the University of Florida for the past eight years. A summary of the work done to date and the status of the development of the cycle is discussed below. The results of a parametric analysis of the cycle using low temperature sensible heat sources are reported in Goswami and Xu [2] and Xu et al.[36]. The analysis established that theoretically, both power and cooling could be obtained from the proposed configuration. Ideal turbine and pump were assumed, heat losses and pressure drops were neglected. The following range of parameters were studied

1.	Boiler Temperature	:	400 K
2.	Condenser Temperature	:	350 K – 400 K
3.	Turbine Inlet Temperature	:	410 K – 500 K
4.	Turbine Inlet Pressure	:	18 bar – 32 bar
5.	Ammonia Concentration	:	0.20 – 0.55
6.	Absorber Temperature	:	280 K
7.	Recovery HX. Exit Temp.	:	350 K

The parametric study results indicate the general behavior of the cycle. Figure 1.7 shows the effect of turbine inlet pressure on the thermal efficiency[2] of the cycle. For a set absorber pressure (as in a parametric analysis), the pressure ratio increases with a higher pressure, but the vapor generation rate drops until the pressure becomes too large to generate any vapor at all. A similar effect is seen with the cooling capacity. A larger pressure ratio results in a larger temperature drop in the turbine, but the drop in vapor generation rate limits cooling at higher pressures (see Fig. 1.8).

The boiler temperature strongly influences the output, as the vapor generated goes up. The heat input also goes up with increased vapor generation; therefore the thermal efficiency reaches a limit after initially increasing. The cooling capacity of the cycle is strongly influenced by the superheater and condenser temperatures. A higher superheater temperature raises the turbine exit temperature, until no refrigeration is produced at all.

The parametric study also clearly shows that there is an optimum value of parameters for the best operation of the cycle. Based on these results, Lu and Goswami [3] performed a mathematical optimization of the efficiency of the cycle using an optimization program that uses the Generalized Reduced Gradient (GRG) algorithm.

The optimization program has since then been used extensively to maximize the thermodynamic output of the cycle in several studies [5,6]. Lu and Goswami [4] also used the program to determine the lowest temperatures that could be achieved using the cycle. They concluded that temperatures as low as 205 K are achievable, however, the vapor generation drops substantially at very low temperatures since lower absorber pressures and purer ammonia vapor generation is required. Hasan and Goswami [5]

[2] See Table 1.1 for the definition of efficiency

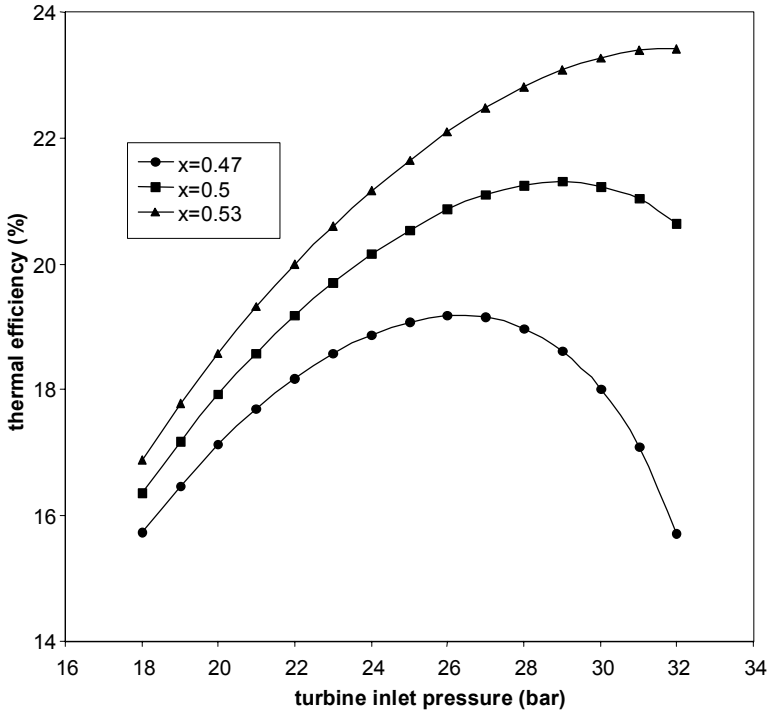

Fig. 1.7 Effect of turbine inlet pressure on the thermal efficiency (%) of the cycle [2]

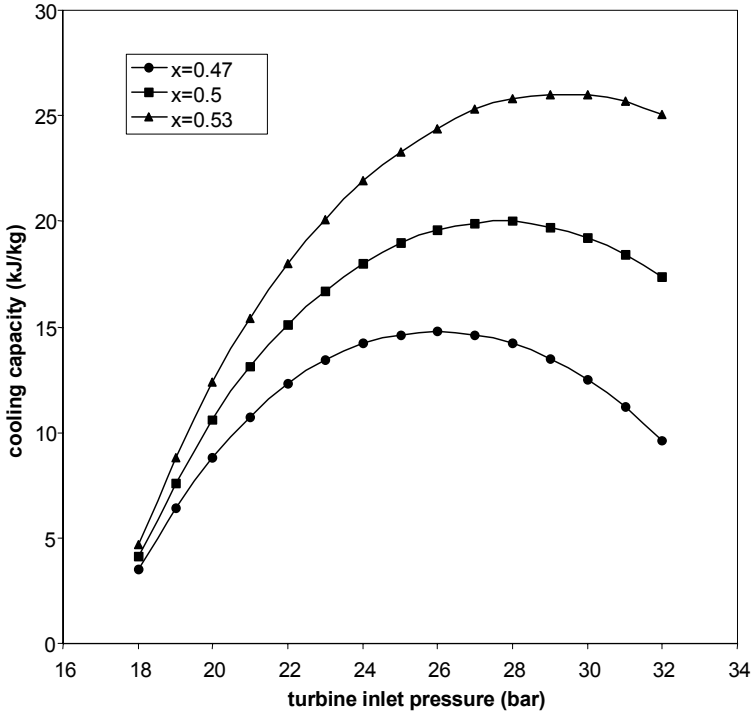

Fig. 1.8 Effect of turbine inlet pressure on the cooling capacity (kJ/kg) of the cycle [2]

performed an exergy analysis of results optimized for second law efficiency and looked at various aspects of the optimized results such as the refrigeration to work output ratio, pressure ratio etc.

An experimental system was built to verify the actual performance of the combined power and cooling cycle. The initial system was a simplified version of the cycle without an actual turbine present. A throttling valve and a heat exchanger performed the functions of expanding and cooling the vapor, thus simulating the turbine in the loop. The experimental system also lacked a rectification arrangement that would have been useful to purify the vapor. Operating this limited version of the cycle [8] verified the boiling and absorption processes. The results indicated that both power and cooling can be obtained simultaneously and that efficiencies close to the predicted values should be achievable.

Specific motivation for work in this dissertation

Efficiency definition. While a significant amount of work has been done on the theoretical analysis of the cycle, there are some shortcomings that need to be addressed. The first question deals with the right efficiency definitions for the cycle. Since the output consists of both power and cooling, the questions that arises is how the two components would be added so as to arrive at a meaningful efficiency definition. Table 1.1 summarizes the efficiency definitions used in different papers written on the cycle. Initial papers simply added the work and cooling output to generate an efficiency, which really is an "energy" efficiency. Later papers divided the cooling output by a Carnot *COP* (evaluated at the average of the inlet and exit temperatures of the refrigeration heat

exchanger). Such a definition gives a very small weight to the cooling output. The subject of efficiency definitions is discussed further in chapter 2.

Table 1.1 Efficiency Definitions used in Various Papers Published on the Cycle

Reference	First Law Definition	Second Law Definition
Goswami and Xu [2]	$(W_{net} + Q_c)/Q_h$	N.A.
Xu et al. [36]		
Lu and Goswami [3]	$(W_{net} + Q_c)/Q_h$	$(W_{net} + Q_c)/E_{hs,in}$
Hasan and Goswami [5]	$(W_{net} + Q_c)/Q_h$	$[W_{net} + (Q_c/COP_{carnot})]/E_{hs,in}$
Tamm et al. [7]		

Cycle simulation. The cycle simulation program written by Lu and Hasan had some shortcomings that were discovered when early simulations were being performed to compare results. These are listed below:

- A pinch point check was not implemented in the recovery heat exchanger. Sometimes the strong solution starts boiling there resulting in the pinch point condition being violated
- The fraction of the strong solution stream entering the rectifier was calculated by setting the temperature after the rectifier and using an energy balance. This temperature need not be set; it can actually be optimized.
- The liquid condensate in the rectifier was assumed to return to the boiler and boil as a separate stream. Yet this was not considered when calculating pinch point in the boiler. The result was that the pinch point was improperly calculated. In addition, the design of such a heat exchanger with three streams is also complicated.

Working fluid. All the work performed so far has been based on using an ammonia-water mixture as the working fluid. It is logical to assume that other mixtures could also be used in this new thermodynamic cycle to provide simultaneous power and cooling output. Organic fluids have been used in Rankine cycles designed for low

temperature heat sources. Therefore, these fluids seem like natural choice for use in this cycle.

Based on these motivations, the work presented in the subsequent chapters follows an outline as follows. First, there is a discussion of the various efficiency definitions that can be used for this cycle. That is followed by a description of the simulation and optimization methods. The basic cycle configuration is optimized using the proposed efficiency definitions, the results of which are discussed in chapter 4. Chapter 5 contains results of simulations performed using organic fluid mixtures and an analysis of the results. Some modified and improved configurations of the cycle are proposed and discussed in chapter 6. The final chapter suggests some directions for the development of the cycle in the light of this study.

CHAPTER 2
EFFICIENCY DEFINITIONS FOR THE COMBINED CYCLE

The combined power and cooling cycle is a combination of the Rankine cycle and an absorption refrigeration cycle. Evaluating the efficiency of this cycle is made difficult by the fact that there are two different simultaneous outputs, namely power and refrigeration. An efficiency expression has to appropriately weigh the cooling component in order to allow comparison of this cycle with other cycles. This chapter develops several expressions for the first law, second law and exergy efficiencies for the combined cycle based on existing definitions in the literature. Some of the developed equations have been recommended for use over others, depending on the comparison being made. Finally, some of these definitions are applied to the cycle and the performance of the cycle optimized for maximum efficiency. A Generalized Reduced Gradient (GRG) method was used to perform the optimization. This method is described in detail in the following chapter.

Conventional Efficiency Definitions

Performance of a thermodynamic cycle is conventionally evaluated using an efficiency or a coefficient of performance (*COP*). These measures of performance are generally of the form

$$\textit{measure of performance} = \textit{useful output / input} \tag{2.1}$$

First Law Efficiency

The first law measure of efficiency is simply a ratio of useful output energy to input energy. This quantity is normally referred to simply as efficiency, in the case of power cycles, and as a coefficient of performance for refrigeration cycles. Table 2.1 gives two typical first law efficiency definitions. For the case of an absorption refrigeration cycle, the input is in the form of heat and pump work. Therefore, its COP is expressed in terms of refrigeration output, heat input, and pump work as [37]

$$COP = Q_c / \left(Q_h + W_p\right) \tag{2.2}$$

Exergy Efficiency

The first law fails to account for the quality of heat. Therefore, a first law efficiency does not reflect all the losses due to irreversibilities in a cycle. Exergy efficiency measures the fraction of the exergy going into the cycle that comes out as useful output [38]. The remaining exergy is lost due to irreversibilitites in devices.

$$\eta_{exergy} = \Sigma E_{out} / \Sigma E_{in} \tag{2.3}$$

Two examples are given in table 2.1. For the absorption refrigeration cycle, the corresponding exergy efficiency expression is given as

$$\eta_{exergy} = E_c / \left(E_{in} + W_{in}\right) \tag{2.4}$$

Here E_c is the change in exergy of the cooled medium.

A resource utilization efficiency [39] is a special case of the exergy efficiency that is more suitable for use in some cases. Consider for instance a binary geothermal power cycle, where the geofluid is reinjected into the ground after transferring heat to the cycle working fluid. In this case, the unextracted availability of the geofluid that is lost on

Table 2.1 Some examples of efficiencies applied to the Rankine cycle and the vapor compression refrigeration cycle

Cycle Type	Rankine	Vapor Compression
First Law	$\eta_I = W_{net}/Q_h$ (2.5)	$COP = Q_c/W_{in}$ (2.8)
Exergy	$\eta_{exergy} = W_{net}/E_{in}$ (2.6)	$\eta_{exergy} = E_c/W_{in}$ (2.9)
Second Law	$\eta_{II} = \eta/\eta_{rev}$ (2.7)	$\eta_{II} = COP/COP_{rev}$ (2.10)

reinjection has to be accounted for. Therefore, a modified definition of the form

$$\eta_R = \Sigma E_{out}/E_{hs} \tag{2.11}$$

is used, where the E_{hs} is the exergy of the heat source.

Another measure of exergy efficiency found in the literature is what is called the exergy index defined as the ratio of useful exergy to exergy loss in the process [40],

$$i_{exergy} = \frac{\Sigma E_{useful}}{\Sigma E_{in} - \Sigma E_{useful}} \tag{2.12}$$

Second Law Efficiency

Second law efficiency is defined as the ratio of the efficiency of the cycle to the efficiency of a reversible cycle operating between the same thermodynamic conditions.

$$\eta_{II} = \eta/\eta_{rev} \tag{2.13}$$

The reversible cycle efficiency is the first law efficiency or COP depending on the cycle being considered. The second law efficiency of a refrigeration cycle (defined in terms of a COP ratio) is also called the thermal efficiency of refrigeration [37]. For constant temperature heat addition and rejection conditions, the reversible cycle is the Carnot cycle. On the other hand for sensible heat addition and rejection, the Lorenz cycle is the applicable reversible cycle [41].

The exergy efficiency and second law efficiency are often similar or even identical. For example, in a cycle operating between a hot and a cold reservoir (see Fig. 2.1), the exergy efficiency is

$$\eta_{exergy} = \frac{W_{net}}{Q_h\left(1 - T_0/T_h\right)} \tag{2.14}$$

while the second law efficiency is

$$\eta_{II} = \frac{W_{net}}{Q_h\left(1 - T_c/T_h\right)} \tag{2.15}$$

Where T_0 is the ambient or the ground state temperature. For the special case where the cold reservoir temperature T_r is the same as the ground state temperature T_0, the exergy efficiency is identical to the second law efficiency.

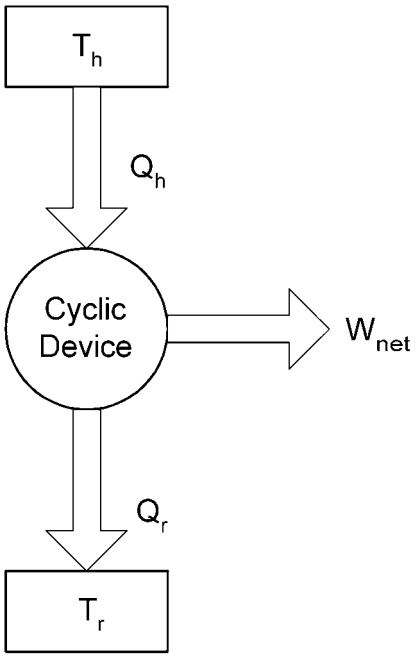

Fig. 2.1 A cyclic heat engine working between a hot and cold reservoir

The Choice of Efficiency Definition

The first law, exergy and second law efficiency definitions can be applied under different situations. The first law efficiency has been the most commonly used measure of efficiency. The first law does not account for the quality of heat input or output. Consider two power plants with identical first law efficiencies. Even if one of these power plants uses a higher temperature heat source (that has a much higher availability), the first law efficiency will not distinguish between the performance of the two plants. Using an exergy or second law efficiency though will show that one of these plants has higher losses than the other. The first law efficiency, though, is still a very useful measure of plant performance. For example, a power plant with a 40% first law efficiency rejects less heat than one of the same capacity with a 30% efficiency; and so would probably have a smaller condensor. An exergy efficiency or second law efficiency is an excellent choice when comparing energy conversion options for the same resource. Ultimately, the choice of conversion method is based on economic considerations.

Efficiency Expressions for the Combined Cycle

The performance evaluation functions discussed above will be applied to the combined power and cooling cycle. When evaluating the performance of a cycle, there are normally two goals. One is to pick parameters that result in the best cycle performance. The other goal is to compare this cycle with other energy conversion options. For instance, to compare the novel cycle with a power cycle that uses waste heat to run an absorption refrigeration system.

First Law Efficiency

Following the pattern of first law efficiency definitions given in the previous section, a simple definition for the first law efficiency would be

$$\eta_I = (W_{net} + Q_c)/Q_h \tag{2.16}$$

Equation (2.16) overestimates the efficiency of the cycle, by not attributing a quality to the refrigeration output. Using this definition, in some cases, the first law efficiency of the novel cycle approaches Carnot values or even exceeds them. Such a situation appears to violate the fact that the Carnot[3] efficiency specifies the upper limit of first law conversion efficiencies. The confusion arises due to the addition of work and refrigeration in the output. Refrigeration output cannot be considered in an efficiency expression without accounting for its quality. To avoid this confusion, it may be better to use the definition of the first law efficiency given as

$$\eta_I = (W_{net} + E_c)/Q_h \tag{2.17}$$

The term E_c represents the exergy associated with the refrigeration output. In other words, this refers to the exergy transfer in the refrigeration heat exchanger. Depending on the way the cycle is modeled, this could refer to the change in the exergy of the working fluid in the refrigeration heat exchanger. Alternately, to account for irreversibilities of heat transfer in the refrigeration heat exchanger, the exergy change of the chilled fluid would be considered.

$$E_c = \dot{m}\left[h_{cf,in} - h_{cf,out} - T_o\left(s_{cf,in} - s_{cf,out}\right)\right] \tag{2.18}$$

Rosen and Le [42] studied efficiency expressions for processes integrating combined heat and power and district cooling. They recommended the use of an exergy efficiency in which the cooling was weighted using a Carnot COP. However, the Carnot

[3] The Carnot cycle is not the reversible cycle corresponding to the combined cycle. This is discussed later in this chapter.

COP is based on the minimum reversible work needed to produce the cooling output. This results in refrigeration output being weighted very poorly in relation to work.

Exergy Efficiency

Following the definition of exergy efficiency described previously Eq.(2.3), the appropriate equation for exergy efficiency to be used for the combined cycle is given below. Since a sensible heat source provides the heat for this cycle, the denominator is the change in the exergy of the heat source, which is equivalent to the exergy input into the cycle.

$$\eta_{exergy} = \left(W_{net} + E_c\right) / \left(E_{hs,in} - E_{hs,out}\right) \tag{2.19}$$

Second Law Efficiency

The second law efficiency of the combined cycle needs a suitable reversible cycle to be defined. Once that is accomplished, the definition of a second law efficiency is a simple process.

Lorenz cycle

The Lorenz cycle is the appropriate "reversible cycle" for use with variable temperature heat input and rejection. A T-S diagram of the cycle is shown in Fig. 2.2.

$$\eta_{Lorenz} = 1 - \frac{Q_{34}}{Q_{12}} \tag{2.20}$$

If the heat input and rejection were written in terms of the heat source and heat rejection fluids, the efficiency would be given as:

$$\eta_{Lorenz} = 1 - \frac{m_{hr}\left(h_{hr,out} - h_{hr,in}\right)}{m_{hs}\left(h_{hs,in} - h_{hs,out}\right)} \tag{2.21}$$

Knowing that processes 4-1 and 2-3 are isentropic, it is easily shown that in terms of specific entropies of the heat source and heat rejection fluids that

$$\frac{m_{hs}}{m_{hr}} = \frac{\left(s_{hr,out} - s_{hr,in}\right)}{\left(s_{hs,in} - s_{hs,out}\right)} \tag{2.22}$$

The efficiency expression for the Lorenz cycle then reduces to

$$\eta_{Lorenz} = 1 - \frac{\left(h_{hr,out} - h_{hr,in}\right)/\left(s_{hr,out} - s_{hr,in}\right)}{\left(h_{hs,in} - h_{hs,out}\right)/\left(s_{hs,in} - s_{hs,out}\right)} \tag{2.23}$$

This can also be written as

$$\eta_{Lorenz} = 1 - \frac{\left(\overline{T}_s\right)_{hr}}{\left(\overline{T}_s\right)_{hs}} \tag{2.24}$$

Here, the temperatures in the expression above are entropic average temperatures, of the form

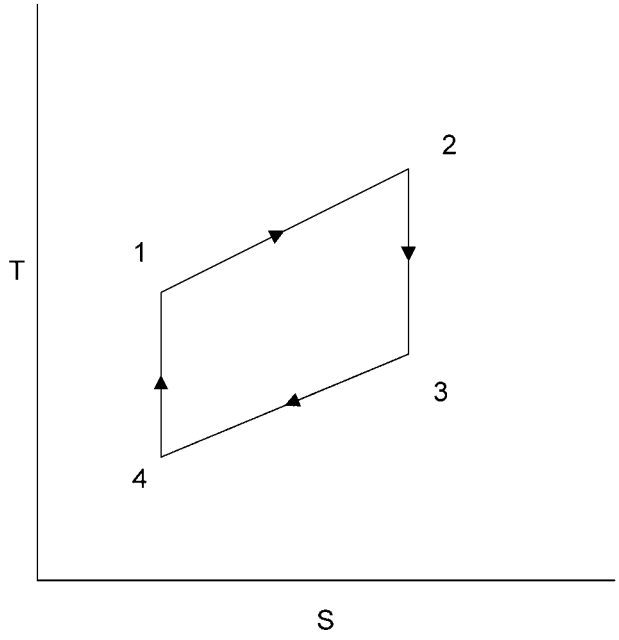

Fig. 2.2 The T-S diagram for a Lorenz cycle

$$\overline{T}_s = \frac{\left(h_2 - h_1\right)}{\left(s_2 - s_1\right)} \tag{2.25}$$

For constant specific heat fluids, the entropic average temperature can be reduced to

$$\overline{T}_s = \frac{(T_2 - T_1)}{\ln(T_2/T_1)} \tag{2.26}$$

The Lorenz efficiency can therefore be written in terms of temperatures as

$$\eta_{Lorenz} = 1 - \frac{(T_{hr,out} - T_{hr,in})/\ln(T_{hr,out}/T_{hr,in})}{(T_{hs,in} - T_{hs,out})/\ln(T_{hs,in}/T_{hs,out})} \tag{2.27}$$

It is easily seen that if the heat transfer processes were isothermal, like in the Carnot cycle, the entropic average temperatures would reduce to the temperature of the heat reservoir, yielding the Carnot efficiency. Similarly the *COP* of a Lorenz refrigerator can be shown to be

$$COP_{Lorenz} = \frac{(\overline{T}_s)_{cf}}{(\overline{T}_s)_{hr} - (\overline{T}_s)_{cf}} \tag{2.28}$$

Cascaded cycle analogy

An analogy to the combined cycle is a cascaded power and refrigeration cycle, where part of the work output is directed into a refrigeration machine to obtain cooling. If the heat engine and refrigeration machine were to be treated together as a black box, the input to the entire system is heat, while output consists of work and refrigeration. This looks exactly like the new combined power/refrigeration cycle. Figure 2.3 shows the analogy, with a dotted line around the components in the cascaded cycle representing a black box.

One way to look at an ideal combined cycle would be as two Lorenz cycle engines cascaded together (Fig 2.3b). Assume that the combined cycle and the cascaded arrangement both have the same thermal boundary conditions. This assumption implies

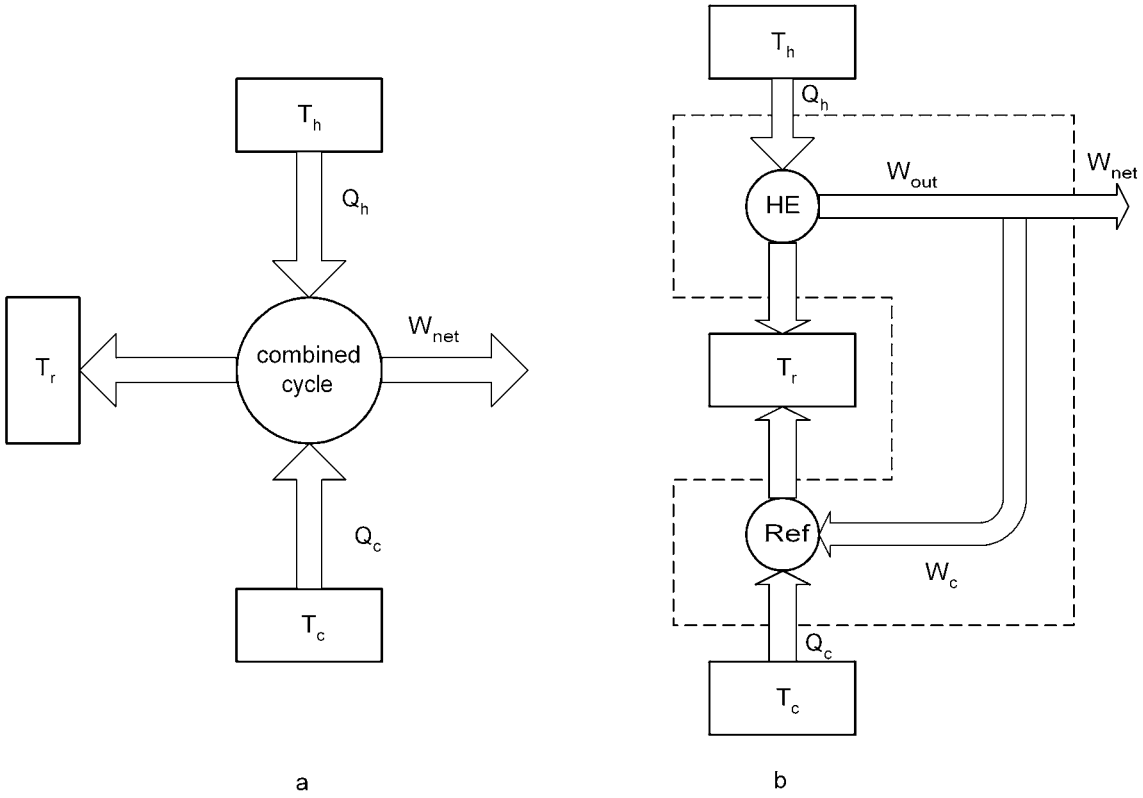

Fig. 2.3 Thermodynamic representation of (a) combined power/cooling cycle and (b) cascaded cycle

that the heat source fluid, chilled fluid and heat rejection fluid have identical inlet and exit temperatures in both cases. The first law efficiency of the cascaded system, using a weight factor f for refrigeration is

$$\eta_{I,sys} = \frac{W_{out} - W_c + fQ_c}{Q_h} \tag{2.29}$$

The weight factor, f is a function of the thermal boundary conditions. Therefore, the first law efficiency of the combined cycle can also be written as

$$\eta_I = \frac{W_{net} + fQ_c}{Q_h} \tag{2.30}$$

The work and heat quantities in the cascaded cycle can also be related using the efficiencies of the cascaded devices

$$W_{out} = Q_h \eta_{HE} \tag{2.31}$$

$$W_c = Q_c / COP \tag{2.32}$$

By specifying identical refrigeration to work ratios (r) in the combined cycle and the corresponding reversible cascaded cycle as

$$r = Q_c / W_{net} \tag{2.33}$$

and using Eq.(2.29) and Eqs.(2.31 - 2.33), one can arrive at the efficiency of the cascaded system as

$$\eta_{I,sys} = \eta_{HE}\left[1 + \frac{r\left(f - 1/COP\right)}{1 + r/COP}\right] \tag{2.34}$$

assuming the cascaded cycle to be reversible, the efficiency expression reduces to

$$\eta_{I,rev} = \eta_{Lorenz}\left[1 + \frac{r\left(f - 1/COP_{Lorenz}\right)}{1 + r/COP_{Lorenz}}\right] \tag{2.35}$$

Here η_{Lorenz} is the first law efficiency of the Lorenz heat engine and COP_{Lorenz} is the COP of the Lorenz refrigerator. A second law efficiency would then be written as

$$\eta_{II} = \eta_I / \eta_{I,rev} \tag{2.36}$$

If the new cycle and its equivalent reversible cascaded cycle have identical heat input (Q_h), the second law efficiency can also be written as

$$\eta_{II} = \frac{\eta_I}{\eta_{I,rev}} = \frac{W_{net} + fQ_c}{W_{net,rev} + fQ_{c,rev}} \tag{2.37}$$

This reduces further to

$$\eta_{II} = \frac{W_{net}}{W_{net,rev}} \frac{\left(1 + fr\right)}{\left(1 + fr\right)} = \frac{W_{net}}{W_{net,rev}} \tag{2.38}$$

Evidently, the refrigeration weight factor (*f*) does not affect the value of the second law efficiency. This is true as long as f is a factor defined such that it is identical for both the combined cycle and the analogous cascaded version. This follows if *f* is a function of the thermal boundary conditions. Assuming a value of unity for *f* simplifies the second law efficiency expression even further. The corresponding reversible cycle efficiency would be,

$$\eta_{I,rev} = \eta_{Lorenz}\left[\frac{1+r}{1+r/COP_{Lorenz}}\right] \tag{2.39}$$

The resulting second law efficiency equation is a good choice for second law analysis. The expression does not have the drawback of trying to weight the refrigeration with respect to the work output. Being a second law efficiency, the expression also reflects the irreversibility present in the cycle, just like the exergy efficiency.

Validity of Expressions

Expressions for the first law, exergy and second law efficiencies have been recommended for the combined power and cooling cycle in Eqs. (2.17), (2.19) and (2.37) respectively. These definitions give thermodynamically consistent evaluations of cycle performance, but they are not entirely suitable for comparing the cycle to other energy conversion options. Substituting for refrigeration with the equivalent exergy is equivalent to replacing it with the minimum work required to produce that cooling. This would be valid if in the equivalent cascaded arrangement, the refrigeration machine were reversible. Therefore, when comparing the combined cycle with other options, such a substitution is debatable. This is where the difficulty arises in arriving at a reasonable definition of efficiency. Two cases are discussed here to illustrate the point.

Case 1: Comparing this Cycle to Other Combined Cooling and Power Generation Options

Consider the situation where the novel cycle is being designed to meet a certain power and refrigeration load. The goal then, would be to compare the thermodynamic performance of the novel cycle with other options designed to meet the same load. If the performance of both cycles were evaluated using Eqs.(2.17), (2.19) and (2.35), such a comparison would be perfectly valid.

Case 2: Comparing a Combined Cycle to a Power Cycle

In some instances, a combined cycle would have to be compared to a power cycle. For example, this cycle could be configured so as to operate as a power cycle. In this situation, the refrigeration would have to be weighted differently, so as to get a valid comparison. One way of doing this would be to use a practically achievable value of refrigeration COP to weight the cooling output. Another option is to divide the exergy of cooling by a reasonable second law efficiency of refrigeration (also called thermal efficiency of refrigeration). Such efficiencies are named "effective" efficiencies in this study.

$$\eta_{I,eff} = \frac{\left(W_{net} + Q_c / COP_{practical}\right)}{Q_h} \tag{2.40}$$

$$\eta_{I,eff} = \frac{\left(W_{net} + E_c / \eta_{II,ref}\right)}{Q_h} \tag{2.41}$$

$$\eta_{exergy,eff} = \left(W_{net} + Q_c / COP_{practical}\right) / \left(E_{hs,in} - E_{hs,out}\right) \tag{2.42}$$

$$\eta_{exergy,eff} = \left(W_{net} + E_c / \eta_{II,ref}\right) / \left(E_{hs,in} - E_{hs,out}\right) \tag{2.43}$$

Some Examples of Application to the Combined Cycle

An optimization program was used to optimize the performance of the Goswami cycle. A description of the methodology adopted is given in the following chapter. Optimization results using different efficiency definitions as objective functions are given in this section. The cycle simulations were performed using simple energy and mass balances. Approach temperature limits of 5 K were imposed on all heat exchangers. Boiler pinch points were assumed to be at least 5 K. It was assumed that there were no pressure losses in the devices and that the turbine and pump operated isentropically. The vapor at the turbine exit is constrained to be at least 90% dry. A turbine exit temperature of 270 K or lower was required to generate refrigeration. The optimization was also constrained so that refrigeration was always generated.

The heat source fluid was assumed to be hot water at 400 K at the saturation pressure of water at that temperature. The absorber temperature was 5 K above the ambient which was assumed to be 298 K. Saturation conditions were assumed in the absorber to fix the concentration of ammonia in the binary mixture. The schematic of the cycle in Fig.1.6 differs slightly from previously published versions in that the liquid reflux from the rectifier is sent back to the absorber.

The optimization results of the cycle evaluated using the exergy efficiency and second law efficiency Eqs.(2.19) and (2.36) are both identical. That is not surprising, since exergy efficiency and second law efficiency are very similar. The cycle parameters are presented in Table 2.2. It was assumed that the chilled fluid was liquid water for these simulations.

Table 2.2 Cycle parameters that yield optimum exergy and second law efficiencies.

Parameters	Optimized Case
η_{exergy} (%)	61.35
η_{II} (%)	61.35
$T_{boiler,exit}$ (K)	395
$T_{rectifier,exit}$ (K)	365.15
$T_{superheater,exit}$ (K)	365.15
$T_{turbine,exit}$	269.96
p_{high} (bars)	10.84
p_{low} (bars)	1.00
x_{basic} , Ammonia mass fraction in absorber	0.288
$\dot{m}_{hs}$, Mass flow rate of heat source (kg/s)	10.93
$\dot{m}_{basic}$, Mass flow rate of basic solution (kg/s)	3
W_{net} , Net work output (kW)	79.15
Q_c , Cooling output (kW)	25.99

Tables 2.3 and 2.4 give results optimized for effective efficiencies. Different second law efficiencies of refrigeration were assumed. The exergy of cooling was calculated on the working fluid side. It is seen that assuming different second law efficiencies of refrigeration has a significant effect on the equivalent exergy efficiency.

Table 2.3 Efficiency and cycle parameters optimized for effective exergy efficiency

Parameters	Case I	Case II	Case III	Case IV
$\eta_{II,ref}$ (%)	30	50	70	100
$\eta_{exergy,eff}$ (%)	72.52	65.20	62.74	62.10
$\eta_{I,eff}$ (%)	17.70	15.89	15.11	15.08
$T_{boiler,exit}$ (K)	395	395	395	395
$T_{rectifier,exit}$ (K)	342.85	343.88	368.75	370.67
$T_{superheater,exit}$ (K)	342.85	343.88	368.75	370.67
$T_{turbine,exit}$	253.68	252.10	270	270
p_{high} (bars)	16.7	15.3	17.4	18.0
p_{low} (bars)	1.8	1.64	2.0	1.96
x_{basic}, Ammonia mass fraction in absorber	0.374	0.360	0.390	0.388
$\dot{m}_{hs}$, Mass flow rate of heat source	10.82	10.79	10.92	10.95
$\dot{m}_{basic}$, Mass flow rate of basic solution	3	3	3	3
W_{net}, Net Work Output	69.2	72.2	97.4	87.63
Q_c, Cooling Output	59.1	58.1	34.2	30.55

Table 2.4 Efficiency and cycle parameters optimized for effective first law efficiency

Parameters	Case I	Case II	Case III	Case IV
$\eta_{II,ref}$ (%)	30	50	70	100
$\eta_{I,eff}$ (%)	17.73	15.92	15.21	15.08
$T_{boiler,exit}$ (K)	395	395	395	395
$T_{rectifier,exit}$ (K)	343.69	344.92	348.99	370.67
$T_{superheater,exit}$ (K)	343.69	344.92	348.99	370.67
$T_{turbine,exit}$	253.08	251.49	249.72	270
p_{high} (bars)	16.79	15.46	13.37	18.0
p_{low} (bars)	1.74	1.59	1.31	1.96
x_{basic}, Ammonia mass fraction in absorber	0.369	0.355	0.327	0.388
$\dot{m}_{basic}$, Mass flow rate of basic solution	3	3	3	3
W_{net}, Net work output	64.5	66.83	68.26	87.63
Q_c, Cooling output	55.1	53.80	48.18	30.55

To get a feel for second law efficiencies, a typical 10 EER vapor compression air conditioning system operates at a COP of around 3 at the standard rated conditions. The corresponding Carnot COP, assuming 280 K cold temperature and an ambient temperature of 308 K (selected based on standard rating conditions) is around 10. This implies a second law efficiency of 30%. Refrigeration cycles are inherently irreversible since they include a throttling process. The last case in tables 2.3 and 2.4 is the case where a second law efficiency of refrigeration is not considered. It is interesting to note that the optimization results in table 2.3, case IV are different from those in table 2.2. The reason for the difference is that irreversibilites in the refrigeration heat exchanger are considered in the optimization in table 2.2. The exergy of cooling E_c, is calculated on the working fluid side in both tables 2.3 and 2.4.

Conclusions

In defining efficiencies of a combined power and cooling cycle, it is necessary to weight the refrigeration output to obtain meaningful values. Definitions of first law, exergy and second law efficiencies have been developed in this chapter. From the basis of a strict thermodynamic analysis, the definitions given in Eqs. (2.17) and (2.19) are the correct efficiency definitions of the cycle. However, these definitions do not realistically weight the cooling content. When comparing the combined power and cooling cycle to one producing work alone, effective efficiencies defined in Eqs. (2.41) and (2.43) are recommended. It has also been shown in this paper that the weight assigned to refrigeration output has an impact on the optimum parameters for the cycle.

CHAPTER 3
CYCLE SIMULATION AND OPTIMIZATION

The combined cycle has been studied by a simple simulation model coupled to an optimization algorithm. The simulation model is simplistic, and is based on simple mass and energy balances. Ammonia water properties are calculated using a Gibbs free energy based method [43] while organic fluid properties were estimated using a NIST program that is based on a corresponding states method (see Appendix A). The optimization is performed by a search method. Search methods require an initial point to be specified. From there the algorithm searches for a "better" point in the feasible domain of parameters. This process goes on until certain criteria that indicate that the current point is optimum are satisfied.

Optimization Method Background

The optimization of the working of the cycle is a non linear programming (NLP) problem. A NLP is one in which either the objective function or one of the constraints are non-linear functions. The cycle optimization method chosen for the analysis of this cycle is a search method. Search methods are used to refer to a general class of optimization methods that search within a domain to arrive at the optimum solution. It is necessary to specify an initial starting point in search schemes. The optimization algorithm picks a new point in the neighborhood of the initial point such that the objective function (the function being optimized) value improves without violating any constraints. A simple method of determining the direction of change is to calculate the

gradient of the objective function at the current point [44]. Such methods are also classified as steepest ascent (or descent) methods, since the algorithm looks for the direction of maximum change. By repeating these steps until a termination condition is satisfied, the algorithm is able to arrive at an optimized value of the objective.

When implementing steepest ascent type methods for constrained optimization problems, the constraints pose some limits on the search algorithm. If a constraint function is at its bound, the direction of search might have to be modified such that the bounds are not violated. The Generalized Reduced Gradient (GRG) method was used to optimize the cycle. GRG is one of the most popular NLP methods in use today. A description of the GRG method can be found in several sources [44-46].

There are several variations of the GRG algorithm. A commercially available program called the GRG2 was used for ammonia water optimization, and a more recent version called the LSGRG2 was used for alternate fluid work. LSGRG2 is able to handle more variables and constraints than the GRG2 code, and is based on a sparse matrix representation of the problem Jacobian (matrix of first partial derivatives). The method used in the software has been discussed by Himmelblau et al. [46] and Lasdon et al. [47]. A brief description of the concept of the algorithm, heavily adapted [46, 47] is presented below:

Consider the optimization problem defined as:

Minimize objective function: $g_{m+1}(X)$

Subject to equality and inequality type constraints as given below

$$g_i(X) = 0, \qquad i = 1,...,neq \tag{3.1}$$

$$0 \le g_i(X) \le ub(n+i), \qquad i = neq+1,...,m \tag{3.2}$$

The variables are constrained by an upper and lower bound.

$$lb(i) \le X_i \le ub(i), \quad i = 1,...,n \tag{3.3}$$

Here X is the variable vector consisting of *n* variables.

As in many optimization algorithms, the inequality constraints are set to equality form by adding slack variables, $X_{n+1},...,X_{n+m}$

The optimization program then becomes

Minimize: $g_{m+1}(X)$

Subject to:

$$g_i(X) - X_{n+i} = 0, \qquad i = 1,...,m \tag{3.4}$$

$$lb(i) \le X_i \le ub(i), \qquad i = 1,...,n+m \tag{3.5}$$

$$lb(i) = ub(i) = 0, \qquad i = n+1,...,n+neq \tag{3.6}$$

$$lb(i) = 0, \qquad i = n+neq+1,...,n+m \tag{3.7}$$

The last two equations specify the bounds for the slack variables. Eq. (3.6) specifies that the slack variables are zero for the equality constraints, while the variables are positive for the inequality constraints. The variables $X_1,...,X_n$ are called the natural variables.

Consider any feasible point (satisfies all constraints), which could be a starting point, or any other point after each successful search iteration. Assume that *nb* of the constraints are binding, or in other words, hold as equality constraints at a bound. In the GRG algorithm used in the GRG2 and LSGRG2 software, using the *nb* binding constraint equations, *nb* of the natural variables (called basic variables) are solved for in terms of

the remaining *n-nb* natural variables and the *nb* slack variables associated with the binding constraints. These *n* variables are called the nonbasic variables.

The binding constraints can be written as

$$g(y,x)=0 \tag{3.8}$$

Here *y* and *x* are vectors of the *nb* basic and *n* nonbasic variables respectively and *g* is a vector of the binding constraint functions. The binding constraints Eq. (3.8) can be solved for *y* in terms of *x*, reducing the objective to a function of *x* only.

$$g_{m+1}(y(x),x)=F(x)$$

This equation is reasonably valid in the neighborhood of the current point to a simpler reduced problem.

Minimize $F(x)$

Subject to the variable limits for the components of the vector *x*.

$$l \le x \le u \tag{3.9}$$

The gradient of the reduced objective $F(x)$, $\nabla F(x)$ is called the reduced gradient. Now the search direction can be determined from the reduced gradient. A basic descent algorithm can now be used to determine an improved point from here. The choice of basic variables is determined by the fact that the *nb* by *nb* basis matrix consisting of $(\partial g_i/\partial y_j)$should be nonsingular terms should be nonsingular at the current point.

A more detailed description of the theory and the implementation of the GRG algorithm and the optimization program can be found elsewhere [46-48]. This algorithm is a robust method that appears to work well for the purposes of optimizing this cycle, the way it has been implemented in our study.

Search Termination

The search will terminate if an improved feasible point cannot be found in a particular iteration. A well known test for optimality is by checking if the Kuhn-Tucker conditions are satisfied. The Kuhn-Tucker conditions are explained in detail in [45,46]. It can be mathematically explained in terms of the gradients of the objective functions and inequality constraints as:

$$\nabla g_{m+1}(X) + \sum_{j=1}^{j=m} u_j \nabla g_j(X) = 0 \tag{3.10}$$

$$u_j \geq 0, \;\; u_j \left[g_j(X) - ub(j) \right] = 0 \tag{3.11}$$

$$g_j(X) \leq ub(j), \;\; j = 1,...,m \tag{3.12}$$

Here, u_j is a Lagrange Multiplier for the inequality constraints.

Unfortunately, the Kuhn-Tucker conditions are valid only for strictly convex problems, a definition that most optimization problems do not satisfy. A disadvantage of using a search method, such as the GRG algorithm that has been used in this study, is that the program can terminate at a local optimum. There is no way to conclusively determine if the point of termination is a local or global optimum [46]. The procedure is to run the optimization program starting from several initial points.

Sensitivity Analysis

The sensitivity of the results to the active constraints can be determined using the corresponding Lagrange multipliers.

$$u_j = \frac{-\partial V}{\partial ub(j)} \tag{3.13}$$

Where, V is the value of the objective at the optimum.

Application Notes

There are some factors in the optimization of the cycle studied using GRG2 and LSGRG2 that are interesting to mention. In a search scheme, it is possible that the termination point could be a local optimum, or not an optimum at all. It is necessary to determine the nature of the "optimum" returned by the program. Prior to the optimization, during setup, close attention should be paid to:

- Scaling of the variables
- Limits set for different convergence criteria
- Method used to numerically calculate the gradient

The relative scaling of the variables affects the accuracy of the differentiation and the actual value of the components in the gradient, which determines the search direction. Experimenting with the numerical calculation of the gradient is useful during scaling. Too small a convergence criterion, particularly for the Newton-Raphson method used during the one-dimensional search can cause premature termination of the optimization program. The accuracy of the numerical gradient affects the search process. This was clearly seen when setting up the program with the SUPERTRAPP program. A forward differencing scheme was not accurate enough for the search to proceed forward.

Once the program was setup, the following methods were used in the process in order to obtain a global optimum:

- For each case, several runs were performed, from multiple starting points.
- Optimized results using different objective functions were useful as starting points for other cases.
- Examining the constraints indicated if the point was truly an optimum. For instance, at maximum second law efficiencies, the pinch point in the boiler was expected to be at its lower bound.
- The results were perturbed and optimized, particularly with respect to what would be expected to very sensitive variables, to see if a better point could be obtained.

For example, in RUE optimization, the heat source flow rate is a very sensitive variable. Perturbing the optimum results w.r.t the heat source flow rate was very useful to get better points.

- Another method is to change the scaling of variables that appear to be insensitive to check if better points can be obtained.
- For each configuration, comparing the results for different heat source and turbine exit temperatures was used to identify non-optimum and local optimum points.

At the end of this exhaustive process, it is assumed with reasonable confidence that the resulting point is indeed a global optimum. The optimization process using GRG is to a certain extent "art" not "science". Unfortunately, this is a problem with almost all NLP methods currently in use.

Cycle Modeling

Several cycle configurations have been studied in this dissertation. The model used for the basic cycle configuration shown in Fig. 3.1 is first discussed. The modeling of additional features in modified configurations is discussed, if necessary, when the alternate configuration is introduced. Consider the basic cycle configuration shown in Fig. 3.1

Eight independent variables are sufficient to determine the operation of the cycle. Two more variables are required to determine heat source conditions. Pressure drops and heat losses are neglected.

- Cycle high pressure
- Cycle low pressure
- Absorber temperature
- Temperature at boiler exit
- Temperature at rectifier / condenser exit
- Superheater exit temperature

- Effectiveness of the heat recovery heat exchanger, R_1
- Ratio of the mass flow rates of the strong solution in the heat recovery heat exchanger and the rectifier, R_2
- Heat source temperature
- Mass flow rate of heat source

The absorber temperature is set a little above the ambient temperature. The following general assumptions were used in the simulation

- Pressure losses in piping and equipment are neglected.
- An isentropic efficiency is assumed for the pump and turbine
- All processes are assumed to end in equilibrium thermodynamic states.

Using the variables and assumptions listed above, the properties at all state points in the cycle can be determined. For a binary mixture, two intensive properties and the composition of the mixture are sufficient to establish all the other properties. Some combinations include pressure, temperature and composition (*p,T,x*); pressure, specific enthalpy and composition (*p,h,x)*; or pressure, specific entropy and composition (*p,s,x*). Property calculation methods are discussed in Appendix B.

State Point Calculation

The calculation of state points for each state in Fig. 3.1 is described below.

State point 1

The mixture in the absorber is assumed to be at saturation conditions. The low pressure of the cycle and the temperature of the absorber allow the calculation of ammonia concentration of the basic solution. Absorber temperature is assumed to be 5 K above ambient temperature. A reference flow rate is assumed and all other flow rates in the

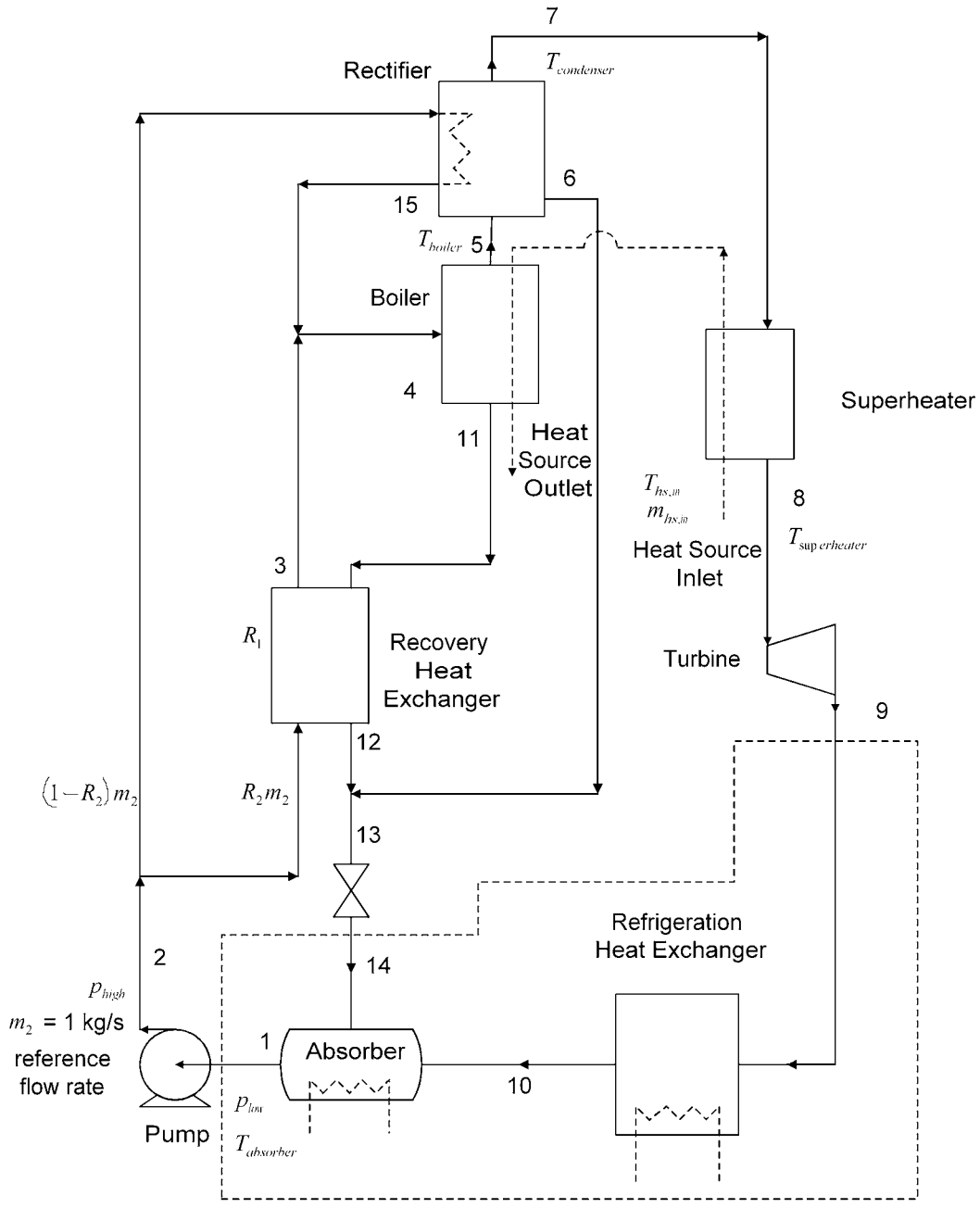

Fig. 3.1 The basic cycle configuration with the variables shown

system are scaled to this value. The choice of reference flow rate is to an extent decided by the optimization program. The value is determined after a few trials so that other parameters (particularly heat source mass flow rate) are reasonably large. This is important so that error in gradient calculation is limited. Relative magnitudes of the optimized variables are important to ensure reasonable values in gradient calculations. In equation form:

$$T_1 = T_{absorber} \tag{3.14a}$$

$$p_1 = p_{low} \tag{3.14b}$$

$$x_1 = satcon(p_1, T_1) \tag{3.14c}$$

$$\dot{m}_1 = 3 \tag{3.14d}$$

Satcon is a function in the ammonia-water properties program to calculate saturated liquid concentration given the pressure and temperature. Knowing three properties, the remaining properties of the binary mixture can be determined. This is implicit in the rest of this section.

Point 2

The pump pressurizes the strong solution to the high pressure in the cycle. Knowing the isentropic efficiency of the pump, the pressure and enthalpy at state 2 is easily computed. The composition of the solution remains the same as in state 1.

$$p_2 = p_{high} \tag{3.15a}$$

$$s_{isen} = s_1 \tag{3.15b}$$

$$x_2 = x_1 \tag{3.15c}$$

Calculate enthalpy at pump exit, h_{isen}, for isentropic compression. Then, knowing the pump efficiency, the actual enthalpy can be calculated using Eq. (3.15d) below.

$$\eta_p = \frac{h_2 - h_1}{h_{isen} - h_1} \tag{3.15d}$$

Points 5 and 11

Since the boiler exit temperature and pressure are known, vapor-liquid equilibrium correlations yield the vapor and liquid compositions leaving the boiler. A mass balance is used to determine the vapor and liquid mass fractions.

$$T_5 = T_{11} = T_{boiler} \tag{3.16a}$$

$$p_5 = p_{11} = p_{high} \tag{3.16b}$$

Use VLE data to get equilibrium compositions of vapor and liquid. The vapor and liquid mass fractions in the boiler can be computed from a mass balance as shown below.

$$vmf_{boiler} = \frac{x_4 - x_{11}}{x_5 - x_{11}} \tag{3.16c}$$

$$lmf_{boiler} = \frac{x_5 - x_4}{x_5 - x_{11}} \tag{3.16d}$$

Therefore, the mass flow rates would be

$$\dot{m}_5 = vmf_{boiler}\dot{m}_4 \tag{3.16e}$$

$$\dot{m}_{11} = lmf_{boiler}\dot{m}_4 \tag{3.16f}$$

Points 6 and 7

The rectifier exit temperature and pressure are known, as well as the boiler vapor mass fraction and composition. This allows the calculation of vapor and liquid compositions and mass fractions leaving the rectifier.

$$T_6 = T_7 = T_{rectifier} \tag{3.17a}$$

$$p_6 = p_7 = p_{high} \tag{3.17b}$$

VLE data is used to get equilibrium compositions of vapor and liquid. Once again, a mass balance gives the vapor and liquid mass fraction leaving the rectifier as

$$vmf_{rectifier} = \frac{x_5 - x_6}{x_7 - x_6} \tag{3.17c}$$

$$lmf_{rectifier} = \frac{x_6 - x_5}{x_7 - x_6} \tag{3.17d}$$

Therefore, the mass flow rates would be

$$\dot{m}_7 = vmf_{rectifier}\dot{m}_5 \tag{3.17e}$$

$$\dot{m}_6 = lmf_{rectifier}\dot{m}_5 \tag{3.17f}$$

Point 8

The superheater exit temperature is specified for each simulation, and the pressures and composition of the vapor are known.

$$T_8 = T_{superheater} \tag{3.18a}$$

$$p_8 = p_{high} \tag{3.18b}$$

$$x_8 = x_7 \tag{3.18c}$$

Point 9

The turbine isentropic efficiency is assumed, the turbine exit pressure is the system low pressure and the composition of the vapor is known. Therefore state points at the turbine exit can be calculated.

$$p_9 = p_{low} \tag{3.19a}$$

$$s_{isen} = s_8 \tag{3.19b}$$

$$x_9 = x_8 \tag{3.19c}$$

Calculate an enthalpy corresponding to isentropic expansion and use in equation below to calculate enthalpy at turbine exit.

$$\eta_t = \frac{h_8 - h_9}{h_8 - h_{isen}} \tag{3.19d}$$

Point 10

If the vapor is cold enough, it is assumed that the vapor leaves the refrigeration heat exchanger at 5 K below ambient. If the vapor leaving the turbine is not cold enough to yield refrigeration, state 10 is identical to state 9. The pressure and composition are already known.

If $T_9 \leq T_{\min}$

$$T_{10} = T_0 - 5 \tag{3.20a}$$

$$p_{10} = p_9 \tag{3.20b}$$

$$x_{10} = x_9 \tag{3.20c}$$

Else, point 10 is identical to state point 9.

Points 12 and 3

The maximum heat recovered from the weak solution is decided by the approach temperature limits. A fraction of this heat (variable R_1) is recovered.

$$x_{12} = x_{11} \tag{3.21a}$$

$$p_{12} = p_{11} \tag{3.21b}$$

A 5 K approach temperature difference is assumed in the recovery heat exchanger, i.e., $T'_{12} = T_2 + 5$. Other properties at the state point are calculated using this temperature to obtain maximum possible heat transfer. This assumption eliminates the use of a constraint at that point.

$$\dot{Q}_{HRHX,\max,hot} = \dot{m}_{11}\left(h_{11} - h'_{12}\right) \tag{3.21c}$$

On the other side of the heat exchanger,

$$p_3 = p_{high} \tag{3.21d}$$

$$x_3 = x_2 \tag{3.21e}$$

$$\dot{m}_3 = R_2 \dot{m}_2 \tag{3.21f}$$

Set the maximum temperature at the heat exchanger outlet

$$T'_3 = T_{11} - 5 \tag{3.21g}$$

Now a cold side maximum heat transfer can be calculated

$$\dot{Q}_{HRHX,\max,cold} = \dot{m}_3\left(h'_3 - h_3\right) \tag{3.21h}$$

The smaller of the values from Eq. (3.21c) and Eq. (3.21h) represents the maximum heat transfer possible. Now, using the ratio of the actual heat transfer to the maximum possible heat transfer, R_1, enthalpy h_{12} is calculated as

$$h_{12} = h_{11} - \frac{R_1 \dot{Q}_{HRHX,\max}}{\dot{m}_{11}} \tag{3.21i}$$

$$h_3 = h_2 + \left(R_1 \dot{Q}_{HRHX,\max} / \dot{m}_3\right) \tag{3.21j}$$

This allows the calculation of other state points. Note that R_1 is a pseudo heat exchanger effectiveness. The advantage of this assumption is that approach temperature constraints can be eliminated for the heat exchanger.

Point 13

The liquid reflux stream from the rectifier, and that from the boiler mix to form the fluid at state 13. The mixing is modeled as a constant total enthalpy process.

$$p_{13} = p_{high} \tag{3.9a}$$

$$h_{13} = \frac{\dot{m}_6 h_6 + \dot{m}_{12} h_{12}}{\dot{m}_{13}} \tag{3.9b}$$

$$x_{13} = \frac{\dot{m}_6 x_6 + \dot{m}_{12} x_{12}}{\dot{m}_{13}} \tag{3.9c}$$

Point 14

The weak solution at high pressure is throttled to a low pressure. The throttling is modeled as a constant enthalpy process.

$$h_{14} = h_{13} \tag{3.10a}$$

$$p_{14} = p_{low} \tag{3.10b}$$

$$x_{14} = x_{13} \tag{3.10c}$$

Point 15

The heat lost by the condensing fluid in the rectifier is recovered by the part of the strong solution stream flowing through the rectifier. A simple energy balance allows the determination of the state of the fluid at point 15.

$$p_{15} = p_{high} \tag{3.12a}$$

$$x_{15} = x_2 \tag{3.12b}$$

$$\dot{m}_{15} = (1 - R_2)\dot{m}_2 \tag{3.12c}$$

$$\dot{Q}_{rectifier} = \dot{m}_5 h_5 - \dot{m}_6 h_6 - \dot{m}_7 h_7 \tag{3.12d}$$

$$h_{15} = h_2 + \dot{Q}_{rectifier} \big/ \dot{m}_{15} \tag{3.12e}$$

Point 4

The two strong solution streams mix to form the fluid at state 4. This is also modeled as a constant total enthalpy process, as in state13. The composition of the two streams are the same, and hence no mass balance is needed.

$$h_4 = h_3 + h_{15} \tag{3.13a}$$

$$x_4 = x_2 \tag{3.13b}$$

$$p_4 = p_{high} \tag{3.13c}$$

Variable Limits

In any constrained optimization problem, limits of variable values have to be specified. The purpose of specifying limits is to ensure that the values at optimum

conditions are achievable, meaningful, and desirable in practice. An upper and lower bound is specified for the variables in the GRG optimization program. If the variable is to be held fixed, the upper bound is set to be equal to the lower bound, both of which are set equal to the value of the parameter. Unbounded variables are specified by setting a very large limit. Table 3.1 shows the upper and lower bounds of the variables used in the cycle optimization. Some of the bounds are arbitrarily specified when a clear value was

Table 3.1 Independent cycle parameters and their limits

Variable	**Lower Limit**	**Upper Limit**	**Name and Units**
$T_{absorber}$	$T_0 + 5$	$T_0 + 5$	Absorber Temperature (K)
T_{boiler}	$T_0 + 5$	$T_{heatsource} - 5$	Boiler Exit Temperature (K)
$T_{rectifier}$	$T_0 + 5$	$T_{heatsource} - 5$	Rectifier Exit Temperature (K)
$T_{superheater}$	$T_0 + 5$	$T_{heatsource} - 5$	Superheater Exit Temperature (K)
P_{high}	2	100	Cycle High Pressure (bars)
P_{low}	1	100	Cycle Low Pressure (bars)
$T_{heatsource}$	$T_{heatsource}$	$T_{heatsource}$	Heat Source Temperature (K)
$\dot{m}_{heatsource}$	0	18	Mass Flow Rate of Heat Source Fluid (kg/s)
R_1	0	1	Pseudo Heat Exchanger Effectiveness
R_2	0.01	0.99	Flow Split Ratio

not available. For instance, although the rectifier exit temperature can reach its upper limit, the value always has to be below the boiler exit temperature. The actual domain in which these variables may vary is further restricted by additional constraints that are specified. The lower limit for the low pressure is set at 1 bar, to avoid vacuum pressures anywhere in the system. At vacuum pressures, non-condensable gases enter the system. Additional equipment is required to remove these gases. The highest pressures in the optimization are set arbitrarily at around 100 bars.

Constraint Equations

To ensure that cycle parameters stay within limits that are practical and physically achievable, it is necessary to specify limits in the form of constraint equations. Constraints are implemented in GRG2 by defining constraint functions and setting an upper and lower bound for the function. Table 3.2 summarizes the constraint equations used for simulation of the basic cycle. If the constraint is unbounded in one direction, a value of the order of 10^{30} is specified. In GRG2, the objective function is also specified among the constraint functions. The program treats the objective function as unbounded.

A brief discussion of the constraints specified in Table 3.2 follows. The rectifier/condenser exit temperature should be below the boiler temperature and superheater temperature. A minimum approach temperature of 5K is assumed for all devices. A pinch point temperature difference of 5K is also assumed in the boiler. For the contingency that boiling could begin in the rectifier or recovery heat exchanger, a pinch point calculation is implemented in those two devices also. To ensure that the reflux flow from the boiler is in the right direction, a constraint is used to maintain that value positive. Additional constraints are used to keep the vapor mass fraction at the turbine exit (dryness of vapor) greater than 90%. Two additional constraints (that might

Table 3.2 Constraints used in the optimization

Constraint	Description	Lower Limit	Upper Limit
$T_{rectifier} - T_{boiler}$	Measure of condensation in the rectifier	-1E+30	0
$T_{rectifier} - T_{\sup erheater}$	Measure of Superheating	-1E+30	0
$T_6 - T_2$	Rectifier exit approach ΔT	5	1E+30
$T_5 - T_{15}$	Rectifier inlet approach ΔT	5	1E+30
$T_{hs,II} - T_7$	Boiler exit approach ΔT	5	1E+30
$T_{hs,III} - T_4$	Boiler inlet approach ΔT	5	1E+30
$T_{pinch,boiler}$	Pinch Point ΔT in Boiler	5	1E+30
$T_{pinch,HRHX}$	Pinch ΔT in HRHX (if applicable)	5	1E+30
$T_{pinch,rectifier}$	Pinch ΔT in Rectifier (if applicable)	5	1E+30
$\dot{m}_{11} \times 100$	Boiler reflux mass flow rate	0	1E+30
$vmf_{turbine} \times 100$	Vapor mass fraction at turbine exit	90	100
$vmf_{boiler} \times 100$	Vapor mass fraction at boiler exit	1E-05	100
$lmf_{rectifier} \times 100$	Liquid mass fraction	1E-05	100
Q_c	Cycle Cooling Output	0.1	1E+30
Objective	Efficiency Percentage	0	100

be redundant) are used to ensure that some vapor is generated in the boiler and that there is some condensation in the rectifier. These ensure that there is no heat addition to the vapor in the rectifier. A final constraint is used so that there is always some minimum positive cooling achieved in the cycle. This is to make sure that the cycle behavior does not go into a mode where only power is produced.

Model Limitations

The model used to simulate the cycle is a simple one with the advantage of being computationally fast. The results are expected to give a good idea of the trends that would be seen in real equipment. Such simple models are regularly found in the literature for preliminary analysis of thermodynamic cycles. The efficiencies obtained from such models would be higher than actually achievable efficiencies.

While the results of the optimization study will indicate an approximate value for the maximum efficiency of the cycle, the cycle parameters are not necessarily practical. The ultimate predictor of the usefulness of the cycle is in the economics of using it.

CHAPTER 4
OPTIMIZATION OF BASIC CYCLE CONFIGURATION USING AMMONIA-WATER MIXTURE AS THE WORKING FLUID

Initial parametric studies of the combined power and cooling cycle using ammonia-water mixtures as the working fluid suggested that some optimum conditions of operation exist for the cycle performance [2,36]. An optimization scheme was implemented to determine the best conditions of operation (from a thermodynamic efficiency perspective) for various applications [3], such as for utilizing geothermal and solar resources, and for achieving very low temperature cooling. Work done in the past has used a variety of different efficiency definitions. In this chapter, some of the past optimization work has been repeated with the efficiency definitions discussed in chapter 2. Additional results are presented, that use isentropic efficiencies for the turbine and pump.

The modeling of the cycle in earlier work was improved upon for the optimization work discussed in this chapter. Two additional variables were added to vary the effectiveness of the Heat Recovery Heat eXchanger (HRHX) and to control the ratio in which the strong solution stream was split between the HRHX and the rectifier. Earlier modeling had the liquid reflux from the rectifier going back into the boiler and boiling as a separate stream. Such a model makes the pinch point calculation in the boiler difficult. The stream was diverted to a point after the recovery heat exchanger. Additional pinch point checks were introduced in the rectifier and HRHX to account for the possibility of the start of boiling of the strong solution before entering the boiling heat exchanger.

Simulated Conditions

The modeling of the cycle in the optimization study carried out here has been discussed in the previous chapter. One of the questions that remained unanswered in earlier optimization work is the influence of the turbine exit temperature (the low temperature in the cycle) on the optimized efficiencies. Turbine exit temperatures were varied from 255 K to 280 K in 5 K increments. Optimizing for work output maximization, one ends up working with a cycle similar to the Maloney and Robertson cycle. A low pressure limit of 5 bars was used in the work optimization in order that the cycle remained an absorption type cycle. This limit was arbitrarily set so that there is a reasonable amount of absorbent in the basic solution at the absorber temperature.

To study the effect of heat source temperatures, four values, 360 K, 400 K, 440 K and 480 K were picked for simulation. This covers a range of low to medium temperature solar heat. The heat source was assumed to be water at the saturation pressure corresponding to the heat source temperature. The ambient temperature was assumed to be 298 K for all simulations. The objective functions corresponding to efficiency definitions developed in chapter 2 are shown in Eqs. (4.1-4.5)

$$Obj_R = \eta_R = \left(W_{net} + E_c\right) / E_{hs,in} \tag{4.1}$$

$$Obj_{exergy} = \eta_{exergy} = \left(W_{net} + E_c\right) / \left(E_{hs,in} - E_{hs,out}\right) \tag{4.2}$$

$$Obj_I = \eta_I = \left(W_{net} + E_c\right) / Q_h \tag{4.3}$$

$$Obj_{R,eff} = \eta_{R,eff} = \left(W_{net} + E_c / \eta_{II,ref}\right) / E_{hs,in} \tag{4.4}$$

$$Obj_{exergy,eff} = \eta_{exergy,eff} = \left(W_{net} + E_c / \eta_{II,ref}\right) / \left(E_{hs,in} - E_{hs,out}\right) \tag{4.5}$$

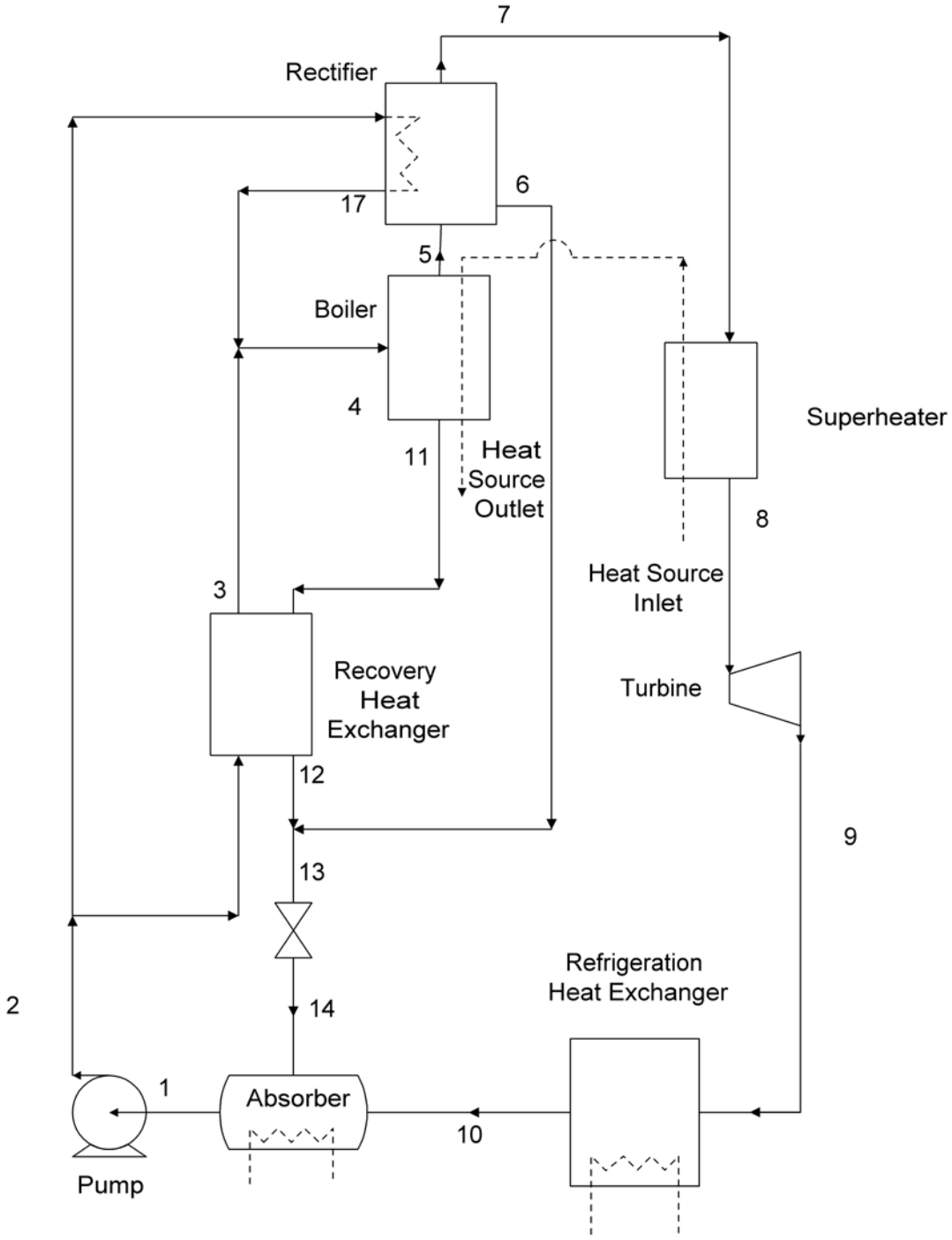

Fig. 4.1 Block diagram showing the basic scheme of the combined power and cooling cycle. Same as Fig. 1.6

Exergy losses in each component were calculated in the optimized results using the entropy generation in each device. The turbine and pump were the only devices assumed without losses in the model. Results discussed later in this chapter assume a value for isentropic efficiencies for these devices. The exergy loss in each process is calculated using the Guoy-Stodola theorem, from an entropy balance on each device, as in Eq. (4.6).

$$E_{loss} = T_0 S_{gen} = T_0 \left(\Sigma S_{out} - \Sigma S_{in} \right) \tag{4.6}$$

Here, T_0 is the ground state temperature with respect to which exergy is defined, set at 298 K for all cases. The ground state pressure was set at 1.013 bar (1 atmosphere).

Optimization results

Resource Utilization Efficiency

The resource utilization efficiency is the recommended choice in evaluating an energy conversion device for resources that are "discarded" after use in the cycle. A good example is the case of a geothermal application, where, the heating fluid is reinjected into the ground after extraction of energy from it in the power plant. The availability of the geofluid at the point of reinjection is wasted exergy that the power plant is incapable of utilizing. This efficiency can also be applied to other applications. In a coal power plant, the resource utilization efficiency would consider either the exergy of the coal and the air used for combustion, or the exergy of the products of combustion (hot gases and any solid residue such as ash). Unutilized exergy leaving the power plant through hot combustion products leaving the smokestack and in hot ash dumped into an ash pit is wasted. Optimizing for resource utilization efficiency is a good choice to

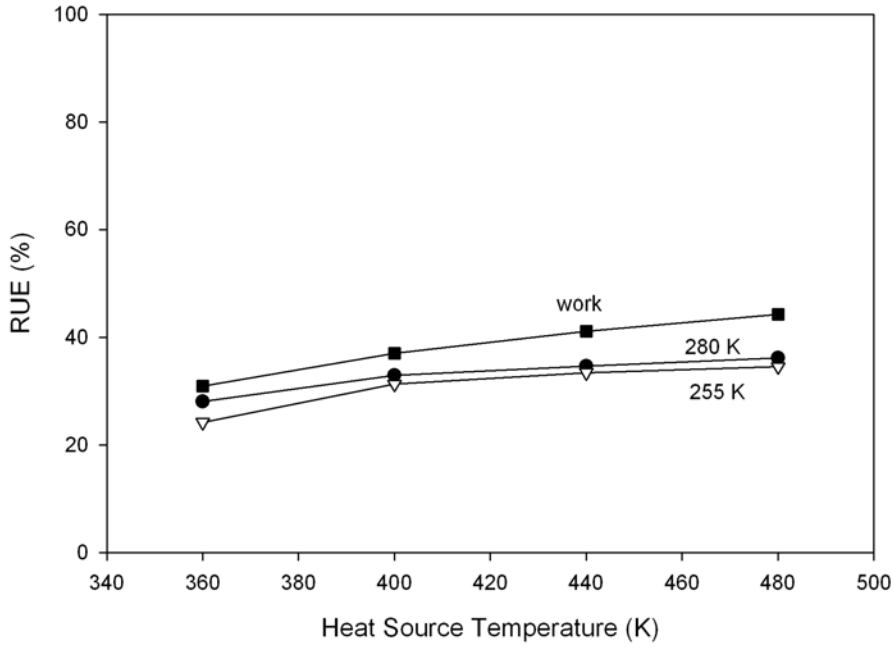

Fig. 4.2 Optimized resource utilization efficiencies for the basic cycle configuration

ensure that maximum use is made of the energy source or fuel. The resource utilization efficiency is written as (also see Eqs. (4.3) and (2.11))

$$\eta_R = \frac{(W_{net} + E_c)}{\dot{m}_{hs}\left[h_{hs,in} - h_o - T_o\left(s_{hs,in} - s_o\right)\right]} \tag{4.7}$$

The specific enthalpy h_o and specific entropy s_o are calculated at the ground state. To maximize the efficiency of Eq. (4.7), the sum of the net work output and the exergy of cooling has to be increased, while the mass flow rate of the heat source is decreased. The objective function, therefore, is very sensitive to the flow rate of the heat source.

The optimum resource utilization efficiencies (RUE) are shown in Fig. 4.2. Three different cases have been plotted. Maximum efficiency obtained using two different turbine exit temperature limits are shown. There is a slight drop off in RUE with lower

turbine exit temperatures. Optimizing purely for work output gives a better RUE value. An upper limit of 5 bars (0.5 MPa) was used for the work maximization simulations. Without this constraint, the optimum conditions were seen to be at conditions where the cycle operates using nearly pure ammonia as a Rankine cycle. The absorber model used is not valid at those conditions and the results are also not valid.

Exergy Efficiency

In solar thermal power plants, normally solar energy is collected and stored in a heat storage medium. This medium acts as the heat source for the power plant. The exergy of the heat source is not lost in the unextracted heat leaving in the fluid exiting the cycle because it is recirculated through the collector system to the storage tank. In such a case, the exergy efficiency is a reasonable choice for the objective function. This assumes though that the collection system efficiency is unrelated to the inlet and outlet temperatures of the cycle, which might not be the case. Even for solar resources, ultimately, resource utilization efficiency can be calculated, if the solar radiation were to be treated as the input. The definition of exergy of solar radiation is still being debated , but the values of different definitions in the literature give values that are fairly close to each other.

Exergy efficiency is defined in terms of the exergy transferred from the heat source fluid to the working fluid in the boiler. This function is relatively less sensitive to mass flow rate of the heat source. Changing the mass flow rate would be compensated by a change in specific exergy change in the heat source fluid, in the denominator of the exergy efficiency equation, Eq. (4.6). A large heat source flow rate results in a small temperature drop of the heat source and a bad thermal match in the boiler.

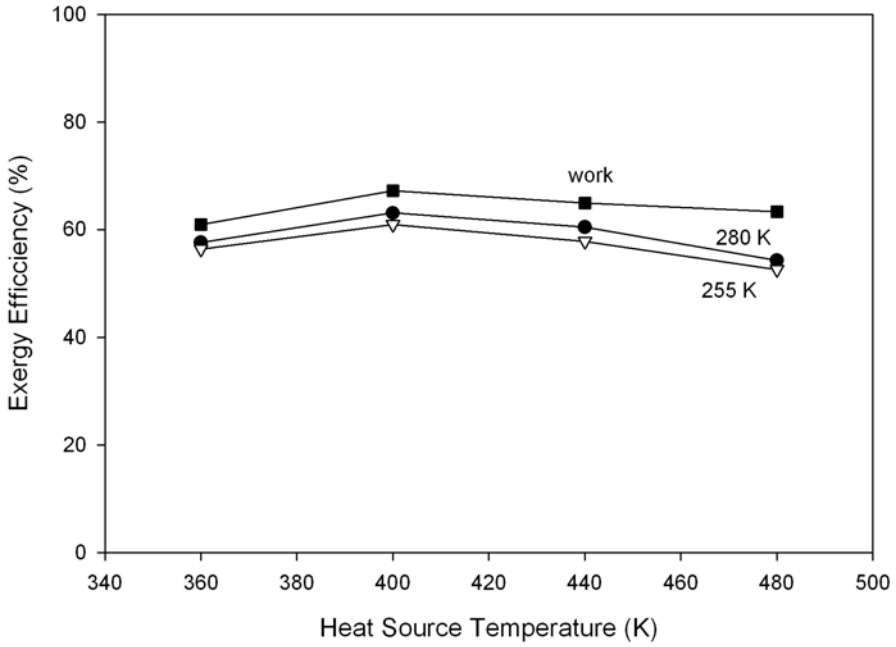

Fig.4.3 Optimized exergy efficiencies for the basic cycle configuration

$$\eta_{exergy} = \frac{(W_{net} + E_c)}{\dot{m}_{hs}\left[h_{hs,in} - h_{hs,out} - T_o\left(s_{hs,in} - s_{hs,out}\right)\right]} \tag{4.6}$$

For the exergy efficiency case, as seen in Fig. 4.3, efficiency is maximum at 400 K (of the four temperatures considered here), which is still lower than the efficiency in the work output optimized case, with a 5 bar upper limit on pressure. The optimized results are not bound at the 5 bar pressure limit. The reason for the drop in efficiency at higher temperatures is primarily due to the boiler temperature not increasing corresponding to the increase in heat source temperatures. There are limits to the temperatures in the boiler and condenser at which refrigeration can be obtained efficiently, since it becomes difficult to achieve sufficient temperature drop in the turbine across a given pressure ratio. A similar effect can also be seen in first law efficiency optimization (see Fig. 4.4)

where the efficiency curve plateaus at higher heat source temperatures. The effect of lower turbine exit temperatures is to lower optimum efficiencies slightly.

First Law Efficiency

The first law efficiency is not sensitive to mass flow rate of the heat source. Once the optimum operating conditions of the cycle are determined, as long as the pinch point conditions are not violated, changing the mass flow rate does not affect the first law efficiency at all, since the heat input to the cycle remains the same. An advantage of using a binary mixture is the improved thermal matching in the boiler. Since the first law efficiency does not account for the heat source behavior, the exergy efficiency is a better choice for evaluating binary mixtures. It might be a better choice to use the first law efficiency corresponding to the optimum exergy efficiency.

A first law efficiency is a useful measure of the cycle's performance. It is a direct measure of the heat transfer requirements in the boiler and condenser. A cycle with a high first law efficiency would have a much smaller boiler heat transfer area requirement per unit work output. Similarly, the condenser load being smaller, would use a much smaller condenser for the same boiler size. Note that this is a simplistic statement. Several other factors such as the heat transfer coefficients and pressures play a role in the size of the equipment.

Optimized first law efficiencies in the refrigeration domain are shown in Fig.4.4 Once again, the work optimization results show a higher value of efficiency. The effect of lower temperatures in the cycle is a small drop off in efficiency. It is also seen from the results that the cycle optimized in the refrigeration domain fails to take advantage of higher heat source temperatures. The optimized parameter values for heat source

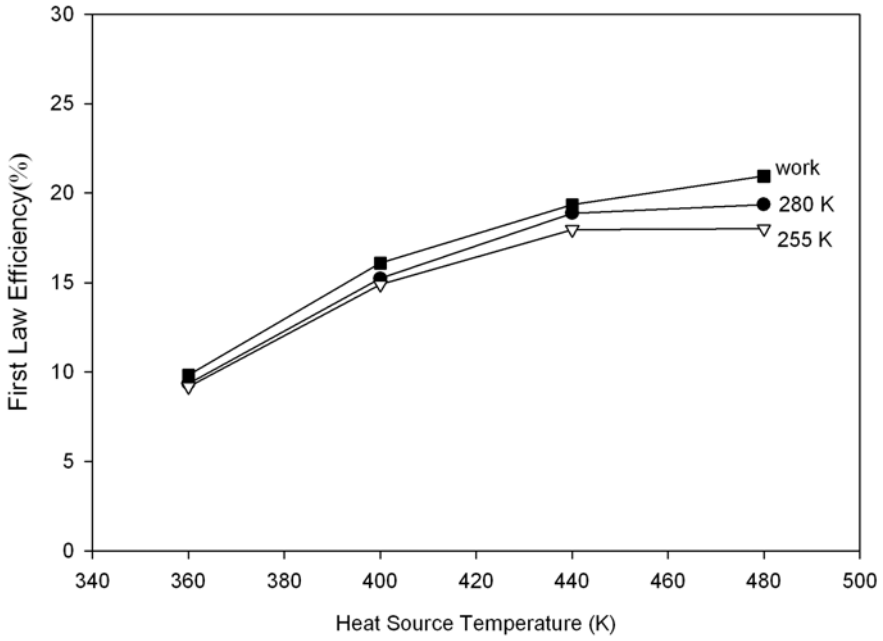

Fig. 4.4 Optimized First Law Efficiencies for the Cycle Configuration in Fig. 4.1

temperatures of 440 and 480 K are almost identical. Optimizing in the work output domain, one sees an increase in efficiency going from 440 K to 480 K. This implies that while the first law efficiency improves, a corresponding increase in exergy efficiency is not seen.

Exergy Analysis

An exergy analysis was performed to determine the various pathways of losses in the cycle. For the optimized RUE results, the major exergy losses in different parts of the cycle are plotted in Figs. 4.5 and 4.6. Figure 4.5 shows the losses occurring for the case where cooling is produced and the turbine exit temperature limit was set to 280 K. A large fraction of the exergy of the heat source is lost in the fluid leaving the cycle. Approximately 30 % of the exergy available in the heat source is lost in this fashion. The

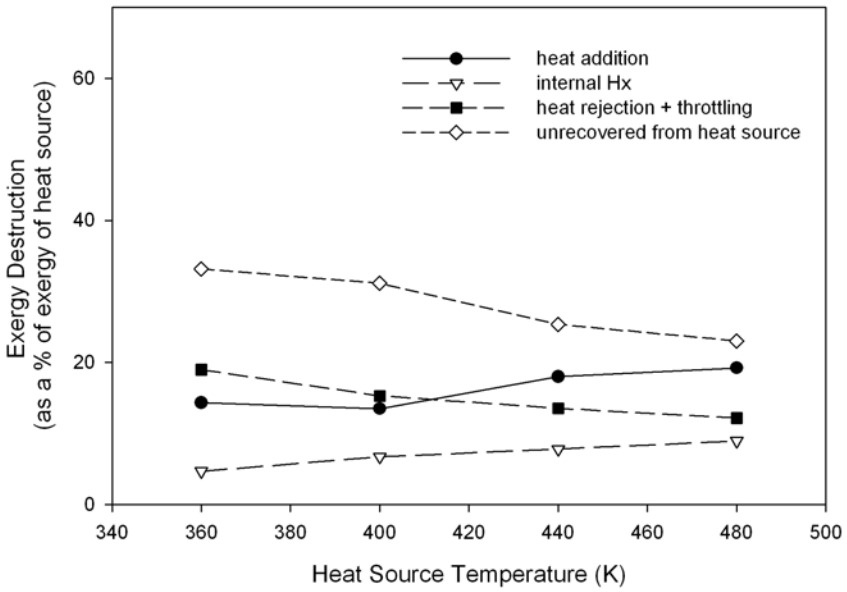

Fig. 4.5 Exergy destruction in the cycle represented as a percentage of exergy of the heat source, for optimized RUE corresponding to 280 K turbine exit temperature

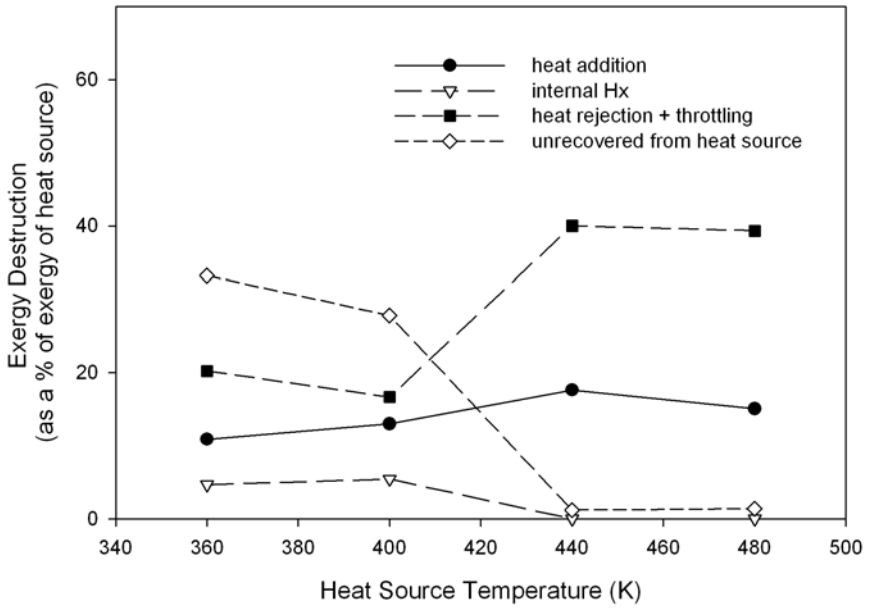

Fig. 4.6 Exergy destruction in the cycle represented as a percentage of exergy of the heat source, for optimized RUE corresponding to pure work output

losses in the heat addition process (boiler and superheater combined) are also high due to the poor thermal matching in the boiler. At the optimized condition, the mass flow rate of the heat source is very small. At these conditions, the strong solution enters the boiler at a temperature slightly above the bubble point. This removes the pinch point constraint in the boiler and allows a small heat source flowrate at the expense of thermal matching.

In the work domain, there is no rectification at optimum conditions. The process of rectification is a source of exergy loss and is unnecessary if refrigeration is not desired. At higher heat source temperatures (440 K and 480 K), there is no heat recovered in the solution heat exchanger under optimum conditions. The hot weak solution is throttled and then cooled in the absorber, with considerable losses. The heat source is used to preheat the working fluid and therefore leaves the cycle at low temperatures. As a result, the exergy losses in heat rejection and throttling go up, while the loss through unrecovered exergy in the heat source drops (Fig. 4.6).

Similar plots are shown for exergy destruction in the optimized exergy efficiency cases in Figs. 4.7 and 4.8. In the case with cooling output, the losses in the boiler are small. There is good thermal matching in the boiler, except at the 480 K heat source temperature. The exergy loss during heat rejection, in the absorber, is a major source of irreversibility in the system. That is surprising because the vapor has been expanded to very low temperatures and a large fraction of the heat recovered from the weak solution. Apparently, the mixing and absorption losses are high.

Once again the optimum parameters in the work domain do not show any rectification. The internal heat exchange category in Fig. 4.8 is the sum of exergy destruction in the solution heat exchanger and rectifier. It is seen that exergy destruction

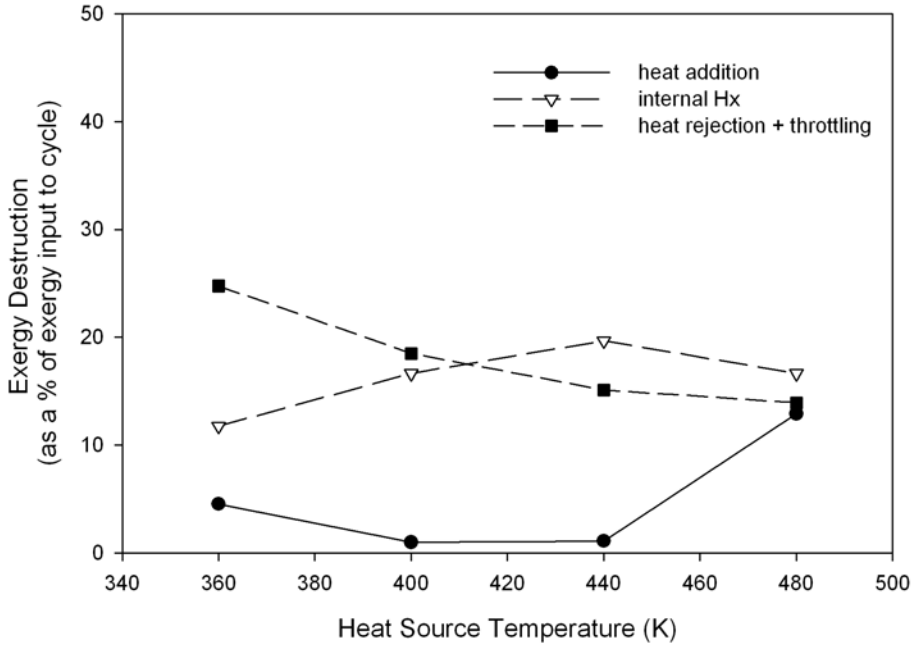

Fig. 4.7 Exergy destruction in the cycle for optimized exergy efficiency corresponding to 280 K turbine exit temperature

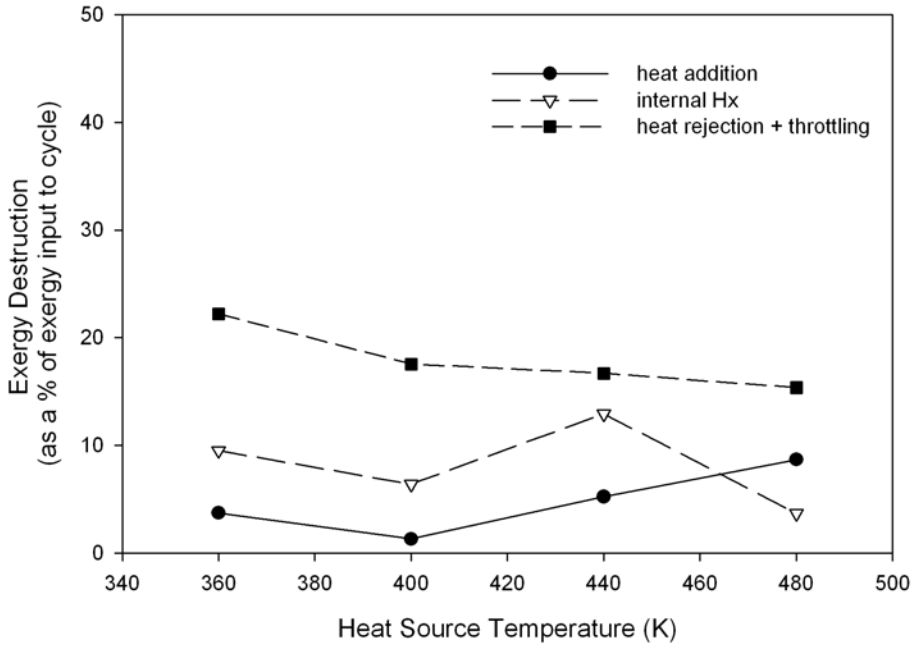

Fig. 4.8 Exergy destruction in the cycle for optimized exergy efficiency corresponding to pure work output

in the boiler and superheater is small. The thermal matching in the boiler is reasonably good in the exergy efficiency optimized cases, but it appears to be poorer than in the cooling domain. In the work domain, the requirement for work output does not limit the boiler exit temperature. However, the superheating seen at optimum conditions is larger and therefore, the thermal match in the boiler is poorer. In addition, the vapor fraction in the boiler is large enough that there is not enough weak solution to preheat the strong solution sufficiently to eliminate the pinch point in the boiler at 440 K and 480 K. This accounts for the odd looking inflections in the curves in Fig. 4.8 and contributes to increased exergy losses in the boiler.

Optimization Considering Losses

The optimization discussed so far assumes isentropic turbine and pump. Only approach temperature constraints are placed on the solution heat exchanger. The resulting effectiveness is close to 95%. Additional simulations were performed considering the turbine and pump as non ideal devices and using a lower effectiveness for the recovery heat exchanger. Optimization calculations were also performed using effective efficiency definitions developed in chapter 2.

An isentropic efficiency of 0.85 was assumed for the turbine, while a value of 0.8 was assumed for the pump. The values assumed are relatively optimistic, actual values would depend on the type of expander used and the size and scale of the equipment. Although the effect is predictable, the basic cycle configuration was also optimized using heat exchangers with lower effectiveness of 70 % and 80%. A turbine exit temperature limit of 270 K was set for all simulations.

The optimized RUE is plotted in Fig. 4.9. The effect of including an isentropic efficiency for the turbine and pump is to lower the RUE (see Fig. 4.2). In effective

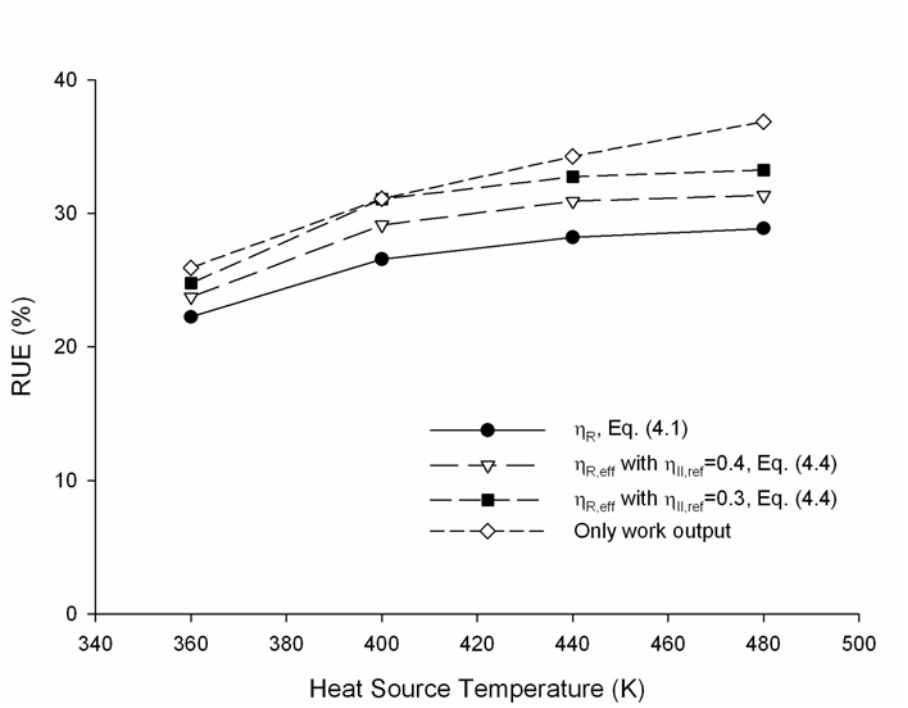

Fig. 4.9 Optimized RUE for the basic cycle configuration using a non isentropic turbine and pump

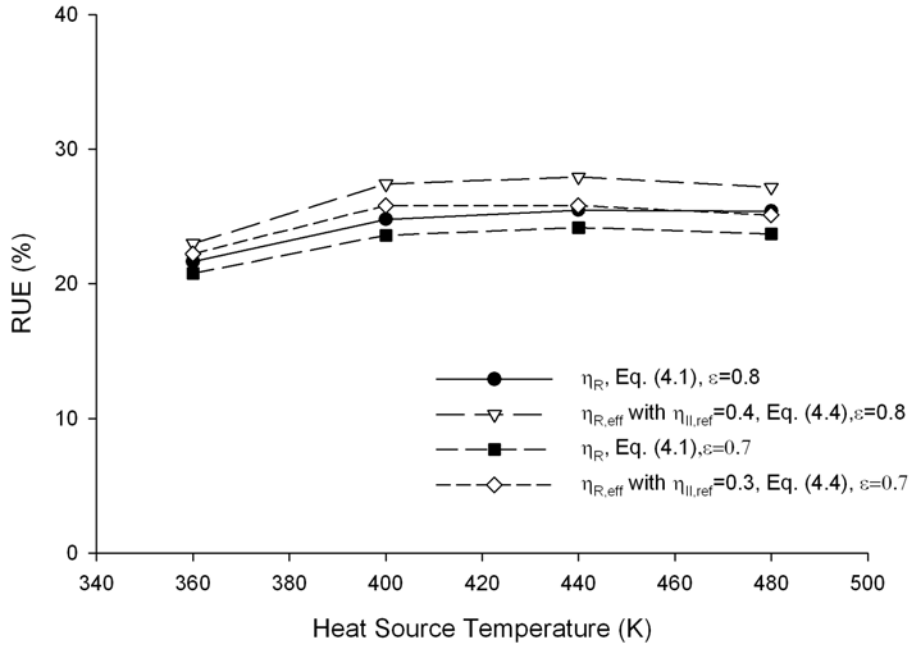

Fig. 4.10 Effect of recovery heat exchanger effectiveness on RUE at optimum RUE conditions, with cooling output

efficiency definitions, as discussed earlier, the cooling component is given a larger weight. Therefore, better efficiencies are obtained and a larger amount of refrigeration is produced at optimum conditions. The cycle was also optimized so as to obtain maximum work output with an upper limit on low pressure set at 5 bars, as in the previous optimizations. As seen in the earlier results, the efficiency is higher when optimizing for work output. It can be seen that with sufficient weight given to the refrigeration output, the cycle could have a higher effective efficiency in the refrigeration mode. Figure 4.10 represents the effect of solution heat exchanger effectiveness on the RUE. As expected, a lower effectiveness results in a lower efficiency.

Figures 4.11 and 4.12 show optimized exergy efficiencies for the cycle with an irreversible turbine and pump. It is seen that effective exergy efficiencies are comparable to the optimum efficiencies obtained for pure work output at lower heat source temperatures. At higher source temperatures, the optimum conditions in the pure work output case are still superior. The best efficiency in the refrigeration domain is seen at the heat source temperature of 400 K. At higher source temperatures, the boiler exit temperature does not get very close to the heat source inlet temperature because it is difficult to drop to cold temperatures through the turbine if the inlet temperature is very high. The effect of lower recovery heat exchanger effectiveness is a drop in efficiency.

The exergy destruction in some of the major processes in the cycle (appropriately normalized), when optimized for RUE and exergy efficiency in the cooling domain, is plotted in Figs. 4.13 and 4.14. It is seen that the effect of turbine irreversibility is to lower the RUE by about 5% (absolute) and the exergy efficiency by about 10%. Once again the largest source of losses in the RUE optimization is the

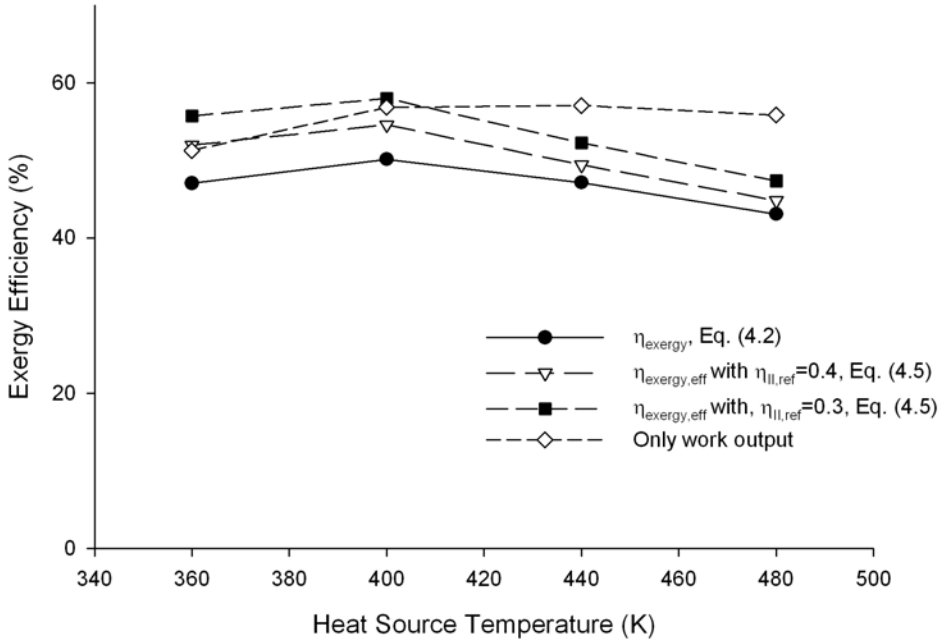

Fig. 4.11 Optimized exergy efficiencies for the basic cycle configuration using a non isentropic turbine and pump

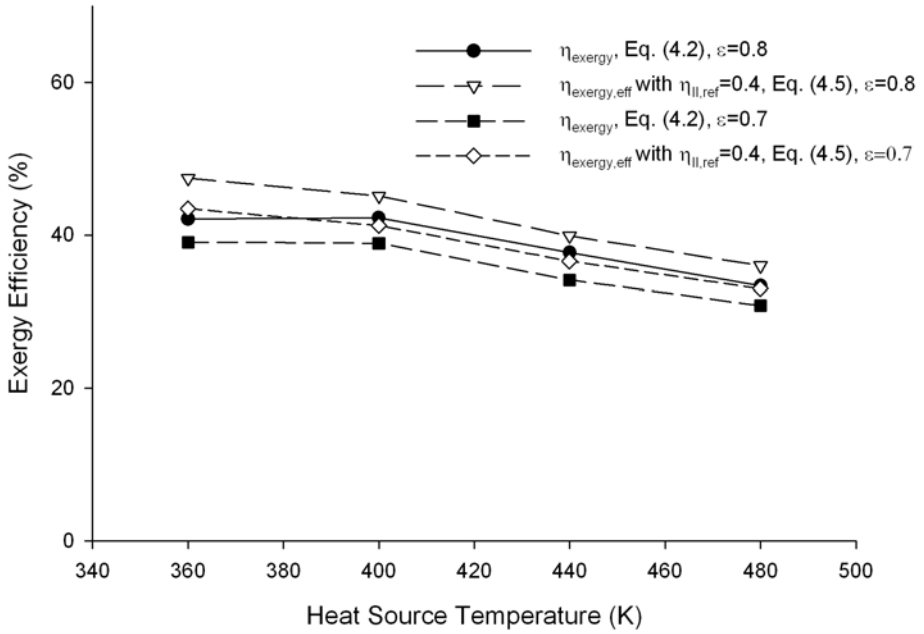

Fig. 4.12 Effect of recovery heat exchanger effectiveness on effective efficiency

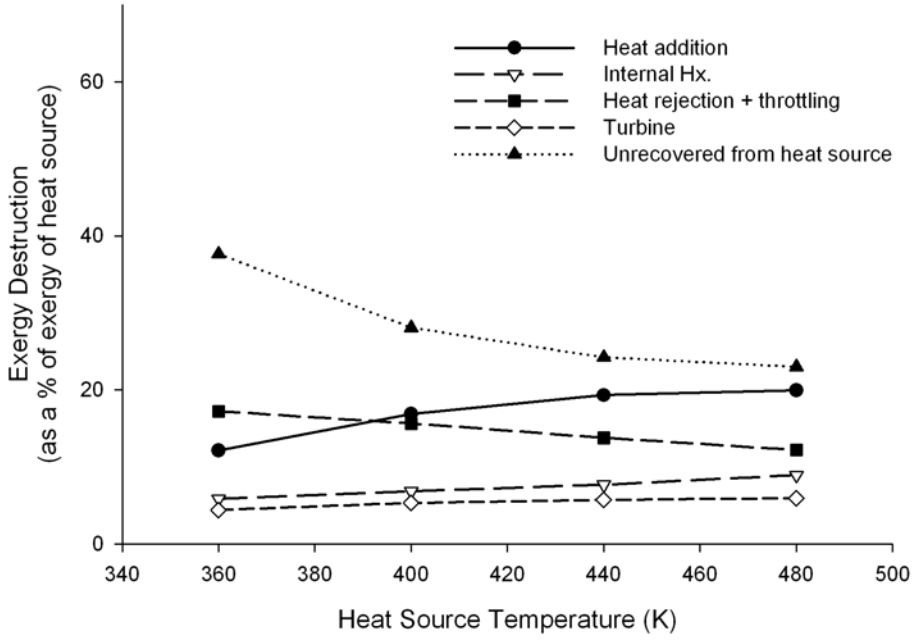

Fig. 4.13 Exergy destruction in the optimized RUE case

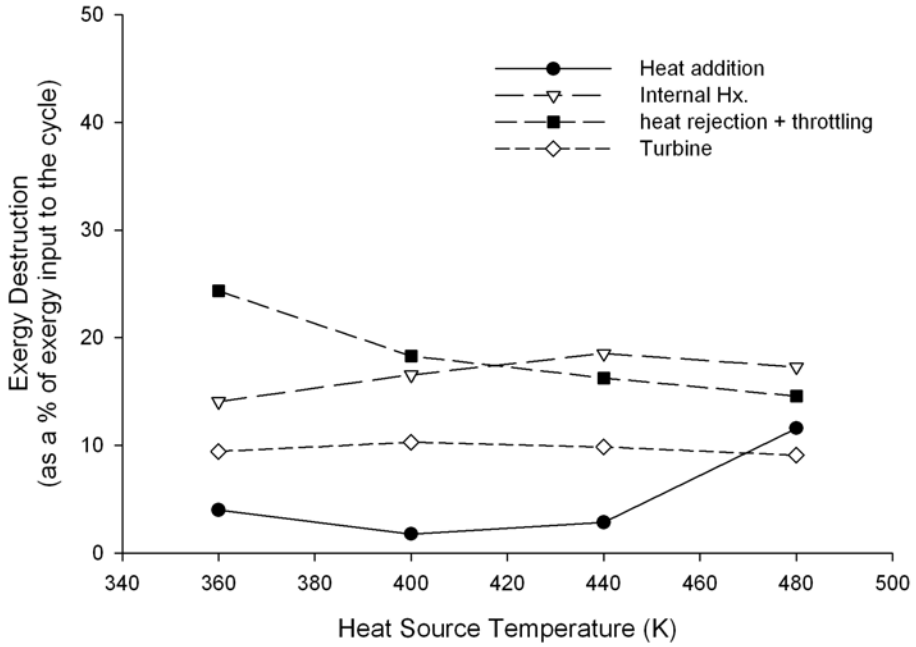

Fig. 4.14 Exergy destruction in the optimized exergy efficiency case

unrecovered exergy lost from the heat source. The bad thermal match in the boiler is reflected in the large exergy destruction during heat addition. The losses in the absorber are also quite big. The dominant losses when maximizing exergy efficiency (Fig. 4.14) are in the absorber and the internal heat recovery process.

Discussion

The basic configuration of the cycle has been optimized in order to gauge its thermodynamic performance. An exergy analysis is performed to determine the potential areas of improvement in the cycle. The results of the exergy analysis are applied to improving the performance of the cycle, which is discussed in a later chapter.

It is seen that RUE values obtained with the cycle are quite low. The optimized cycle state points show that the strong solution starts boiling before entering the boiler (in the HRHX and rectifier), thereby eliminating the "pinch point" in the boiler. Figures 4.15 and 4.16 show the boiler inlet and exit conditions of the working fluid at the heat source temperatures studied. The cycle performance is maximized by reduction of mass flow rate of the heat source until the approach temperature constraint at the boiler entrance (state 4 in Fig. 4.1) is at the bound. High exergy destruction occurs in the boiler, when the parameters are set to yield maximum RUE while providing both power and cooling (see Figs. 4.5 and 4.13). The reason for the observed trend is the low vapor fraction in the cycle (boiler) when operated to produce power and refrigeration (see Fig. 4.15). It is seen that the vapor fraction is between 9 and 15 % when producing work and cooling at high efficiency, while in the work domain it is between 20 and 28 % (Fig. 4.16). In order to expand the vapor to low temperatures, relatively high concentration vapor is required. Other requirements include a high pressure ratio, and lower pressures at the turbine exit such that the temperature drop in the turbine is high. All these factors

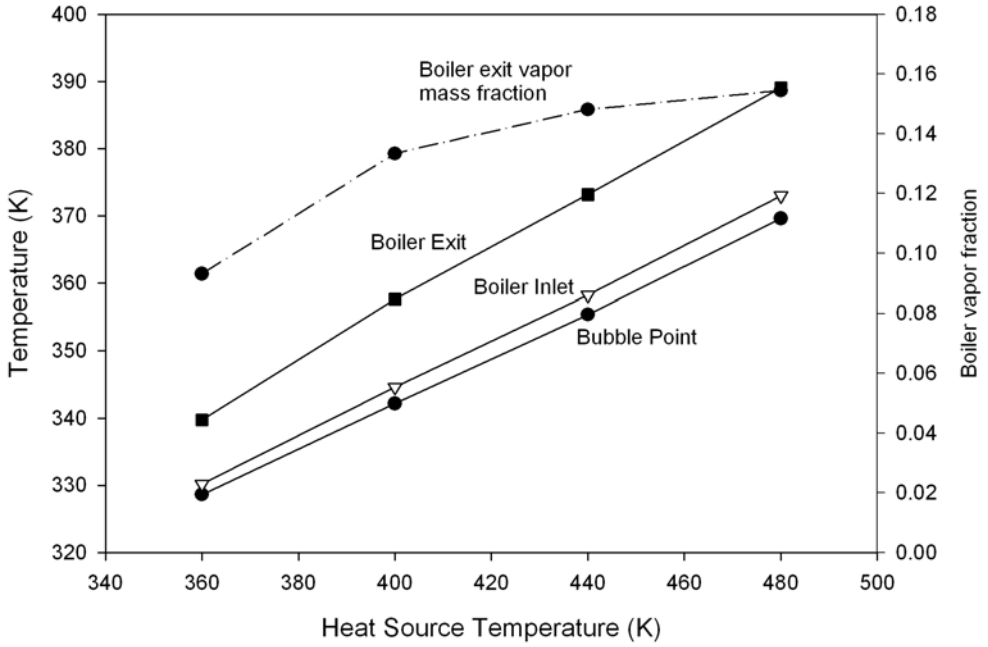

Fig. 4.15 Working fluid temperatures and vapor fractions in boiler: at maximum RUE and with cooling

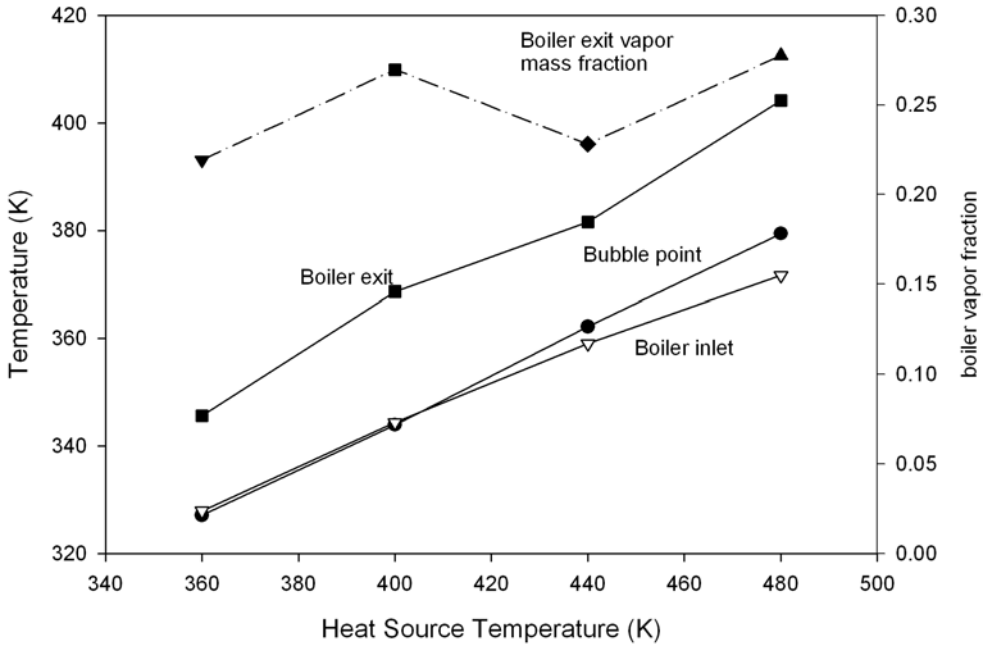

Fig. 4.16 Working fluid temperatures and vapor fractions in boiler: at maximum RUE with pure work output

promote low vapor fraction in the boiler. Consequently, there is a large temperature difference at the boiler exit (between heat source state II and vapor at state 5) and the result is poor thermal matching in the boiler. A large temperature glide would be needed for good thermal matching in the boiler, which only occurs at large vapor fractions.

From Fig. 4.1, it can be seen that the exergy in the heat source fluid leaving the boiler is not utilized elsewhere. In order to remove as much of the exergy out of the heat source as possible, the temperature of the heat source should be dropped to the maximum extent possible in the boiler.

Since the fluid enters the boiler at a condition where it is beginning to boil, the bubble point of the strong solution should be low. This is achieved by having a high basic (strong) solution concentration and lower boiler pressures. However when operating at these conditions, the pressure ratios are lower resulting in a lower temperature drop in the turbine.

Figure 4.17 clearly shows that the pressure ratios are lower in the RUE optimized results compared to the exergy efficiency optimized results. Interestingly, it is seen that setting a lower limit for recovery heat exchanger effectiveness results in a substantial reduction in pressure ratio in the optimized exergy efficiency results. With ammonia-water mixtures, lower absorber pressures result in higher pressure ratios. However, the basic (strong) solution concentration then becomes smaller limiting the vapor fractions in the boiler. With the resulting increase in the weak solution flow, the load on the recovery heat exchanger goes up. A reduction in the effectiveness of the recovery unit pushes the optimum towards higher absorber pressures and lower pressure ratios.

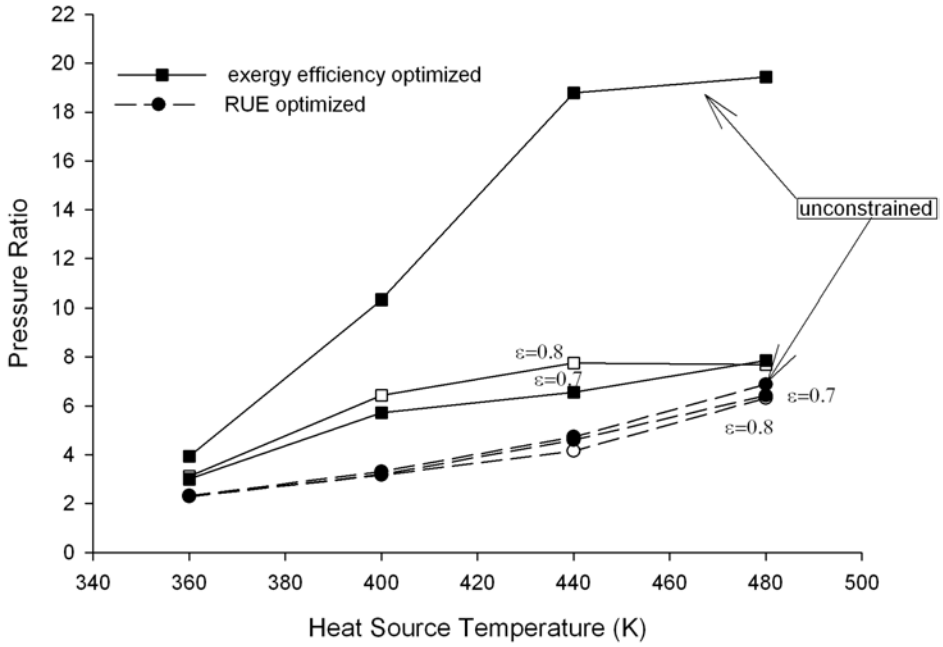

Fig.4.17 Cycle pressure ratios and the influence of solution heat exchanger effectiveness

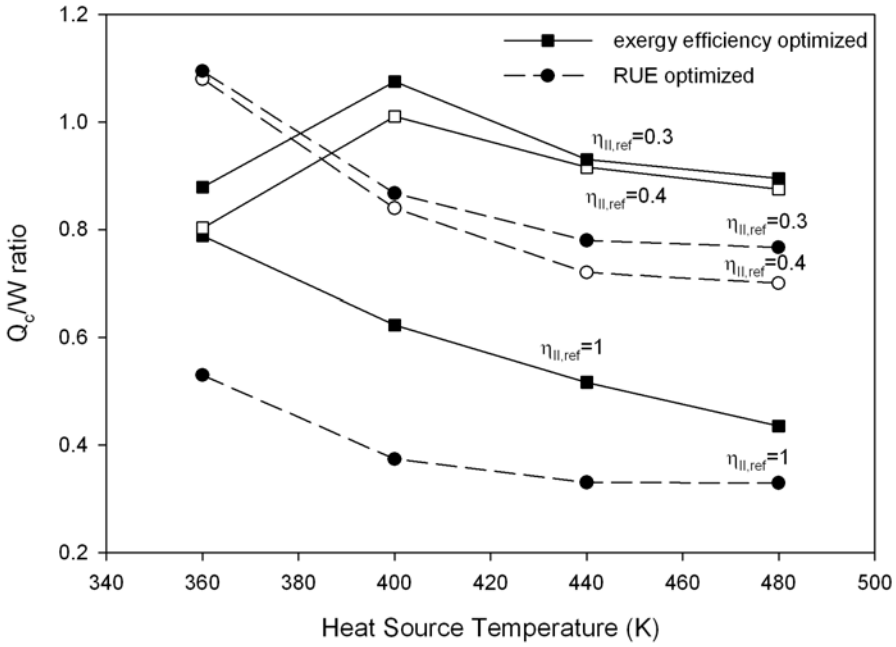

Fig.4.18 Cooling to work output ratios at optimum conditions

Figure 4.18 shows the cooling to work output ratio at optimum conditions using the basic cycle configuration. Clearly, assigning a larger weight to the refrigeration output results in a larger cooling output at optimum conditions in the cooling domain. Unlike classic refrigeration cycles, the cold fluid is in the form of dry or slightly wet vapor. The cooling is by sensible heating of the vapor, and not by the vaporization of a two-phase mixture as in a typical evaporator. When weight assigned to cooling is larger, in some cases, the turbine output temperature drops well below the set limit of 270 K in the simulations.

The corresponding first law efficiency of the cycle at optimum exergy efficiency and optimum RUE conditions is plotted in Fig. 4.19 and 4.20 respectively. Since the heat source temperature is low, the corresponding first law efficiency is generally low.

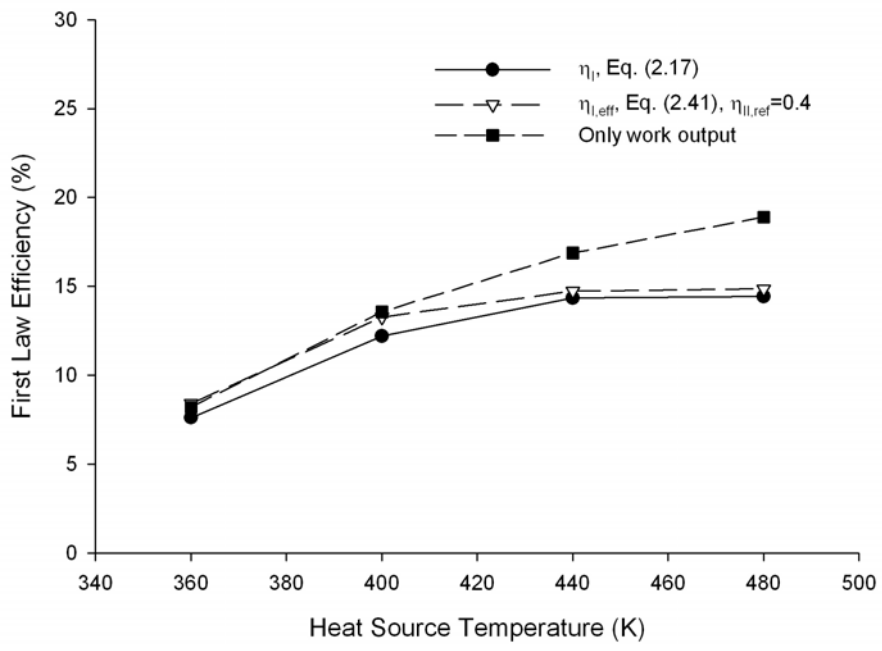

Fig. 4.19 First law efficiency at optimized exergy efficiency conditions

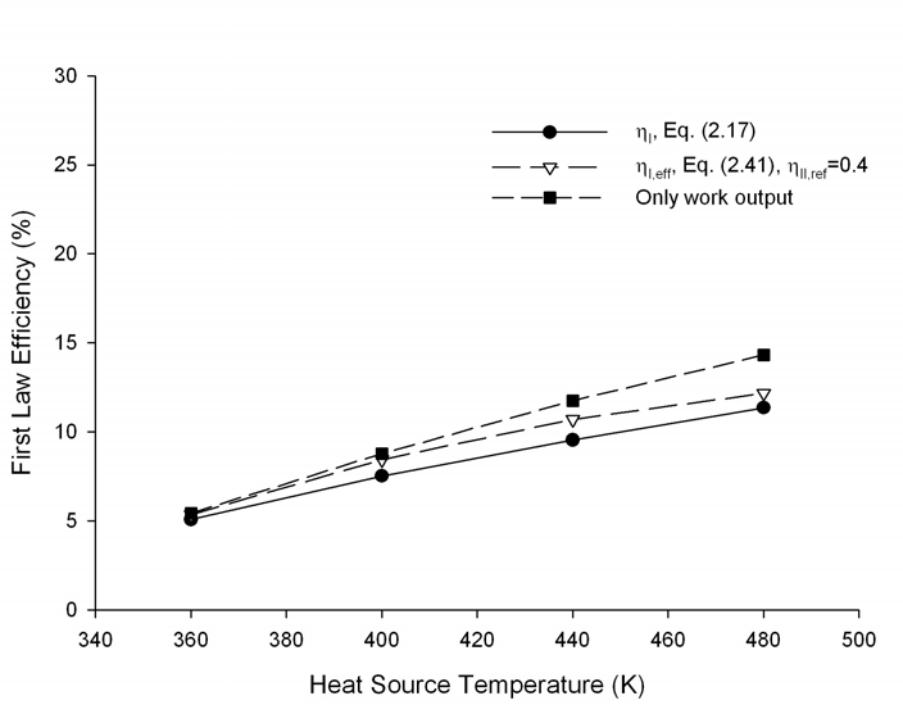

Fig. 4.20 First law efficiency at optimum RUE conditions

The first law efficiency corresponding to the RUE is lower. This is because for high RUE, the goal is to remove as much energy from the heat source as possible.

Conclusions

The basic cycle configuration has been optimized for maximum resource utilization efficiency and exergy efficiency. It is seen that the RUE values obtained with this configuration are low, primarily because of the difficulty in removing heat from the source fluid while maintaining high efficiencies. The exergy efficiency values appear to be relatively high at 360 K and 400 K. At higher values of 440 K and 480 K, the second law efficiency is lower.

When the cycle is operated to give only work output the efficiencies are higher in almost all cases. However, when considering effective efficiencies, the basic

configuration performs comparably in the cooling domain or the pure work output domain, at low heat source temperatures. At higher temperatures (440 K and 480 K), this configuration does not efficiently produce both work and cooling simultaneously.

CHAPTER 5
RESULTS AND DISCUSSION: ORGANIC WORKING FLUIDS

The combined power and cooling cycle has been extensively studied using a binary mixture of ammonia and water as the working fluid. Ammonia, however, is a corrosive fluid and poses some challenges in turbine design, particularly in limiting the leakage at the seals and in material compatibility issues. While a limited number of ammonia based (Kalina) power plants have been built in the past few years, hydrocarbon mixtures would be easier to work with. Hydrocarbons and halocarbons have been used in binary geothermal power plants for the last couple of decades and the industry has significant experience with them.

Working Fluid Selection

There are several considerations for desirable properties of working fluids used in thermodynamic cycles. There are some obvious general properties that would be ideal to have in a working fluid. The working fluid should be

- Stable
- Non Fouling
- Non Corrosive
- Non Toxic
- Non Flammable

The working fluid stability at the pressures and temperatures encountered in the cycle, and over long term use is critical. Non corrosive, non fouling, non toxic, non flammable fluids simplify the design and cost of a power plant significantly. A suggested application of this cycle is in small power plants sized for residential, commercial and

industrial buildings. For some of these cases, a non toxic, non flammable fluid would help to meet building code requirements. The organic working fluids considered in this chapter all have high flammability. The heavier components are skin and eye irritants. Data available on long term temperature and pressure stability appears limited, but indications are that the compounds are stable and that hazardous polymerization is not a concern.

Several references [16,35, 49-54] were used to shortlist working fluids and for background on the properties of working fluids required in cycles of the type considered here. The list consists of alkanes, alkenes and dienes. The optimization work discussed in this chapter focuses on mixtures of saturated hydrocarbons (alkanes). Halocarbons are not considered due to concerns about their environmental friendliness. The NIST Database 4, also called the NIST Thermophysical Properties of Hydrocarbon Mixtures Database or SUPERTRAPP is used to calculate property data for the working fluids. This database includes a properties subroutine source code, which was adapted for use in cycle simulations. Properties were available in this database for a majority of the candidate fluid pairs that were identified. A list of the fluids considered for initial study is given in table 5.1. To determine the performance of the cycle with a given working fluid pair, the performance of the cycle was optimized using that pair as the working fluid. After studying initial optimization and simulation results, the list of working fluids was extended such that higher efficiencies are obtained.

When picking the working fluid components for this cycle, it is important that the low boiling component be volatile. If the low boiling component is not volatile,

Table 5.1 List of Working Fluids Considered Initially

No.	Fluid	Mol. Wt.	T_m (K)	T_b (K)	T_c (K)	p_c (MPa)
1	water	18.02	273.15	373.15	646.99	22.06
2	ammonia	17.03	195.3	239.85	405.5	11.35
3	methane	16.04	90.7	111.6	190.5	4.60
4	ethane	30.07	90.3	184.5	305.4	4.88
5	ethylene	28.05	104	169.4	282.3	5.04
6	propane	44.10	85.5	231.0	369.8	4.25
7	propylene	42.08	87.9	225.3	364.8	4.601
8	n-butane	58.12	134.9	272.6	425.1	3.78
9	isobutane	58.12	134.8	261.4	407.8	3.63
10	n-pentane	72.15	143.15	309.25	469.7	3.36
11	cyclopentane	70.13	179.3	322.4	511.7	4.51
12	n-hexane	86.18	178.15	342.15	507.7	3.01

vacuum pressures will be needed at the turbine exit in order to attain low temperatures. This is generally not desirable, since then the problem of air leaking into the system arises. The volatile component can be chosen from any of the compounds containing 1 to 4 carbon atoms in table 5.1. Methane, ethane and ethylene would not be good choices, since the vapor pressure at ambient conditions are high. The pressure needed to maintain a binary mixture containing these fluids in a liquid state in the absorber would be very

large. The corresponding cycle high pressures would be large, and pressure ratios and efficiencies low. In addition, the costs of building equipment rated at the high pressures encountered would be much higher compared to other fluids. Note that these fluids also have a low critical temperature and relatively larger critical pressure, compared with the other fluids in the table 5.1. From the remaining fluids listed in the table, propane and isobutane were selected for study as the volatile component.

Preliminary Simulation

The basic cycle configuration shown again in Fig 5.1 was simulated using different hydrocarbon working fluid pairs selected from table 5.1. Reasonable low temperatures were only obtained using hexane as the higher boiling component. It was seen in preliminary simulations that low temperatures achievable were limited in comparison to those with ammonia-water mixtures. Therefore it was assumed that if a minimum turbine exit temperature of 285 K (12 $^{\circ}$C) was not achieved, useful refrigeration could not be obtained, for an ambient temperature of 298 K (25 ºC). The other assumptions used were similar to those described for ammonia-water simulations, including assumptions of isentropic turbine and pump, minimum 5 K approach and pinch temperatures in heat exchangers etc. Heat source temperatures of 360, 400 and 440 K were studied. With a search based method, it is necessary to have many feasible or near feasible initial points for the optimization. The following procedure proved to be very effective in the optimization:

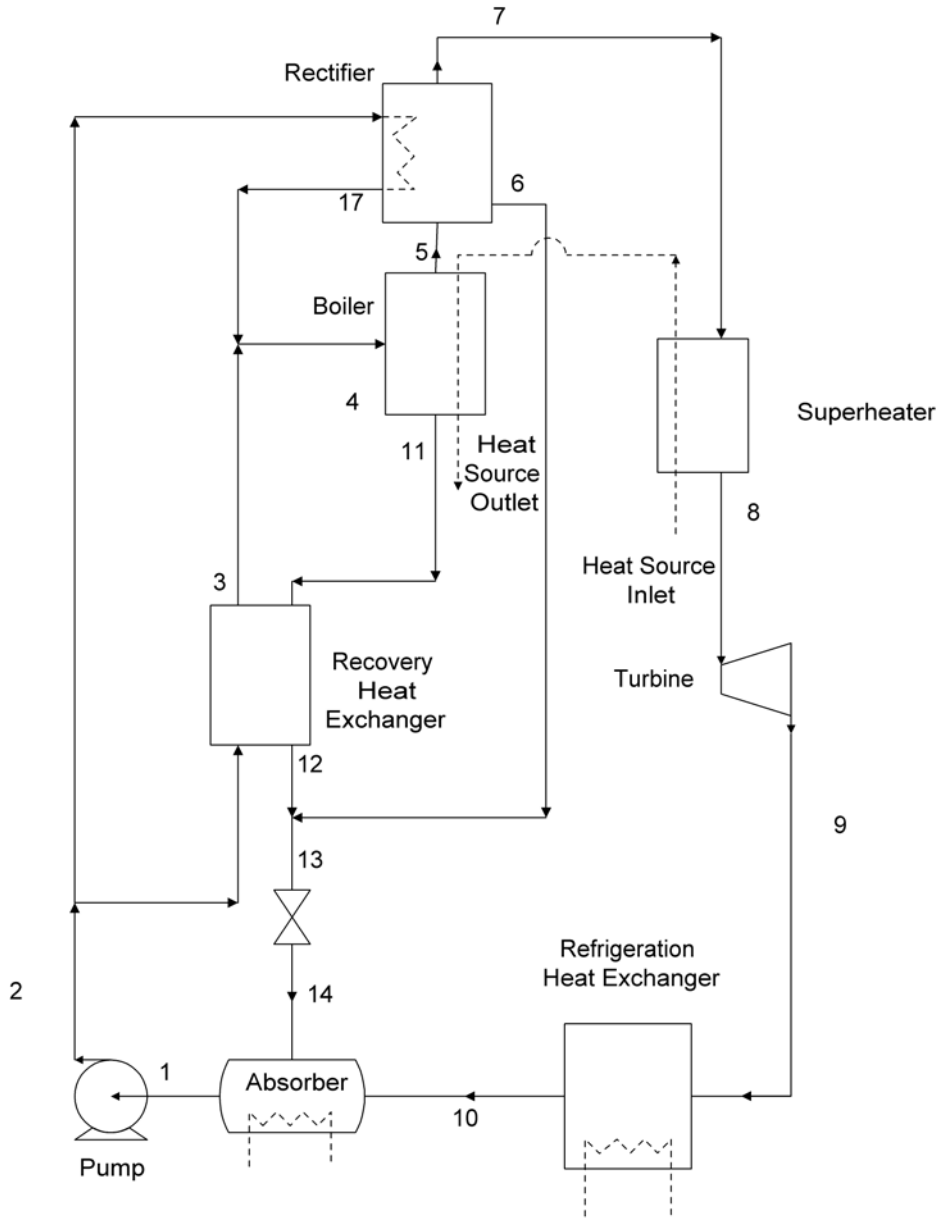

Fig. 5.1 Basic configuration simulated. In this configuration, the condensate from the rectifier is redirected to the absorber.

1. Run the optimization program to *minimize* turbine exit temperature starting from randomly chosen feasible starting points. A constraint equation was set such that the turbine exit temperature would not go below 285 K.

2. Using the termination points from simulations in the previous step, optimizations are run to maximize the exergy of cooling (E_c), output of the cycle. This second step was used because optimizations used to minimize turbine exit temperature tend

to terminate at points where vapor generation is also minimal, due to large rectification requirements.

3. The termination points from steps (1) and (2) can then be used as initial points for different optimizations for exergy and resource utilization efficiency. The termination points from these optimizations yield more initial points for additional optimizations.

4. Some state points in the optimum conditions from step (3) are perturbed to see if further improvement is possible.

After step (1), it was concluded that sufficiently low temperatures were not achieved with pentane as the heavy component. 285 K turbine exit temperature could not be achieved using an isobutane-hexane pair for the cycle configuration being simulated. In fact, temperatures below ambient were not obtained in step (1). Optimized exergy and resource utilization efficiency are plotted for the three temperatures studied using ethane and propane as the volatile component and hexane as the second component of the binary mixture, in Fig. 5.2.

The optimized exergy and resource utilization efficiencies are defined as in previous chapter, and are repeated in Eqs. (5.1) and (5.2) for convenience.

$$\eta_{exergy} = \left(W_{net} + E_c\right) / \left(E_{hs,in} - E_{hs,out}\right) \tag{5.1}$$

$$\eta_R = \left(W_{net} + E_c\right) / \left(E_{hs,in}\right) \tag{5.2}$$

It can be seen that the efficiencies with ethane as the volatile component are extremely low. The absorber pressure is large and the corresponding boiler pressure is also very high, while the pressure ratio obtained across the expander is small. The optimization procedure sometimes returned meaningless values since portions of the cycle entered the supercritical region. The properties program is invalid near or above critical conditions.

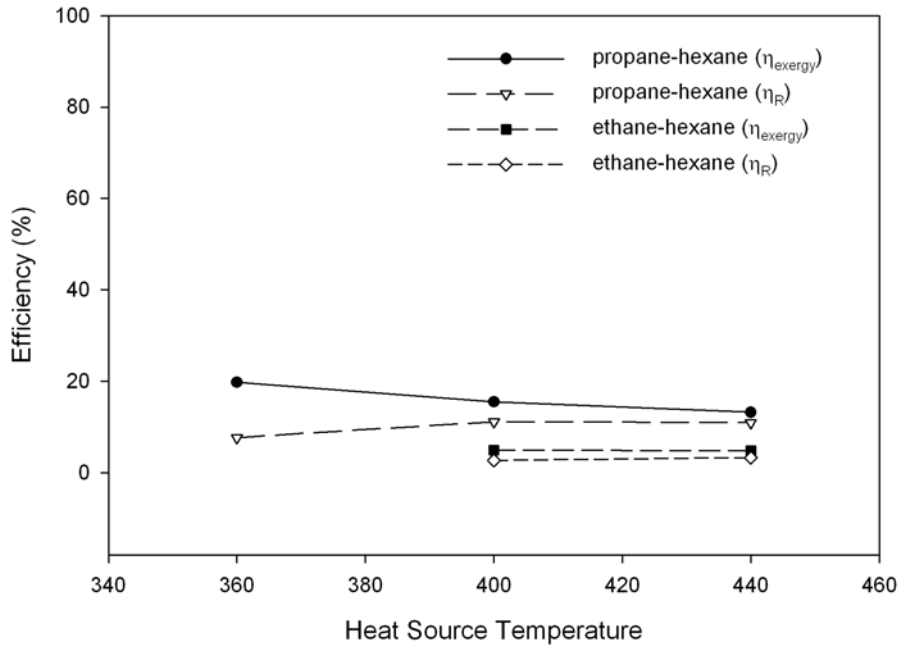

Fig. 5.2 Optimized second law efficiencies of the combined power and cooling cycle using organic working fluid pairs

A rather large amount of rectification was observed in these optimized cases. Figure 5.3 shows a different configuration for the cycle, where the reflux from the rectifier joins with the strong solution stream entering the boiler. Generally, the liquid reflux from the rectifier has a high volatile component concentration. Therefore, the advantage of the configuration in Fig. 5.3 is that the strong solution entering the boiler has a higher concentration of the volatile component. This results in larger vapor generation and consequently, an improvement in efficiency. Figure 5.4 shows the improvement obtained by using the modified configuration of Fig. 5.3.

The efficiency numbers seen with organic fluid pairs considered so far are poor when compared to ammonia water mixtures. The data showed that the vapor has a lower concentration of volatile component, and significant rectification is required to obtain

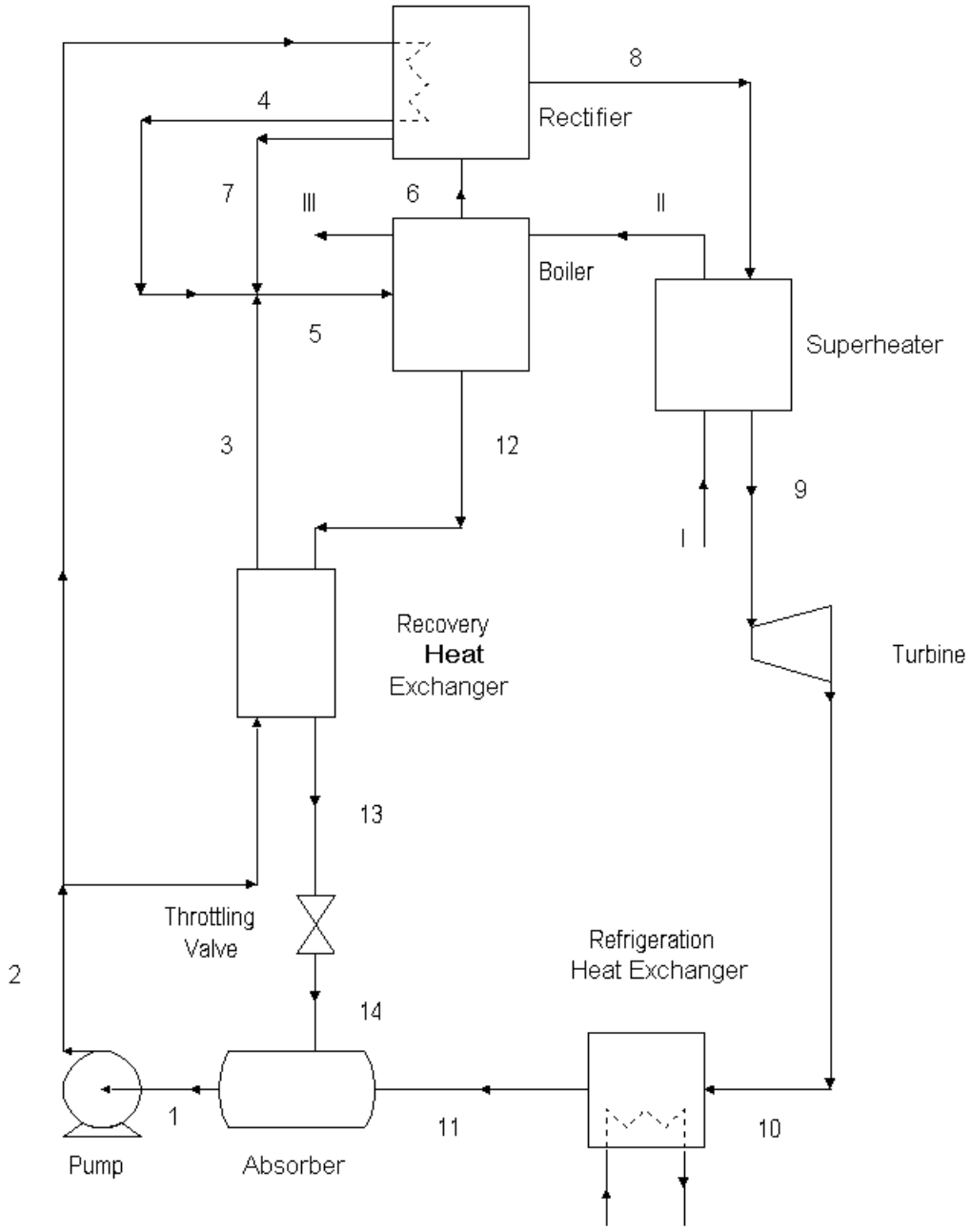

Fig. 5.3 Alternate configuration, where the condensate from the rectifier is mixed with the strong solution inlet stream to the boiler.

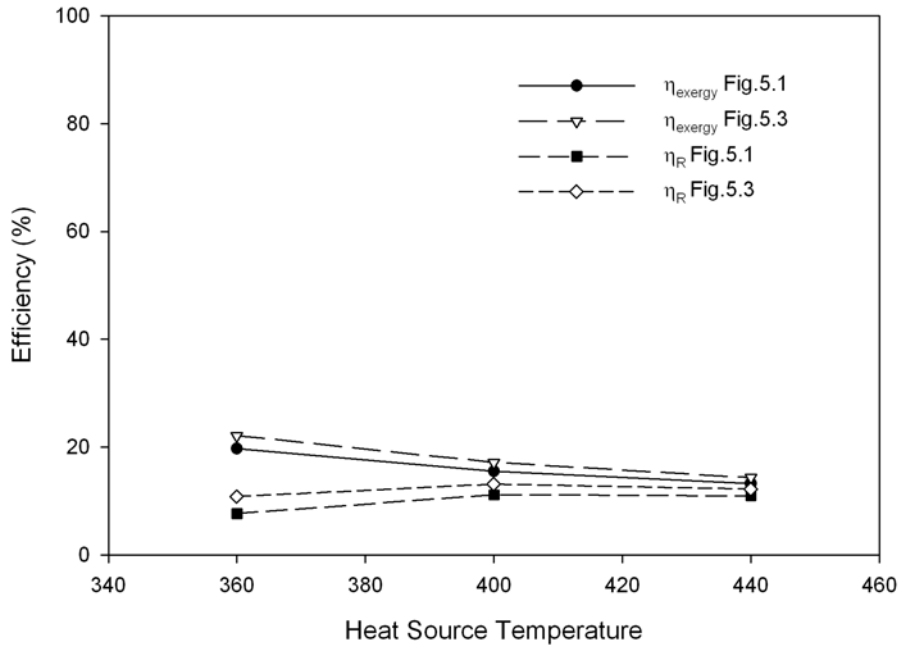

Fig. 5.4 Comparison of the second law efficiency performance of the two configurations in Fig. 5.1 and 5.3, using a propane-hexane mixture as the working fluid

high concentration vapor. This appears to indicate that the volatility ratio is low. In other words, more of the high boiling component tends to vaporize out initially with the volatile component.

Simulation of Higher Boiling Components

Higher molecular weight components were then studied with propane and isobutane (see table 5.2). These new binary components work much better in the cycle. Optimized second law efficiency results are shown in Figs. 5.5 and 5.6. The efficiency increases by selecting higher boiling components. Using propane, the second law efficiencies show an increase on moving from n-octane to n-dodecane in table 5.2, as the second component. The improvement seen rapidly diminishes and the efficiency improves very little from n-decane to n-dodecane.

Table 5.2 Higher boiling components considered

No.	Fluid	Mol. Wt.	T_m (K)	T_b (K)	T_c (K)	p_c (MPa)
1	n-octane	114.23	216.3	398.8	568.9	2.493
2	n-nonane	128.60	219.6	424.0	594.6	2.288
3	n-decane	142.29	243.4	447.3	617.7	2.104
4	n-undecane	156.39	247.5	469.1	638.8	1.966
5	n-dodecane	170.34	263.5	489.5	658.2	1.824

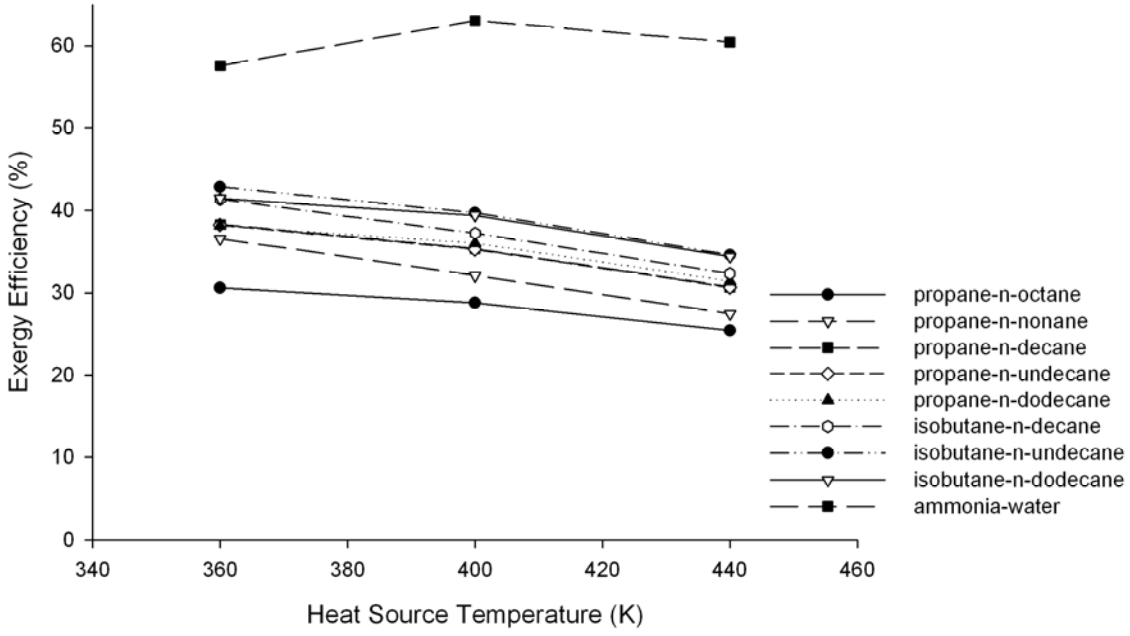

Fig. 5.5 Optimized exergy efficiency using higher boiling non volatile mixtures

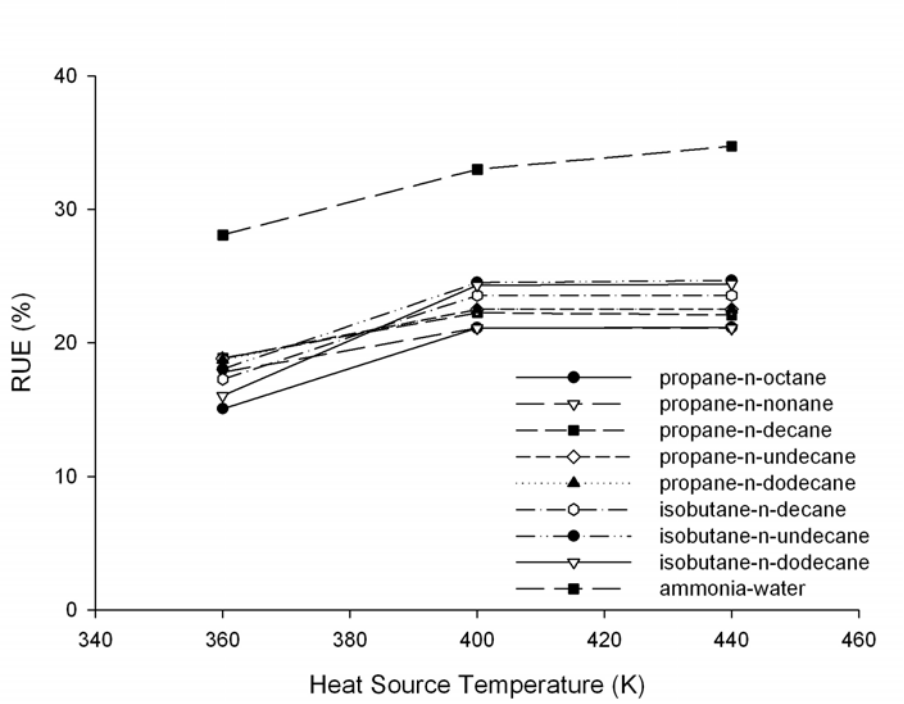

Fig. 5.6 Optimized resource utilization efficiency using higher boiling non volatile mixtures

The use of isobutane as the volatile component appears to give better RUE than propane. The best efficiency is seen with an isobutane-n-undecane pair. The next higher combination of isobutane-n-dodecane has slightly lower efficiencies. Comparing the results to those using ammonia-water mixtures, it is seen from Figs. 5.5 and 5.6 that the performance of the organic fluid mixtures is relatively poor.

A summary of the results of optimization performed using organic working fluids in the combined power and cooling cycle are as follows:

- The efficiencies are much lower than those obtained with ammonia-water mixtures.
- Low temperatures that are obtainable are limited, compared to those using NH_3-H_2O mixtures.
- The pressure ratios across the turbine are lower.

- Substantial condensation occurs during rectification, which is accompanied by a large temperature drop.
- The concentration of vapor is extremely high at optimum conditions. The mass fraction of the volatile component in the vapor is greater than 0.99, which is higher than the concentrations seen with ammonia-water mixtures.
- Mixtures with heavier (higher boiling) nonvolatile fraction appear to improve performance, although the improvement is very small beyond a certain point.
- The optimum exergy efficiency decreases with temperature in the range studied, while with ammonia-water an optimum exists within that range.
- Among the combinations studied, the best efficiency was observed with a isobutane-n-undecane mixture.

The pressure ratios at optimum conditions are plotted in Figs. 5.7 and 5.8. It is seen that isobutane based mixtures have higher pressure ratios. With both isobutane and propane, the combination giving higher efficiency has a greater pressure ratio. The data also shows a trend of higher boiler exit temperatures and better temperature matching in the boiler using heavier molecular weight components. The working fluid boiler exit temperature does not increase much as the source temperature is increased from 400 K to 440 K, when optimizing for exergy efficiency. This result is similar to what is seen with ammonia-water optimization when comparing the source temperatures of 440 K and 480 K. The reason for this trend is the inability to expand the high temperature fluid at the turbine inlet to low turbine exit temperatures while maintaining efficiency. Cycle parameters optimized for resource utilization efficiency do not show a good thermal match in the boiler, which is similar to the results for ammonia-water mixtures. Instead, the mass flow rate of the heat source is minimized to the extent allowed by the approach temperature constraint at the boiler inlet.

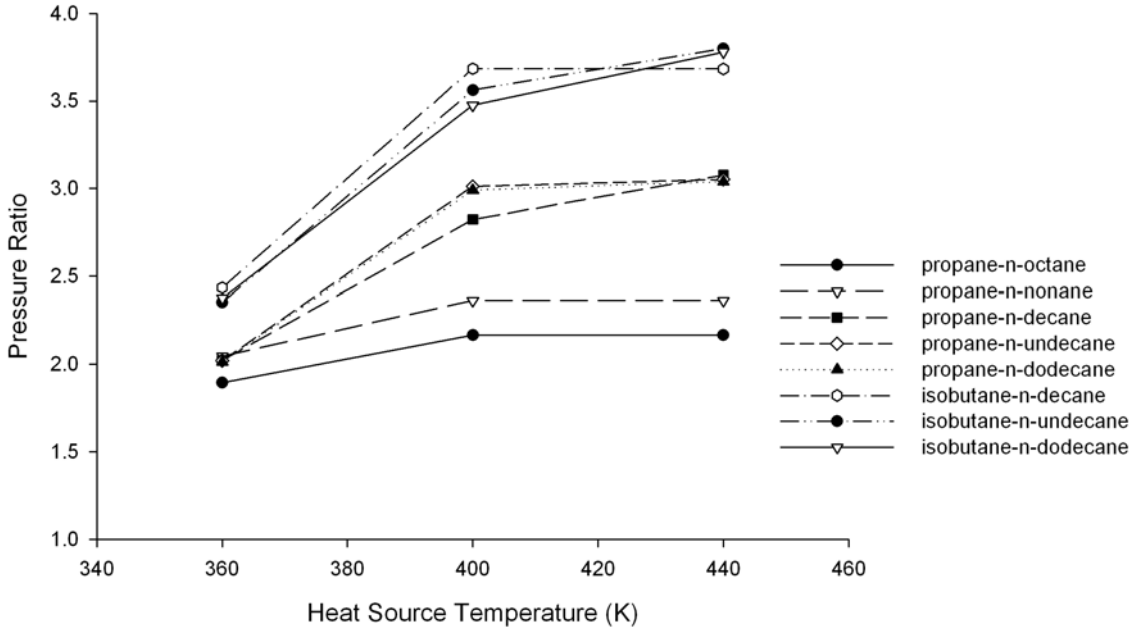

Fig. 5.7 Pressure ratios at optimum exergy efficiency

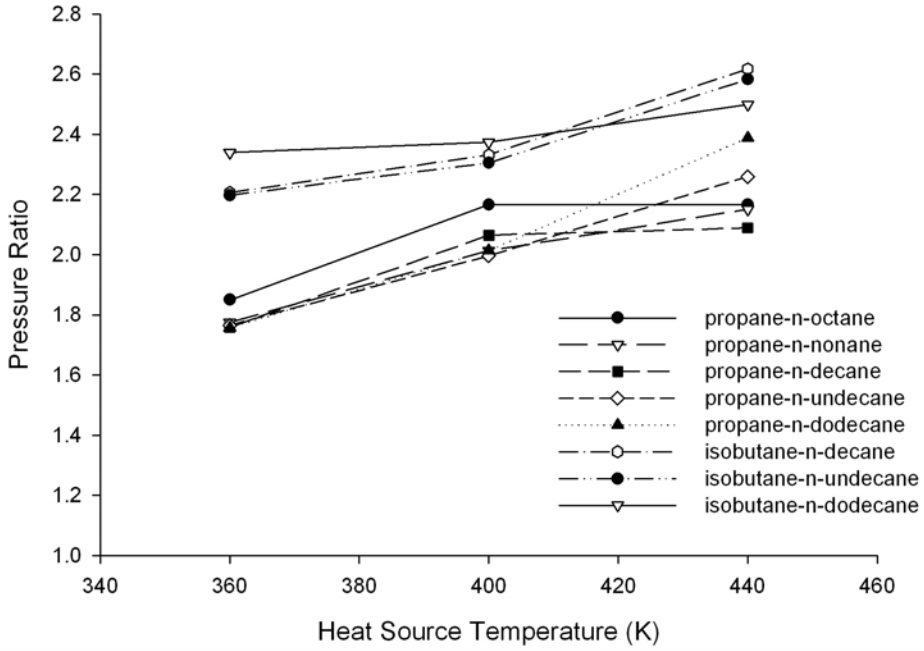

Fig. 5.8 Pressure ratios at optimum RUE

Discussion

A reason for the poorer performance seen with the organic fluids considered here appears to be lower pressure ratios. The pressure ratios seen with ammonia-water mixtures are much larger in comparison. The maximum pressure achievable at a certain basic solution concentration and heat source temperature is determined by the bubble pressure at the highest possible boiler temperature. In some cases, the turbine exit dryness constraint also limits the pressure ratio, which is not considered in Fig. 5.9. This limiting pressure ratio is plotted for two of the best performing organic fluid mixtures and for ammonia-water combination, in Fig. 5.9. It is clear that the limiting pressure ratio is much larger with ammonia-water mixtures. The limiting pressure ratio curve for the ammonia-water mixtures also shows a large reduction from lower to higher ammonia-mass fraction in the basic solution. At lower basic solution concentrations, a higher pressure ratio is achievable. However, vapor generation and the ammonia concentration in the vapor might be limited at the lower absorber pressures.

When the cycle is operated to obtain refrigeration, there are several tradeoffs that come into play during operation. The low pressure has to be small enough that the vapor remains relatively dry at the cold temperature condition at the turbine exit. Therefore, the vapor in the turbine has to be rich in the volatile component to produce refrigeration. A higher concentration of the basic solution (larger absorber pressure) would allow more vapor generation since there is more volatile component present, but the purity required in the vapor is larger since the dryness constraint could be violated at the pressures and temperatures of the turbine exit. Further, for higher mass fractions in the absorber, the

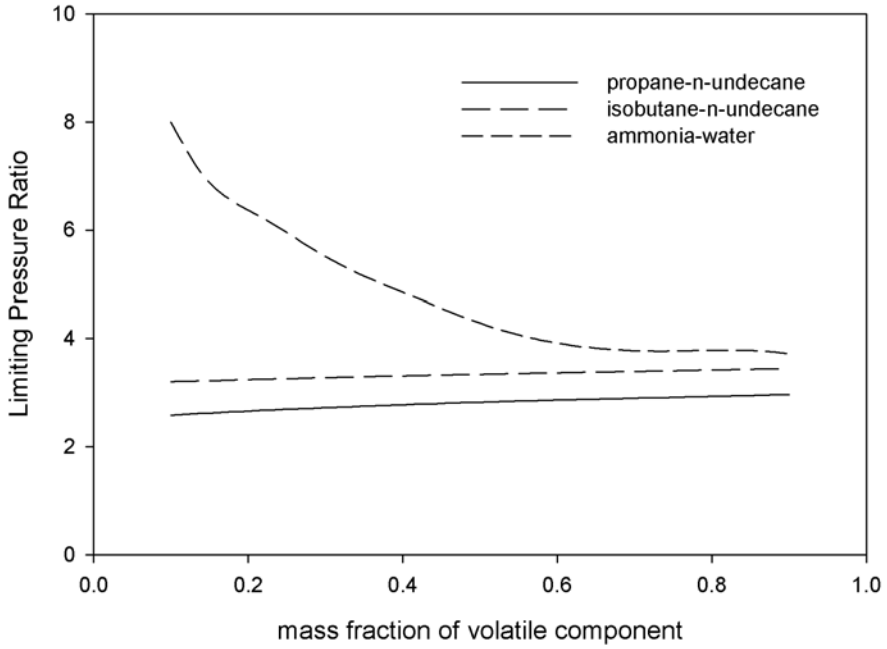

Fig. 5.9 Maximum (limiting) pressure ratio using some working fluid mixtures at various basic solution concentrations in the absorber and using a 360 K heat source

limiting pressure ratio is lower which affects the temperature drop that could be achieved. The temperature drop of the vapor on expansion over a certain pressure ratio is a property of the fluid. If the temperature drop is not large, the rectification may be used to lower the turbine inlet temperature such that the desired cold temperature is reached at the turbine exit.

Factors Affecting Cycle Performance

A general discussion on the effect of mixture properties and some cycle parameters on the behavior of the cycle follows.

Rectification

A common characteristic in all optimized results is the requirement of rectification where the vapor is partially condensed resulting in a drop in temperature of the vapor

going into the turbine (assuming no superheating). Rectification increases the concentration of the vapor such that the mass fraction of the volatile component is larger. Figures 5.10 and 5.11 show on a phase diagram, some of the state points of the cycle optimized for exergy efficiency, using a mixture of isobutane and n-decane as the working fluid. The heat source fluid inlet temperature is 400 K. Figure 5.10 consists of two sets of bubble and dew point lines, corresponding to the system high and low pressure. Several horizontal lines indicating the temperature at different points in the cycle are drawn on the plot. The point at which the absorber temperature line intersects the low pressure bubble point curve (location 1) determines the strong solution concentration. When this solution is heated to the boiler exit temperature (location 2), the point at which the boiler temperature line intersects the high pressure dew point curve gives the equilibrium vapor concentration. A partial condensation process (rectification) would result in a higher concentration vapor (location 4), which can then be expanded to low temperatures. Figure 5.11 shows a portion of Fig. 5.10 in more detail.

If no rectification were to be done, the vapor exiting the boiler would expand through the turbine to the low pressure at condition 5'. Rectification allows the expansion to condition 5, which is at a much lower temperature. Rectification reduces the temperature at the turbine inlet which produces lower temperatures at the turbine exit when expanded over the allowable pressure ratio.

Boiler Conditions

Vapor produced in the boiler should be of high concentration so that rectification required is small. Rectification is an additional process that involves irreversibility and lowers the amount of vapor available to spin the turbine. Minimizing the need for

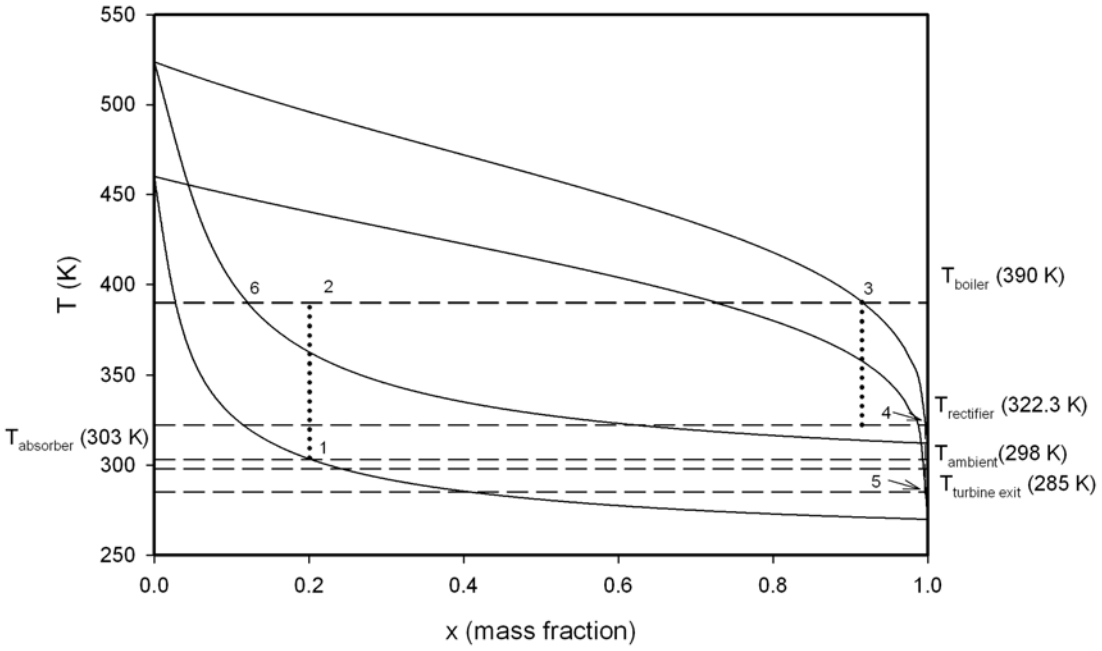

Fig. 5.10 Phase diagram of a part of the cycle using isobutane-n-decane at 400 K, optimized for exergy efficiency

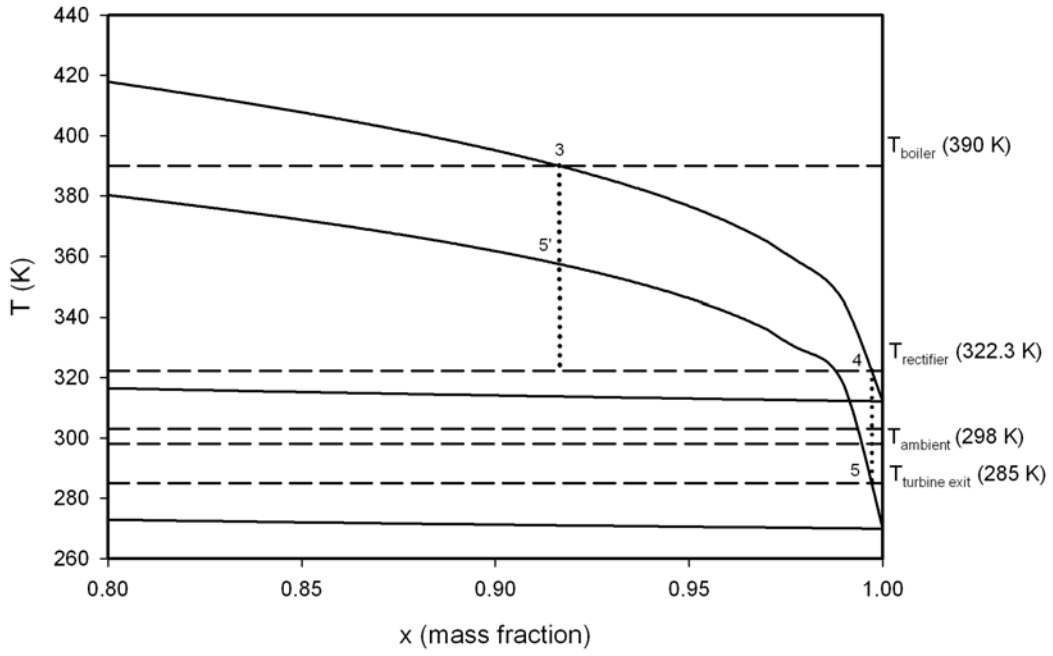

Fig. 5.11 Close up of a portion of Fig. 5.10

rectification will improve the efficiency of the cycle. For a given concentration of the basic solution (also called strong solution) and boiler pressure, a higher vapor fraction in the boiler results in vapor with a lower concentration of the volatile component, requiring more rectification.

The influence of the vapor fraction on the exergy efficiency can be explained from the efficiency definition in Eq. (5.1). Since the contribution of the cooling component is small, consider the approximate expression given below.

$$\eta_{exergy} \approx \left(W_{net}\right)/\left(E_{hs,in} - E_{hs,out}\right) \tag{5.3}$$

This can also be written, on the basis of Fig. 5.1 as

$$\eta_{exergy} \approx \dot{m}_8\left(h_8 - h_9\right)/\dot{m}_{hs}\left(\varepsilon_{hs,in} - \varepsilon_{hs,out}\right) \tag{5.4}$$

Here ε is the specific exergy of the heat source fluid. In the optimized case, the goal is to maximize the numerator while minimizing the denominator. The work output requires large vapor flow rate and enthalpy drop across the turbine. Specific enthalpy drop across the turbine for a given working fluid is a strong function of the pressure ratio in the cycle. The low pressure is governed by the absorber temperature and strong solution concentration. The high pressure is limited by the heat source inlet temperature and the basic solution concentration and the resulting ability to produce vapor. The vapor mass flow rate is a function of the heat source temperature, strong solution concentration (mass fraction), system high pressure and rectifier exit temperature.

In the denominator, a large heat source flow rate generally results in a smaller specific exergy drop for the fluid. Naturally a tradeoff exists, where at optimum conditions, a small heat source flow rate is desirable, along with a moderate temperature drop in the heat source fluid.

The effect of vapor fraction in the boiler can be qualitatively analyzed by considering the cycle shown in Fig. 5.1. A part of the strong solution is boiled to produce vapor and hot weak solution. A portion of the heat supplied in the boiler is utilized in generating vapor. The remaining heat is used to raise the temperature of the solution. This heat is subsequently recovered in the solution (recovery) heat exchanger, and used to preheat the strong solution. If the vapor fraction in the boiler is very low, the fraction of heat transferred to the vapor is low. Since it is the vapor that expands through a turbine to produce work, the cycle efficiency is smaller under these conditions. A reasonably high vapor fraction is required to get good efficiencies.

Basic Solution Concentration

Figure 5.12 shows the effect of a lower pressure on the low temperature achievable in a cycle. The T-x diagram shows the optimized case obtained using a propane-n-hexane mixture with the heat source at 400 K. The low pressure was 3.45 bars (0.345 MPa). The bubble and dew point curves for 3 bar (0.3 MPa) are also shown in the figure. The vapor leaving the turbine is at location 5 in figure, under optimized conditions, with a 285 K limit imposed for refrigeration at turbine exit. If the low pressure was 3 bars, it can be seen that:

- A lower turbine exit temperature would be achieved (5'). Note that propane is a wetting fluid, unlike isobutane.
- The basic solution concentration would be lower (1').
- The vapor fraction produced would be lower

Pressure and Temperature Ratio

The temperature drop across a turbine is determined by the pressure ratio. The pressure ratio is also a measure of specific work output in the turbine. A qualitative

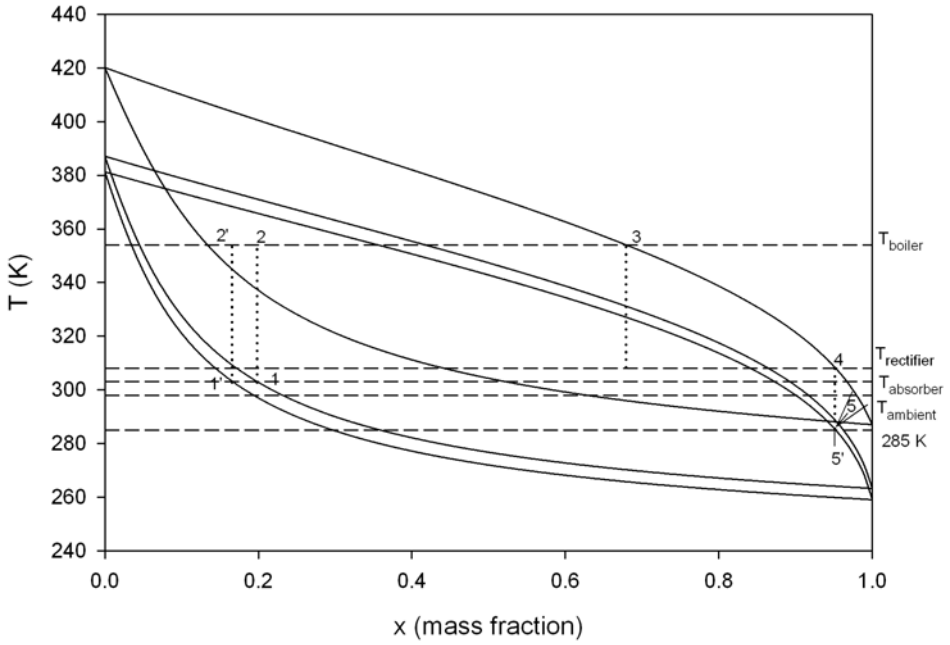

Fig. 5.12 Effect of low pressure (propane-hexane mixture as working fluid)

understanding of achievable temperature drops with pressure ratios can be obtained by considering perfect gas behavior. Assume that the vapor is superheated throughout the expansion process and also that the vapor behaves as a perfect gas with constant specific heat in the expander. These assumptions are not really valid for the results discussed in this dissertation. Superheating at optimum conditions is seen only in few of the ammonia-water mixture optimized results. Since the vapor is in or close to the two-phase region during expansion, perfect gas behavior is not expected. The relatively small temperature range considered here does support the assumption of constant specific heat.

For a perfect gas, the change in entropy can be related as

$$s_2 - s_1 = c_p \ln(T_2/T_1) - R \ln(p_2/p_1) \qquad (5.5)$$

For isentropic expansion, it is easily seen that

$$\frac{T_2}{T_1} = \left(\frac{p_2}{p_1} \right)^{\frac{R}{c_p}} \tag{5.6}$$

The non-dimensional term, R/c_p, is a predictor of the ability to obtain low temperatures at the turbine exit with reasonable pressure ratios. Table 5.3 gives a list of fluids and the temperature ratio that would be obtained for certain pressure ratios.

Table 5.3 Calculated R/c_p values for certain gases in the temperature range of the cycle being studied

Gas	c_p (J/mol.K)	R/c_p
water (steam)	37.1	0.2243
ammonia	36.5	0.2275
air	29.4	0.2827
ethane	58.1	0.1431
propane	92.9	0.0895
isobutane	116.2	0.0715

It is seen that for the same pressure ratio, organic working fluids have a much smaller temperature ratio. The optimum pressure ratio is limited by several factors. The system high pressure is limited by the heat source temperature and the basic solution concentration. The low pressure is limited, once again by the heat source temperature and the high pressure, since if the pressure is too low, the basic solution concentration is also lowered. This increases the bubble point in the boiler and limits the vapor fraction.

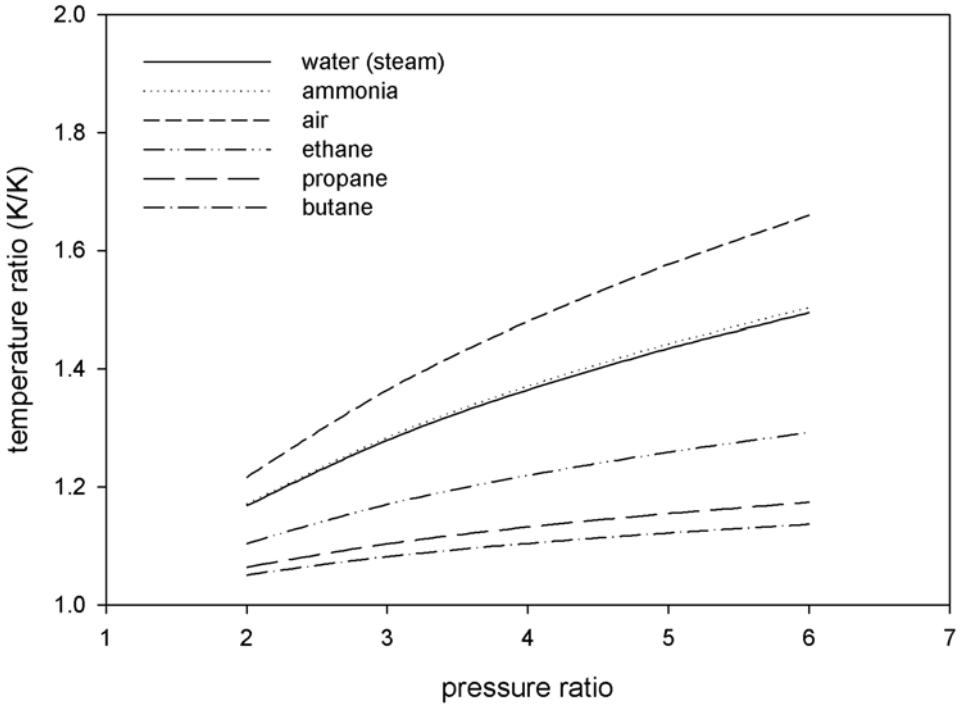

Fig. 5.13 Calculated isentropic temperature ratio as a function of pressure ratio using perfect gas assumptions

Another factor limiting the pressure ratio is the tendency to form wet vapor. Certain fluids tend to go into the two-phase region during expansion. While this is not a constraint for the organic fluids considered here, it is definitely a limiting factor for ammonia. The constraint setting dryness at the turbine exit is never at the bound in any of the organic fluid simulations. That is not the case in simulations with ammonia-water.

The temperature drop during expansion in the two-phase region for a binary mixture is difficult to study analytically. For pure components, the Clausius-Clapeyron equation (Eq. 5.5) relates temperature change to pressure change in the two-phase region.

$$\left(\frac{dT}{dp}\right)_{sat} = \frac{v_{fg}}{s_{fg}} \tag{5.7}$$

A higher ratio of specific volume change to entropy change would be desirable for the volatile component used in the cycle.

Volatility Ratio

The shape of the bubble and dew point curve plays a role in the efficiency that can be obtained using a certain working fluid pair in the combined power and cooling cycle. The difference in boiling points of the two fluids is a parameter that would clearly affect the shape of the curve. Another measure of the shape of the diagram is the volatility ratio. The volatility ratio is defined as [55]

$$\alpha_{21} = \frac{y_{2g}/y_{2f}}{y_{1g}/y_{1f}} = \frac{x_{2g}/x_{2f}}{x_{1g}/x_{1f}} \tag{5.8}$$

Here α_{21} is the volatility ratio of component 2 of the (binary) mixture with respect to component 1. This is defined as the ratio of the mole fraction y (or mass fraction x) of the components in the vapor and liquid phases. In general, the volatility ratio is a measure of the shape of the vapor liquid equilibrium (VLE) curves. Pairs with a higher volatility ratio will boil off more of the volatile component than the higher boiling component. Similarly, during condensation, the non volatile fluid will condense out more easily.

The volatility ratio as defined in Eq. (5.8) is an inconsistent factor. The volatility ratio changes with temperature between the bubble and dew points. The definition given here would give a single value at a given pressure only if the bubble and dew point curve can be fitted to exponential functions. Most binary pairs do not fit that description. It is therefore not easy to use this definition to compare working fluids. Table 5.4 lists the

volatility ratio of some pairs of working fluids considered. The evaluations in this table were done at the pressure corresponding to the optimum efficiency at 400 K and at the average of the bubble and dew point temperatures corresponding to a concentration of 50% by mass.

Among the components listed in Table 5.4, for a given volatile component, the absorbent pair with a higher volatility ratio performs better. However, with isobutane as the volatile component, there was a drop off in efficiency between using n-undecane and n-dodecane. Therefore, there may be a point where the high volatility ratio is not advantageous anymore.

Table 5.4 Volatility ratio of selected pairs

Volatile	Absorbent	α_{21}	Pressure bars
ammonia	water	17.0	20.0
propane	hexane	16.9	7.0
propane	decane	62.8	15.8
isobutane	hexane	6.1	6.6
isobutane	decane	71.3	5.3

Liquid Formation During Expansion

The slope of the dew point intercept on a T-s projection of the phase diagram would determine the tendency of the working fluid to form liquid during isentropic expansion. In the literature, a factor known as the *I* factor is used to determine the

tendency of the (pure) working fluid to form liquid during isentropic expansion. The non-dimensional quantity, *I* is defined as [50, 51]:

$$I = 1 - \left(\frac{ds}{dT} \frac{T}{c_p} \right)_{sat.vap.} = 1 - T \left(\frac{ds}{dh} \right)_{sat.vap.} \tag{5.7}$$

The factor has a small dependence on the temperature at which it is evaluated. Nevertheless, the *I* value gives a fair idea of the "wetting tendency" of the fluid. The tendency of a working fluid to enter the two phase region can be determined from the slope of the line partitioning the vapor and two phase region in the T-s diagram.

Table 5.5 *I* values of certain pure components at 300 K and corresponding saturation pressure

Fluid	Index I Evaluated at 300 K
Water	3.10
Ammonia	4.55
Propane	1.21
iso-butane	0.82
n-hexane	0.74

A value of *I* greater than 1 means that the fluid becomes wet on isentropic expansion. If *I* is less than 1, the vapor is always superheated at the turbine exit. It is seen that the hydrocarbon working fluids considered here have small values of *I*, while ammonia and water have values that are substantially larger than 1. Ammonia has a relatively larger tendency to form liquid in the turbine. Hydrocarbons therefore can be expanded over a larger pressure ratio in the turbine without the two-phase region being a

problem. Ammonia and water are highly wetting fluids compared to the organic working fluids considered here.

There is an interesting aspect of binary mixture wetting behavior that was observed using the properties programs. The wetting tendency of the fluid changes with even a small amount of non volatile component present. This is particularly pronounced when the difference in boiling points is very high. Figures 5.14-5.17 show the projection into the T-s plane of the bubble and dew point of three organic fluid pairs and the ammonia-water pair. The change in the slope of the vapor dome is clearly seen. Figure 5.15 shows how a non-wetting isobutane mixture becomes wetting with small amounts of n-undecane. Note that due to the concentrated nature of the vapor, the dryness fraction would remain high even if all of the higher boiling component condenses.

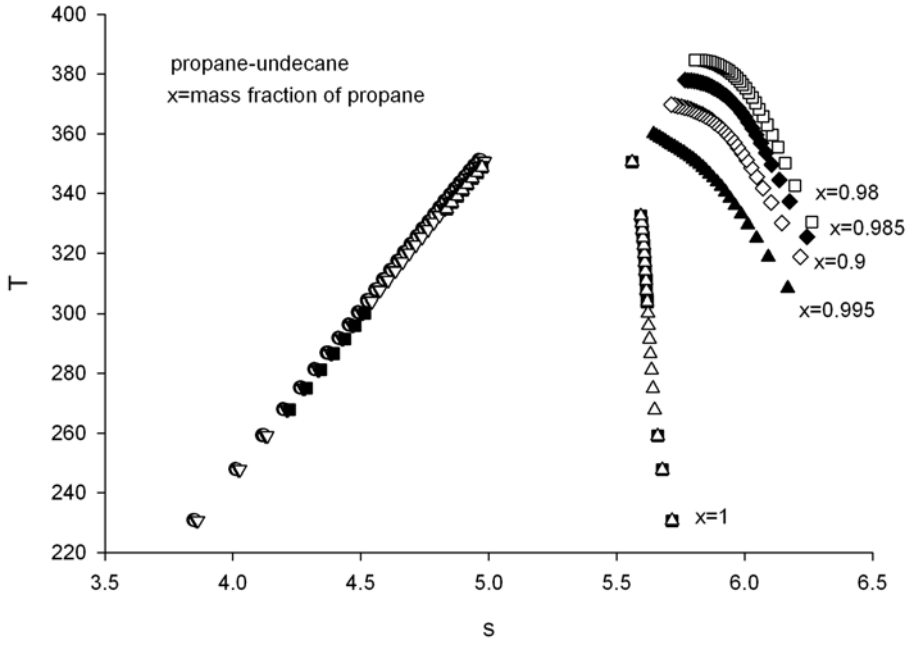

Fig. 5.14 T-s diagram for concentrated propane-n-undecane mixtures

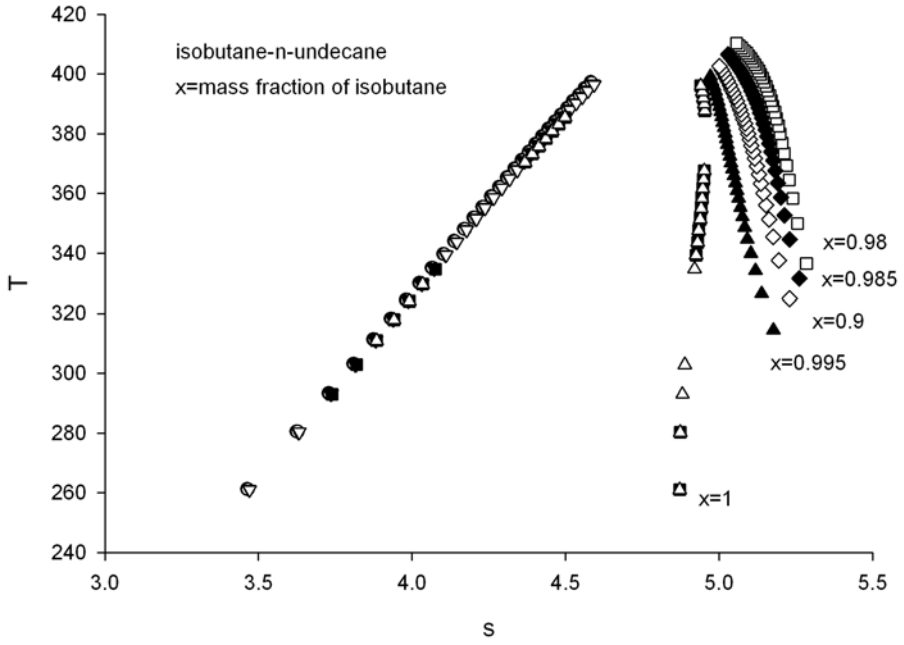

Fig. 5.15 T-s diagram for concentrated isobutane-n-undecane mixtures

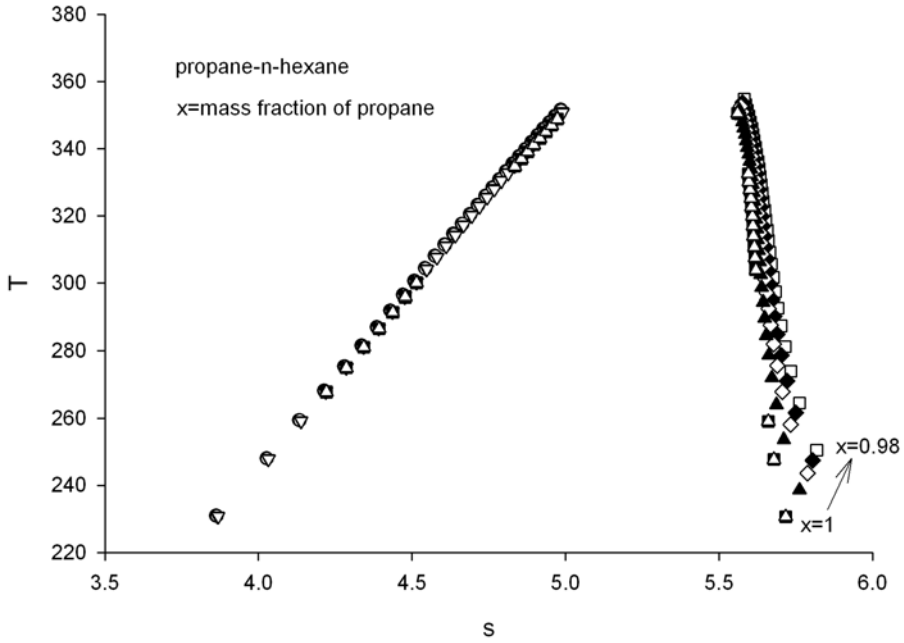

Fig. 5.16 T-s diagram for concentrated propane-n-hexane mixtures

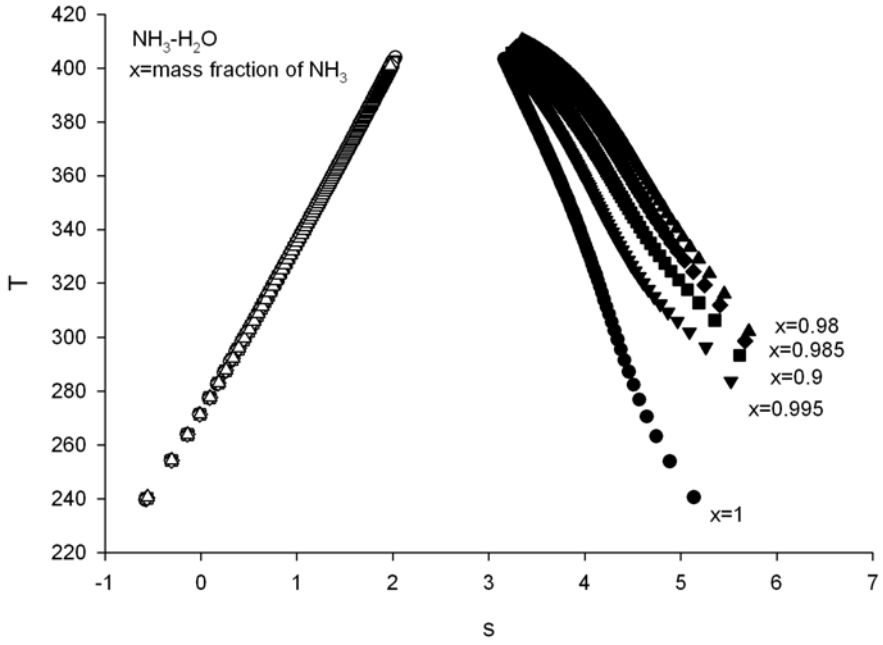

Fig. 5.17 T-s diagram for concentrated ammonia-water mixtures

Conclusions

It is shown that organic working fluids can be used in a combined power and cooling cycle. Based on the optimization studies, ammonia-water mixtures give better efficiencies when used in the cycle, as compared to a mixture of organic working fluids. The low temperature range that can be achieved using these mixtures is also limited, when compared with the ammonia-water pair.

These fluids have a large molar specific heat c_p , that limits the ability to get low temperatures over reasonable pressure ratios. Therefore, substantial rectification is required in order to get purer vapor and lower temperatures at turbine inlet to get sufficiently low temperatures. In the organic fluid mixtures considered, isobutane

performs better as the volatile component that propane. A higher volatility ratio of the mixture appears to improve the performance in the cycle.

CHAPTER 6
RESULTS AND DISCUSSION: IMPROVED CONFIGURATIONS

Motivation

Optimization results of the cycle using the basic configuration given in Fig. 4.1 clearly show that the basic cycle configuration has some limitations. At conditions giving maximum RUE, there is a large unutilized fraction of heat source exergy lost due to the inability of the cycle to remove heat from the source fluid. This leads to low values of resource utilization efficiency. The optimum exergy efficiencies obtained using the cycle are reasonably good.

In order to improve the performance of the cycle, modifications to the basic cycle configuration were proposed to utilize the available energy better. Various configurations were modeled and optimized using ammonia-water mixtures as the working fluid. Some of the combinations showed improved efficiencies, particularly with respect to resource effectiveness (RUE). The assumptions used for all the optimization in this chapter are similar to those described in Chapters 3 and 4. Isentropic efficiencies were assumed for the turbine and pumps. A turbine exit temperature upper limit of 270 K was set for all simulations.

Reflux Mixed with Boiler Inlet

A slight improvement in efficiency can be achieved by modifying the configuration such that the condensate from the rectifier mixes with the strong solution stream entering

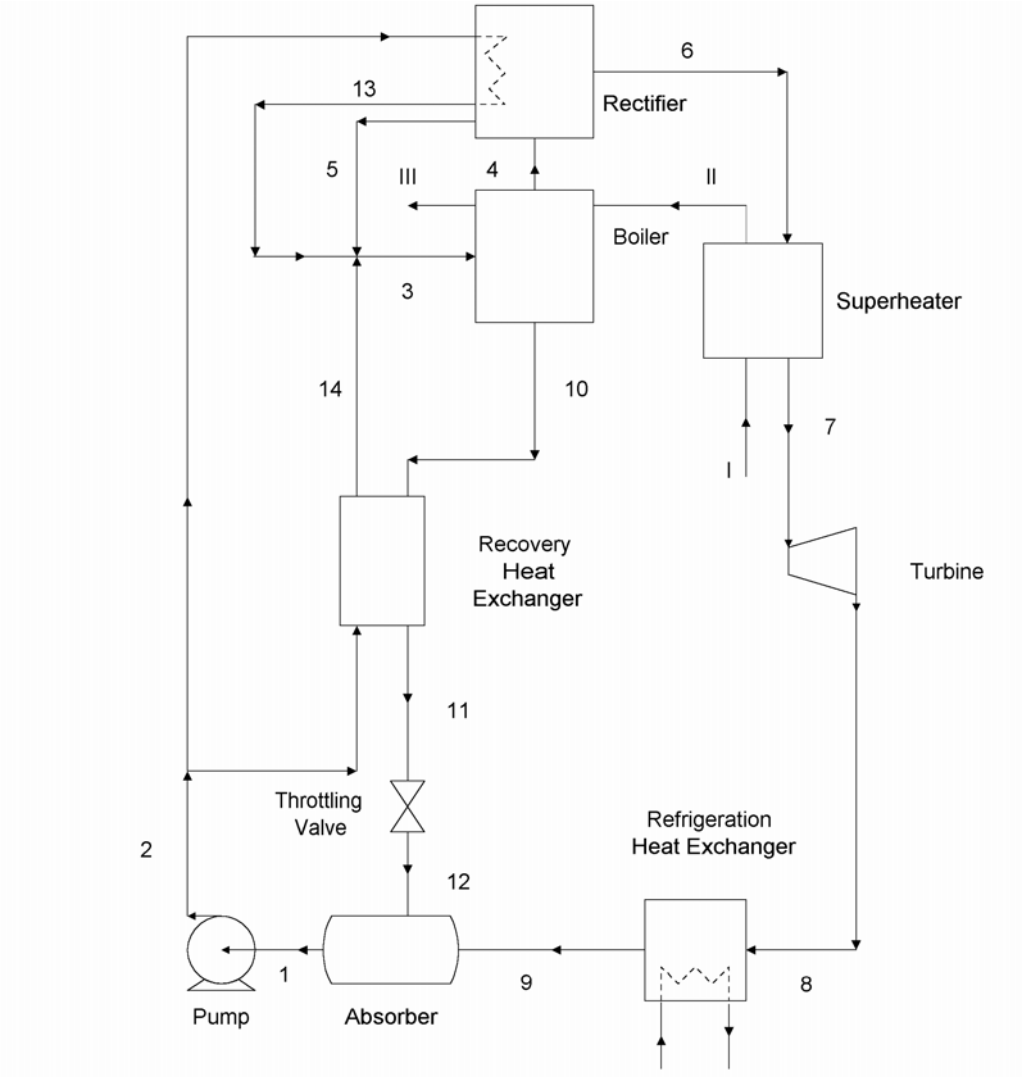

Fig. 6.1 Modification of the basic cycle configuration which has the liquid condensate from the rectifier mixed with the strong solution at the boiler inlet

the boiler. This configuration is shown in Fig. 6.1. The condensate from the rectifier is richer in ammonia content compared to the strong solution stream. Therefore it is possible to increase the concentration of the boiler inlet stream by this mixing process. A higher concentration results in a higher vapor fraction in the boiler. Note that in the configuration shown in Fig. 6.1 pressure drop between the boiler inlet and the rectifier is neglected. In reality, a pressure drop will exist and some sort of pumping arrangement

will be needed to get the liquid from state 5 to mix with streams 13 and 14. There are other alternate designs that can be used in practice to approximate this configuration.

The improvement in RUE seen with this modified configuration is small. However, exergy efficiencies improve noticeably (see Fig. 6.2). The improvement seen is larger at the higher heat source temperatures of 440 and 480 K. At these temperatures, the base cycle configuration shows a limited increase in boiler exit temperatures (from the 400 K case) and a larger rectification requirement. This results in lower exergy destruction in the boiler (hear addition) due to better thermal matching, as shown by comparing Figs. 6.3 and 4.14. The boiler vapor fraction is slightly higher in the modified configuration.

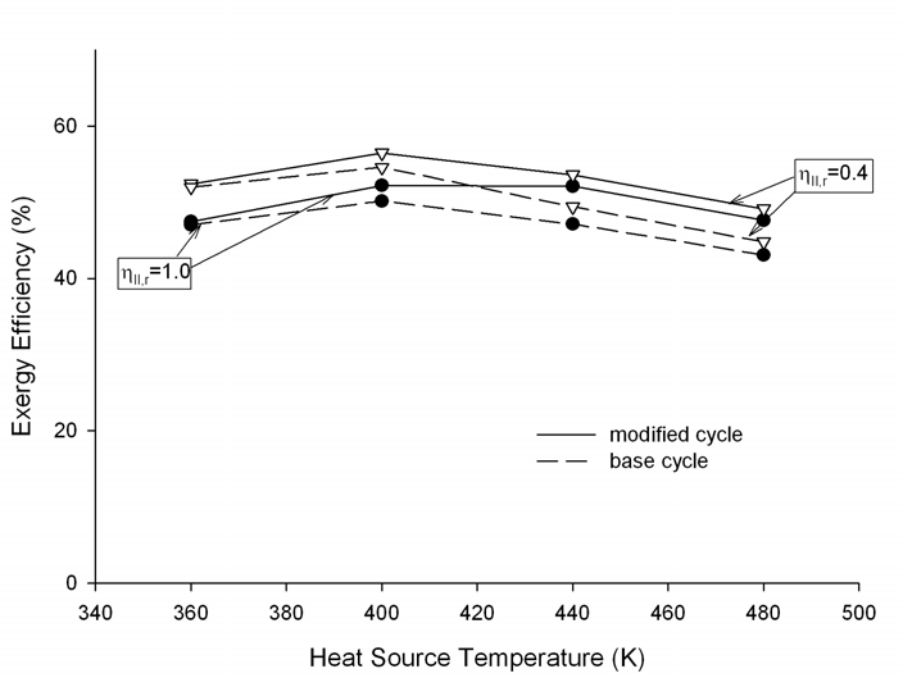

Fig. 6.2 Optimum exergy efficiencies obtained with the modified configuration shown in Fig. 6.1

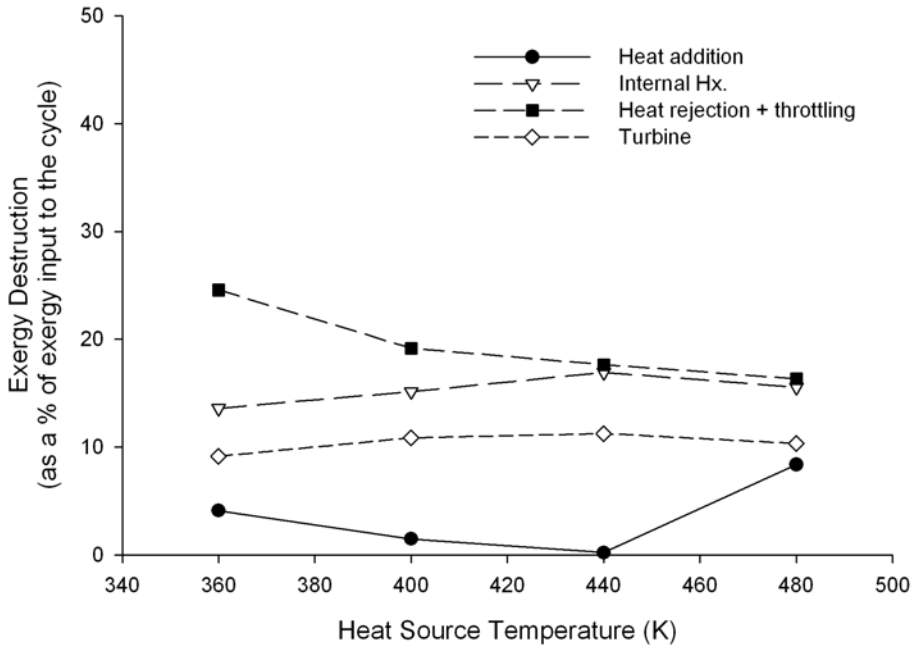

Fig. 6.3 Major exergy destruction categories for the modified cycle, at optimum exergy efficiency conditions.

Addition of a Preheater

Two configurations of the cycle have been discussed thus far. These are the basic cycle configuration in Fig. 4.1 and the one shown in Fig. 6.1, where the condensate from the rectifier is assumed to be mixed with the strong solution feed entering the boiler. The RUE is low in both these configurations. High RUE is important for the use of this cycle in geothermal and waste heat recovery applications. An exergy analysis has shown that the largest losses are due to the unrecovered exergy from the heat source. A slightly different configuration is shown in Fig. 6.4 that has the strong solution stream split into three parts after the system pump. One stream (2-3 in Fig. 6.4) is used to recover heat from the weak solution. The second stream (2-5) is used to recover the heat of condensation from the rectifier. The heat source fluid preheats the third stream (2-4).

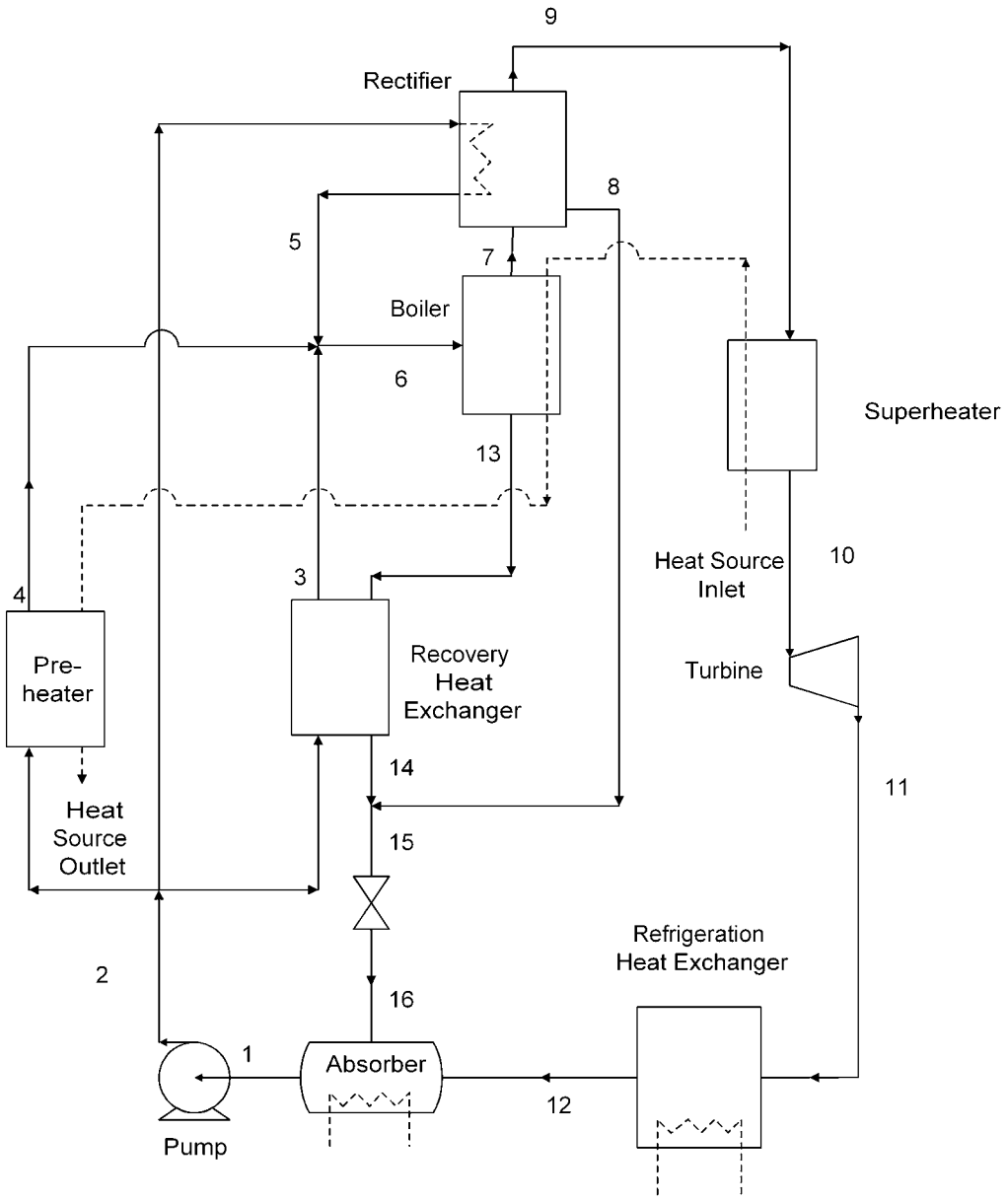

Fig. 6.4 Modified cycle configuration with part of the basic solution being preheated by the heat source fluid.

This configuration allows the removal of more heat from the heat source at the expense of recovering heat from the weak solution, with a possible increase in optimum RUE. However, the modified configuration does not lead to an increase in the exergy efficiency. Unrecovered exergy in the heat source fluid has no influence on the exergy efficiency. Instead, it is more important to recover exergy from the weak solution in the recovery heat exchanger. This was also clear from optimization results, since the flow through the preheater was seen to be zero under maximum exergy efficiency conditions.

When optimizing the cycle configuration shown in Fig. 6.4 with respect to RUE, an improvement is seen in the values. Figure 6.5 shows optimum efficiencies using a strict definition of RUE, Eq. (4.1) and an effective efficiency assuming the second law efficiency of refrigeration production to be 40 %. An improvement in efficiency is clearly seen in both cases. The resulting optimum conditions are seen to have larger absorber pressures, and higher vapor fractions in the boiler. Similarly, this configuration optimized for work output alone also performs better than the basic cycle configuration (data not shown in plots). As expected, an exergy analysis shows much lower losses through the pathway of unrecovered exergy in the heat source, while the losses associated with throttling and heat rejection increase, since all the heat is not recovered due to the lower flow. From the perspective of system design, this indicates a requirement for larger heat transfer area in the absorber. The size of the recovery heat exchanger would be smaller, but a separate preheater would be required adding to heat transfer area requirements.

Jet Pump Assisted Cycle

It would be desirable to have a low turbine exit pressure order to have higher pressure ratio and temperature drop through the turbine. However, higher absorber

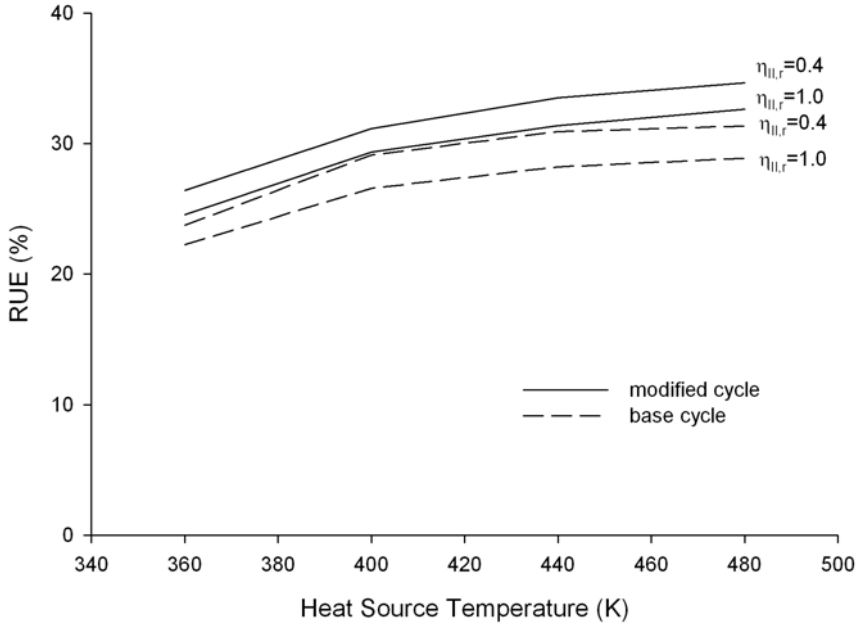

Fig. 6.5 Optimized RUE for the modified configuration in Fig. 6.4 compared to the base configuration in Fig. 4.1

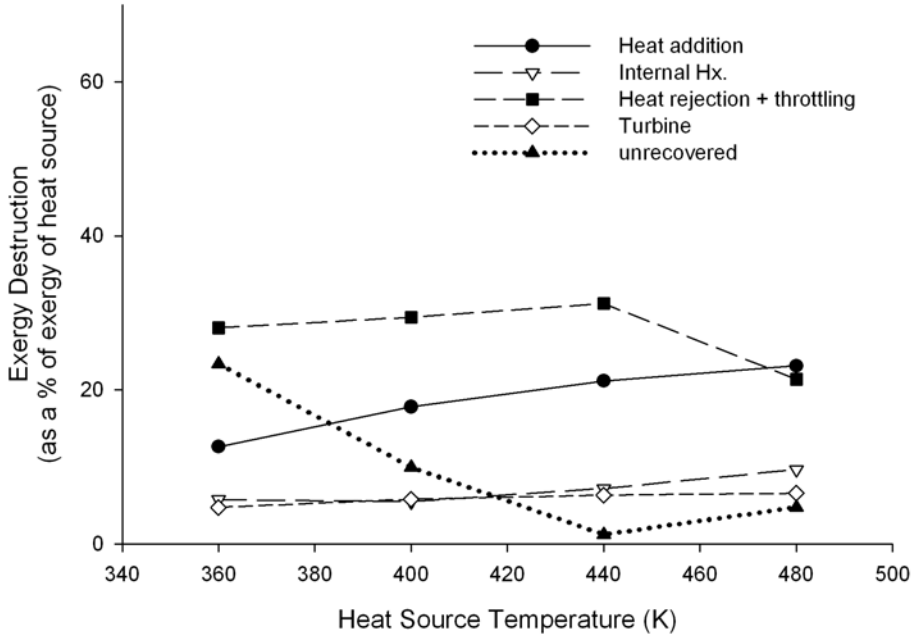

Fig. 6.6 Major exergy losses in different parts of the modified cycle, optimized for RUE

pressures are desirable so that the basic solution mass fraction is high resulting in higher vapor flow rates. All the cycle configurations studied so far have the absorber pressure set to be the same as the turbine exit pressure. In practice, taking into account pressure drops in the system, the absorber pressure would be a little lower than the turbine exit pressure. One of the ways of boosting the absorber pressure above turbine exit would be to use a jet pump to raise the pressure of vapor leaving the turbine. The high pressure liquid returning from the boiler to the absorber would be the high pressure primary fluid that is used to raise the pressure.

The advantages of using a jet pump in the combined power and cooling cycle are the following:

- The expansion in the turbine can be carried out to a pressure lower than the absorber pressure.
- Higher absorber pressures allow for lower bubble points of the strong solution and larger vapor fractions in the boiler.
- Lower rectification would be required to achieve lower temperatures.
- The vapor will be well mixed and entrained in the liquid in the form of small bubbles. This will simplify the design of the absorber condenser substantially.

Jet Pump Background

Jet pumps and ejectors are a class of fluid pumping devices that have been studied for a number of years. In a jet pump, a high pressure primary fluid is expanded through a primary nozzle. At the low pressure region after the primary nozzle exit, a secondary nozzle is used to introduce the secondary fluid. A mixing section follows in which momentum and kinetic energy is transferred from the primary fluid to the secondary fluid and the secondary fluid is properly entrained and mixed in the primary fluid flow. A diffuser is then used to raise the pressure of the mixture. The primary and secondary

fluids could be any combination of liquid, gas, or a two-phase mixture. An ejector is a term that generally refers to a device where both the primary and secondary fluids are gases.

There are several well known applications of jet pumps and ejectors. In steam jet refrigeration, water is used as the working fluid. High pressure steam is used as the primary fluid in an ejector to compress the water vapor from the evaporator. Jet pumps are also used to create and maintain vacuum in several chemical operations such as distillation and evaporation and to remove accumulated non-condensable gases from steam power plant condensers. Ejectors are also found in jet propulsion systems such as an ejector ramjet type engine. The use of jet pumps, ejectors or similar devices have been suggested also been suggested in power and refrigeration cycles. Different configurations have been investigated [56], which involves using ejectors in ammonia – water mixture based absorption refrigeration cycles. Nord et al. [57] discuss a combined power and cooling cycle, primarily for space applications that uses a jet pump. A patent search showed an idea very similar to the one being studied in this section. The patent [58] proposes the use of a device called a “hydrokinetic amplifier”, which somewhat resembles a jet pump, in absorption refrigeration cycles and power cycles. Unfortunately, there is no other literature or operational data available on this device or its application to ammonia-water based cycles.

Jet Pump Analysis

It is proposed that the liquid weak solution from the boiler be used as the primary fluid in the jet pump. Simulation results indicated that the subcooled weak solution that has given up heat in the recovery heat exchanger does not provide much of a pressure boost. The hot, saturated weak solution works best for that purpose. The secondary fluid

is the low-pressure vapor exiting the refrigeration heat exchanger. The primary fluid is accelerated through a nozzle in order to achieve a higher velocity. This high speed primary fluid exits the nozzle with a large velocity and low static pressure. At this point, the secondary fluid (ammonia rich vapor) is introduced through a secondary nozzle into a mixing chamber. The secondary fluid is entrained in the primary fluid jet inside the mixing chamber. Mixing chambers are generally classified as two types, even though many mixing chamber geometries do not fit either category. These are the constant pressure type and constant area type mixing chambers. Within the mixing chamber, the secondary fluid is entrained in and accelerated by the primary jet. There is a transfer of momentum and kinetic energy from the primary jet to the secondary fluid. Assuming the mixing chamber is long enough, it is reasonable to say that the two streams are completely mixed at its exit.

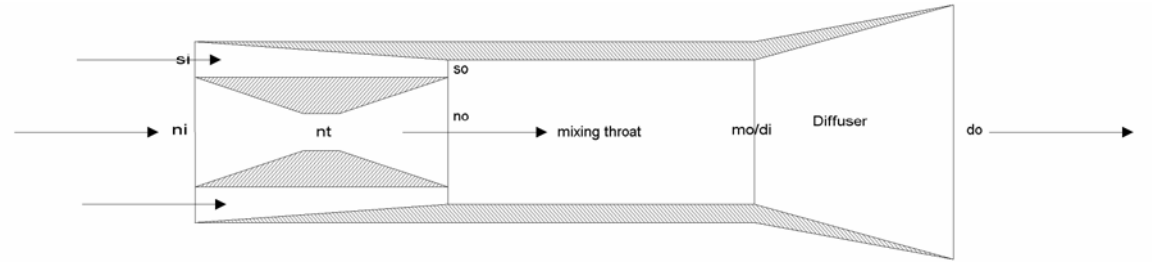

Fig. 6.7 Schematic drawing of a jet pump showing the different sections and the flow through it

The mixed stream subsequently enters the diffuser where the flow is slowed down and kinetic energy is used to compress the mixture. This compressed mixture would then be routed to the absorber-condenser where heat is removed from it and the vapor condenses back into the liquid.

The analysis presented here discusses the operation of a jet pump, as a part of the (ammonia-water based) combined power and cooling cycle. The model presented here is that used by Sherif et al. [59]. This model is then further simplified for use in the simulations.

An ideal nozzle would be modeled as an isentropic device. To incorporate losses, an isentropic efficiency is assumed for the nozzle. Since the primary fluid is a saturated binary liquid mixture, several issues become important in the analysis. As the pressure drops within the nozzle, the fluid in the nozzle begins to vaporize accompanied by a drop in the temperature of the fluid. Since, the speed of sound in a two-phase mixture is significantly lower than that in a liquid there is a possibility that sonic conditions could be achieved within the nozzle. In this case, the nozzle would have to be designed as a converging diverging nozzle in order to achieve the desired pressure at the nozzle exit. For analysis purposes, the flow would also have to be assumed to be homogeneous. In other words, the gas is evenly distributed in the liquid phase or vice versa. Choking at the nozzle throat would also limit the achievable mass flow rate in a given nozzle geometry. The nozzle would have to be suitably designed in order to accommodate the design mass flow rate of primary fluid in the cycle.

In the mixing section, the primary and secondary streams mix and exchange momentum and kinetic energy. Since the volume of liquid is very small in comparison to the volume of vapor, it is assumed that the liquid would be finely dispersed as droplets within the vapor at the mixing section exit.

The mixture then enters the diffuser where the velocity is slowed down accompanied by an increase in pressure, and partial condensation of some vapor back

into liquid. If the flow in the mixing chamber is supersonic in nature, a shock wave can be expected at or close to the diffuser entrance. Since the pressure at the diffuser exit will be much lower than that of the primary fluid entering the nozzle, condensation is not expected to be significantly large. Further, the binary mixture nature of the fluid also implies a lack of a sharp phase transition. Therefore, the phenomenon of condensation shock is not expected within the diffuser. Equations that describe the behavior of the jet pump are discussed below. The flow is assumed to be one dimensional, and homogenous at every point that a two phase mixture is analyzed.

Primary nozzle

In the ideal case, the nozzle is treated as an isentropic expansion device without any losses. If the occurrence of supersonic conditions were not a concern, the expansion through the nozzle would be treated as an isentropic process. The equations that need to be satisfied are the continuity and energy relationships.

Continuity:

$$\rho_{ni} V_{ni} A_{ni} = \rho_{no} V_{no} A_{no} \tag{6.1}$$

Energy:

$$h_{ni} + \frac{1}{2} V_{ni}^2 = h_{no} + \frac{1}{2} V_{no}^2 \tag{6.2}$$

Isentropic Condition:

$$s_{ni} = s_{no} \tag{6.3}$$

Knowing the exit pressure condition, and assuming an isentropic process, the remaining state properties can be calculated. The resulting enthalpy and density values should satisfy the continuity and energy equation respectively. An iterative process might be required to determine the nozzle design. The speed of sound in a two-phase mixture can

be very low. For example, the speed of sound in a 50-50 volumetric mixture of air and water is 1.5% of the speed of sound in water, and 6.8% of the speed of sound in air. That fact should indicate the possibility for sonic conditions being achieved in the nozzle. Therefore, it would be more likely that the nozzle is a converging – diverging nozzle that will have to be analyzed in two sections. From the inlet to the throat and from the throat to the nozzle outlet.

The fundamental equations are the same.

$$\rho_{ni} V_{ni} A_{ni} = \rho_{nt} V_{nt} A_{nt} \tag{6.4}$$

$$h_{ni} + \frac{1}{2} V_{ni}^2 = h_{nt} + \frac{1}{2} V_{nt}^2 \tag{6.5}$$

$$s_{ni} = s_{nt} \tag{6.6}$$

In addition, the condition for choked flow at the nozzle throat applies, which means that the Mach number at the throat is unity. The local speed of sound at the throat is calculated as:

$$a_{nt} = \sqrt{\left(\frac{\partial p}{\partial \rho}\right)_s} \tag{6.7}$$

$$M_{nt} = \frac{V_{nt}}{a_{nt}} = 1 \tag{6.8}$$

Obviously, this condition limits the mass flow rate through a given throat cross-sectional area. The throat to nozzle outlet calculations can be performed easily assuming isentropic expansion. It would be reasonable to assume that the flow would not revert to subsonic conditions within the nozzle. From the energy equation, it can be seen that the change in enthalpy of the fluid through the nozzle is converted to a gain in the kinetic energy of the weak solution.

Secondary nozzle

The low pressure secondary fluid, which in this case is ammonia rich vapor from the refrigeration heat exchanger is introduced via a secondary nozzle into the mixing section entrance of the jet pump. An isentropic assumption allows for the calculation of the condition of the secondary fluid at the mixing section inlet. The pressure is assumed to be the same as the primary nozzle outlet pressure.

$$\rho_{si} V_{si} A_{si} = \rho_{so} V_{so} A_{so} \tag{6.9}$$

$$h_{si} + \frac{1}{2} V_{si}^2 = h_{so} + \frac{1}{2} V_{so}^2 \tag{6.10}$$

$$s_{si} = s_{so} \tag{6.11}$$

Mixing section

The mixing section is probably the most critical of all the components of a jet pump. There are two standard configurations that are assumed while modeling jet pumps in the literature. A constant area mixing section that has a uniform cross sectional area and a constant pressure mixing section which is shaped such that the pressure is constant throughout the mixing section length. Obviously, a constant pressure mixing section would be more difficult to design in practice. The primary fluid jet that enters the mixing section would start breaking up after a few diameters past the nozzle at its edges. Viscous interaction at the boundary of the primary jet and the secondary stream would entrain some of the secondary fluid into the flow. The jet would start breaking up at the boundaries. After a sufficient length of flow, one would expect to see a completely mixed flow.

One concern is the occurrence of what is called Fabri choking in the mixing section. For the case where there is a very small viscous interaction between the primary

and secondary streams, as the primary flow from the nozzle expands in the mixing section, the available flow area for the secondary flow reduces. It then becomes possible that the secondary flow would get choked, limiting the entrainment ratio achievable with a given jet pump/ejector.

The fluid that exits from the nozzle is a mixture of vapor and saturated liquid. It is assumed that the temperature difference between the secondary and primary streams is small enough not to have a significant effect on the liquid vapor equilibrium. For the constant pressure case, it is reasonable to assume that there is no condensation in the mixing section. For the constant area case (or in general, for all mixing sections excluding the constant pressure type), a rise in pressure would result in some condensation accompanied with a temperature rise. To model the mixing section the following equations are used. Define the mass entrainment ratio as:

$$\Phi = \frac{\dot{m}_s}{\dot{m}_p} \tag{6.12}$$

Equations of mass conservation, momentum and energy have to be solved in conjunction with the equation of state (properties correlations) to determine conditions at the mixing section exit

$$\dot{m}_p(1+\Phi) = p_{mo} A_{mo} V_{mo} \tag{6.13}$$

$$p_{no} A_{no} + p_{so} A_{so} - p_{mo} A_{mo} = \dot{m}_p(1+\Phi) V_{mo} - \dot{m}_p V_{no} - \dot{m}_p \Phi V_{so} \tag{6.14}$$

$$h_{no} + \frac{1}{2} V_{no}^2 + \Phi\left(h_{so} + \frac{1}{2} V_{so}^2\right) = (1+\Phi)\left(h_{mo} + \frac{1}{2} V_{mo}^2\right) \tag{6.15}$$

For the constant pressure case, the exit pressure is known while for the constant area solution, a value of pressure would have to be assumed and iterated until convergence. Notice that the analysis above assumes that the flow is completely mixed

at the mixer exit. The mixing section would have to be long enough for this to be accomplished. It has been experimentally verified for the case of LJG (Liquid Jet Gas compression) pumps that if mixing continues into the diffuser, there is degradation in the performance of the jet pump [60].

Diffuser

There is a very high chance that the flow at the diffuser inlet is supersonic, especially since it would be a relatively homogeneous mixture of liquid and gas. As this flow is decelerated to subsonic speeds, there is a good possibility of a shock wave developing. In practice, there are two ways that a supersonic mixture could be dealt with in a diffuser.

Case a: The diffuser inlet could be set to supersonic mixer exit conditions. An isentropic process is assumed. This is called the *second solution* of the diffuser flow problem. Operation in such a mode, while theoretically and experimentally possible, is very difficult. This is due to the stringent requirements on the geometry of the diffuser and the need for specific inlet conditions for the diffuser.

Case b: A more common solution, called the *first solution* assumes shock at the nozzle inlet. The Rankine-Hugoniot equations are used to model shock. The equations then would be as follows.

$$\rho_{mo} V_{mo} = \rho_{ss} V_{ss} \tag{6.16}$$

$$p_{mo} + \rho_{mo} V_{mo}^2 = p_{ss} + \rho_{ss} V_{ss}^2 \tag{6.17}$$

$$h_{mo} + \frac{1}{2} V_{mo}^2 = h_{ss} + \frac{1}{2} V_{ss}^2 \tag{6.18}$$

$$\rho = \rho(p, h) \tag{6.19}$$

Once the conditions after the shock are determined, isentropic assumptions can be used to determine the conditions at the diffuser exit.

Simplified Model Used in Simulation

For the purposes of integrating a jet pump with the cycle simulation, a more simplified model is used, which does not involve as many parameters as in the model discussed above, and is free of dimensional information about the jet pump. The simplified model assumes the following

1. The effect of choking in the primary nozzle is neglected. The nozzle is modeled with an isentropic efficiency of 0.6. Nozzles are generally efficient devices. The low isentropic efficiency assumed is in order to compensate for assuming an ideal mixing section.
2. The pressure drop in the secondary nozzle is neglected.
3. Mixing section is assumed to be without any losses. In general, the process of mixing usually is where the most losses occur in a jet pump. This section has a high speed jet mixing with and entraining the secondary flow. Although the momentum transfer is relatively efficient, the transfer of kinetic energy between the streams is not. Mixing losses are lumped with the primary nozzle isentropic efficiency.
4. Shock at the diffuser inlet is ignored. The diffuser is modeled using an isentropic efficiency of 0.8.

This model is somewhat similar to assuming an expander-compressor tandem operating to expand the primary stream and compress the mixed primary-secondary streams. Jet pumps are normally low efficiency devices. The assumptions above imply a total efficiency of 0.48 for the jet pump, which might be a slightly optimistic assumption. Efficiencies of up to 0.40 have been reported for liquid-air jet pumps [61].

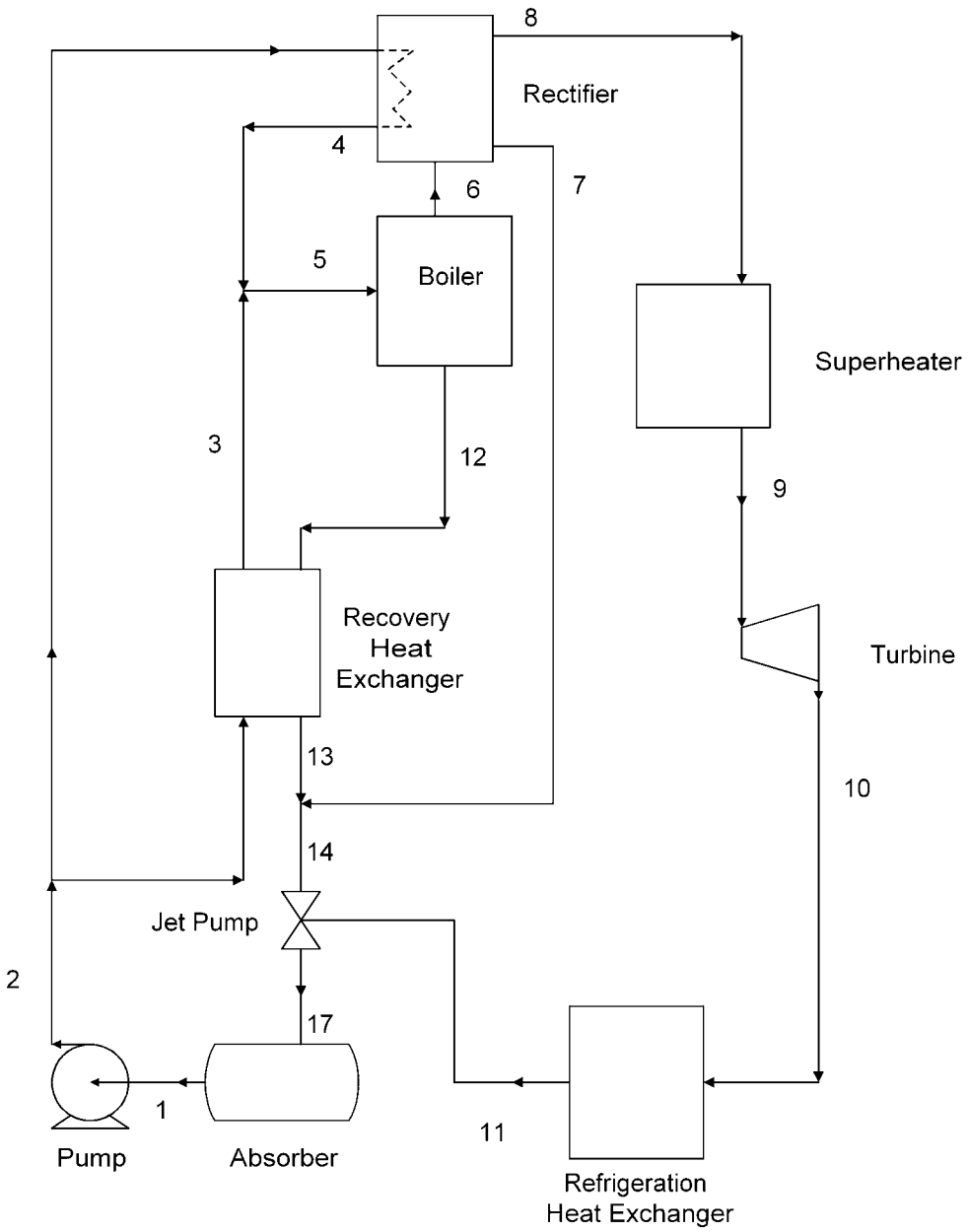

Fig. 6.8 Cycle configuration incorporating the jet pump

Results

It was observed that the pressure improvement observed with LGJ pumps, where the weak solution, after heat recovery is used to pressurize the gas; was very small. Looking at the volumetric entrainment ratio and comparing with data from the literature

and that for commercially available jet pumps, it was determined that the ratio in our case is too large to give a useful pressure increase. Another alternative is to use the high temperature saturated weak solution leaving the boiler/separator as the primary fluid. The process of expansion through a nozzle will result in a high velocity two-phase mixture leaving the primary nozzle. Simulating this case produces a larger pressure boost. A disadvantage here is that the preheating of the strong solution prior to the boiler is mostly done by the heat source. Therefore, while improved resource utilization efficiencies can be achieved, the exergy efficiency does not improve

Maximizing resource utilization efficiency results in a small improvement. The results of simulations using a non isentropic turbine and pump are shown in Fig. 6.9. It is seen that the improvement is larger at heat source temperatures of 400 K and 440 K, while at 480 K, there is actually a decrease in efficiency by using a jet pump. Since the jet pump is an inefficient device, it appears that it is more effective to recover the exergy in the hot weak solution through the recovery heat exchanger than to use it in the jet pump to compress the vapor exiting the turbine. Optimizations performed using higher, and possibly unrealistic efficiency for the jet pump show a dramatic improvement in resource utilization efficiency at all temperatures.

Further, since the jet pump allows a lower turbine exit pressure at a given absorber pressure, the extra work is obtained by additional expansion in the turbine. The limits set on low temperature at the turbine exit also influence efficiency, as seen in Fig. 6.10. Higher vapor concentrations and/or lower turbine exit pressures are needed for achieving lower temperatures. A higher low temperature allows larger turbine exit pressures and even higher absorber pressures.

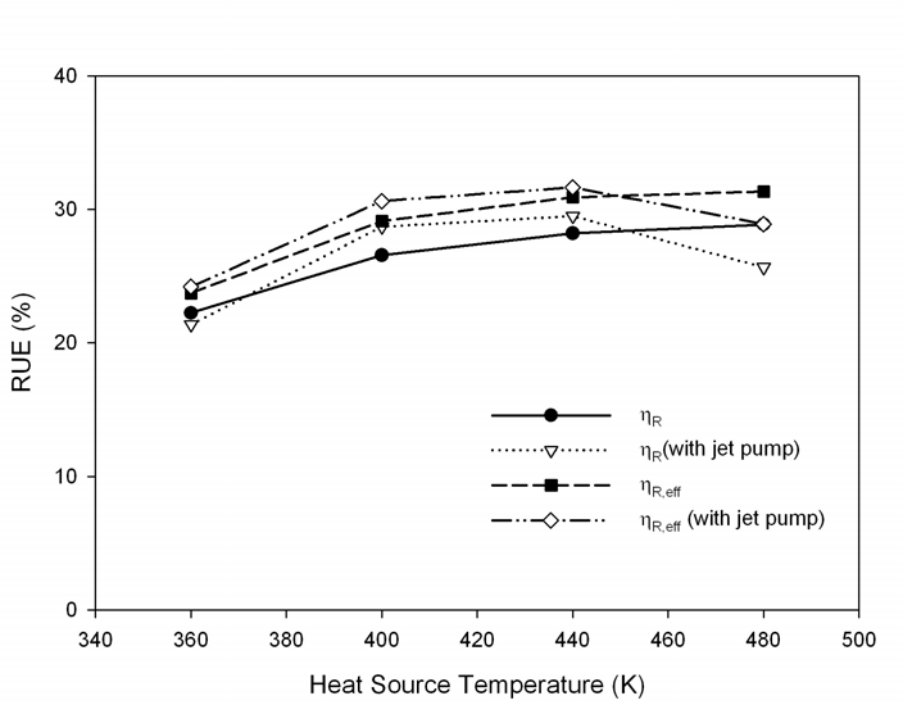

Fig. 6.9 Improvement in resource utilization efficiency with the addition of a jet pump.

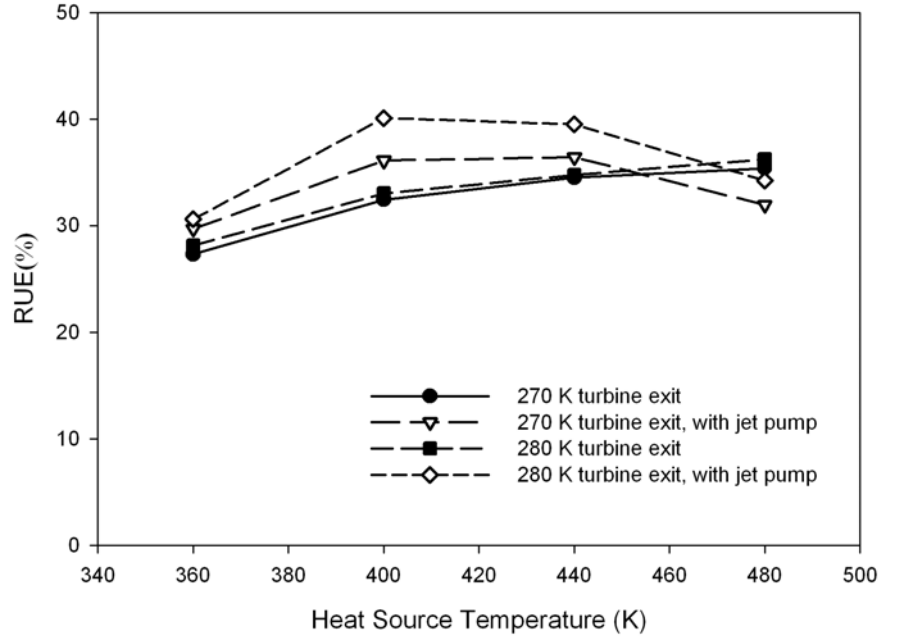

Fig. 6.10 Influence of the choice of turbine exit temperatures on the improvement achievable with a jet pump using an isentropic turbine and pump.

Conclusions

A jet pump used in the cycle as shown in Fig. 6.8 will improve the efficiency of the cycle at certain heat source temperatures. Two important factors affecting the improvement are the efficiency of the jet pump and the efficiency of the turbine being used. Jet pumps are low efficiency devices and contribute substantially to losses in the cycle. The fluids considered here for use in the jet pump are parts of a miscible refrigerant-absorbent pair. The primary fluid is in fact a binary mixture. More work and experimentation are required in order to estimate the performance of a jet pump with this combination better. The addition of a preheater to the basic cycle configuration, discussed in the previous section, gives a larger improvement in efficiency than with using a jet pump. Other configurations that have some separation between the absorber and turbine exit pressures are discussed in the following section.

Distillation (Thermal Compression) Methods

The use of a jet pump in the cycle showed that separation of absorber and turbine exit pressures results in improvement in RUE of the cycle. Due to the low efficiencies of the jet pump, the RUE does not improve much with that device used in the cycle. There is another method described in the literature, that can be adapted to achieve a similar effect as with the jet pump. In the first Kalina cycle that was proposed [20], a distillation arrangement was described in which hot vapor from the turbine exhaust is used in a distillation column. The vapor generated in the distiller is used to increase the concentration of the strong solution going to the boiler. In this configuration, the turbine exit pressure does not directly limit the strong solution concentration. This method has been called a “thermal-compression” method in some papers.

Two different configurations are discussed below that incorporate the thermal compression feature in the combined power and cooling cycle. Since the cycle has cold vapor at the turbine exhaust, the vapor cannot be used as a source of heat in the distiller. Two different configurations are discussed below. In the first case, the heat source fluid is used to produce vapor in the distiller. In the second case, the weak solution and vapor streams are mixed and the heat of condensation of the resulting mixture is used to produce vapor in the distiller.

Using Heat Source

The configuration of the cycle discussed in this section is shown in Fig. 6.11. This configuration has some additional components when compared to the basic cycle configuration. There is an extra absorber, an additional recovery heat exchanger and a distillation column. Some of the ammonia-water mixture in the low pressure absorber is pumped into the high pressure absorber at a slightly higher pressure. The remaining solution is sent to the distiller where the heat source is used to boil off a fraction into vapor that is rich in ammonia. This vapor is routed into the high pressure absorber where is it recombined with the solution pumped there. The resulting solution in the high pressure absorber has a higher mass fraction of ammonia. This high concentration strong solution is partially vaporized in the boiler. The higher mass fraction of ammonia in the strong solution entering the boiler results in a higher vapor fraction. The distiller portion also helps in extracting more energy (and exergy) from the heat source. Consequently, the exergy lost in the heat source leaving the cycle is lower. The pressure difference between the LP and HP absorbers results in a higher pressure ratio in the cycle. The extra expansion possible permits lower temperatures at the turbine exit and more work output in the turbine.

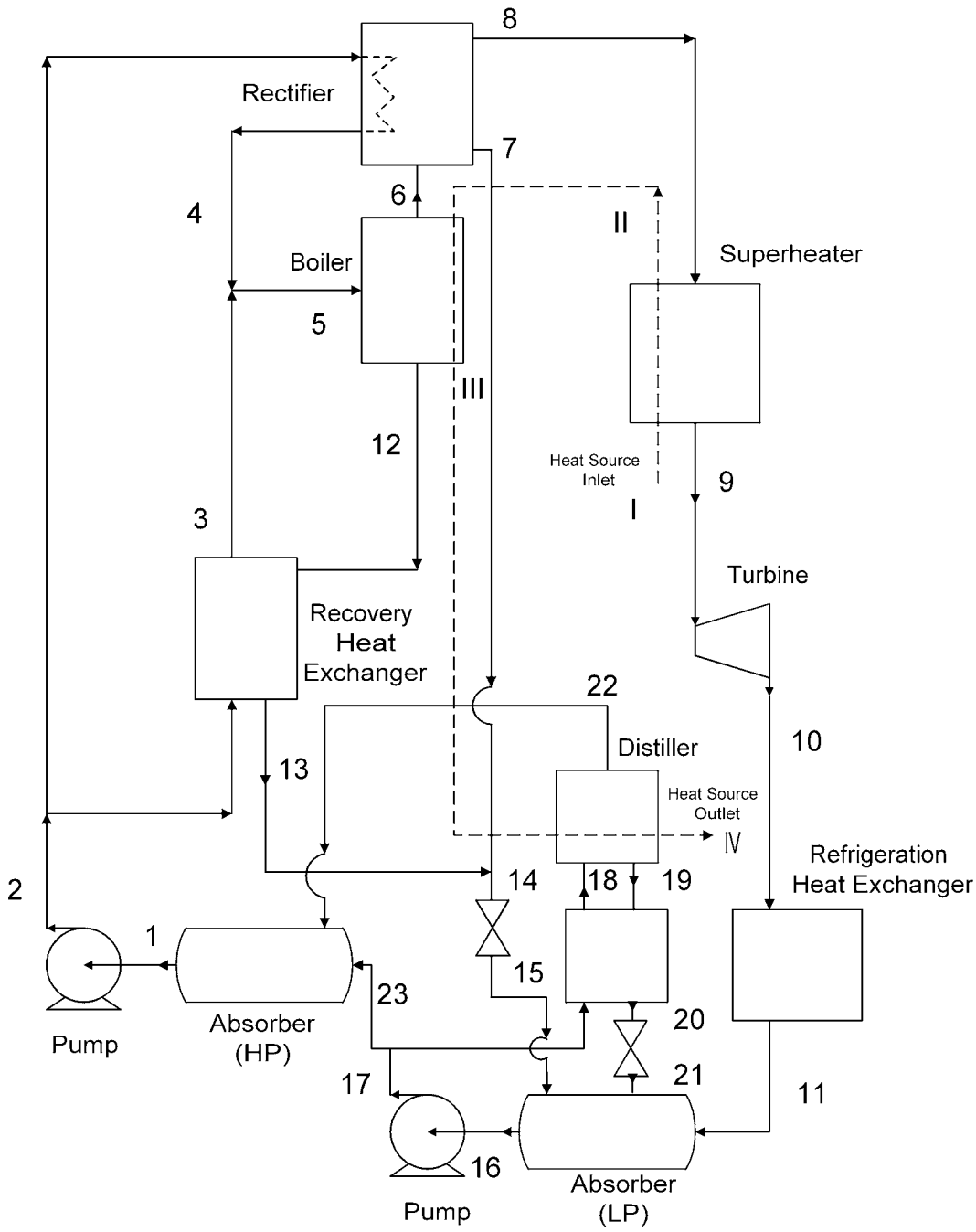

Fig. 6.11 Cycle configuration using the heat source to produce vapor in the distiller

The optimized RUE values obtained using this cycle configuration are plotted in Fig. 6.12. Three cases are plotted. One case uses a definition of effective RUE with a second law efficiency of refrigeration of 100%. The second case uses a second law efficiency of refrigeration of 40%. The third efficiency that is considered is the case where only work output is considered (work domain). Corresponding maximum efficiencies of the basic cycle configuration are also plotted for comparison. The modified configuration greatly improves the optimum RUE of the cycle, with the largest improvement being at lower heat source temperatures. Once again, the optimum RUE in the work domain is substantially higher. The first law efficiency of the modified cycle at optimum RUE conditions is plotted in Fig. 6.13. Comparing with Fig. 4.20 in chapter 4, it is clearly seen that the first law efficiency improves significantly over the basic cycle configuration..

The exergy destruction through major processes in the cycle in the cooling and work domain is shown in Figs. 6.14 and 6.15 respectively. Comparing Figs. 4.13 and 6.14, it is evident that the loss through unrecovered exergy is much lower in the modified configuration. The losses through heat rejection in the absorbers are higher in comparison. This can be explained by the fact that the amount of heat addition is larger, since the heat source provides heat in both the boiler and the distiller. Therefore, there is larger heat rejection in the absorber. The exergy destruction in the boiler itself is lower in the modified configuration, since the higher strong solution concentration and resulting larger vapor fractions result in higher boiler exit temperatures and better thermal matching in the boiler. However, the irreversibility of heat addition, including the distiller, is higher in the modified cycle.

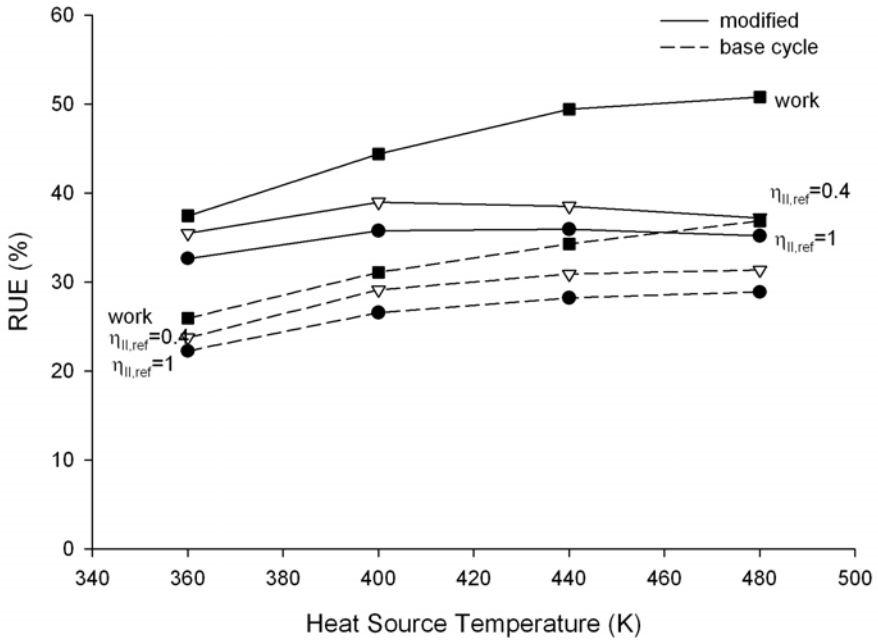

Fig. 6.12 Maximum RUE of the cycle configuration modified with heat source fluid powered thermal compression modification

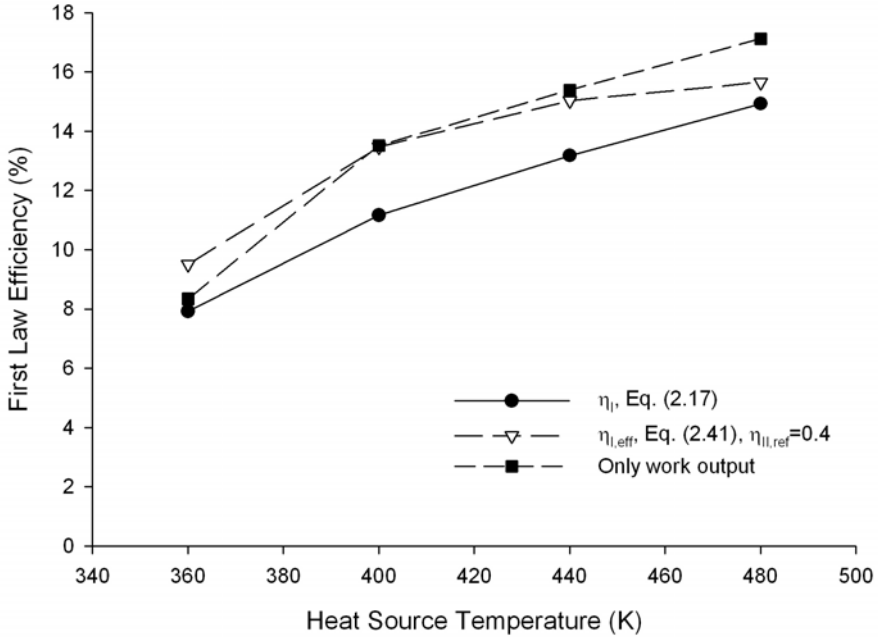

Fig. 6.13 First law efficiency at maximum RUE conditions for configuration with heat source powered thermal compression modification

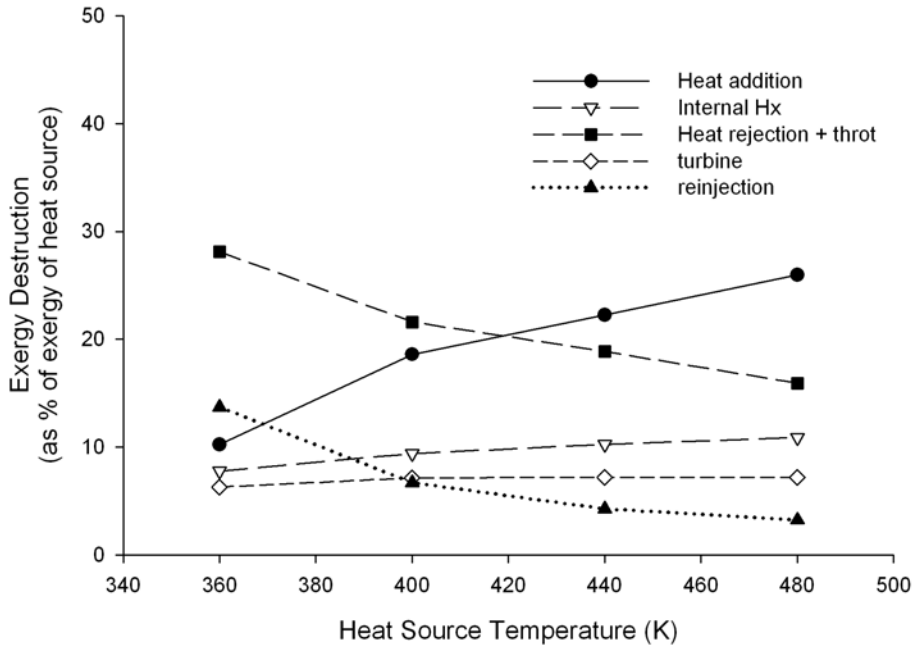

Fig. 6.14 Exergy destruction in the cycle with heat source powered thermal compression modification, when operated to provide power and cooling

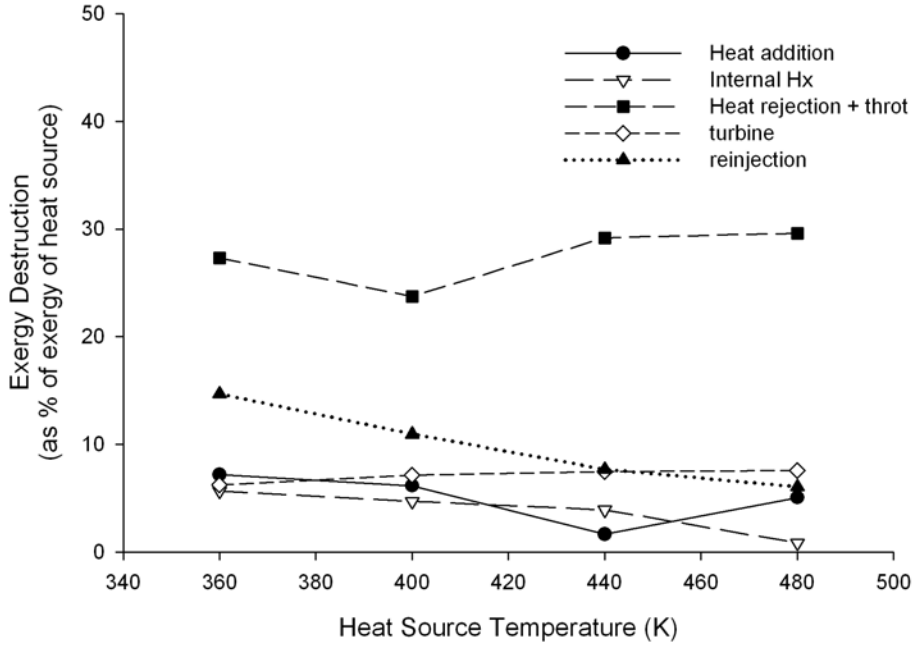

Fig. 6.15 Exergy destruction in the cycle with heat source powered thermal compression modification, when operated to provide only power output

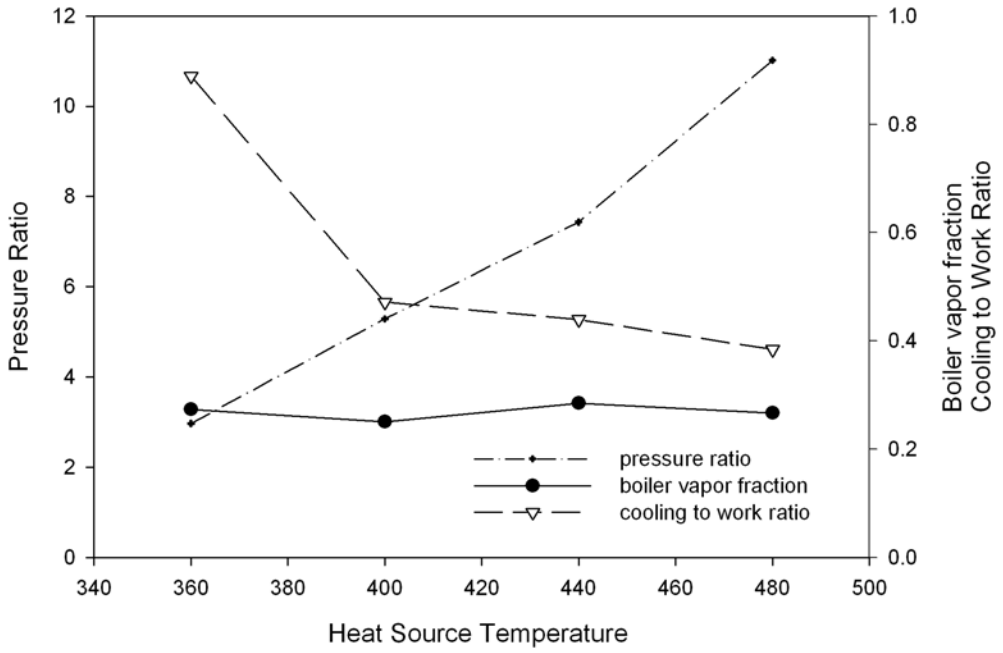

Fig. 6.16 Some parameters for optimized RUE conditions in the cooling domain

The vapor fractions produced in the modified configuration are plotted in Fig. 6.16, and the values are up to 3 times higher than the basic cycle configuration. Comparing Fig. 6.16 with Fig. 4.17, it is seen that the pressure ratios are also improved in the modified configuration. This is expected since the turbine exit pressure is not the same as the strong solution saturation pressure with the thermal compression scheme implemented. Figure 6.17 shows the pressure ratios and boiler vapor fractions for the optimum conditions in the work domain. The vapor fractions observed are substantially higher in the work domain, since the vapor does not have to be expanded to low temperatures and therefore can have a large concentration of water. In fact, at higher temperatures (440 K and 480 K), almost all of the strong solution is boiled off in the boiler. Since the simulation model has the boiling heat exchanger set up as a single pass

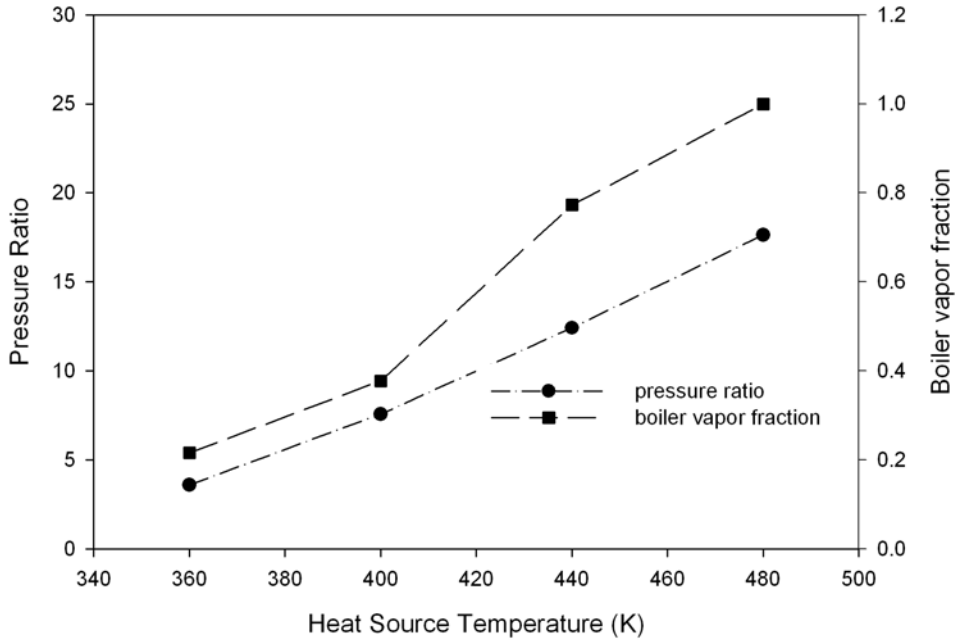

Fig. 6.17 Some parameters for optimized RUE in the work domain

counter current type, the higher vapor fractions may not be easily achievable in practice. The modified configuration is not suitable for improving exergy efficiency, since the increased heat addition in the distiller increases the exergy input to the cycle without a proportionate improvement in output. However, it is interesting to note that the pressures of operation for the modified cycle in the work domain are rather low. Lower pressures could translate to lower equipment costs.

Using Absorber Heat Recovery

The heat supplied to the distiller can come from different sources. Kalina uses the heat of condensation of the hot exhaust vapor coming out of the turbine for boiling in the distiller. This cycle, when operating in the refrigeration mode is designed to produce cold vapor through the turbine. The weak solution is one available source, but by itself

does not match very well with the heating profile of the liquid entering the distiller. Some simulations were performed to confirm this. However, if the weak solution were to be mixed with the vapor, the heat of condensation of the two-phase mixture would match well with the requirements of boiling in the distiller. The challenge then is in mixing the vapor and liquid streams. A jet pump like device (without a diffuser section to slow the stream and raise the pressure) could be used to mix the two streams. Other configurations possible include absorber designs built so as to recover the heat of condensation from it. Such designs have already been developed for GAX (Generator-Absorber Exchange) type of absorption refrigeration cycles. These cycles use heat from the absorber to preheat the working fluid entering the generator (boiler).

In the simulations performed for the results presented in this section, the mixing process is modeled as isenthalpic. While this may be difficult to achieve in practice, the results of these simulations give a general idea of what is achievable. A diagram of this configuration is shown in Fig. 6.18. An actual design would probably differ in some ways from the schematic presented here.

The optimized RUE values are plotted for the new configuration in Fig. 6.19. As in earlier cases, the work domain gives the best results. In the cooling domain, the modified configuration shows a distinct improvement over the basic cycle configuration. While the configuration studied in the previous section has higher RUE at lower temperatures, at higher heat source temperatures, the present configuration works better. In the work domain, the optimum efficiency of the configuration using the condensing mixture as the heat source is better. However, the first law efficiency is poor and is comparable to the values obtained for the basic cycle configuration (See Fig. 6.20).

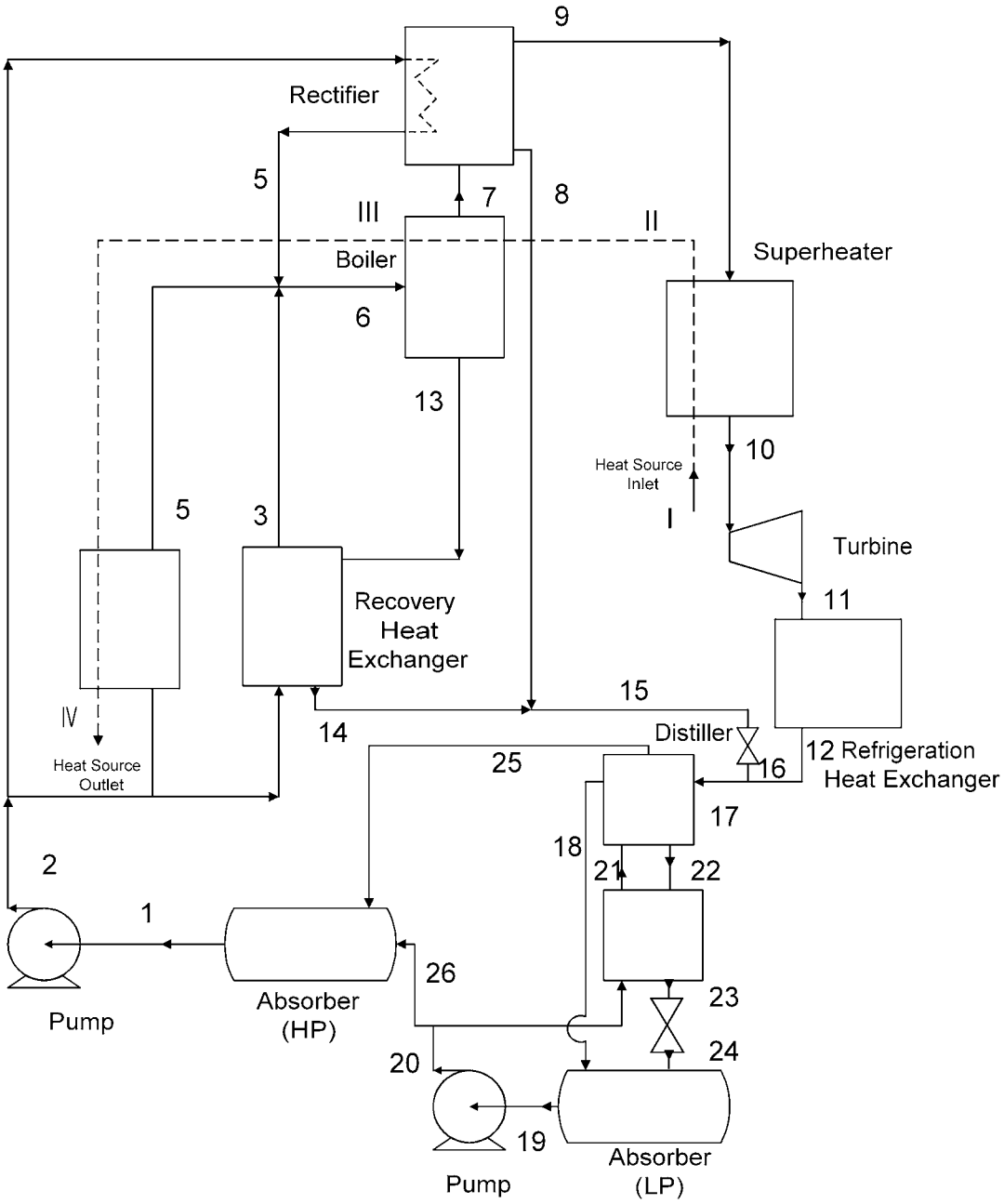

Fig. 6.18 Cycle configuration using heat of condensation to produce vapor in the distiller

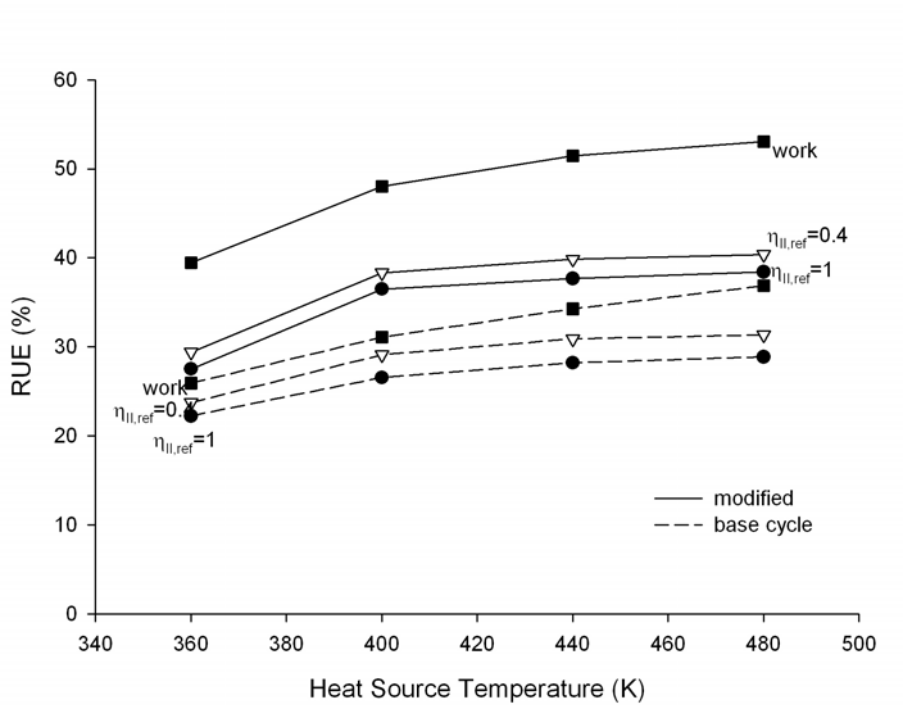

Fig. 6.19 Maximum RUE of the cycle configuration modified with a condensing mixture providing heat of distillation

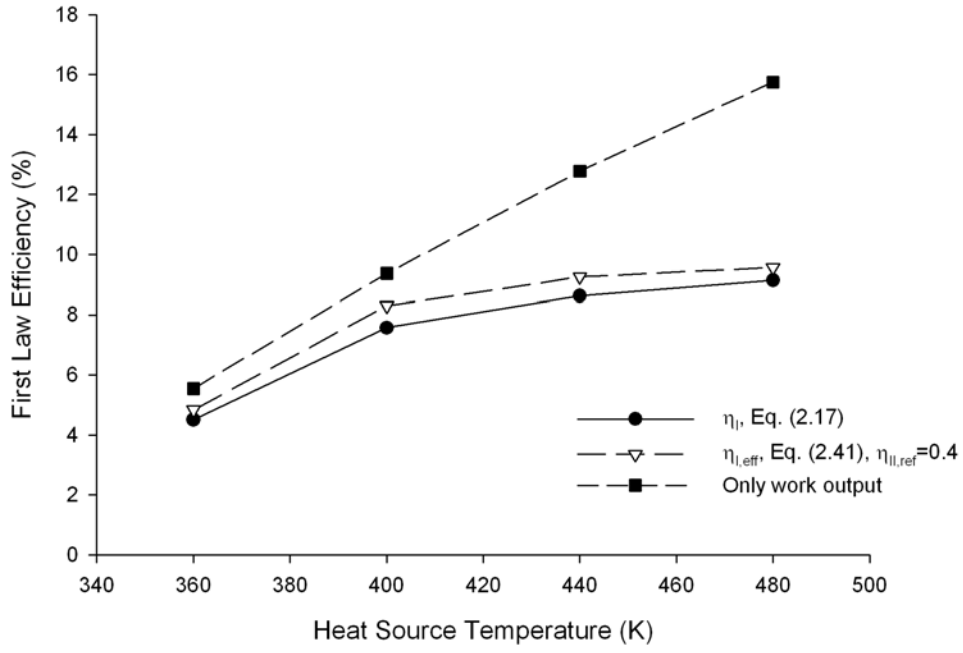

Fig. 6.20 First law efficiency at maximum RUE conditions for configuration using heat of condensation to produce vapor in the distiller

The exergy destruction plots once again show a much lower fraction of exergy lost in the heat source fluid leaving the boiler. In this configuration, the heat source is used to preheat a portion of the strong solution and that process lowers the temperature of the heat source exiting the cycle. The major losses are through exergy destruction in heat addition (boiler, superheater and preheater), and in the absorbers (heat rejection). In the work mode, the exergy losses due to heat addition are lower than in the refrigeration mode. This is attributable to better thermal matching in the boiler, since higher temperatures are attained at the boiler exit with the higher vapor fractions.

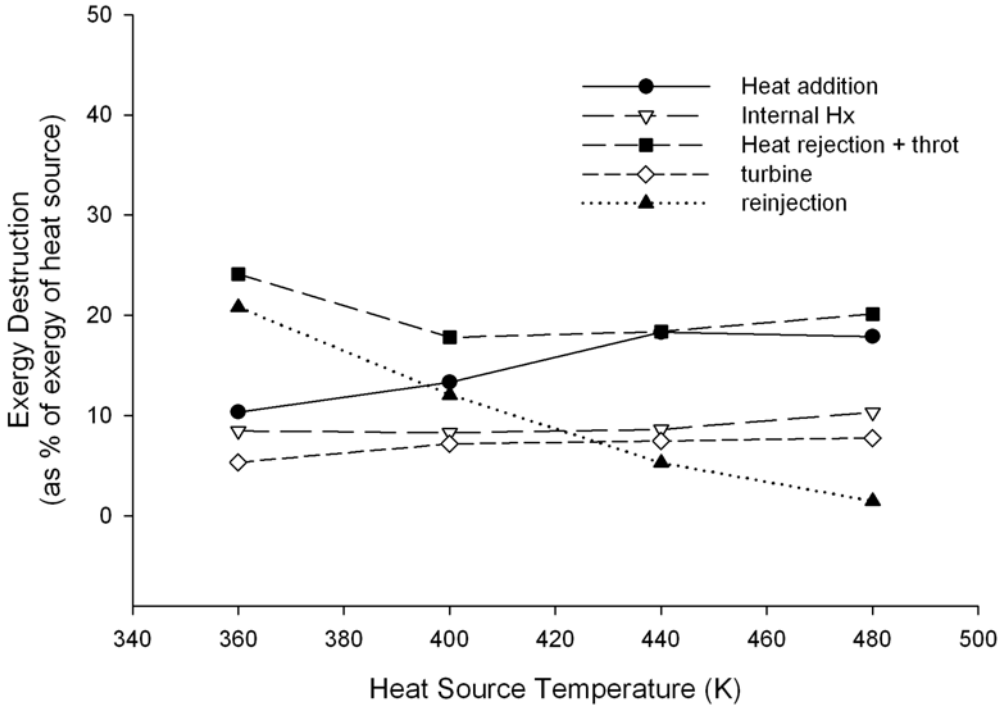

Fig. 6.21 Exergy destruction in cooling domain in modified cycle with a condensing mixture providing heat of distillation

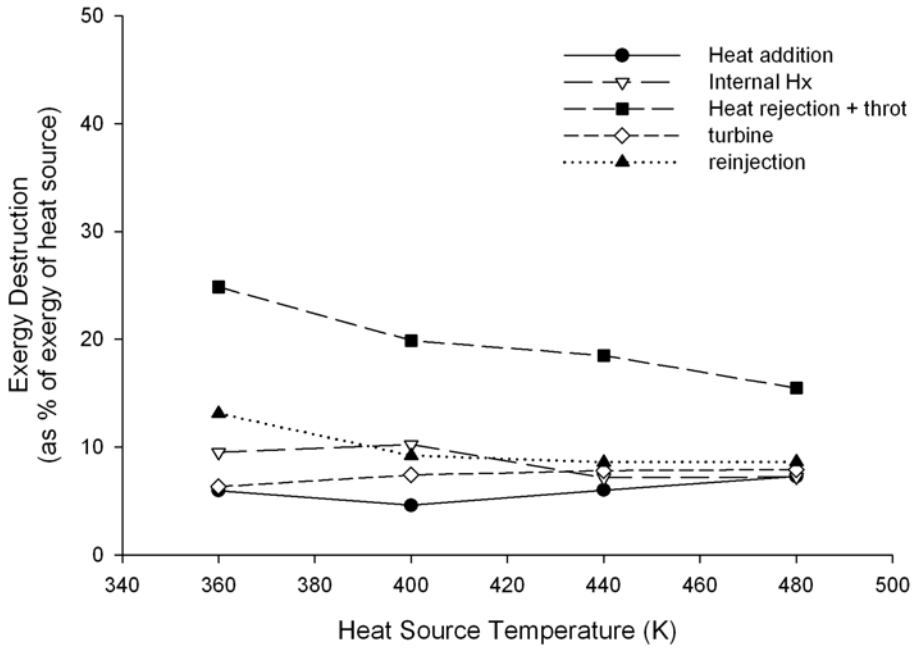

Fig. 6.22 Exergy destruction in work domain with a condensing mixture providing heat of distillation

The pressure ratios are higher in this configuration (Fig. 6.21) than in the basic cycle configuration or in the modified configuration discussed in earlier in this chapter where a preheater is added to the basic cycle configuration. The boiler vapor fraction is again high compared to the basic cycle configuration. In the work domain, the boiler vapor fraction at optimum conditions approaches unity at 440 K and 480 K. This means that there is no weak solution reflux stream returning from the boiler. Consequently, the cycle configuration becomes similar to the basic Kalina cycle configuration (Fig. 1.3). Once again, the question of once through boiling of all of the strong solution arises. It remains to be seen if that can be accomplished effectively.

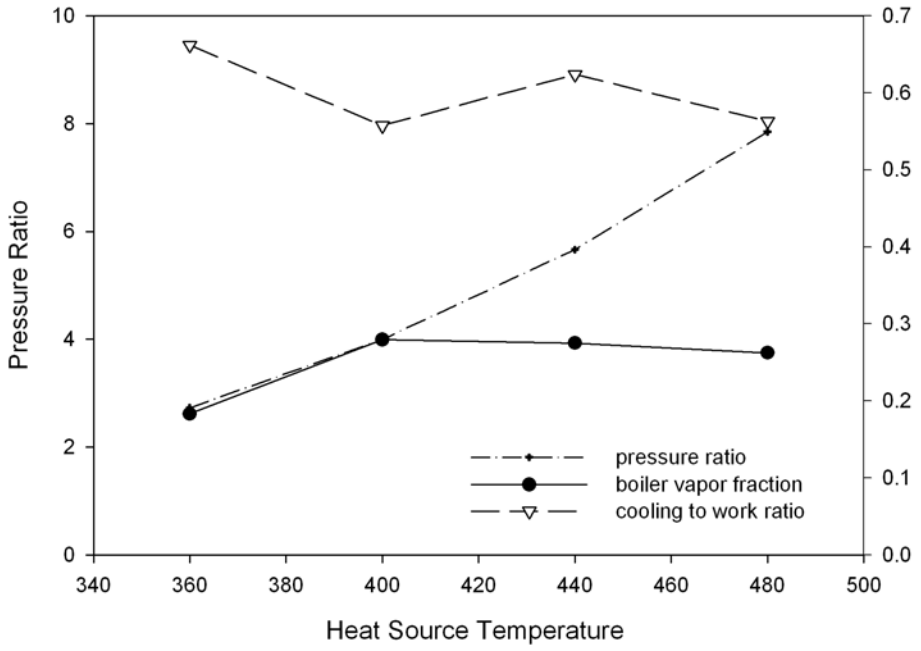

Fig. 6.23 Some parameters for optimized RUE (strict definition) in the cooling domain for the modified cycle with a condensing mixture providing heat of distillation

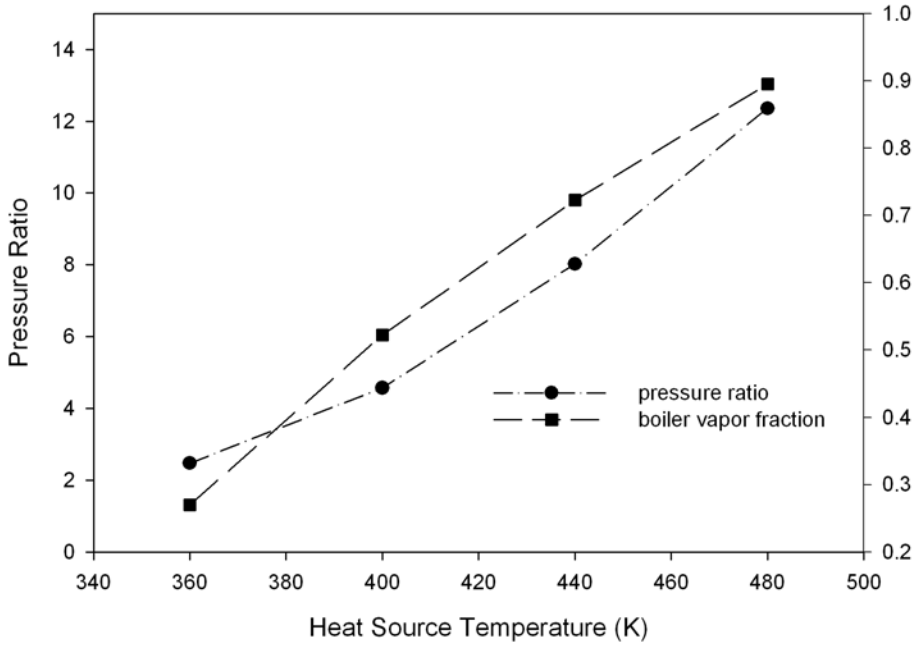

Fig. 6.24 Some parameters for optimized RUE in the work domain for the modified cycle with a condensing mixture providing heat of distillation

Conclusions

Several configurations of the combined power and cooling cycle have been simulated and optimized. Most of the configurations discussed improve the RUE of the cycle. The exergy efficiency of the basic cycle configuration itself is relatively high. Most of the configurations considered did not show a better exergy efficiency. The simplest method of increasing RUE is to add another heat exchanger where the heat source is used to preheat a portion of the strong solution, before the boiler.

A jet pump was added in the cycle configuration in order to use the high pressure weak solution and raise the pressure of the vapor after the refrigeration heat exchanger. Due to the low efficiency of jet pumps, the improvement seen in efficiency is small. Another means of achieving the same effect as using a jet pump is to use the distillation compression method proposed by Kalina. Two configurations implementing that method were simulated. In one case, heat from the heat source was used for the distillation, while in the other case; a condensing mixture of weak solution and vapor was used. Both methods improved RUE. When optimized to provide work output, both cycles tend to have very high vapor fractions in the boiler, especially at higher heat source temperatures. The efficiencies at maximum work RUE conditions are also much higher. The advantage of operating in the work mode is that there is no restriction on the composition of the vapor. Therefore, a large fraction of the binary mixture can be boiled off, taking advantage of the larger temperature glide available.

CHAPTER 7
CONCLUSIONS

The combined power and cooling cycle has been studied. The methodology followed for the study consists of optimizing a simple simulation model of the cycle. Four sensible heat source temperatures were studied that covered the range of low to moderate temperature solar and geothermal sources.

Summary of Results

The work performed in this study builds on previous theoretical and experimental work on the combined cycle. The following are the contributions of this study:

1. Efficiency definitions were developed for the combined power and cooling cycle. It was shown that it is important to assign a realistic weight to the refrigeration output of the cycle, when defining the efficiency.
2. The basic cycle configuration of the cycle (see Fig. 4.1) was optimized for maximum second law efficiency. These optimizations differed from earlier work since the calculations used the new efficiency definitions, and considered isentropic efficiencies for the turbine and pump.
3. The basic cycle configuration was shown to have reasonable exergy efficiencies and poor resource utilization efficiencies.
4. The cycle was shown to have a better exergy efficiency using lower temperature heat sources, when operated to deliver both power and cooling.
5. Binary mixtures of alkanes were considered as working fluids for the combined cycle. It was shown that power and cooling could be obtained simultaneously using these fluids.
6. The organic fluids considered performed poorly compared to the original choice of ammonia-water mixtures.
7. Among the organic fluid mixtures, it was found that combinations with higher volatility ratios and higher limiting pressure ratios performed better.
8. Alternate configurations of the cycle were investigated in order to improve the RUE.
9. Configurations that decouple the absorber and turbine exit pressure were shown to perform better than the basic cycle configuration.
10. While using a jet pump to decouple the pressures had a small effect on the cycle RUE, other configurations using a Kalina thermal compression scheme performed very well.

11. In all cases, the cycle operated in the work domain gave a higher RUE than when operated to yield simultaneous power and cooling output.

A set of thermodynamic efficiency definitions was developed for this novel cycle, which has simultaneous power and refrigeration output. It has been recommended that the refrigeration output be assigned a weight that reflects the efficiency of a comparable refrigeration cycle. Efficiency definitions have been developed that are based on a second law efficiency of a comparable refrigeration cycle. The optimum parameters are found to be different when assigning a larger weight to refrigeration.

The basic configuration of the cycle (shown in Fig. 4.1) was optimized for exergy and resource utilization efficiency. Since the cycle can either provide work and cooling output, or alternately simply provide work output, both cases were considered. When only providing work output, the cycle is essentially a Maloney Robertson (M-R) cycle. The configuration is different from the original M-R cycle [19] in that a superheater is added in the combined power and cooling cycle. Substantial superheating is seen in the optimized results. It is seen that based on an effective exergy efficiency, the cycle operating in the cooling mode has efficiencies comparable to the M-R cycle. Overall, while the exergy efficiencies seem reasonable, the resource utilization values are very low. The primary reason for the low RUE is the limited ability of the cycle to remove heat from the heat source.

Binary mixtures of alkanes were investigated as alternate working fluids in the cycle. These fluids were selected on the basis of their previous application in organic Rankine cycles. The second law efficiencies (exergy and RUE) achievable are lower with these fluid mixtures. Further, the low temperature that can be obtained using these fluids is also limited. The temperature drop with pressure drop is higher using ammonia

in a turbine. The limiting pressure ratios that can be obtained are also much higher using ammonia-water mixtures. Comparing organic working fluid mixtures, while isobutane has a lower temperature drop with pressure drop in the turbine, the limiting pressure ratios (and optimum pressure ratios) are higher. Mixtures containing isobutane give a better efficiency than mixtures with propane. A higher volatility ratio between the two components appears to be advantageous when operating in the cooling mode.

Several configurations were studied in order to improve the efficiency of the cycle. A modified cycle, where a heat exchanger was used to preheat part of the working fluid stream using the heat source, while the remaining preheating was done in the recovery heat exchanger improves the RUE of the cycle.

A jet pump was proposed in the cycle so that the weak solution at the high pressure could be used to compress the vapor from the refrigeration heat exchanger into the absorber. The most efficient use would have been to use a LJG compressor. Unfortunately, the liquid stream volume is too small in relation to the vapor to be compressed; in other words, the entrainment ratio is too high for a LJG pump to work. Assuming a two-phase jet pump that expands hot, saturated weak solution in the primary nozzle indicated the possibility of some improvement. The very low efficiency of the jet pumps limits the improvement substantially.

Another method of raising the concentration of the working solution entering the boiler without increasing the turbine exit pressure is to use a modification of the so-called thermal compression method introduced by Kalina. Kalina uses the heat recovered from the hot vapor exiting the turbine to distil an ammonia water mixture. The distilled vapor is combined with some of the original mixture to make a concentrated solution, which is

boiled and expanded in the turbine. In the cycle studied here, the vapor leaving the turbine is cold, and therefore it is unsuitable for providing the heat of distillation. The weak solution is also badly matched to the requirement of providing heat in the distiller. The cycle on the other hand is limited in the amount of heat that it is able to remove from the heat source. Therefore, using the heat source itself in the distiller is a possible source of heat. This solution improved the RUE of the cycle (while producing cooling) substantially over the base cycle values. An effective efficiency of about 39 % was obtained at 400 K heat source temperature. Another method of recovering heat in the distillation section is to use the heat of condensation from the absorber. Such a model shows a slightly improved resource utilization efficiency of the cycle. The model used for simulation assumes the condensation in a heat exchanger with countercurrent flow, of a mixture of the weak solution and the condensed vapor. Such a design may not be easy to implement in practice. The condensing vapor matches better with the boiling liquid in the distiller.

Both models also show much higher RUE with pure work output. Under optimum conditions, the absorber heat recovery model begins to appear very similar to the basic Kalina cycle, with only a negligible weak solution flow from the boiler/separator. Under these conditions, where only work output is desired, these configurations appear to have the advantage of having low pressures of operation.

Future Work

More work is needed to better understand the performance of a power plant built on the combined power and cooling cycle. While some work is already in progress, some recommendations to extend the results of this work are presented below. The suggestions are listed and a discussion elaborating on some of these topics follows.

1. The simulation study has to be extended using more realistic models incorporating losses such as pressure losses and device efficiencies.
2. Additional inputs required such as cooling fluid pumping work should be considered.
3. Cycle performance should be evaluated for the demands and conditions of some actual applications, which might be currently satisfied by other cycles, such as ORCs.
4. An economic analysis is important to determine the feasibility of actually using this cycle.
5. The search for working fluid pairs is not over. Simply pairing ammonia with a better absorbent than water might give an improved efficiency.
6. The Kalina thermal compression schemes do not show high exergy efficiency. Nevertheless, when considering the efficiency of the collector, it might prove to be advantageous in that application. This should be investigated.
7. The application of jet pumps in the cycle still holds some promise. Some work needs to be done to investigate jet pumps using the fluid combination proposed here. Some commercial products in the market may also hold promise.

All the theoretical work done so far on the cycle has been on the basis of simple simulation models. While such models are useful for determining the advantages and disadvantages of different cycle configurations and an approximate idea of different parameters, more realistic models are necessary to determine the sizes of different equipment and the losses expected in the cycle.

While the models consider the turbine work output and pump input, additional power consumption such as power required for circulating the cooling fluid in the absorber condenser and the heat source are not considered. Energy is also consumed in removing non-condensable gases from the absorber. This additional power consumed comes under the category of parasitic losses. While parasitic losses are small in power plants converting high temperature heat sources, they tend to become significant in low temperature power plants.

Another point of concern is the size (scale) of the power plant. The scale of the project will have an influence on the selection of the expander. While steam turbines in

large power plants are very efficient, at smaller sizes, the effect of losses such as blade tip leakage losses becomes larger. Efficiencies expected at smaller sizes might be smaller.

In this study, the cycle is optimized from the point of view of optimum thermodynamic performance. High recovery heat exchanger effectiveness is permitted. Relatively low pinch points and approach temperature limits are assumed. It is important to recognize that the ultimate determining factor in cycle design for most applications is the cost. For instance, it might be more economical to have a smaller recovery heat exchanger. An economic analysis is required to determine these factors.

Some case studies where a cycle design is developed for specific applications might be useful. For instance, a solar, geothermal, and waste heat conversion application can be considered. Each of these applications has different requirements. For example, there is a limit in geothermal applications on the temperature of the brine (geofluid) leaving the cycle, to prevent silica precipitation. The cycle designs developed can be compared to standard cycles in use now and to the most promising alternative determined, particularly through an economic analysis.

The search for better working fluids can be expanded on the basis of some of the conditions discussed here. Ammonia is a good choice of volatile component. There may be a better choice of absorbent in the place of water such that the pair has an even higher volatility ratio. More complex (ternary) mixtures may also prove to be an option.

The optimization program can be setup to handle a more complicated simulation model. A key criteria to keep in mind would be the computational requirements for a given simulation. Since the model involves calculating the gradients for all variables, which requires invoking the function several times for each step, the computational time

requirements can dramatically increase. The model, as it exists now can easily be optimized on a PC.

The configurations based on the Kalina thermal compression arrangement would be the best choice for geothermal and waste heat applications. The basic cycle configuration is better suited to utilizing solar resources. The Kalina compression based cycles may have some advantage when considering the effect of heat source exit temperature on collector system efficiency. These have to be computed.

The use of a jet pump was shown to have a slight advantage under certain conditions. The main reason for the lack of improvement is the low efficiency of the jet pump itself. If it were possible to build an improved jet pump, the use of that device in the cycle would be advantageous. A company has claimed to have a very efficient jet pump like device (hydrokinetic amplifier) that may work well in such applications. Keeping that in mind, it might be worthwhile to pursue the jet pump method further and to try to improve the efficiency of these devices.

APPENDIX A
WORKING FLUID PROPERTY CALCULATION

The simulation of the combined cycle and its accuracy depend substantially on the accuracy of prediction of the working fluid properties. In the work presented here, a properties program written by Xu (see Xu and Goswami [43]) has been utilized for ammonia-water mixture properties. For hydrocarbon mixtures, the program SUPERTRAPP (TRAnsport Properties Prediction) program, available from NIST was used. A brief discussion on the property prediction methods for binary mixtures is given below, using ammonia-water mixtures as an example, along with a summary of the theory behind the programs used in this study.

Property Prediction Methods

The experimental measurement of properties of working fluids at all possible pressures and temperatures is very difficult. The normal practice is to make accurate measurements in a relatively small number of points within the range of values desired, and to then use theories on thermophysical properties of substances to predict the properties at all other values.

Some of the commonly used thermophysical property prediction methods for binary mixtures can be broadly classified as those based on (see Thorin et al. [62])

- Equations of State
- Gibbs excess energy
- Law of corresponding states

Equations of state based methods use equations of state defined for the fluid mixtures to compute properties at all points. Some equations that are commonly used are the Helmholtz equations of state, cubic equations of state, and virial equations of states. Helmholtz equations of state are the most common form of accurate equations of states being developed with a large range of applicability [63]. For ammonia water mixtures, one of the more recent methods used to predict properties is one developed at NIST, using reduced Helmholtz equations of state [64]. Cubic equations of state, such as the Peng Robinson equation or the Redlich Kwong equation are recommended for use when no other equations are available. For instance, Elnick et al. [65] found that a Peng-Robinson equation based method was less accurate than the WATAM proprietary properties code developed by Exergy Inc. Cubic equations have parameters that can be correlated with a limited amount of experimental data [63]. For the prediction of properties of organic mixtures, the Benedict-Webb-Rubin equation, which is a more complicated (and not a cubic) equation of state used to be a popular choice. Virial equations are truncated power series functions in terms of molar volumes or pressures. The coefficients of the power terms can be empirically correlated using PVT data or estimated using molecular thermodynamics [63].

Gibbs energy function is a characteristic function, i.e., a function from which all other thermodynamic properties can be derived by simple algebra or calculus. Gibbs excess energy methods use correlations for the Gibbs energies of the pure components and correlations for the excess free energy of mixtures to account for their mutual interaction. The properties program used in our study uses a Gibbs excess energy based method.

The principle of corresponding states correlates the behavior of substances using reduced properties. To introduce the concept simplistically, using reduced properties that are normalized using critical properties, given as $p_r = p/p_{crit}$, $T_r = T/T_{crit}$ and $v_r = v/v_{crit}$, an equation of state could be written as

$$p_r = f(v_r, T_r) \tag{A.1}$$

Principles of statistical mechanics can be used to improve the quality of prediction of the corresponding states methods. Corresponding states methods do not always have the accuracy of empirical correlations, but these are very useful to estimate properties beyond the range of existing data.

Methods Used for Properties in this Study

Ammonia Water Properties Prediction

Xu and Goswami [43] describe in detail the ammonia-water properties program used in this study. A program written by Xu in the C language was modified and used in this study. A small error in the implementation of the calculation of specific volume was corrected and additional functions added for convenience, during the course of this study.

The method combines the Gibbs free energy method for mixture property prediction and bubble and dew point correlations for phase equilibrium. Ammonia-water mixtures in the vapor state are assumed to be ideal mixtures, such that the properties of pure water and ammonia are added up by weighting with the composition of the mixture. For the liquid state on the other hand, an excess Gibbs energy term is used to account for the deviation from ideal solution behavior. The entropies in both states (liquid and vapor) are naturally, not additive. Entropy of mixing term is used to account for the additional irreversibility of mixing. Phase equilibrium calculations are performed using

equations developed by El-Sayed and Tribus [66]. These correlations directly yield the bubble and dew point values, therefore avoiding the iterative method of equating fugacity coefficients of each component in the vapor and liquid state in equilibrium. Xu [67] gives a review of ammonia-water mixture property prediction methods as well as a detailed description of the method used in this study.

The properties predicted by these correlations were compared to measured values in the literature and the agreement was found to be good [43]. The property correlations used are valid in the 0.2-110 bar (0.02 MPa to 11 MPa) range, and from -43 to 327 ºC (230 to 600 K) range.

Organic Fluid Mixture Properties

The SUPERTRAPP program for mixtures, developed at NIST, is one of the five computerized databases distributed by the Standard Reference Data (SRD) Program of NIST. Although the database was developed with an emphasis on accurate density prediction, the calculation of other properties is excellent also [68]. An earlier version of this program was used for the calculations in the DOE heat cycle research program conducted at Idaho National Engineering Laboratory.

The properties calculation can be performed using extended corresponding states (EXCST) models or a Peng-Robinson equation of state (PRS) equation based model. Vapor liquid equilibrium calculations are always performed using a PRS model. For simulations, the EXCST model was used for phase calculations and the PRS for phase equilibrium predictions.

Mason and Uribe [69] provide an excellent review of the EXCST, along with application to dilute gases and a short description of the historical evolution of the method. Huber and Hanley [70] review the application of the method to dense fluids

with particular reference to the SUPERTRAPP program. Nowarski and Friend [71] describe the application of the extended corresponding states method to the calculation of ammonia-water mixture thermodynamic properties. Simply put, the basic corresponding states principle is extended by knowledge of the intermolecular interactions to come up with the extended corresponding states method. A brief description of the method, adapted from Huber and Hanley [70], is given below.

Consider a given fluid. The property of this fluid is related to a reference fluid at a corresponding-state point using two functions, F_x and H_x. These are functions of the critical parameters and the acentric factor ω. The Pitzer acentric factor is a parameter based on the slope of the vapor-pressure curve. In the limiting case of a two-parameter corresponding states model between two pure fluids, these functions reduce to a ratio of critical parameters of the fluid with respect to the reference fluid.

$$F_x = \frac{T_{c,x}}{T_{c,0}} \tag{A.2}$$

$$H_x = \frac{\rho_{c,0}}{\rho_{c,x}} \tag{A.3}$$

The subscript 0 refers to the reference fluid, and the subscript *x* to the fluid under consideration. The concept of extended corresponding states broadens considerably, the range of applicability of the corresponding states. The functions given in Eqs.(A.2) and (A.3) are modified by adding "shape factors".

$$F_x = \frac{T_{c,x}}{T_{c,0}} \theta_x \left(\rho_{r,x}, T_{r,x}, \omega_x \right) \tag{A.4}$$

$$H_x = \frac{\rho_{c,0}}{\rho_{c,x}} \phi_x \left(\rho_{r,x}, T_{r,x}, \omega_x \right) \tag{A.5}$$

The shape factors are functions of reduced parameters and the acentric factor.

In the SUPERTRAPP program, the shape factors are calculated semi-empirically using information on the pure fluid components. Mixture properties are calculated using mixing rules. The mixture is first characterized as a hypothetical pure fluid and is related to the reference fluid. The mixing rule equations used are

$$H_x = \sum_{i=1}^{n} \sum_{j=1}^{n} x_i x_j H_{ij} \tag{A.6}$$

$$F_x H_x = \sum_{i=1}^{n} \sum_{j=1}^{n} x_i x_j F_{ij} H_{ij} \tag{A.7}$$

Where,

$$F_{ij} = \sqrt{F_i F_j} \left(1 - k_{ij} \right) \tag{A.8}$$

$$H_{ij} = \left(H_i^{1/3} + H_j^{1/3} \right)^3 \left(\frac{1 - l_{ij}}{8} \right) \tag{A.9}$$

Here x_i is the concentration of the i^{th} component in the mixture of n components. k_{ij} and l_{ij} are binary interaction parameters that can be non zero when $i \neq j$. Additional mixing formulas may be used for transport properties.

The properties predicted by the SUPERTRAPP algorithm worked well with the simulation program. The VLE calculation results were slightly “noisy”, due to which a function written to calculate the saturation concentration at a given temperature and pressure would not converge. Further, it was necessary to use the central differencing

scheme in the gradient calculations in order to prevent the search from terminating at obviously non-optimum points. The numerical error in the central differencing scheme is lower.

APPENDIX B
OPTIMIZED STATE POINTS

The optimized state points for some cycle configurations are tabulated here. The numbers are from computer program outputs and may contain significant figures exceeding the accuracy of the properties program. The state points correspond to the numbers in the respective figures referenced. The following assumptions hold for the simulations.

Conditions

Heat Source Temperature	:	400 K
Ambient Temperature	:	298 K
Dead State Temperature	:	298 K
Reference flow rate	:	1 kg/s
For ammonia-water fluid based Simulations		
Upper limit on Turbine exit Temp.	:	270 K
Turbine isentropic efficiency	:	80 %
Pump isentropic efficiency	:	85 %
For Organic fluid simulations		
Upper limit on Turbine exit Temp.	:	285 K
Turbine isentropic efficiency	:	100 %
Pump isentropic efficiency	:	100 %

Basic Cycle Configuration

Fluid: Ammonia- Water

Exergy Efficiency Optimized

	T	p	x	h	s	flow rate
	K	bars		kJ/kg	kJ/kg.K	kg/s
1	303.00	1.00	0.288	-55.84	0.37	3.000
2	303.10	10.34	0.288	-54.53	0.37	3.000
3	381.84	10.34	0.288	326.71	1.48	2.622
4	382.86	10.34	0.288	342.59	1.52	3.000
5	394.96	10.34	0.831	1718.96	5.46	0.340
6	357.11	10.34	0.391	147.79	1.05	0.081
7	357.11	10.34	0.970	1472.39	4.89	0.259
8	359.82	10.34	0.970	1479.33	4.91	0.259
9	270.00	1.00	0.970	1201.83	5.09	0.259
10	293.00	1.00	0.970	1299.81	5.44	0.259
11	394.96	10.34	0.219	379.33	1.56	2.660
12	308.10	10.34	0.219	3.53	0.49	2.660
13	309.81	10.34	0.224	7.81	0.51	2.741
14	310.01	1.00	0.224	7.81	0.51	2.741
17	389.96	10.34	0.288	452.65	1.80	0.378

Heat Source:
Inlet: 400.00 K
Outlet: 387.86 K
Heat source flowrate: 11.01 kg/s

Effective Exergy Efficiency Optimized
$\eta_{II,ref} = 0.4$

	T	p	x	h	s	flow rate
	K	bars		kJ/kg	kJ/kg.K	kg/s
1	303.00	1.86	0.380	-90.30	0.32	3.000
2	303.18	16.53	0.380	-88.18	0.33	3.000
3	381.82	16.53	0.380	303.14	1.46	2.577
4	382.52	16.53	0.380	314.27	1.49	3.000
5	395.00	16.53	0.905	1617.37	5.03	0.378
6	341.87	16.53	0.601	88.66	0.85	0.085
7	341.87	16.53	0.992	1380.40	4.42	0.293
8	341.87	16.53	0.992	1380.40	4.42	0.293
9	255.26	1.86	0.992	1147.07	4.58	0.293
10	293.00	1.86	0.992	1324.73	5.24	0.293
11	395.00	16.53	0.304	345.20	1.53	2.622
12	308.18	16.53	0.304	-39.39	0.44	2.622
13	310.02	16.53	0.314	-35.39	0.46	2.707
14	310.33	1.86	0.314	-35.39	0.46	2.707
17	386.87	16.53	0.380	382.07	1.66	0.423

Heat Source:
Inlet: 400.00 K
Outlet: 387.52 K
Heat source flowrate: 10.82 kg/s

RUE Optimized

	T K	p bars	x	h kJ/kg	s kJ/kg.K	flow rate kg/s
1	303.00	2.60	0.434	-101.75	0.30	3.000
2	303.08	8.61	0.434	-100.87	0.30	3.000
3	344.16	8.61	0.434	110.06	0.95	2.691
4	344.58	8.61	0.434	117.63	0.97	3.000
5	357.68	8.61	0.960	1491.22	5.02	0.400
6	324.42	8.61	0.542	-5.86	0.60	0.029
7	324.42	8.61	0.993	1371.88	4.68	0.371
8	324.42	8.61	0.993	1371.88	4.68	0.371
9	270.00	2.60	0.993	1235.89	4.77	0.371
10	293.00	2.60	0.993	1316.18	5.05	0.371
11	357.68	8.61	0.353	159.17	1.07	2.600
12	308.08	8.61	0.353	-59.19	0.41	2.600
13	308.37	8.61	0.355	-58.60	0.41	2.629
14	308.50	2.60	0.355	-58.60	0.41	2.629
17	348.34	8.61	0.434	183.65	1.16	0.309

Heat Source:
Inlet: 400.00 K
Outlet: 349.58 K
Heat source flowrate: 3.09 kg/s

Effective RUE Optimized
$\eta_{II,ref} = 0.4$

	T K	p bars	x	h kJ/kg	s kJ/kg.K	flow rate kg/s
1	303.00	2.54	0.430	-101.22	0.30	3.000
2	303.08	8.75	0.430	-100.31	0.31	3.000
3	345.57	8.75	0.430	119.11	0.98	2.569
4	345.70	8.75	0.430	121.49	0.98	3.000
5	357.00	8.75	0.963	1486.45	5.00	0.354
6	312.10	8.75	0.653	-33.68	0.45	0.035
7	312.10	8.75	0.997	1335.00	4.56	0.319
8	312.10	8.75	0.997	1335.00	4.56	0.319
9	261.88	2.54	0.997	1202.28	4.65	0.319
10	293.00	2.54	0.997	1327.63	5.10	0.319
11	357.00	8.75	0.359	154.36	1.06	2.646
12	308.68	8.75	0.359	-58.68	0.41	2.646
13	309.03	8.75	0.363	-58.35	0.42	2.681
14	309.15	2.54	0.363	-58.35	0.42	2.681
17	346.50	8.75	0.430	135.72	1.02	0.431

Heat Source:
Inlet: 400.00 K
Outlet: 350.67 K
Heat source flowrate: 10.82 kg/s

Work Domain
Exergy Efficiency Optimized
Low Pressure Limit of 5 bars.

	T K	p bars	x	h kJ/kg	s kJ/kg.K	flow rate kg/s
1	303.00	1.00	0.288	-55.84	0.37	3.000
2	303.10	10.13	0.288	-54.56	0.37	3.000
3	381.24	10.13	0.288	326.83	1.48	2.601
4	377.99	10.13	0.288	276.15	1.35	3.000
5	395.00	10.13	0.827	1724.77	5.48	0.359
6	395.00	10.13	0.215	381.29	1.56	0.000
7	395.00	10.13	0.827	1724.77	5.48	0.359
8	395.00	10.13	0.827	1724.77	5.48	0.359
9	323.08	1.00	0.827	1412.69	5.65	0.359
10	323.08	1.00	0.827	1412.69	5.65	0.359
11	395.00	10.13	0.215	381.29	1.56	2.641
12	308.10	10.13	0.215	5.66	0.49	2.641
13	308.10	10.13	0.215	5.66	0.49	2.641
14	308.30	1.00	0.215	5.66	0.49	2.641
17	303.10	10.13	0.288	-54.56	0.37	0.399

Heat Source:
Inlet: 400.00 K
Outlet: 382.99 K
Heat source flowrate: 11.04 kg/s

RUE Optimized
Low Pressure Limit of 5 bars

	T K	p bars	x	h kJ/kg	s kJ/kg.K	flow rate kg/s
1	303.00	5.00	0.565	-100.20	0.29	3.000
2	303.17	15.51	0.565	-98.55	0.29	3.000
3	344.45	15.51	0.565	102.23	0.91	2.970
4	344.37	15.51	0.565	100.22	0.90	3.000
5	368.63	15.51	0.968	1483.94	4.74	0.809
6	368.63	15.51	0.416	197.45	1.19	0.000
7	368.63	15.51	0.968	1483.94	4.74	0.809
8	395.00	15.51	0.968	1554.05	4.92	0.809
9	332.98	5.00	0.968	1397.32	5.00	0.809
10	332.98	5.00	0.968	1397.32	5.00	0.809
11	368.63	15.51	0.416	197.45	1.19	2.191
12	308.17	15.51	0.416	-74.72	0.38	2.191
13	308.17	15.51	0.416	-74.72	0.38	2.191
14	308.38	5.00	0.416	-74.72	0.39	2.191
17	303.17	15.51	0.565	-98.55	0.29	0.030

Heat Source:
Inlet: 400.00 K
Outlet: 382.99 K
Heat source flowrate: 6.50 kg/s

Fluid: Propane-n-Undecane

Exergy Efficiency Optimized

	T	p	x	h	s	flow rate
	K	bars		kJ/kg	kJ/kg.K	kg/s
1	303.0	6.337	0.313114	-2291.78	3.481	10.000
2	303.4	19.087	0.313114	-2289.87	3.481	10.000
3	375.1	19.087	0.313114	-2082.67	4.085	8.539
4	375.7	19.087	0.313114	-2080.41	4.091	10.000
5	395.0	19.087	0.967003	-2187.09	5.983	1.752
6	333.2	19.087	0.776900	-2499.30	4.452	0.254
7	333.2	19.087	0.999262	-2351.36	5.639	1.498
8	333.2	19.087	0.999262	-2351.36	5.639	1.498
9	285.0	6.337	0.999262	-2402.74	5.639	1.498
10	293.0	6.337	0.999262	-2386.45	5.696	1.498
11	395.0	19.087	0.174205	-1972.49	3.909	8.248
12	308.4	19.087	0.174205	-2186.99	3.298	8.248
13	309.5	19.087	0.192224	-2196.33	3.336	8.502
14	309.9	6.337	0.192224	-2196.33	3.342	8.502
17	379.0	19.087	0.313114	-2067.21	4.126	1.461

Heat Source:
Inlet: 400.00 K
Outlet: 380.70 K
Heat source flowrate: 8.59 kg/s

RUE Optimized

	T	p	x	h	s	flow rate
	K	bars		kJ/kg	kJ/kg.K	kg/s
1	303.0	6.583	0.334172	-2305.44	3.514	10.000
2	303.2	13.137	0.334172	-2304.45	3.514	10.000
3	342.5	13.137	0.334172	-2185.85	3.877	8.383
4	342.4	13.137	0.334172	-2185.94	3.877	10.000
5	357.8	13.137	0.991529	-2271.69	5.901	1.697
6	314.0	13.137	0.852730	-2596.67	4.411	0.096
7	314.0	13.137	0.999863	-2371.35	5.633	1.601
8	314.0	13.137	0.999863	-2371.35	5.633	1.601
9	285.0	6.583	0.999863	-2403.48	5.633	1.601
10	293.0	6.583	0.999863	-2387.37	5.689	1.601
11	357.8	13.137	0.199785	-2085.04	3.699	8.303
12	308.2	13.137	0.199785	-2204.79	3.339	8.303
13	308.4	13.137	0.207260	-2209.28	3.353	8.399
14	308.6	6.583	0.207260	-2209.28	3.356	8.399
17	342.3	13.137	0.334172	-2186.46	3.875	1.617

Heat Source:
Inlet: 400.00 K
Outlet: 347.44 K
Heat source flowrate: 3.12 kg/s

Fluid: Isobutane-n-Undecane

Exergy Efficiency Optimized

	T	p	x	h	s	flow rate
	K	bars		kJ/kg	kJ/kg.K	kg/s
1	303.0	1.622	0.230908	-2218.66	3.191	10.000
2	303.1	5.778	0.230908	-2218.06	3.191	10.000
3	376.6	5.778	0.230908	-2016.16	3.780	8.812
4	376.8	5.778	0.230908	-2015.49	3.782	10.000
5	391.3	5.778	0.954950	-2125.49	5.294	1.249
6	322.2	5.778	0.741997	-2461.20	3.771	0.217
7	322.2	5.778	0.999666	-2293.93	4.936	1.032
8	322.2	5.778	0.999666	-2293.93	4.936	1.032
9	285.0	1.622	0.999666	-2344.34	4.936	1.032
10	293.0	1.622	0.999666	-2330.66	4.983	1.032
11	391.3	5.778	0.127585	-1943.42	3.713	8.751
12	308.1	5.778	0.127585	-2146.73	3.130	8.751
13	308.5	5.778	0.142432	-2154.33	3.148	8.968
14	308.7	1.622	0.142432	-2154.33	3.150	8.968
17	378.2	5.778	0.230908	-2010.48	3.795	1.188

Heat Source:
Inlet: 400.00 K
Outlet: 381.78 K
Heat source flowrate: 6.38 kg/s

RUE Optimized

	T	p	x	h	s	flow rate
	K	bars		kJ/kg	kJ/kg.K	kg/s
1	303.0	1.895	0.283372	-2248.96	3.239	10.000
2	303.1	4.368	0.283372	-2248.60	3.239	10.000
3	342.5	4.368	0.283372	-2140.56	3.571	8.832
4	342.4	4.368	0.283372	-2140.84	3.570	10.000
5	353.7	4.368	0.989706	-2220.98	5.162	1.179
6	309.3	4.368	0.819779	-2535.06	3.734	0.067
7	309.3	4.368	0.999889	-2313.09	4.911	1.112
8	309.3	4.368	0.999889	-2313.09	4.911	1.112
9	285.0	1.895	0.999889	-2345.64	4.911	1.112
10	293.0	1.895	0.999889	-2331.95	4.958	1.112
11	353.7	4.368	0.189007	-2073.84	3.518	8.821
12	308.3	4.368	0.189007	-2182.02	3.191	8.821
13	308.3	4.368	0.193736	-2184.66	3.196	8.888
14	308.4	1.895	0.193736	-2184.66	3.197	8.888
17	342.0	4.368	0.283372	-2143.01	3.564	1.168

Heat Source:
Inlet: 400.00 K
Outlet: 347.40 K
Heat source flowrate: 2.24 kg/s

Configuration with Preheater

RUE Optimized

	T	p	x	h	s	flow rate
	K	bars		kJ/kg	kJ/kg.K	kg/s
1	303.00	2.87	0.451	-103.92	0.30	3.000
2	303.09	9.49	0.451	-102.94	0.30	3.000
3	361.25	9.49	0.451	388.23	1.74	0.635
4	346.56	9.49	0.451	145.77	1.05	1.864
5	353.84	9.49	0.451	270.30	1.41	0.501
6	350.70	9.49	0.451	217.88	1.26	3.000
7	366.25	9.49	0.945	1525.50	5.07	0.592
8	324.32	9.49	0.569	-1.78	0.60	0.068
9	324.32	9.49	0.994	1366.11	4.62	0.525
10	324.32	9.49	0.994	1366.11	4.62	0.525
11	270.00	2.87	0.994	1231.37	4.71	0.525
12	293.00	2.87	0.994	1315.17	5.00	0.525
13	366.25	9.49	0.329	204.85	1.18	2.408
14	337.08	9.49	0.329	75.34	0.81	2.408
15	337.12	9.49	0.336	73.23	0.81	2.475
16	326.90	2.87	0.336	73.23	0.81	2.475

Heat Source:
Inlet: 400.00 K
Boiler Outlet: 355.69 K
Preheater Outlet: 327.82 K
Heat source flowrate: 3.97 kg/s

Configuration with Jet Pump

RUE Optimized:

	T	p	x	h	s	flow rate
	K	bars		kJ/kg	kJ/kg.K	kg/s
1	303.00	4.20	0.524	-105.18	0.29	3.000
2	303.19	17.00	0.524	-103.22	0.29	3.000
3	303.19	17.00	0.524	-103.22	0.29	2.851
4	357.12	17.00	0.524	198.78	1.19	0.149
5	306.53	17.00	0.524	-88.18	0.34	3.000
6	363.58	17.00	0.978	1454.52	4.62	0.347
7	341.34	17.00	0.616	90.63	0.85	0.014
8	341.34	17.00	0.993	1376.00	4.39	0.333
9	341.34	17.00	0.993	1376.00	4.39	0.333
10	270.00	3.29	0.993	1194.83	4.51	0.333
11	293.00	3.29	0.993	1306.83	4.91	0.333

12	363.58	17.00	0.465	171.07	1.12	2.653
13	363.58	17.00	0.465	171.07	1.12	2.653
14	363.46	17.00	0.466	170.66	1.12	2.667
15	318.31	3.29	0.466	159.54	1.14	2.667
16	317.61	3.29	0.524	286.88	1.56	3.000
17	323.93	4.20	0.524	296.89	1.57	3.000

Heat Source:
Inlet: 400.00 K
Outlet: 311.53 K
Heat source flowrate: 3.29 kg/s

Configuration with Kalina Thermal Compression

Using heat source for distillation

RUE Optimized

	T K	p bars	x	h kJ/kg	s kJ/kg.K	flow rate kg/s
1	303.00	3.68	0.497	-106.26	0.29	1.165
2	303.12	12.38	0.497	-104.94	0.29	1.165
3	350.52	12.38	0.497	193.33	1.19	0.843
4	346.16	12.38	0.497	108.75	0.95	0.322
5	349.28	12.38	0.497	169.96	1.12	1.165
6	373.21	12.38	0.947	1530.72	4.96	0.292
7	343.52	12.38	0.506	78.54	0.86	0.025
8	343.52	12.38	0.988	1409.25	4.63	0.267
9	343.52	12.38	0.988	1409.25	4.63	0.267
10	270.00	2.34	0.988	1217.68	4.76	0.267
11	293.00	2.34	0.988	1304.27	5.06	0.267
12	373.21	12.38	0.347	231.65	1.26	0.873
13	308.12	12.38	0.347	-56.52	0.41	0.873
14	309.34	12.38	0.351	-52.76	0.43	0.898
15	309.55	2.34	0.351	-52.76	0.43	0.898
16	303.00	2.34	0.417	-98.84	0.31	3.000
17	303.02	3.68	0.417	-98.64	0.31	3.000
18	317.17	3.68	0.417	-27.09	0.54	2.001
19	325.86	3.68	0.366	14.06	0.65	1.835
20	308.02	3.68	0.366	-63.97	0.40	1.835
21	308.04	2.34	0.366	-63.97	0.40	1.835
22	325.86	3.68	0.982	1413.54	5.20	0.166
23	303.02	3.68	0.417	-98.64	0.31	0.999

Heat Source:
Inlet: 400.00 K
Boiler Outlet: 354.27 K
Distiller outlet: 322.17 K
Heat source flowrate: 2.34 kg/s

Effective RUE optimized

$\eta_{II,ref} = 0.4$

	T K	p bars	x	h kJ/kg	s kJ/kg.K	flow rate kg/s
1	303.00	3.08	0.463	-105.08	0.30	1.283
2	303.11	11.39	0.463	-103.83	0.30	1.283
3	352.67	11.39	0.463	192.27	1.18	0.973
4	357.08	11.39	0.463	268.13	1.40	0.310
5	353.71	11.39	0.463	210.61	1.24	1.283
6	373.27	11.39	0.940	1541.89	5.02	0.280
7	321.91	11.39	0.651	11.10	0.59	0.046
8	321.91	11.39	0.996	1347.10	4.48	0.235
9	321.91	11.39	0.996	1347.10	4.48	0.235
10	254.56	1.89	0.996	1158.29	4.61	0.235
11	293.00	1.89	0.996	1333.19	5.26	0.235
12	373.27	11.39	0.330	236.51	1.27	1.003
13	308.11	11.39	0.330	-50.72	0.42	1.003
14	309.91	11.39	0.344	-48.04	0.44	1.049
15	309.86	1.89	0.344	-48.04	0.44	1.049
16	303.00	1.89	0.382	-90.92	0.32	3.000
17	303.01	3.08	0.382	-90.75	0.32	3.000
18	318.13	3.08	0.382	-10.86	0.58	1.893
19	328.35	3.08	0.322	39.54	0.70	1.717
20	308.01	3.08	0.322	-48.54	0.42	1.717
21	308.04	1.89	0.322	-48.54	0.43	1.717
22	328.35	3.08	0.973	1432.62	5.34	0.176
23	303.01	3.08	0.382	-90.75	0.32	1.107

Heat Source:
Inlet: 400.00 K
Boiler Outlet: 358.71 K
Distiller outlet: 323.13 K
Heat source flowrate: 2.28 kg/s

Work Optimized

	T K	p bars	x	h kJ/kg	s kJ/kg.K	flow rate kg/s
1	303.00	2.67	0.438	-102.40	0.30	0.962
2	303.09	9.71	0.438	-101.36	0.30	0.962
3	357.61	9.71	0.438	293.36	1.47	0.568
4	303.09	9.71	0.438	-101.36	0.30	0.393
5	348.11	9.71	0.438	132.01	1.01	0.962
6	395.00	9.71	0.818	1736.23	5.52	0.363
7	395.00	9.71	0.208	384.81	1.56	0.000
8	395.00	9.71	0.818	1736.23	5.52	0.363
9	395.00	9.71	0.818	1736.23	5.52	0.363
10	330.44	1.28	0.818	1458.69	5.66	0.363
11	330.44	1.28	0.818	1458.69	5.66	0.363
12	395.00	9.71	0.208	384.81	1.56	0.598
13	308.09	9.71	0.208	9.82	0.49	0.598
14	308.09	9.71	0.208	9.82	0.49	0.598
15	308.27	1.28	0.208	9.82	0.50	0.598
16	303.00	1.28	0.323	-71.09	0.35	3.000

17	303.02	2.67	0.323	-70.89	0.35	3.000
18	324.36	2.67	0.323	31.55	0.68	2.216
19	333.99	2.67	0.269	86.55	0.80	2.038
20	308.02	2.67	0.269	-24.81	0.46	2.038
21	308.04	1.28	0.269	-24.81	0.46	2.038
22	333.99	2.67	0.947	1477.44	5.52	0.177
23	303.02	2.67	0.323	-70.89	0.35	0.784

Heat Source:
Inlet: 400.00 K
Boiler Outlet: 353.11 K
Distiller outlet: 329.36 K
Heat source flowrate: 3.71 kg/s

Using absorber heat recovery for distillation

RUE Optimized

	T K	p bars	x	h kJ/kg	s kJ/kg.K	flow rate kg/s
1	303.00	3.35	0.479	-105.97	0.29	1.438
2	303.10	10.55	0.479	-104.89	0.29	1.438
3	370.38	10.55	0.479	544.39	2.16	0.278
4	370.38	10.55	0.479	544.39	2.16	0.235
5	351.52	10.55	0.479	248.87	1.35	0.925
6	357.97	10.55	0.479	354.32	1.64	1.438
7	375.38	10.55	0.926	1566.02	5.12	0.402
8	332.31	10.55	0.539	30.08	0.71	0.059
9	332.31	10.55	0.992	1384.07	4.63	0.343
10	332.31	10.55	0.992	1384.07	4.63	0.343
11	270.00	2.64	0.992	1226.67	4.73	0.343
12	293.00	2.64	0.992	1311.35	5.03	0.343
13	375.38	10.55	0.306	254.01	1.30	1.036
14	336.08	10.55	0.306	79.91	0.81	1.036
15	336.60	10.55	0.319	77.23	0.81	1.095
16	327.31	2.64	0.319	77.23	0.81	1.095
17	324.63	2.64	0.479	371.42	1.83	1.438
18	315.38	2.64	0.479	225.30	1.37	1.438
19	303.00	2.64	0.437	-102.17	0.30	3.000
20	303.01	3.35	0.437	-102.06	0.30	3.000
21	310.38	3.35	0.437	-65.11	0.42	1.672
22	317.00	3.35	0.398	-33.13	0.52	1.562
23	308.01	3.35	0.398	-72.69	0.39	1.562
24	308.02	2.64	0.398	-72.69	0.39	1.562
25	317.00	3.35	0.988	1387.37	5.17	0.110
26	303.01	3.35	0.437	-102.06	0.30	1.328

Heat Source:
Inlet: 400.00 K
Boiler Outlet: 362.97 K
Preheater outlet: 331.04 K
Heat source flowrate: 2.44 kg/s

Effective RUE Optimized

$\eta_{II,ref} = 0.4$

	T K	p bars	x	h kJ/kg	s kJ/kg.K	flow rate kg/s
1	303.00	3.65	0.496	-106.27	0.29	1.350
2	303.12	11.81	0.496	-105.03	0.29	1.350
3	375.76	11.81	0.496	612.28	2.34	0.251
4	375.76	11.81	0.496	612.28	2.34	0.253
5	358.21	11.81	0.496	345.09	1.61	0.846
6	364.59	11.81	0.496	444.84	1.89	1.350
7	380.76	11.81	0.918	1582.60	5.10	0.423
8	333.82	11.81	0.559	40.42	0.73	0.072
9	333.82	11.81	0.992	1381.30	4.57	0.351
10	333.82	11.81	0.992	1381.30	4.57	0.351
11	270.00	2.85	0.992	1220.89	4.67	0.351
12	293.00	2.85	0.992	1310.00	4.99	0.351
13	380.76	11.81	0.303	279.68	1.37	0.927
14	337.12	11.81	0.303	85.83	0.82	0.927
15	338.03	11.81	0.321	82.55	0.83	0.999
16	329.08	2.85	0.321	82.55	0.83	0.999
17	326.00	2.85	0.496	401.36	1.92	1.350
18	315.17	2.85	0.496	232.15	1.39	1.350
19	303.00	2.85	0.450	-103.84	0.30	3.000
20	303.01	3.65	0.450	-103.72	0.30	3.000
21	309.67	3.65	0.450	-74.13	0.40	1.764
22	316.97	3.65	0.413	-36.34	0.51	1.650
23	309.80	3.65	0.413	-67.98	0.41	1.650
24	309.52	2.85	0.413	-67.98	0.41	1.650
25	316.97	3.65	0.989	1384.51	5.12	0.114
26	303.01	3.65	0.450	-103.72	0.30	1.236

Heat Source:
Inlet: 400.00 K
Boiler Outlet: 369.59 K
Preheater outlet: 333.95 K
Heat source flowrate: 2.54 kg/s

Work Optimized

	T K	p bars	x	h kJ/kg	s kJ/kg.K	flow rate kg/s
1	303.00	2.03	0.394	-93.88	0.32	0.554
2	303.03	4.57	0.394	-93.51	0.32	0.554
3	382.99	4.57	0.394	1043.62	3.53	0.060
4	331.71	4.57	0.394	88.55	0.88	0.006
5	380.03	4.57	0.394	963.41	3.32	0.488
6	380.03	4.57	0.394	963.41	3.32	0.554
7	387.99	4.57	0.647	1934.62	6.17	0.289
8	387.93	4.57	0.117	405.23	1.51	0.000
9	387.93	4.57	0.648	1933.53	6.17	0.289
10	387.93	4.57	0.648	1933.53	6.17	0.289
11	343.50	1.00	0.648	1720.76	6.28	0.289
12	343.50	1.00	0.648	1720.76	6.28	0.289
13	387.99	4.57	0.117	405.69	1.51	0.264
14	326.71	4.57	0.117	145.91	0.78	0.264
15	326.81	4.57	0.117	146.35	0.79	0.265

16	326.88	1.00	0.117	146.35	0.79	0.265
17	341.55	1.00	0.394	967.72	3.66	0.554
18	318.19	1.00	0.394	426.90	2.03	0.554
19	303.00	1.00	0.288	-55.84	0.37	3.000
20	303.01	2.03	0.288	-55.69	0.37	3.000
21	313.16	2.03	0.288	-12.05	0.52	2.534
22	326.72	2.03	0.264	57.55	0.71	2.446
23	316.16	2.03	0.264	12.34	0.57	2.446
24	309.51	1.00	0.264	12.34	0.57	2.446
25	326.72	2.03	0.952	1458.01	5.60	0.088
26	303.01	2.03	0.288	-55.69	0.37	0.466

Heat Source:
Inlet: 400.00 K
Boiler Outlet: 385.03 K
Preheater outlet: 326.60 K
Heat source flowrate: 2.10 kg/s

APPENDIX C
SIMULATION SOURCE CODE

A sample source code used in the simulation of the basic cycle configuration is included here. The programs were written in the C language. The functions used to calculate fluid properties should be clearly identifiable. The code for other cycle configurations can be easily written suing the code below and the description in the text.

Basic Cycle Configuration

Header File

Cycver0.h

```
double x_boiler, y_boiler, x_cond, y_cond;
double t_boilermin, t_condmin, t_dewb, t_bubblec;
double T_coolMax=270 ;
double molarweight_water=18.01528;
 //[Handbook of Chemistry and Physics, 72nd ed.]
double hhs1_massbasis, hhs2_massbasis, hhs3_massbasis,hhsm_massbasis,f_hs;
double amv_boiler, aml_boiler, amv_cond, aml_cond, amv_rcond, aml_rcond;
double ms = 1.;
double x_in, x_sat, r1,r2;
double t_ab, t_boiler, t_cond, t_super, p_high, p_low, p_inter;
double h[18], s[18], v[18], t[18], p[18], x[18], f[18];
double h_is, s_is, v_is, t_is;
double h_boiler[6], s_boiler[6], v_boiler[6];
double irr[11];
double q_absorber, q_boiler, q_cond, q_super, q_cooler, q_hrhx;
double wt, eff, eff_withoutcooling, pump;
double x_turbine, y_turbine;
double amv_turbine, aml_turbine;
double molehs, phs;
double ths1, hhs1, shs1, vhs1;
double ths2, hhs2, shs2, vhs2;
double ths3, hhs3, shs3, vhs3;
double hhs4, shs4, vhs4;
double thsm, hhsm, shsm, vhsm;
double tcf1, hcf1, scf1, vcf1;
```

```
double tcf2, hcf2, scf2, vcf2;
double molecf, pcf;
double td,hd,sd,vd;
double t_pin, h_pin, s_pin, v_pin, q_pin, q_hot, q_cold;
double t0=298, p0, h0, s0, v0;
double exhs,exhs1,exhs2,effrue, effxgy, effex;
double deltat, deltat2, deltat3;
double h_hs_b;
double etaIS_pump=0.8;
double etaIS_turb=0.85;
```

Cycle Simulation

cycver0.c

```
#include <stdio.h>
#include <math.h>
#include "propertyv2.c"
#include "cycver0.h"

/*****************************************************************
1. This program simulates the basic power cooling cycle.
2. No pressure losses are assumed
3. Isentropic Efficiencies are assumed for the turbine and pump

*****************************************************************/

// BOILER
FUNCTION*************************************************
void boiler(double p_boiler_in, double x_in, double t_boiler, double t_cond,
                        double h_boiler[], double s_boiler[], double v_boiler[])
{

// ammonia mass fraction in boiler and condenser, x: liquid, y: vapor

  double h_re, s_re, v_re;


   // incoming mixture property
        t_boilermin=bubble(p_boiler_in, x_in);
        t_dewb=dew(p_boiler_in, x_in);

        amm_fraction(t_boiler, p_boiler_in, &x_boiler, &y_boiler);
        amv_boiler = (x_in - x_boiler)/(y_boiler - x_boiler);
        aml_boiler = (y_boiler - x_in)/(y_boiler - x_boiler);

        //condensor equations
```

```
        t_condmin = dew(p_boiler_in, y_boiler);
        t_bubblec = bubble(p_boiler_in, y_boiler);
                amm_fraction(t_cond, p_boiler_in, &x_cond, &y_cond);

        amv_cond = (y_boiler - x_cond)/(y_cond - x_cond);
        aml_cond = (y_cond - y_boiler)/(y_cond - x_cond);

        // Mass balances implemented

        f[12]=aml_boiler*f[1];
        f[5]=amv_boiler*f[1];
        f[7]=amv_cond*f[5];
        f[6]=aml_cond*f[5];

        mix_l(t_boiler, p_boiler_in, x_boiler, &h_re, &s_re, &v_re);
        h_boiler[2] = h_re;
        s_boiler[2] = s_re;
        v_boiler[2] = v_re;
        mix_v(t_boiler, p_boiler_in, y_boiler, &h_re, &s_re, &v_re);
        h_boiler[3] = h_re;
        s_boiler[3] = s_re;
        v_boiler[3] = v_re;
        mix_l(t_cond, p_boiler_in, x_cond, &h_re, &s_re, &v_re);
        h_boiler[4] = h_re;
        s_boiler[4] = s_re;
        v_boiler[4] = v_re;
        mix_v(t_cond, p_boiler_in, y_cond, &h_re, &s_re, &v_re);
        h_boiler[5] = h_re;
        s_boiler[5] = s_re;
        v_boiler[5] = v_re;
 return;
}

//************ END OF BOILER FUNCTION

void main()
{
 char filename[30];
 FILE *fp;
 double g[17], gub[17], glb[17];
 int i=0;
    gets(filename);
  fp=fopen(filename,"a");
   t_ab=303;
 scanf("%lf",&t_ab);
 scanf("%lf",&t_boiler);
```

```
  scanf("%lf",&t_cond);
  scanf("%lf",&t_super);
  scanf("%lf",&p_high);
  scanf("%lf",&p_low);
  scanf("%lf",&ths1);
  scanf("%lf",&molehs);
  scanf("%lf",&r1);
  scanf("%lf",&r2);

 x_in = sat_con(p_low, t_ab);
 p_inter=p_low;
//HEAT SOURCE HEAT SOURCE HEAT SOURCE HEAT SOURCE HEAT SOURCE HEAT SOURCE
HEAT SOURCE
        f_hs=molehs*molarweight_water;  //flow rate of the heat source in kg/s
        phs = h2o_sat_p(ths1);          //heat source pressure
        steam_l(ths1, phs, &hhs1, &shs1, &vhs1); //molar basis
        hhs1_massbasis=hhs1/molarweight_water;

//HEAT SOURCE HEAT SOURCE HEAT SOURCE HEAT SOURCE HEAT SOURCE HEAT SOURCE
//point 1
        t[1] = t_ab;
        p[1] = p_low;
        x[1] = x_in; // DEFINE AS AN UPPER BOUND LIMIT?
        f[1] = 3.; // REFERENCE FLOWRATE.  HOW TO SCALE?
        mix_l(t[1], p[1], x[1], &h[1], &s[1], &v[1]);
//point 2 (AFTER PUMP)
        p[2] = p_high;
        x[2] = x[1];

//THE NEXT THREE LINES ACCOUNT FOR THE ISENTROPIC EFFICIENCY OF
PUMP.
      s_is=s[1];
      property_s_t(p[2],s_is,x_in,&h_is,&t_is,&v_is);
      h[2]=(h_is-h[1])/etaIS_pump+h[1];

        f[2] = f[1];
        property_h_t(p[2], h[2], x[2], &t[2], &s[2], &v[2]);

// CALL TO BOILER FUNCTION
 boiler(p_high,x_in,t_boiler,t_cond,h_boiler,s_boiler,v_boiler);
 //point 12  Weak solution return from boiler
        t[12] = t_boiler;
        p[12] = p_high;
        x[12] = x_boiler;
        s[12] = s_boiler[2];
        v[12] = v_boiler[2];
```

```
        h[12] = h_boiler[2];
//point 13 and point 3

        t[13] = t[2];
        p[13] = p[12];
        x[13] = x[12];
        f[13] = f[12];
        property(t[13], p[13], x[13], &h[13], &s[13], &v[13]);
        q_hot = f[12]*(h[12] - h[13]);

        t[3] = t[12] ;
        p[3] = p[2];
        x[3] = x[2];
        f[3] = f[2]*r2/100;
        property(t[3], p[3], x[3], &h[3], &s[3], &v[3]);
       q_cold = f[3]*(h[3] - h[2]);
        if(q_hot <= q_cold){
       q_hot = q_hot*r1/100;
        q_hrhx = q_hot;
        h[13]=h[12] - q_hot/f[12];
        property_h_t(p[13], h[13], x[13], &t[13], &s[13], &v[13]);
        h[3] = h[2] + q_hot/f[3];
        property_h_t(p[3], h[3], x[3], &t[3], &s[3], &v[3]);
        }
        else
        {
        q_cold = q_cold*r1/100;
        q_hrhx = q_cold;
        h[13]=h[12] - q_cold/f[12];
        property_h_t(p[13], h[13], x[13], &t[13], &s[13], &v[13]);
        h[3] = h[2] + q_cold/f[3];
        property_h_t(p[3], h[3], x[3], &t[3], &s[3], &v[3]);
        }
//point 5 (Vapor)
        t[5] = t_boiler;
        p[5] = p_high;
        h[5] = h_boiler[3];
        s[5] = s_boiler[3];
        v[5] = v_boiler[3];
        x[5] = y_boiler;
// point 6 Reflux from Rectifier
        t[6] = t_cond;
        p[6] = p[5];
        h[6] = h_boiler[4];
        s[6] = s_boiler[4];
        v[6] = v_boiler[4];
```

```
        x[6] = x_cond;
//point 14 Mixing of Reflux from condensor and weaksolution return from boiler
        p[14] = p[13];
        x[14] = (f[13]*x[13]+f[6]*x[6])/(f[13]+f[6]);
        h[14] = (f[13]*h[13]+f[6]*h[6])/(f[13]+f[6]);
        property_h_t(p[14], h[14], x[14], &t[14], &s[14], &v[14]);
        f[14]=f[13]+f[6];
//point 15
        p[15] = p_low;
        x[15] = x[14];
        h[15] = h[14]; //isenthalpic expansion
        property_h_t(p[15], h[15], x[15], &t[15], &s[15], &v[15]);
        f[15]=f[14];
// point 7 Vapor from Rectifier
        t[7] = t_cond;
        p[7] = p[6];
        x[7] = y_cond;
        h[7] = h_boiler[5];
        s[7] = s_boiler[5];
        v[7] = v_boiler[5];
// point 8   Super Heater
        t[8] = t_super;
        p[8] = p[7];
        x[8] = x[7];
        f[8] = f[7];
        mix_v(t[8], p[8], x[8], &h[8], &s[8], &v[8]);
//point 9  Turbine
        p[9] = p_inter; //new variable
        s_is=s[8];
        x[9] = x[8];
        f[9]=f[8];
   property_s_t(p[9],s_is,x[9],&h_is,&t_is,&v_is);
   h[9]=h[8]-etaIS_turb*(h[8]-h_is);
  property_h_t(p[9], h[9], x[9], &t[9], &s[9], &v[9]);
  amm_fraction(t[9], p[9], &x_turbine, &y_turbine);
        amv_turbine=(y_cond-x_turbine)/(y_turbine-x_turbine);
        aml_turbine=(y_turbine-y_cond)/(y_turbine-x_turbine);
//point 10  isenthalpic expansion -- redundant
        p[10]=p_low;
        x[10] = x[9];
        h[10] = h[9]; //isenthalpic expansion
        property_h_t(p[10], h[10], x[10], &t[10], &s[10], &v[10]);
        f[10]=f[9];
//point 11   cooler
        p[11] = p_low ;
        x[11] = x[10];
```

```
        f[11]=f[10];
        if(t[10]<T_coolMax)
          {
                t[11] = 293.;
                property(t[11], p[11], x[11], &h[11], &s[11], &v[11]);
                q_cooler = ms * f[10] * (h[11] - h[10]);
          }
        else
          {
                q_cooler = 0.;
                t[11] = t[10];
                h[11] = h[10];
                s[11] = s[10];
                v[11] = v[10];
          }
//SUPERHEATER ENERGY BALANCE
        hhs2_massbasis=hhs1_massbasis - f[7]*(h[8]-h[7])/f_hs  ;
// Point 17
        f[17]=(1 - (r2/100))*f[2];
//CONDENSOR ENERGY BALANCE
        h[17]=h[2]+(f[5]*h[5]-f[7]*h[7]-f[6]*h[6])/f[17];
        x[17]=x[2];
        p[17]=p[2];
        property_h_t(p[17], h[17], x[17], &t[17], &s[17], &v[17]);
//point 4
   h[4]=(f[3]*h[3]+f[17]*h[17])/(f[3]+f[17]);
        f[4]=f[3]+f[17];
        x[4]=x[3];
        p[4]=p[3];
        property_h_t(p[4], h[4], x[4], &t[4], &s[4], &v[4]);
//BOILER MASS BALANCE
        hhs3_massbasis=hhs2_massbasis-(f[5]*h[5]+f[12]*h[12]-f[4]*h[4])/f_hs ;
        hhs3=hhs3_massbasis*molarweight_water;
        hhs2=hhs2_massbasis*molarweight_water;
        steam_l_ph(phs, hhsm, &thsm, &shsm, &vhsm);
        steam_l_ph(phs, hhs3, &ths3, &shs3, &vhs3);
        steam_l_ph(phs, hhs2, &ths2, &shs2, &vhs2);
//PINCH POINT EVALUATION
        //HX1
        t_pin = t_boilermin;
        property(t_pin, p_high, x_in, &h_pin, &s_pin, &v_pin);
        if(t[3]>=t_boilermin)
        {
                        h[16] = h[13]+ ms*f[3]*(h_pin-h[2])/f[13];
                        x[16] = x[12];
                        p[16] = p[12];
```

```
                        f[16] = f[12];
                        property_h_t(p[16], h[16], x[16], &t[16], &s[16], &v[16]);
                        deltat=t[16]-t_pin;
        }
        else deltat = t[13]-t[2];
        if(t[4]<t_boilermin)
        {
        hhsm_massbasis=hhs3_massbasis+ ms*f[4]*(h_pin-h[4])/f_hs;
        hhsm=hhsm_massbasis*molarweight_water;
        steam_l_ph(phs, hhsm, &thsm, &shsm, &vhsm);
        deltat3 = thsm-t_pin;
        }
        else deltat3=ths3- t[4];
        if(t[17]>t_boilermin)
        {
                h[16] = h[5]- f[17]*(h[17]-h_pin)/f[5];
                        x[16] = x[5];
                        p[16] = p[6];
                        f[16] = f[5];
                        property_h_t(p[16], h[16], x[16], &t[16], &s[16], &v[16]);
                        deltat2=t[16]-t_pin;
        }

        else deltat2= t[6]-t[2];
        t0=298.0;
       p0=1.013;
      steam_l(t0, p0, &h0, &s0, &v0);
//Heats
  q_boiler = ms * (f[5]*h[5]+f[12]*h[12]-f[4]*h[4]);
  q_cond   = ms * (f[6] * h[6] + f[7] * h[7] - f[5] * h[5]);
  q_super = ms * f[7] * (h[8] - h[7]);
  q_absorber = ms * (f[15] * h[15] + f[11] * h[11]-f[1] * h[1]);
  wt = ms * f[8] * (h[8] - h[9]);
  pump = ms * f[1] * (h[2] - h[1]);
  // eff = ((wt-pump+q_cooler) / (q_super + q_boiler)) * 100;
    eff = (wt-pump+(f[10]*(h[10]-h[11]-t0*(s[10]-s[11])))/0.3)* 100. / (q_super +
q_boiler) ;
     exhs=molehs*((hhs1-h0)-t0*(shs1-s0));
     exhs1=molehs*((hhs1-hhs3)-t0*(shs1-shs3));
//      effrue = (wt-pump+q_cooler)* 100./ exhs ;
       effrue = (wt-pump+ (f[10]*(h[10]-h[11]-t0*(s[10]-s[11])))/0.3)* 100./ exhs ;
//      effrue = ((wt-pump)* (t[10]/(298-t[10]))+q_cooler)* 100./ exhs;
//     effrue = ((wt-pump)* (T_coolMax/(298-T_coolMax))+q_cooler)* 100./ exhs;
//     effrue = (f[10]*(h[10]-h[11]-t0*(s[10]-s[11])))* 100./ exhs ;
//     effrue = (wt-pump)* 100./ exhs ;
```

```
//      effxgy = (wt-pump+q_cooler)* 100./ exhs1 ;
       effxgy = (wt-pump+ (f[10]*(h[10]-h[11]-t0*(s[10]-s[11])))/0.3)* 100./ exhs1 ;
//    effxgy = ((wt-pump)* (t[10]/(298-t[10]))+q_cooler)* 100./ exhs1;
//    effxgy = ((wt-pump)* (T_coolMax/(298-T_coolMax))+q_cooler)* 100./ exhs1;
//    effxgy = (f[10]*(h[10]-h[11]-t0*(s[10]-s[11])))* 100./ exhs1 ;
//    effxgy = (wt-pump)* 100./ exhs1 ;
// constraint functions
  g[1] = t_cond - t_boiler;
  g[2] = t_cond - t_super;
  g[3] = t[12] - t[3];
  g[4] = t[5] - t[17];
  g[5] = ths1 - t[8];
  g[6] = ths2 - t[5];
  g[7] = ths3 - t[4];
  g[8] = deltat;
  g[9] = deltat2;
  g[10]= deltat3;
  g[11]= f[12] * 100.;
  g[12]= amv_turbine * 100.;
  g[13]= amv_boiler*100;
  g[14]= q_cooler;
  g[15]= effrue;
  g[16]= p_high-p_low;
//Irreversibilities
            // Boiler
            irr[0]=t0*(f[5]*s[5] + f[12]*s[12] - f[4]*s[4]+ molehs*(shs3-shs2));
            //Rectifier
            irr[1]=t0*(f[7]*s[7] + f[6]*s[6] + f[17]*s[17] - f[17]*s[2] - f[5]*s[5]);
            //Recup. Hx
            irr[2]=t0*(f[3]*s[3] + f[13]*s[13] - f[3]*s[2] - f[12]*s[12]);
            //Super Heater
            irr[3]=t0*(f[8]*(s[8]-s[7]) + molehs*(shs2-shs1));
            //Throttle Valve
            irr[4]=t0*f[14]*(s[15]-s[14]);
            //Mixing 1
            irr[5]= t0*(f[14]*s[14] - f[6]*s[6] - f[13]*s[13]);
            //Mixing 2
            irr[6]= t0*(f[4]*s[4] - f[17]*s[17] - f[3]*s[3]);
            //Absorber
            irr[7]= t0*(f[1]*s[1] - f[15]*s[15] - f[11]*s[11] + q_absorber/t0);
            //Exergy Lost from Source Reinjection
            irr[8] = exhs-exhs1;
            // Turbine Irreversibility
            irr[9] = t0*f[9]*(s[9] - s[8]);
            // Pump irreversibility
```

```
            irr[10] = t0*f[1]*(s[2] - s[1]);
// Constraint limits
glb[1] =   -1.0e+30  ;  gub[1]  =   0.00     ;
glb[2] =   -1.0e+30  ;  gub[2]  =   0.00     ;
glb[3] =     5.      ;  gub[3]  =   1.0e+30  ;
glb[4] =     5.      ;  gub[4]  =   1.0e+30  ;
glb[5] =     5.      ;  gub[5]  =   1.0e+30  ;
glb[6] =     5.      ;  gub[6]  =   1.0e+30  ;
glb[7] =     5.      ;  gub[7]  =   1.0e+30  ;
glb[8] =     5.      ;  gub[8]  =   1.0e+30  ;
glb[9] =     5.      ;  gub[9]  =   1.0e+30  ;
glb[10] =    5.      ;  gub[10] =   1.0e+30  ;
glb[11] =    0.00    ;  gub[11] =   300      ;
glb[12] =    90.     ;  gub[12] =   1.0e+30  ;
glb[13] =  0.01      ;  gub[13] =   100.0    ;
glb[14] =  0.1       ;  gub[14] =   1.0e+30  ;
glb[15] =  0.0       ;  gub[15] =   100.0    ;
glb[16] =  0.0       ;  gub[16] =   1.0e+30  ;

fprintf(fp,"PARAMETERS OF CYCLE FOR TRANSFER TO SPREADSHEET\n");
  fprintf(fp,"Heat Source Temperature: %f \t Low temperature: %f \t Objective function:
%f \n", ths1, t[10], g[15]);
  fprintf(fp,"t_ambient: %f \t t_ab: %f \n", t0, t_ab);
  fprintf(fp,"\n\n");
         for(i=1;i<=16;i++){
         if(g[i]<glb[i] || g[i]>gub[i]) fprintf(fp,"g[%d]: %f \t0\n", i,g[i]);
          else fprintf(fp,"g[%d]: %f \t1\n", i,g[i]);
}
         for(i=1 ; i<18 ; i++){
      fprintf(fp,"%2i  %6.2f  %5.2f  %5.3f  %7.2f  %8.2f  %8.3f   %7.3f\n",
          i,t[i],p[i],x[i],h[i],s[i],v[i],f[i]);
 }
         fprintf(fp,"pin  %6.2f  %5.2f  %5.3f  %7.2f  %8.2f  %8.3f   %7.3f\n",
          t_pin,p[3],x[3],h_pin,s_pin,v_pin,f[3]);
  fprintf(fp,"\n\n");
  fprintf(fp, "%f \t %f \t %f \n", ths1, hhs1,shs1);
    fprintf(fp, "%f \t %f \t %f \n", ths2, hhs2,shs2);
           fprintf(fp, "%f \t %f \t %f \n", ths3, hhs3,shs3);
             fprintf(fp, "%f \t %f \t %f \n", t0, h0,s0);
  fprintf(fp,"\n\n");
  fprintf(fp," %f \n",t_boiler);
  fprintf(fp," %f \n",t_cond);
  fprintf(fp," %f \n",t_super);
  fprintf(fp," %f \n",p_high);
  fprintf(fp," %f \n",p_low);
  fprintf(fp," %f \n",x_in);
```

```
  fprintf(fp," %f \n",t_dewb);
  fprintf(fp," %f \n",t_boilermin);
  fprintf(fp," %f \n",t[10]);
  fprintf(fp," %f \n",r1);
  fprintf(fp," %f \n",r2);
  fprintf(fp," %f \n",eff);
  fprintf(fp," %f \n",effrue);
  fprintf(fp," %f \n",effxgy);
  fprintf(fp," %f \n",wt-pump);
  fprintf(fp," %f \n",q_cooler);
  fprintf(fp," %f \n",molehs);
  fprintf(fp," %f \n",q_boiler);
  fprintf(fp," %f \n",-1*q_cond);
  fprintf(fp," %f \n",q_hrhx);
  fprintf(fp," %f \n",q_super);
  fprintf(fp," %f \n",q_absorber);
  fprintf(fp," %f \n",ths3);
  fprintf(fp," %f \n",exhs);
  fprintf(fp," %f \n",exhs1);
  fprintf(fp," %f \n",amv_turbine);
  fprintf(fp," %f \n",amv_boiler);



 fprintf(fp,"\n\n");
         for(i=0; i<=10; i++)fprintf(fp," %f \n", irr[i]);
  fprintf(fp,"\n\n");
  fclose(fp);
}
```

Interface to Supertrapp

The program written to interface the cycle simulation to the SUPERTRAPP source code is given below. This program, written in FORTRAN 77 uses subroutines in SUPERTRAPP and has specific subroutines similar to those in the ammonia-water properties program.

Propty.for

```
CCCCCCCCCCCCCCCCCCCCCCCCCCCCCCCCCCCCCCCCCCCCCCCCCCCCCCCCCCCCCCCCCCCCCCCCCCC
C      DRIVER SUBROUTINES TO OBTAIN VARIOUS PROPERTIES NEEDED IN CYCLE
```

```
C      SIMULATION
C
C      INTERNAL UNITS OF THE CODE ARE SPECIFIED BELOW
C          PROPERTY                 UNITS
C        ..........................................................
C          TEMPERATURE              [K]
C          PRESSURE                 [BAR]
C          VOLUME                   [LITER/MOL]
C          DENSITY                  [MOL/L]
C          ENTHALPY                 [CAL/MOL]
C          ENTROPY                  [CAL/MOL.K]
C          CP                       [CAL/MOL.K]
C          CV                       [CAL/MOL.K]
C          SOUND SPEED              [M/SEC]
C          JT COEFFICIENT           [K/BAR]
C          VISCOSITY                [MICROPOISE]
C          THERMAL CONDUCTIVITY     [MW/M.K]
C          COMPOSITION              [MOL FRACTION]
C
C
C
CCCCCCCCCCCCCCCCCCCCCCCCCCCCCCCCCCCCCCCCCCCCCCCCCCCCCCCCCCCCCCCCCCCCCCCCCCCCCCC
      DOUBLE PRECISION FUNCTION WTMOL(P,T,NAME)
      IMPLICIT DOUBLE PRECISION (A-H,O-Z)
      CHARACTER NAME(20)*50
      DIMENSION  X(20,2), FEED(20), AK(20), PROPS(20,2)
      DIMENSION  XL(20),XV(20)
C
C     SELECT EXTENDED CORRESPONDING STATES MODEL, METHOD = 2
      METHOD = 2
      NC = 1
      FEED(1) = 1

C               ADDITIONAL SET UP, REQUIRED EVERY TIME COMPONENTS
C                OR FEED CHANGED
      CALL SETCOM(NAME,FEED,NC,IER)
      IF(IER.NE.0)THEN
        WRITE(*,*)' COMPONENT NAME SPELLED INCORRECTLY, OR '
        WRITE(*,*)' IT IS NOT PRESENT IN THE DATABASE '
        STOP
      ENDIF
C
      CALL FLASH(P,T,FEED,AK,X,PSI,NPH,IER)
      DO 111 I = 1,NC
        XL(I)=X(I,1)
        XV(I)=X(I,2)
111   CONTINUE
C                       EVALUATE PROPERTIES IF NO ERRORS FROM FLASH
      IF(IER.EQ.0)THEN
        CALL PHASEP(P,T,XL,XV,PSI,NPH,METHOD,PROPS,IERPP)
        IF(IERPP.NE.0) THEN
           WRITE(2,*)' FAILURE IN PHASEP '
        ELSE
C                       J = 1 IS LIQUID PHASE, J = 2 IS VAPOR
         WTMOL = PROPS(1,1)*PROPS(2,1)+PROPS(1,2)*PROPS(2,2)
        ENDIF
      ENDIF
```

```
C
C
      RETURN
      END
CCCCCCCCCCCCCCCCCCCCCCCCCCCCCCCCCCCCCCCCCCCCCCCCCCCCCCCCCCCCCCCCCCCCCC
C
      SUBROUTINE PRPTPX(P,T,XIN1,H,S,V,NAME)
      IMPLICIT DOUBLE PRECISION (A-H,O-Z)
      CHARACTER NAME(20)*50
      COMMON/PVARS/NC,METHOD
      DIMENSION  X(20,2), FEED(20), AK(20), PROPS(20,2)
      DIMENSION  XL(20),XV(20)
C
      CALL XC1(XIN1,FEED(1))
      FEED(2) = 1D0-FEED(1)
C                         ADDITIONAL SET UP, REQUIRED EVERY TIME
COMPONENTS
C                         OR FEED CHANGED
      CALL SETCOM(NAME,FEED,NC,IER)
      IF(IER.NE.0)THEN
        WRITE(*,*)' COMPONENT NAME SPELLED INCORRECTLY, OR '
        WRITE(*,*)' IT IS NOT PRESENT IN THE DATABASE '
        STOP
      ENDIF
C
C     FIRST DEMONSTRATE T,P FLASH
C     INTERNAL UNITS   TX[K], PX[BAR]
      CALL FLASH(P,T,FEED,AK,X,PSI,NPH,IER)
      DO 111 I = 1,NC
        XL(I)=X(I,1)
        XV(I)=X(I,2)
111   CONTINUE
C                         EVALUATE PROPERTIES IF NO ERRORS FROM FLASH
      IF(IER.EQ.0)THEN
        CALL PHASEP(P,T,XL,XV,PSI,NPH,METHOD,PROPS,IERPP)
        IF(IERPP.NE.0) THEN
           WRITE(2,*)' FAILURE IN PHASEP VIA PRPTPX '
        ELSE
C                         J = 1 IS LIQUID PHASE, J = 2 IS VAPOR
         H = PROPS(1,1)*PROPS(5,1)+PROPS(1,2)*PROPS(5,2)
         S = PROPS(1,1)*PROPS(6,1)+PROPS(1,2)*PROPS(6,2)
         V = PROPS(1,1)/PROPS(4,1)+PROPS(1,2)/PROPS(4,2)
        ENDIF
      ENDIF
C
C
      CALL UNIT2(FEED(1),H,S,V)
      RETURN
      END
CCCCCCCCCCCCCCCCCCCCCCCCCCCCCCCCCCCCCCCCCCCCCCCCCCCCCCCCCCCCCCCCCCCCCC
C
      SUBROUTINE SPTPX(P,T,XIN1,NP,H,S,V,NAME)
      IMPLICIT DOUBLE PRECISION (A-H,O-Z)
      CHARACTER NAME(20)*50
      COMMON/PVARS/NC,METHOD
      DIMENSION  X(20,2), FEED(20), AK(20), PROPS(20,2)
      DIMENSION  XL(20),XV(20)
```

```
C
      CALL XC1(XIN1,FEED(1))
      FEED(2) = 1D0-FEED(1)
C                    ADDITIONAL SET UP, REQUIRED EVERY TIME
COMPONENTS
C                    OR FEED CHANGED
      CALL SETCOM(NAME,FEED,NC,IER)
      IF(IER.NE.0)THEN
        WRITE(*,*)' COMPONENT NAME SPELLED INCORRECTLY, OR '
        WRITE(*,*)' IT IS NOT PRESENT IN THE DATABASE '
        STOP
      ENDIF
C
C     FIRST DEMONSTRATE T,P FLASH
C     INTERNAL UNITS   TX[K], PX[BAR]
      NPH = NP
      CALL FLASHO(P,T,FEED,AK,X,PSI,NPH,IER)
      DO 111 I = 1,NC
        XL(I)=X(I,1)
        XV(I)=X(I,2)
111   CONTINUE
C                    EVALUATE PROPERTIES IF NO ERRORS FROM FLASH
      IF(IER.EQ.0)THEN
        CALL PHASEP(P,T,XL,XV,PSI,NPH,METHOD,PROPS,IERPP)
        IF(IERPP.NE.0) THEN
           WRITE(2,*)' FAILURE IN PHASEP VIA SPTPX '
        ELSE
C                    J = 1 IS LIQUID PHASE, J = 2 IS VAPOR
         H = PROPS(1,1)*PROPS(5,1)+PROPS(1,2)*PROPS(5,2)
         S = PROPS(1,1)*PROPS(6,1)+PROPS(1,2)*PROPS(6,2)
         V = PROPS(1,1)/PROPS(4,1)+PROPS(1,2)/PROPS(4,2)
        ENDIF
      ENDIF
C
C
      CALL UNIT2(FEED(1),H,S,V)
      RETURN
      END
CCCCCCCCCCCCCCCCCCCCCCCCCCCCCCCCCCCCCCCCCCCCCCCCCCCCCCCCCCCCCCCCCCCCCC
      SUBROUTINE PRPSPX(P,S,XIN1,H,T,V,NAME)
      IMPLICIT DOUBLE PRECISION (A-H,O-Z)
      CHARACTER NAME(20)*50
       COMMON/PVARS/NC,METHOD
      DIMENSION  X(20,2), FEED(20), AK(20), PROPS(20,2)
      DIMENSION  XL(20),XV(20)
C
      CALL UNIT1(XIN1,H,S,V)
      CALL XC1(XIN1,FEED(1))
      FEED(2) = 1D0-FEED(1)
C                ADDITIONAL SET UP, REQUIRED EVERY TIME COMPONENTS
C                OR FEED CHANGED
      CALL SETCOM(NAME,FEED,NC,IER)
      IF(IER.NE.0)THEN
        WRITE(*,*)' COMPONENT NAME SPELLED INCORRECTLY, OR '
        WRITE(*,*)' IT IS NOT PRESENT IN THE DATABASE '
        STOP
      ENDIF
```

```
      CALL FLPS(P,S,FEED,METHOD,XL,XV,T,PSI,NPH,IER)
C
C                       EVALUATE PROPERTIES IF NO ERRORS FROM FLASH
      IF(IER.EQ.0)THEN
        CALL PHASEP(P,T,XL,XV,PSI,NPH,METHOD,PROPS,IERPP)
        IF(IERPP.NE.0) THEN
           WRITE(2,*)' FAILURE IN PHASEP VIA PRPSPX '
        ELSE
C
C                       J = 1 IS LIQUID PHASE, J = 2 IS VAPOR
         H = PROPS(1,1)*PROPS(5,1)+PROPS(1,2)*PROPS(5,2)
         V = PROPS(1,1)/PROPS(4,1)+PROPS(1,2)/PROPS(4,2)
        ENDIF
      ELSE
        WRITE(2,*)' CONVERGENCE FAILURE IN FLPS VIA PRPSPX '
      ENDIF
C
C
      CALL UNIT2(FEED(1),H,S,V)
      RETURN
      END
CCCCCCCCCCCCCCCCCCCCCCCCCCCCCCCCCCCCCCCCCCCCCCCCCCCCCCCCCCCCCCCCCCCCCCCCCCCCCCC
C
C
C
      SUBROUTINE PRPHPX(P,H,XIN1,S,T,V,NAME)
      IMPLICIT DOUBLE PRECISION (A-H,O-Z)
      CHARACTER NAME(20)*50
       COMMON/PVARS/NC,METHOD
      DIMENSION  X(20,2), FEED(20), AK(20), PROPS(20,2)
      DIMENSION  XL(20),XV(20)
C
      CALL UNIT1(XIN1,H,S,V)
      CALL XC1(XIN1,FEED(1))
      FEED(2) = 1D0-FEED(1)
C                       ADDITIONAL SET UP, REQUIRED EVERY TIME
COMPONENTS
C                       OR FEED CHANGED
      CALL SETCOM(NAME,FEED,NC,IER)
      IF(IER.NE.0)THEN
        WRITE(*,*)' COMPONENT NAME SPELLED INCORRECTLY, OR '
        WRITE(*,*)' IT IS NOT PRESENT IN THE DATABASE '
        STOP
      ENDIF
      CALL FLPH(P,H,FEED,METHOD,XL,XV,T,PSI,NPH,IER)
C
C                       EVALUATE PROPERTIES IF NO ERRORS FROM FLASH
      IF(IER.EQ.0)THEN
        CALL PHASEP(P,T,XL,XV,PSI,NPH,METHOD,PROPS,IERPP)
        IF(IERPP.NE.0) THEN
           WRITE(2,*)' FAILURE IN PHASEP VIA PRPHPX '
        ELSE
C
C                       J = 1 IS LIQUID PHASE, J = 2 IS VAPOR
         S = PROPS(1,1)*PROPS(6,1)+PROPS(1,2)*PROPS(6,2)
         V = PROPS(1,1)/PROPS(4,1)+PROPS(1,2)/PROPS(4,2)
        ENDIF
```

```
      ELSE
        WRITE(2,*)' CONVERGENCE FAILURE IN FLPH VIA PRPHPX '
      ENDIF
C
C
      CALL UNIT2(FEED(1),H,S,V)
      RETURN
      END
C
CCCCCCCCCCCCCCCCCCCCCCCCCCCCCCCCCCCCCCCCCCCCCCCCCCCCCCCCCCCCCCCCCCCCCCCCCCCCCCC
C PROPERTIES OF MIXTURE IN VAPOR PHASE
C
      SUBROUTINE VAPTPX(P,T,XIN1,H,S,V,NAME)
      IMPLICIT DOUBLE PRECISION (A-H,O-Z)
      CHARACTER NAME(20)*50
      COMMON/PVARS/NC,METHOD
      DIMENSION  X(20,2), FEED(20), AK(20), PROPS(20,2)
      DIMENSION  XL(20),XV(20)
C
      CALL XC1(XIN1,FEED(1))
      FEED(2) = 1D0-FEED(1)
C                      ADDITIONAL SET UP, REQUIRED EVERY TIME
COMPONENTS
C                      OR FEED CHANGED
      CALL SETCOM(NAME,FEED,NC,IER)
      IF(IER.NE.0)THEN
        WRITE(*,*)' COMPONENT NAME SPELLED INCORRECTLY, OR '
        WRITE(*,*)' IT IS NOT PRESENT IN THE DATABASE '
        STOP
      ENDIF
C
C     FIRST DEMONSTRATE T,P FLASH
C     INTERNAL UNITS   TX[K], PX[BAR]
      CALL FLASH(P,T,FEED,AK,X,PSI,NPH,IER)
      DO 111 I = 1,NC
        XL(I)=X(I,1)
        XV(I)=X(I,2)
111   CONTINUE
C                      EVALUATE PROPERTIES IF NO ERRORS FROM FLASH
      IF(IER.EQ.0)THEN
        CALL PHASEP(P,T,XL,XV,PSI,NPH,METHOD,PROPS,IERPP)
        IF(IERPP.NE.0) THEN
           WRITE(2,*)' FAILURE IN PHASEP VIA VAPTPX '
        ELSE
C                      J = 1 IS LIQUID PHASE, J = 2 IS VAPOR
         H = PROPS(5,2)
         S = PROPS(6,2)
         V = 1/PROPS(4,2)
         ENDIF
      ENDIF
C
C
      CALL UNIT2(FEED(1),H,S,V)
      RETURN
      END
C
```

```
CCCCCCCCCCCCCCCCCCCCCCCCCCCCCCCCCCCCCCCCCCCCCCCCCCCCCCCCCCCCCCCCCCCCCCCCCCCCCCC
C
C     PROPERTIES OF MIXTURE IN LIQUID PHASE
C
      SUBROUTINE LIQTPX(P,T,XIN1,H,S,V,NAME)
      IMPLICIT DOUBLE PRECISION (A-H,O-Z)
      CHARACTER NAME(20)*50
      COMMON/PVARS/NC,METHOD
      DIMENSION  X(20,2), FEED(20), AK(20), PROPS(20,2)
      DIMENSION  XL(20),XV(20)
C
      CALL XC1(XIN1,FEED(1))
      FEED(2) = 1D0-FEED(1)
C                     ADDITIONAL SET UP, REQUIRED EVERY TIME
COMPONENTS
C                     OR FEED CHANGED
      CALL SETCOM(NAME,FEED,NC,IER)
      IF(IER.NE.0)THEN
        WRITE(*,*)' COMPONENT NAME SPELLED INCORRECTLY, OR '
        WRITE(*,*)' IT IS NOT PRESENT IN THE DATABASE '
        STOP
      ENDIF
C
C     FIRST DEMONSTRATE T,P FLASH
C     INTERNAL UNITS   TX[K], PX[BAR]
      CALL FLASH(P,T,FEED,AK,X,PSI,NPH,IER)
      DO 111 I = 1,NC
        XL(I)=X(I,1)
        XV(I)=X(I,2)
111   CONTINUE
C                     EVALUATE PROPERTIES IF NO ERRORS FROM FLASH
      IF(IER.EQ.0)THEN
        CALL PHASEP(P,T,XL,XV,PSI,NPH,METHOD,PROPS,IERPP)
        IF(IERPP.NE.0) THEN
           WRITE(2,*)' FAILURE IN PHASEP VIA LIQTPX '
        ELSE
C                     J = 1 IS LIQUID PHASE, J = 2 IS VAPOR
         H = PROPS(5,1)
         S = PROPS(6,1)
         V = 1/PROPS(4,1)
        ENDIF
      ENDIF
C
C
      CALL UNIT2(FEED(1),H,S,V)
      RETURN
      END
CCCCCCCCCCCCCCCCCCCCCCCCCCCCCCCCCCCCCCCCCCCCCCCCCCCCCCCCCCCCCCCCCCCCCCCCCCCCCCC
C
C
C     BUBBLE AND DEW POINT DATA ROUTINES
C
      SUBROUTINE BUBLT(PX,TX,XIN1,NAME)
      IMPLICIT DOUBLE PRECISION (A-H,O-Z)
       COMMON/PVARS/NC,METHOD
      PARAMETER (MX = 20)
      CHARACTER NAME(MX)*50
```

```
      DIMENSION FEED(MX),X(MX,2),PROPS(20,2),XL(20),XV(20)
C
      CALL XC1(XIN1,FEED(1))
      FEED(2) = 1D0-FEED(1)
C                       ADDITIONAL SET UP, REQUIRED EVRY TIME
COMPONENTS
C                       OR FEED CHANGED
      CALL SETCOM(NAME,FEED,NC,IER)
      IF(IER.NE.0)THEN
        WRITE(*,*)' COMPONENT NAME SPELLED INCORRECTLY, OR '
        WRITE(*,*)' IT IS NOT PRESENT IN THE DATABASE '
        STOP
      ENDIF
C
C
C                       USE BUBT TO GET SATURATION VALUES FOR PURE
COMPONENT
      CALL BUBT(PX,TX,FEED,AK,X,PSI,NPH,IER)
C
      RETURN
      END
C
CCCCCCCCCCCCCCCCCCCCCCCCCCCCCCCCCCCCCCCCCCCCCCCCCCCCCCCCCCCCCCCCCCCCCCCCCCCCCCC
C
      SUBROUTINE DT(PX,TX,XIN1,NAME)
      IMPLICIT DOUBLE PRECISION (A-H,O-Z)
       COMMON/PVARS/NC,METHOD
      PARAMETER (MX = 20)
      CHARACTER NAME(MX)*50
      DIMENSION FEED(MX),X(MX,2),PROPS(20,2),XL(20),XV(20)
C
      CALL XC1(XIN1,FEED(1))
      FEED(2) = 1D0-FEED(1)
C                       ADDITIONAL SET UP, REQUIRED EVRY TIME
COMPONENTS
C                       OR FEED CHANGED
      CALL SETCOM(NAME,FEED,NC,IER)
      IF(IER.NE.0)THEN
        WRITE(*,*)' COMPONENT NAME SPELLED INCORRECTLY, OR '
        WRITE(*,*)' IT IS NOT PRESENT IN THE DATABASE '
        STOP
      ENDIF
C
C
C                       USE DEWT TO GET SATURATION VALUES FOR PURE
COMPONENT
      CALL DEWT(PX,TX,FEED,AK,X,PSI,NPH,IER)
C
      RETURN
      END
C
CCCCCCCCCCCCCCCCCCCCCCCCCCCCCCCCCCCCCCCCCCCCCCCCCCCCCCCCCCCCCCCCCCCCCCCCCCCCCCC
C        BUBBLE POINT PRESSURE CALCULATION
C
      SUBROUTINE BUBLP(PX,TX,XIN1,NAME)
      IMPLICIT DOUBLE PRECISION (A-H,O-Z)
       COMMON/PVARS/NC,METHOD
```

```
      PARAMETER (MX = 20)
      CHARACTER NAME(MX)*50
      DIMENSION FEED(MX),X(MX,2),PROPS(20,2),XL(20),XV(20)
C
      CALL XC1(XIN1,FEED(1))
      FEED(2) = 1D0-FEED(1)
C                         ADDITIONAL SET UP, REQUIRED EVRY TIME
COMPONENTS
C                         OR FEED CHANGED
      CALL SETCOM(NAME,FEED,NC,IER)
      IF(IER.NE.0)THEN
        WRITE(*,*)' COMPONENT NAME SPELLED INCORRECTLY, OR '
        WRITE(*,*)' IT IS NOT PRESENT IN THE DATABASE '
        STOP
      ENDIF
C
C
C                         USE BUBP TO GET SATURATION VALUES FOR PURE
COMPONENT
      CALL BUBP(PX,TX,FEED,AK,X,PSI,NPH,IER)
C
      RETURN
      END
CCCCCCCCCCCCCCCCCCCCCCCCCCCCCCCCCCCCCCCCCCCCCCCCCCCCCCCCCCCCCCCCCCCCCC
C
      SUBROUTINE DP(PX,TX,XIN1,NAME)
      IMPLICIT DOUBLE PRECISION (A-H,O-Z)
       COMMON/PVARS/NC,METHOD
      PARAMETER (MX = 20)
      CHARACTER NAME(MX)*50
      DIMENSION FEED(MX),X(MX,2),PROPS(20,2),XL(20),XV(20)
C
      CALL XC1(XIN1,FEED(1))
      FEED(2) = 1D0-FEED(1)
C                         ADDITIONAL SET UP, REQUIRED EVRY TIME
COMPONENTS
C                         OR FEED CHANGED
      CALL SETCOM(NAME,FEED,NC,IER)
      IF(IER.NE.0)THEN
        WRITE(*,*)' COMPONENT NAME SPELLED INCORRECTLY, OR '
        WRITE(*,*)' IT IS NOT PRESENT IN THE DATABASE '
        STOP
      ENDIF
C
C
C                         USE DEWP TO GET SATURATION VALUES FOR PURE
COMPONENT
      CALL DEWP(PX,TX,FEED,AK,X,PSI,NPH,IER)
C
      RETURN
      END
C
CCCCCCCCCCCCCCCCCCCCCCCCCCCCCCCCCCCCCCCCCCCCCCCCCCCCCCCCCCCCCCCCCCCCCCC
C
C
C           SUBROUTINE FOR VAPOR AND LIQUID CONCENTRATIONS
C
```

```
      SUBROUTINE VAPLIQ(P,T,XIN1,XV,XL,NAME)
      IMPLICIT DOUBLE PRECISION (A-H,O-Z)
       COMMON/PVARS/NC,METHOD
      CHARACTER NAME(20)*50
      DIMENSION  X(20,2), FEED(20), AK(20), PROPS(20,2)
C
      CALL XC1(XIN1,FEED(1))
      FEED(2) = 1D0-FEED(1)
C                     ADDITIONAL SET UP, REQUIRED EVERY TIME
COMPONENTS
C                     OR FEED CHANGED
      CALL SETCOM(NAME,FEED,NC,IER)
      IF(IER.NE.0)THEN
        WRITE(*,*)' COMPONENT NAME SPELLED INCORRECTLY, OR '
        WRITE(*,*)' IT IS NOT PRESENT IN THE DATABASE '
        STOP
      ENDIF
C
C     INTERNAL UNITS   TX[K], PX[BAR]
      CALL FLASH(P,T,FEED,AK,X,PSI,NPH,IER)
      IF (NPH.EQ.0)THEN
      CALL XD1(X(1,2),XV)
      XL=0
      ELSEIF(NPH.EQ.1)THEN
      XV=0
      CALL XD1(X(1,1),XL)
      ELSEIF(NPH.EQ.2)THEN
      CALL XD1(X(1,1),XL)
      CALL XD1(X(1,2),XV)
      ENDIF
      RETURN
      END
C
CCCCCCCCCCCCCCCCCCCCCCCCCCCCCCCCCCCCCCCCCCCCCCCCCCCCCCCCCCCCCCCCCCCCCCC
C
C     SUBROUTINE TO CALCULATE LIQUID AND VAPOR FLOW FRACTIONS
C     UNTESTED 01/28/03, TEST BEFORE USING!!!!
CCCCCCCCCCCCCCCCCCCCCCCCCCCCCCCCCCCCCCCCCCCCCCCCCCCCCCCCCCCCCCCCCCCCCCC
C
      SUBROUTINE VLFLOW(P,T,XIN1,FV,FL,NAME)
      IMPLICIT DOUBLE PRECISION (A-H,O-Z)
       COMMON/PVARS/NC,METHOD
       COMMON/MW/WTMOL1,WTMOL2
      CHARACTER NAME(20)*50
      DIMENSION  X(20,2), FEED(20), AK(20), PROPS(20,2)
      DIMENSION  XL(20),XV(20)

C
      CALL XC1(XIN1,FEED(1))
      FEED(2) = 1D0-FEED(1)
C                     ADDITIONAL SET UP, REQUIRED EVERY TIME
COMPONENTS
C                     OR FEED CHANGED
      CALL SETCOM(NAME,FEED,NC,IER)
      IF(IER.NE.0)THEN
        WRITE(*,*)' COMPONENT NAME SPELLED INCORRECTLY, OR '
        WRITE(*,*)' IT IS NOT PRESENT IN THE DATABASE '
```

```
        STOP
       ENDIF
C
C      INTERNAL UNITS   TX[K], PX[BAR]
       CALL FLASH(P,T,FEED,AK,X,PSI,NPH,IER)
       DO 111 I = 1,NC
         XL(I)=X(I,1)
         XV(I)=X(I,2)
111    CONTINUE
C                        EVALUATE PROPERTIES IF NO ERRORS FROM FLASH
       IF(IER.EQ.0)THEN
         CALL PHASEP(P,T,XL,XV,PSI,NPH,METHOD,PROPS,IERPP)
         IF(IERPP.NE.0) THEN
            WRITE(2,*)' FAILURE IN PHASEP VIA VLFLOW '
         ELSE
C                        J = 1 IS LIQUID PHASE, J = 2 IS VAPOR
         FL=PROPS(1,1)*PROPS(2,1)
         FV=PROPS(1,2)*PROPS(2,2)

           ENDIF
        ENDIF

       RETURN
       END
C
CCCCCCCCCCCCCCCCCCCCCCCCCCCCCCCCCCCCCCCCCCCCCCCCCCCCCCCCCCCCCCCCCCCCCCCCCCCCCCC
C
C
C      SUBROUTINE FOR SATURATION CONCENTRATION IN ABSORBER
C      WILL WORK FOR NON AZEOTROPIC FLUID MIXTURES.
C     DO NOT USE FOR OTHERS.
CCCCCCCCCCCCCCCCCCCCCCCCCCCCCCCCCCCCCCCCCCCCCCCCCCCCCCCCCCCCCCCCCCCCCCCCCCCCCCC
C
C
       SUBROUTINE SATC(PX,TX,XIN1,NAME)
       IMPLICIT DOUBLE PRECISION (A-H,O-Z)
       LOGICAL IEQ
       PARAMETER (MX = 20)
       CHARACTER NAME(MX)*50
       XIN11=1.0D0
       XIN12=0.0D0
       CALL BUBLT(PX,TX1,XIN11,NAME)
       CALL BUBLT(PX,TX2,XIN12,NAME)
       IF(TX.GT.TX1.AND.TX.GT.TX2) THEN
          WRITE(*,*)'NO SAT. LIQUID AT THIS TEMPERATURE AND PRESSURE'
       ENDIF
C
C221    IF(TX.LT.TX1.AND.TX.LT.TX2) THEN
C           NCOUNT = 0
C          DX=1.0D-04
C           ERROR = (TX-TX1)/TX
C           ERROR = DABS(ERROR)
C           PRINT*, ERROR
C225        IF(ERROR.GT.1.0D-10)THEN
C             XIN12 = XIN11-DX
C             CALL BUBLT(PX,TX2,XIN12,NAME)
C             S =(TX2-TX1)/(XIN12-XIN11)
```

```
C              PRINT*,S
C              XNEW = (TX-TX1)/S + XIN11
C              CALL BUBLT(PX,TNEW,XNEW,NAME)
C              XIN12 = XNEW + DX
C230           CALL BUBLT(PX,TX2,XIN12,NAME)
C              SNEW =(TX2-TNEW)/(XIN12-XNEW)
C              R = SNEW/S
C              IF(R.LT.0)THEN
C                 XNEW = (XIN11+XNEW)/2
C              GO TO 230
C              ENDIF
C              ERROR = (TX-TNEW)/TX
C              ERROR = DABS(ERROR)
C              XIN11 = XNEW
C              TX1 = TNEW
C              GO TO 225
C             ENDIF
C           ENDIF
C           RETURN
C           END

       NCOUNT=0
       ERR=1.0
222    IF(ERR.GT.1D-12.AND.NCOUNT.LT.1000) THEN
          S=(XIN11-XIN12)/(TX1-TX2)
          XIN11=(TX-TX2)*S
          WRITE(*,*)XIN11,TX1,TX2
          CALL BUBLT(PX,TX1,XIN11,NAME)
          ERR=(TX-TX1)/TX
          ERR=DABS(ERR)
          NCOUNT=NCOUNT+1
          GO TO 222
        ELSEIF(ERR.LE.1D-12) THEN
          XIN1=XIN11
           TX=TX1
        ENDIF
        RETURN
        END
C
CCCCCCCCCCCCCCCCCCCCCCCCCCCCCCCCCCCCCCCCCCCCCCCCCCCCCCCCCCCCCCCCCCCCCCC
C
C
C     MASS TO MOL
      SUBROUTINE XC1(XMAS,XMOL)
      IMPLICIT DOUBLE PRECISION (A-H,O-Z)
       COMMON/MW/WTMOL1,WTMOL2
       XMOL = XMAS*WTMOL2/((1.0D0-XMAS)*WTMOL1+XMAS*WTMOL2)
      RETURN
      END
C
C     MOLE TO MASS
      SUBROUTINE XD1(XMOL,XMAS)
      IMPLICIT DOUBLE PRECISION (A-H,O-Z)
       COMMON/MW/WTMOL1,WTMOL2
       XMAS =  XMOL*WTMOL1/(XMOL*WTMOL1 + (1.0D0-XMOL)*WTMOL2)
      RETURN
      END
```

```
C  UNIT1 CONVERTS DATA FROM SI UNITS TO
C  SUPERTRAPP DEFAULT UNITS, NEEDS MASSFRACTION.
      SUBROUTINE UNIT1(X1,H,S,V)
      IMPLICIT DOUBLE PRECISION (A-H,O-Z)
       COMMON/MW/WTMOL1,WTMOL2
       H = H*WTMOL1*WTMOL2/(4.1868D0*(X1*(WTMOL2-WTMOL1)+WTMOL1))
       S = S*WTMOL1*WTMOL2/(4.1868D0*(X1*(WTMOL2-WTMOL1)+WTMOL1))
       V = V*WTMOL1*WTMOL2/(X1*(WTMOL2-WTMOL1)+WTMOL1)
      RETURN
      END
C
C  UNIT2 CONVERTS DATA FROM  SUPERTRAPP DEFAULT UNITS
C   TO SI UNITS, NEEDS MOL FRACTION INPUT.
      SUBROUTINE UNIT2(X1,H,S,V)
      IMPLICIT DOUBLE PRECISION (A-H,O-Z)
       COMMON/MW/WTMOL1,WTMOL2
      H = H*4.1868D0/(X1*(WTMOL1-WTMOL2)+WTMOL2)
      S = S*4.1868D0/(X1*(WTMOL1-WTMOL2)+WTMOL2)
      V = V/(X1*(WTMOL1-WTMOL2)+WTMOL2)
      RETURN
      END



CCCCCCCCCCCCCCCCCCCCCCCCCCCCCCCCCCCCCCCCCCCCCCCCCCCCCCCCCCCCCCCCCCCCCCCCCCCCCCC
C
C     SUBROUTINES FOR WATER PROPERTIES
CCCCCCCCCCCCCCCCCCCCCCCCCCCCCCCCCCCCCCCCCCCCCCCCCCCCCCCCCCCCCCCCCCCCCCCCCCCCCCC
C
      SUBROUTINE STEAML(TX,PX,HH2OL, SH2OL,VH2OL)
      IMPLICIT DOUBLE PRECISION (A-H,O-Z)
C
C     CONSTANTS
      TB = 100
      PB = 10
      R = 8.3144
      H2OLRO = 21.821141
C
      H2OA1 = 2.748796D-02
      H2OA2 = -1.016665D-05
      H2OA3 = -4.452025D-03
      H2OA4 = 8.389246D-04
C
      H2OB1 = 12.14557
      H2OB2 = -1.898065
      H2OB3 = 0.2911966
C
      H2OTD = 5.0705
      H2OPD = 3.0000
C
      H2OSLD = 5.733498
C
      TR=TX/TB
      PR=PX/PB
CCCCCCCCCCCCCCCCCCCCCCCCCCCCCCCCCCCCCCCCCCCCCCCCCCCCCCCCCCCCCCCCCCCCCCCCCCCCCCC
C
```

```
      H = -H2OLRO + H2OB1*H2OTD + H2OB2/2*(H2OTD**2 + TR**2)+
     1 H2OB3/3*(H2OTD**3 - TR**3) - H2OB1*TR - H2OB2*(TR**2) +
     2 (H2OA4*(TR**2) - H2OA1)*(PR - H2OPD)- H2OA2/2*(PR**2 - H2OPD**2)
      HH2OL = -R*TB*H
C
      S = -H2OSLD - H2OB1*log(TR/H2OTD) + H2OB2*(H2OTD - TR)
     3 + H2OB3/2*(H2OTD**2 - TR**2)+(H2OA3 + 2*H2OA4*TR)*(PR - H2OPD)
      SH2OL = -R*S
C
      V = H2OA1 + H2OA2*PR + H2OA3*TR + H2OA4*TR**2
      VH2OL = R*TB/PB*V
C
      RETURN
      END
CCCCCCCCCCCCCCCCCCCCCCCCCCCCCCCCCCCCCCCCCCCCCCCCCCCCCCCCCCCCCCCCCCCCCCCCCCCCCCC
C
      SUBROUTINE STEAMV(TX,PX,HH2OV, SH2OV,VH2OV)
      IMPLICIT DOUBLE PRECISION (A-H,O-Z)
C     CONSTANTS
      TB = 100.0D0
      PB = 10.0D0
      R = 8.3144D0
C
      H2OGRO = 60.965058
      H2OD1 = 4.019170
      H2OD2 = -5.175550D-02
      H2OD3 = 1.951939D-02
C
      H2OC1 = 2.136131D-02
      H2OC2 = -31.69291
      H2OC3 = -4.634611D04
      H2OC4 = 0.0
C
      H2OTD = 5.0705
      H2OPD = 3.0000
C
      H20SGD = 13.453430
C
      TR=TX/TB
      PR=PX/PB

CCCCCCCCCCCCCCCCCCCCCCCCCCCCCCCCCCCCCCCCCCCCCCCCCCCCCCCCCCCCCCCCCCCCCCCCCCCCCCC
C
       H = -H2OGRO + H2OD1*H2OTD + H2OD2/2*(H2OTD**2 + TR**2)
     1  + H2OD3/3*(H2OTD**3 - TR**3) - H2OD1*TR
     2  - H2OD2*(TR**2) - H2OC1*(PR - H2OPD)
     3  + H2OC2*4*(H2OPD/H2OTD**3 - PR/TR**3)
     4  + H2OC3*12*(H2OPD/H2OTD**11 - PR/TR**11)
     5  + H2OC4*4*(H2OPD**3/H2OTD**11 - PR**3/TR**11)
        HH2OV = -R*TB*H
C
        S = -H20SGD - H2OD1*LOG(TR/H2OTD) + H2OD2*(H2OTD - TR)
     6  + H2OD3/2*(H2OTD**2 - TR**2) + LOG(PR/H2OPD)
     7  + 3*H2OC2*(H2OPD/H2OTD**4 - PR/TR**4)
     8  + 11*H2OC3*(H2OPD/H2OTD**12 - PR/TR**12)
     9  + 11/3*H2OC4*(H2OPD**3/H2OTD**12 - PR**3/TR**12)
        SH2OV = -R*S
```

```
C
        V = TR/PR + H2OC1 + H2OC2/TR**3 + (H2OC3 + H2OC4*PR*PR)/TR**11
        VH2OV = R*TB/PB*V
C
      RETURN
      END
CCCCCCCCCCCCCCCCCCCCCCCCCCCCCCCCCCCCCCCCCCCCCCCCCCCCCCCCCCCCCCCCCCCCCCCCCCCCCCC
C
C
C
      SUBROUTINE H2OSP(TX,PX)
      IMPLICIT DOUBLE PRECISION (A-H,O-Z)
      DIMENSION FRRAY(10)
      DATA FRRAY /0.0, -7.691234564, -2.608023696D01, -1.681706546D02,
     1            6.423285504D01, -1.189646225D02, 4.16711732,
     2            2.09750676D01, 1.0D09, 6.0/
      ZT = TX/647.3D0
      ZTT = 1 - ZT
      PK = 0
      DO 30 I = 6,1,-1
      PK = PK * ZTT + FRRAY(I)
 30   CONTINUE
       PK = PK / (ZT * (1 + FRRAY(7) * ZTT + FRRAY(8) * ZTT * ZTT))
       PK = PK - ZTT / (FRRAY(9) * ZTT * ZTT + FRRAY(10))
       PX = EXP(PK) * 221.20
       RETURN
      END
CCCCCCCCCCCCCCCCCCCCCCCCCCCCCCCCCCCCCCCCCCCCCCCCCCCCCCCCCCCCCCCCCCCCCCCCCCCCCCC
C
C
C
        SUBROUTINE STMLPH(PX, HX, TH2OL, SH2OL, VH2OL)
      IMPLICIT DOUBLE PRECISION (A-H,O-Z)
      TT1 = 300.0D0
      TT2 = 500.0D0
      TT=0
      SS=0
      HH=0
      VV=0
      ERR=1
50    IF(ERR.GT.1D-20)THEN
       TTOLD = TT
       TT = (TT1+TT2)/2
       CALL STEAML(TT, PX, HH, SS, VV)
        IF(HH.GT.HX) THEN
          TT2=TT
        ELSE
          TT1=TT
        ENDIF
        ERR = TT-TTOLD
        ERR = DABS(ERR)
        GO TO 50
      ENDIF
      TH2OL = TT
      SH2OL = SS
      VH2OL = VV
      RETURN
```

```
      END
C
CCCCCCCCCCCCCCCCCCCCCCCCCCCCCCCCCCCCCCCCCCCCCCCCCCCCCCCCCCCCCCCCCCCCCCCC
```

LIST OF REFERENCES

1. Goswami, D. Y., 1995, "Solar Thermal Power – Status and Future Directions," *Proceedings of the 2nd ISHMT-ASME Heat and Mass Transfer Conference*, S. Murthy and Y. Jaluria, eds., Tata McGraw Hill, New Delhi, pp. 57-60.

2. Goswami, D. Y., and Xu, F., 1999, "Analysis of a New Thermodynamic Cycle for Combined Power and Cooling Using Low and Mid Temperature Solar Collectors," Journal of Solar Energy Engineering, **121**(2), pp. 91-97.

3. Lu, S., and Goswami, D. Y., 2002, "Optimization of a Novel Combined Power/Refrigeration Thermodynamic Cycle," Journal of Solar Energy Engineering, **125**(2), pp. 212-217.

4. Lu, S., and Goswami, D. Y., 2002, "Theoretical Analysis of Ammonia Based Combined Power/Refrigeration Cycle at Low Refrigeration Temperatures," *Solar Engineering 2002*, ASME, NY, pp. 117-126.

5. Hasan, A. A. and Goswami, D. Y., 2003, "Exergy Analysis of a Combined Power and Refrigeration Cycle Driven by a Solar Heat Source," Journal of Solar Energy Engineering, **125**(1), pp. 55-60.

6. Hasan, A. A., Goswami, D. Y., and Vijayaraghavan, S., 2002, "First and Second Law Analysis of a New Power and Refrigeration Thermodynamic Cycle Using a Solar Heat Source," Solar Energy, **73**(5), pp. 385-393.

7. Tamm, G., and Goswami, D. Y., Lu, S., and Hasan, A.A., 2003, "A Novel Combined Power and Cooling Cycle for Low Temperature Heat Sources – Part I: Theoretical Investigation," Journal of Solar Energy Engineering, **125**(2), pp. 218-222.

8. Tamm, G., and Goswami, D. Y., 2003, "A Novel Combined Power and Cooling Cycle for Low Temperature Heat Sources – Part II: Experimental Investigation," Journal of Solar Energy Engineering, **125**(2), pp. 223-229.

9. Valentini, M., 2002, "Reaching for 60 Percent," Mechanical Engineering, **124**(4), pp. 35-39.

10. Sonntag, R. E., Borgnakke, C., and Van Wylen, G. J., 1998, *Fundamentals of Thermodynamics*, John Wiley and Sons, NY, pp. 348-365, Chap. 11.

11. Babcock and Wilcox Company, 1978, *Steam/Its Generation and Use*, Babcock and Wilcox Company, NY.

12. Larson, D. L., 1987, "Performance of the Coolidge Solar Thermal Electric Power Plant," Journal of Solar Energy Engineering, **109**(1), pp. 2-8.

13. Angelino, G., and Paliano, P. C. D., 1998, "Multicomponent Working Fluids for Organic Rankine Cycles," Energy, **23**(6), pp. 449-463.

14. Demuth, O. J., 1980, "Analysis of Binary Thermodynamic Cycles for a Moderately Low-Temperature Geothermal Resource," *Proceedings of the 15th Intersociety Energy Conversion Engineering Conference*, **1**, AIAA, NY, pp. 798-803.

15. Demuth, O. J., 1981, "Analysis of Mixed Hydrocarbon Binary Thermodynamic Cycles for a Moderate Temperature Geothermal Resources," *Proceedings of the 16th Intersociety Energy Conversion Engineering Conference*, **2**, IEEE, NY, pp. 1316-1321.

16. Iqbal, K. Z., Fish, L. W., and Starling, K. E., 1976, "Advantages of Using Mixtures as Working Fluids in Geothermal Binary Cycles," Proceedings of Oklahoma Academy of Sciences, **56**, pp. 110-113.

17. Demuth, O. J., 1984, "Heat Cycle Research Program," Transactions- Geothermal Resources Council, **8**, pp. 41-46.

18. Boretz, J. E., 1986, "Supercritical Organic Rankine Engines (SCORE)," *Proceedings of the 21st Intersociety Energy Conversion Engineering Conference*, ACS, Washington D. C., pp. 2050-2054.

19. Maloney, J. D. Jr., and Robertson, R. C., 1953, "Thermodynamic Study of Ammonia-Water Heat Power Cycles," Report No. 53-8-43, Oakridge National Laboratory, 60p.

20. Kalina, A. I., 1983, "Combined Cycle and Waste Heat Recovery Power Systems Based on a Novel Thermodynamic Energy Cycle Utilizing Low-Temperature Heat for Power Generation," *Paper # 83-JPGC-GT-3*, American Society of Mechanical Engineers, NY, pp. 1-5.

21. Kalina, A. I., 1984, "Combined-Cycle System with Novel Bottoming Cycle," *Journal of Engineering for Gas Turbines and Power*, **106**, pp. 737-742.

22. Kalina, A. I., and Leibowitz, H. M., 1987, "Applying Kalina Technology to a Bottoming Cycle for Utility Combined Cycles," *Paper # 87-GT-35*, American Society of Mechanical Engineers, NY, 6p.

23. El-Sayed, Y. M., and Tribus, M., 1985, "Theoretical Comparison of the Rankine and Kalina Cycles," *ASME Special Publications*, **AES -1***,* American Society of Mechanical Engineers, NY, pp. 97-102.

24. Park, Y. M., and Sonntag, R. E., 1990, "A Preliminary Study of the Kalina Power Cycle in Conjunction with a Combined Cycle System," International Journal of Energy Research, **14**, pp. 153-162.

25. Nag, P. K., and Gupta, A. V. S. S. K. S., 1998, "Exergy Analysis of the Kalina Cycle," Applied Thermal Engineering, **18**(6), pp. 427-439.

26. Marston, C. H., 1990, "Parametric Analysis of the Kalina Cycle," Journal of Engineering for Gas Turbines and Power, **112**, pp. 107-116.

27. Kalina, A. I., and Leibowitz, H. M., 1989, "Application of the Kalina Cycle Technology to Geothermal Power Generation," Transactions-Geothermal Resources Council, **13**, pp. 605-611.

28. Bliem, C. J., 1989, "Aspects of the Kalina Technology Applied to Geothermal Power Production," Report No. EGG-EP-8708, Idaho National Engineering Laboratory, 67p.

29. Bliem, C. J., and Mines, G. L., 1990, "Advanced Binary Geothermal Power Plants Limits of Performance," *Proceedings of the 25th Intersociety Energy Conversion Engineering Conference*, IEEE, NY, **5**, pp. 85-90.

30. Ibrahim, O. M., and Klein, S. A., 1996, "Absorption Power Cycles," Energy, **21**, pp. 21-27.

31. Mlcak, H. A., 2001, "Design and Start-Up of the 2 MW Kalina Cycle Orkuveita Husavikur Geothermal Power Plant in Iceland," *European Geothermal Energy Council, 2nd Business Seminar*. Available on http://www.exrg.com/ January 10th, 2003.

32. Leibowitz, H. M., and Mirolli, M., 1997, "First Kalina Combined-Cycle Plant Tested Successfully," Power Engineering, **101**(5), pp. 44-48.

33. Rogdakis, E. D., and Antonopoulos, K.A., 1991, "A High Efficiency NH_3/H_2O Absorption Power Cycle," Heat Recovery Systems and CHP, **11**, pp. 263-275.

34. Kouremenos, D. A., Rogdakis, E. D., and Antonopoulos, K. A., 1994, "Cogeneration with Combined Gas and Aqua-Ammonia Absorption Cycles," *Thermodynamics and the Design, Analysis and Improvement of Energy Systems*, **AES – Vol. 33**, ASME, N.Y.

35. Demuth, O. J., and Kochan, R. J., 1982 "Analysis of Mixed Hydrocarbon Binary Thermodynamic Cycles for Moderate Temperature Geothermal Resources Using Regenerative Techniques," *Proceedings of the 17th Intersociety Energy Conversion Engineering Conference*, **2**, IEEE, NY, pp. 1104-1109.

36. Xu, F., Goswami, D. Y., and Bhagwat, S. S., 2000, "A Combined Power/Cooling Cycle," Energy, **25**(3), pp. 233-246.

37. ASHRAE Handbook of Fundamentals, 1997, American Society of Heating, Refrigerating and Air-Conditioning Engineers, Inc., Atlanta, SI Edition.

38. Szargut, J., Morris, D. R., and Steward, F. R., 1988, *Exergy Analysis of Thermal, Chemical and Metallurgical Processes*, Hemisphere, NY, 332p.

39. DiPippo, R., 1980, *Geothermal Energy as a Source of Electricity: a Worldwide Survey of Design and Operation of Geothermal Power Plants*, U.S. Department of Energy, Washington, D.C., 388p.

40. Abrahamsson, K., Jernqvist, A., Aly, G., 1994, "Thermodynamic Analysis of Absorption Heat Cycles," *Proceedings of the International Absorption Heat Pump Conference*, **AES-Vol. 31**, ASME, NY, pp. 375-383.

41. Lorenz, V. H., 1894, "Die Ausnützung der Brennstoffe in den Kühlmaschinen," Zeitschrift für die gesammte Kälte-Industrie, **1**, pp. 10-15.

42. Rosen, M.A., and Le, M., 1995, "Efficiency Measures for Processes Integrating Combined Heat and Power and District Cooling," *Thermodynamics and the Design, Analysis, and Improvement of Energy Systems*, **AES-Vol. 35**, pp. 423- 434.

43. Xu, F., and Goswami, D. Y., 1999, "Thermodynamic Properties of Ammonia-Water Mixtures for Power-Cycle Applications," Energy, **24**, pp. 523-536.

44. Stoecker, W. F., 1989, *Design of Thermal Systems*, McGraw-Hill, NY, 565p.

45. Reklaitis, G. V., Ravindran, A., and Ragsdell, K. M., 1983, *Engineering Optimization: Methods and Applications*, John Wiley and Sons, NY, 684p.

46. Edgar, T. F., Himmelblau, D. M., and Lasdon, L.S., 2001, *Optimization of Chemical Processes*, McGraw-Hill, NY, 650p.

47. Lasdon, L. S., Warren, A. D., Jain, A., and Ratner, M., 1978, "Design and Testing of a Generalized Reduced Gradient Code for Nonlinear Programming," ACM Transactions on Mathematical Software, **4**, pp. 34-50.

48. Lasdon, L. S., and Warren, A. D., 1997, *GRG2 User's Guide*, Unpublished Manuscript, University of Texas, Austin, Dept. of General Business, 26p.

49. Gawlik, K., and Hassani, V., 1997, "Advanced Binary Cycles: Optimum Working Fluids," *Proceedings of the 32nd Intersociety Energy Conversion Engineering Conference*, **3-4**, IEEE, NY, pp.1809-1814.

50. Iqbal, K. Z., West, H., H., and Starling, K. E., 1978, "Hydrocarbon Working Fluid and Operating Condition Selection for the Conventional Geothermal Binary Cycle," *Proceedings of the 13th Intersociety Energy Conversion Engineering Conference*, SAE, Warrendale PA, pp.1114-1120.

51. Kihara, D. H., and Fukunaga, P. S., 1975, "Working Fluid Selection and Preliminary Heat Exchanger Design for a Rankine Cycle Geothermal Power Plant," *Proceedings of Second United Nations Symposium on the Development and Use of Geothermal Resources*, **3**, United Nations, NY, pp.2013-2020.

52. ASHRAE Handbook of Fundamentals, 1997, "Characteristics of Refrigerant-Absorbent Pairs," pp. 1.15-1.16.

53. Walter, R. A., and Wilson, S. W., 1976, "Economic Optimization of Binary Fluid Cycle Power Plants for Geothermal Systems," *Proceedings of the 11th Intersociety Energy Conversion Engineering Conference*, pp. 731-738.

54. Jacob, X., Albright, L. F., and Tucker, W. H., 1969, "Factors Affecting the Coefficient of Performance for Absorption Air-Conditioning Systems," ASHRAE Transactions, pp. 103-110.

55. Gyftopolous, E. P., and Berretta, G. P., 1991, *Thermodynamics: Foundations and Applications*, Macmillan Publishing Company, NY, 658p.

56. Alexis, G. K., and Rogdakis, E. D., 2002, "Performance Characteristics of two Combined Ejector-Absorption Cycles," Applied Thermal Engineering, **22**, pp. 97-106.

57. Nord, J. W., Lear, W. E., and Sherif, S. A., 2001, "Analysis of Heat-Driven Jet-Pumped Cooling System for Space Thermal Management," Journal of Propulsion and Power, **17**, pp. 566-570.

58. Nicodemus, C., 1996, "Thermal Absorption Compression Cycle," *United States Patent No. #5,586,442.*

59. Sherif, S. A., Lear, W. E., Steadham, J. M., Hunt, P L., and Holladay, J. B., 2000, "Analysis and Modeling of a Two-Phase Jet Pump of a Thermal Management System for Aerospace Applications," International Journal of Mechanical Sciences, **42**, pp. 185-198.

60. Cunningham, R. G., and Dopkin, R. J., 1974, "Jet Breakup and Mixing Throat Lengths for the Liquid Jet Gas Pump," ASME Journal of Fluids Engineering, **96**(3), pp. 216-226.

61. Cunningham, R. G., 1974, "Gas Compression with Liquid Jet Pump," ASME Journal of Fluids Engineering, **96**(3), pp. 203-215.

62. Thorin, E., Dejfors, C., and Svedberg, G., 1998, "Thermodynamic Properties of Ammonia-Water Mixtures for Power Cycles," International Journal of Thermophysics, **19**, pp. 501-510.

63. de Reuck, K. M., Craven, R. J. B., and Elhassan, A. E., 1996, "Equations of State," *Transport Properties of Fluids: Their Correlation, Prediction and Estimation*, J. Millat et al., eds., IUPAC, Cambridge University Press, NY, pp. 165-188.

64. Tillner-Roth, R., and Friend, D. G., 1998, "A Helmholtz Free Energy Formulation of the Thermodynamic Properties of the Mixture {Water + Ammonia}," Journal of Physical Chemistry, **27**, pp. 63-77.

65. Elnick, R. M., Donahey, G. P., and Holsinger, M., 1998, "Modelling the High-Pressure Ammonia-Water System with WATAM and the Peng-Robinson Equation of State for Kalina Cycle Studies," Industrial Engineering Chemistry Research, **37**, pp. 1644-1650.

66. El-Sayed, Y. M., and Tribus, M., 1986, "Thermodynamic Properties of Water-Ammonia Mixtures: Theoretical Implementation for Use in Power Cycles," *ASME Special Publications*, **AES-1**, ASME, NY.

67. Xu, F., 1997, "Analysis of a Novel Combined Thermal Power and Cooling Cycle using Ammonia-Water Mixture as a Working Fluid," Ph.D. Dissertation, University of Florida, Gainesville, FL.

68. Friend, D. G. and Huber, M. L., 1994, "Thermophysical Property Standard Reference Data from NIST," International Journal of Thermophysics, **15**(6)**,** pp. 1279-1287

69. Mason, E. A., and Uribe, F. J., 1996, "The Corresponding –States Principle: Dilute Gases," *Transport Properties of Fluids: Their Correlation, Prediction and Estimation*, J. Millat et al., eds., IUPAC, Cambridge University Press, NY, pp. 250-282.

70. Huber, M. L., and Hanley, H. J. M., 1996, "The Corresponding –States Principle: Dense Fluids," *Transport Properties of Fluids: Their Correlation, Prediction and Estimation*, J. Millat et al., eds., IUPAC, Cambridge University Press, NY, pp. 283-295.

71. Nowarski, A., and Friend, D. G., 1998, "Application of the Extended Corresponding States Method to the Calculation of the Ammonia-Water Mixture Thermodynamic Properties," International Journal of Thermophysics, **19**(4), pp. 1133-1142.

BIOGRAPHICAL SKETCH

Sanjay Vijayaraghavan was born on June 23, 1976, in the village of Kodakara in the southern state of Kerala, India. He was brought up entirely in the coastal city of Chennai (formerly known as Madras), the capital of the state of Tamilnadu. In June 1997, he graduated with a bachelor's degree in mechanical engineering from the University of Roorkee (now called the Indian Institute of Technology, Roorkee) located in the new state of Uttaranchal, 15 miles south of the Himalayan foothills. Places and institutions he is associated with tend to change names and shape, so watch out Gainesville and UF.

Sanjay enrolled in the Department of Mechanical Engineering at the University of Florida in the fall of 1997 and worked on photocatalytic detoxification of contaminated water for his master's degree. He stayed on for a Ph.D. and spent almost a year working on antenna solar energy conversion. After preparing a "roadmap" for research on the topic and not being sure of his competence to implement it, has been working on the topic of this dissertation. In the meantime, the merger of two departments resulted in the *new* Mechanical and Aerospace Engineering Department.